The Dissertation Committee for Jason Henry Ideker Certifies that this is the approved version of the following dissertation:

Early-Age Behavior of Calcium Aluminate Cement Systems

Committee:

Kevin J. Folliard, Supervisor

Michael D.A. Thomas, Co-Supervisor

Maria C.G. Juenger

David W. Fowler

Kitty L. Milliken

Early-Age Behavior of Calcium Aluminate Cement Systems

by

Jason Henry Ideker, B.S.C.E.; M.S.E.

Dissertation

Presented to the Faculty of the Graduate School of

The University of Texas at Austin

in Partial Fulfillment

of the Requirements

for the Degree of

Doctor of Philosophy

The University of Texas at Austin

May 2008

Dedication

To my parents for their unconditional support, encouragement and the lifelong love of learning that they instilled in me.

Acknowledgements

Pursuing the doctoral degree does not represent the accomplishments of a single individual; it represents the combined efforts of a large group of people that have provided support for this individual over the course of their study. This support may be physical, emotional or financial. An individual must possess a strong desire for mental and physical challenge, a realization that great accomplishment is often preceded by numerous failed experiments and trials and an undying passion for the material they are studying while pursuing a doctoral degree. None of this is possible, or enjoyable without a community of support to guide and encourage you along the way. While I hope to recognize everyone who has made this dream a reality, I am likely to unintentionally omit several people who deserve my thanks, so let me say thank you to them now.

First I want to thank my parents. Your continued support throughout my collegiate career is unparalleled. I could not have asked for better parents and as each day passes I am more and more cognizant of how amazing you both are to me. This dissertation is dedicated to you because the person I have become took a lot of hard work from both of you and that effort does not go unrecognized or under-appreciated.

I have some of the most amazing friends in the world and I am grateful to each one of you for your support, friendship and camaraderie over the years. Dr. Heather Bean, we've gone through this process together and have been a constant source of support for one another. Your friendship and love has been and continues to be invaluable. I couldn't have made it through the rough spots if it wasn't for your wisdom, laughter and advice. We have had so much fun traveling all over the world for our studies and for fun and I hope we can continue this into the future. Kenny Mobley, you have been and continue to be one of my best friends. It is refreshing to see this world from another perspective through your eyes. Your positive attitude and encouragement

have kept me going and I really do appreciate that. If I ever need a laugh, and it is the beste medicine, Melina Johnson you have always been there to provide that. For you and BJ to come visit me in Switzerland in 2006 was an amazing and cherished experience. Ashley Prisant and Amanda Prisant, two sisters and two amazing friends, you have also followed me to the ends of the earth and our time together is filled with laughter, great conversation and adventure. Ashley, you are one of the most goal-oriented people I know and for that I am grateful. Amanda, no one share our love of the Dave Matthews Band and I know that music is an important part of our lives that has enriched our experiences and followed us along this journey through life. Donna and Jeremy Blalock, thank you for always supporting me and for being so thoughtful and caring with your friendships and decisions in life. Bradley East you have been a great new addition to my circle of friends and the entire group you run with has been so inviting and supportive. You have all enriched my time here in Austin and I look forward to continuing our friendship in the future. Racheal Lute, you have become one of my close friends in the past few years and we have had so much fun together in Europe and at the lab. You were my writing buddy as you worked to complete your thesis at the same time I was working on this dissertation. Your constant communication and encouragement never let me lose my spirit for doing this work, thank you so much. I know the lab is left in good hands with Anthony taking on so much responsibility and always smiling through a face covered in concrete, soil and candy. You became a close friend this year and want to thank you for listening and never turning down an invite to get a beer. Thano Drimalas, you have been there sitting across from me at work to share insight, a good laugh, name songs on the internet and to provide a calming influence in my hectic life. I value our friendship greatly and look forward to many years of working with one of my best friends.

The support from our laboratory at the Concrete Durability Center at The University of Texas at Austin is truly amazing. We have some of the most amazing facilities in which to work and the support of a countless supply of undergraduate research assistants makes the enormous amount of work that everyone performs at the laboratory possible. I have worked with so many undergraduates over the past 6 years and I could not have accomplished my goals without your help. I have also been fortunate enough to work with several undergraduate research assistants specifically on this research project. Ari Eisenberg your dedicated work on the pore press was invaluable and I knew I could always count on you for a good laugh at work. Cynthia Hua, thank you so much for putting up with my crazy schedule and involvement with multiple research projects. You helped to keep me sane by taking on so much responsibility and dedication to high-level analytical techniques. Racheal, if it was not for all of your hard work on the chemical shrinkage and autogenous shrinkage testing we could have never made the great discoveries that we did as part of this study. Thanks also for your work on isothermal calorimetry. I know great things are in your future. Evan Wehrle, you have not only been one of the hardest working and most dedicated people with whom I have ever worked, you have also become a close friend. You challenged me to become a better teacher and role model as we worked through this project together. This research would never have come together if you and I had not put in so much hard work in on this project. Working with you over the past year has been an amazing experience and it has made this project a great success.

The staff at our laboratory has also contributed greatly to the success of this project. David Whitney, thank you so much for your great ideas and support of our research project. Mike Rung, your practical knowledge of so many testing methods and experience has brought a wealth of understanding to this project and I appreciate your

involvement and genuine concern for the success of research at the lab. Thank you for all of your electronics expertise. As we rely more and more on advanced data acquisition equipment you are an invaluable resource at the lab. Sherian Williams, as I have said before, you are someone that truly makes my life easier. You are an amazing and inspiring individual and I want you to know how much I respect your courage, positive attitude and amazing work ethic. Kerry Rothenbach, you always kept my spirits high at the lab and you could work at pace that few others could ever reach. I have missed your presence in the last year but am glad we have remained in touch. The lab certainly misses your "can-do" attitude and your ability to beautifully finish 36 concrete prism molds in less than 10 minutes.

Dr. Maria Juenger, I was so fortunate to work with you as a master's student at UT Austin. You have provided me with opportunities to collaborate on several research projects and I look forward to working with you in the future. I truly do appreciate your constructive criticism for my writing and presentations. You have made me a better communicator and researcher.

Dr. Michael Thomas, when I first heard of you it was from my undergraduate advisor Dr. Kimberley Kurtis. I never thought that we would end up working together on so many projects, traveling all over the world to study concrete and develop a great friendship as well. Thank you so much for the way in which you mentor, your great advice and the fun that you bring to this industry. I look forward to working with you for the rest of my career.

I want to thank Dr. Kimberly Kurtis for seeing some spark in me that might get "hooked" on concrete. I would not be where I am today if it wasn't for your guidance, inspiring instruction and advice. I still consider you one of my most important mentors and hope to work with you more in the future.

Last but certainly not least for my thanks is my advisor, mentor and friend, Dr. Kevin Folliard. I cannot adequately put into words my gratitude for the opportunities you have given me. I never dreamed that my experience as a graduate student could be so enjoyable, completely busy and rewarding as it has been, and that is a direct result of you. Your infectious love of this unassuming material, concrete, permeates every project that you undertake. I hope to be a fraction of the researcher and investigator that you are and I try to follow your example every day. While it will be sad to leave UT Austin, I know we will continue to work together on a variety of projects for the rest of our careers. Over the years we have developed a strong friendship that I treasure and I thank you for taking the time to be a mentor, advisor and friend.

Early-Age Behavior of Calcium Aluminate Cement Systems

Publication No._____

Jason Henry Ideker, Ph.D.

The University of Texas at Austin, 2008

Supervisors: Kevin J. Folliard and Michael D.A. Thomas

Compared to the knowledge base for ordinary portland cement concrete (OPCC), relatively little information exists for calcium aluminate cement concrete (CACC), despite its existence for over 100 years. There is particularly a lack of knowledge related to early-age behavior of CACC, specifically volume change and cracking potential. To assess these early-age properties, two unique pieces of equipment were developed and employed: a rigid cracking frame and free deformation frame which enabled quantification of restrained stress generation and unrestrained autogenous deformation, respectively. These two pieces of equipment employed active temperature control and allowed a wide range of isothermal and realistic temperature conditions to be imposed upon hydrating cementitious samples. Match-cured samples (i.e. identical temperature curing to that in the frames) enabled the quantification of mechanical property development.

Samples cured at discrete isothermal temperatures up to 30 °C developed tensile forces in the rigid cracking frame and exhibited shrinkage phenomena in the free deformation frame. At temperatures above 30 °C, the converse was true and significant

compressive forces developed in restrained testing and expansion was observed in unrestrained testing. It was found that this was a direct result of microstructural development related to the formation of metastable phases (associated with shrinkage) and stable phases (expansion as a result of conversion from metastable to stable phases). Proper use of this material must take into account behavior associated with both types of hydrate assemblages, metastable and stable.

Realistic time-temperature histories were also investigated based on field-scale concrete cast as part of this research project. It was found that volume change at early-age was dominantly controlled by thermal history. Furthermore, it was not simply the maximum temperature reached, but the rate of temperature rise during hydration and the resulting duration of time spent at high temperature that profoundly influenced volume change and property development. The research described in this dissertation represents a significant advancement of the state-of-knowledge of this unique material and has further elucidated the role of temperature during hydration of CACC.

Table of Contents

List of Tables

List of Figures

1 Introduction

Calcium aluminate cement concrete (CACC) has been successfully used in a variety of applications for 100 years. Concrete made with calcium aluminate cement (CAC) offers several distinct advantages over portland cement concrete, including rapid strength gain with customizable setting time (adjusted with proper admixture dosage), better abrasion resistance and improved resistance to aggressive environments. While these cements have been used in a wide range of applications, they have not been studied to the same extent as ordinary portland cement (OPC). Unique to calcium aluminate cements is that the hydration process may result in the formation of stable hydrates, metastable hydrates and more commonly mixtures of the two. The metastable hydrates will inevitably go through a process referred to as conversion whereby less dense metastable hydrates convert to denser stable hydrates, leaving behind porosity which may or may not be water-filled. This conversion process in an already hardened microstructure results in a significant reduction in strength due to porosity increase. While attempts over the years have been made to eliminate the conversion process, this is an inevitable feature of this unique material and the best approach is to ensure that the converted strength is properly quantified and that the converted (minimum strength) meets the design requirements for the desired application. An early lack of understanding of this fundamental property of calcium aluminate cement concrete, combined with misuse of the material during rapid rebuilding phases after World Wars I and II, led to several failures where calcium aluminate cement concrete was at least partially implicated. The negative incidents hindered a more widespread use of this material and are at least partially to blame for the general lack of understanding of other engineering properties of this material.

To facilitate more advanced research on CAC, especially aimed at usage for rapid construction or extreme environments, a Scientific Network was established in the fall of 2004 by Kerneos Aluminate Technologies (formerly LaFarge Aluminates) to generate some of the fundamental knowledge that is lacking for these specialty cements. The Scientific Network is comprised of several university researchers working in conjunction with Kerneos Aluminate Technologies in several topical areas. The first area of research selected was early-age volume change and early-age behavior of the calcium aluminate cement concrete. Due to the rapid hydration, much of the future performance of CACC is dictated by what happens in the first 12-24 hours after casting. There was also a desire to investigate the potential for early-age cracking risk of these materials compared to ordinary portland cement concrete (OPCC) as this is often a concern in rapid construction applications. This work was initiated at The University of Texas at Austin under the direction of Dr. Kevin J. Folliard (and through the research performed by Jason Ideker, Ph.D. candidate). Since the inception of the network, three additional universities have been integrated into the Scientific Network. Under the direction of Dr. Karen Scrivener at Ecole Polytechnique Federale de Lausanne (EPFL) in Lausanne Switzerland, Christophe Gosselin is working to characterize microstructural development of CAC pastes and mortar with and without supplementary cementing materials (SCMs), including fly ash and ground granulated blast furnace slag. Recently research under the direction of Dr. Michael Thomas at the University of New Brunswick (UNB) in Fredericton, New Brunswick, Canada has been initiated to characterize the durability of CAC systems in laboratory testing and outdoor exposure. There is also collaboration with Laval University in Quebec City, Quebec, Canada under the direction of Dr. Marc Jolin.

1.1 RESEARCH SCOPE

The goal of this dissertation research was to investigate early-age behavior, specifically volume change, of calcium aluminate cement systems. The majority of testing was performed on micro-concrete; less emphasis was placed on testing concrete, mortar and paste. The aim of the research was to correlate early-age volume change to the potential for early-age cracking in field applications. While "early-age" is a somewhat vague term in this context, there is specific interest in volume change and stress generation in the first 24 hours of the lifespan of a given calcium aluminate cement system. The resulting microstructure that forms in the first 24 hours is critical to determining the future performance of these systems and the majority of testing methods as part of this dissertation are monitored for at least 5 full days with some methods monitored for much longer periods of time.

Because this dissertation is one of the more comprehensive studies on calcium aluminate cements, an extensive literature review is presented in Chapter 2. The focus of the literature review is to familiarize the reader with the material, bring to light recent findings and portray, in general, the current knowledge about calcium aluminate cement systems. Lastly, this chapter identifies key research needs to advance the state of the art of CAC-based systems.

Chapter 3 is brief and describes the materials and mixture proportions used in this research. The nomenclature for mixtures is also explained to give the reader guidance on how to identify and interpret materials and mixtures described throughout this dissertation. Although the mixture proportions are presented in general terms in this chapter, every figure in this dissertation contains the vital information (testing temperature, w/cm, admixtures, date cast) to inform the reader of key details.

Chapter 4 summarizes research into the chemical shrinkage of calcium aluminate cement and ordinary portland cement pastes. Testing was performed across a wide range of isothermal temperatures to characterize chemical shrinkage associated with stable and metastable hydrate formation. Chemical shrinkage has been used as a successful testing tool to estimate the potential for autogenous shrinkage in ordinary portland cement paste, and as such, significant research was performed to generate similar data for CAC-based systems.

The most substantial chapter of the dissertation is Chapter 5 which is the crux of the research program. This chapter presents results from investigations into early-age behavior in an innovative testing apparatus: rigid cracking and free deformation frames. These frames allow for the quantification of restrained stress generation as well as free movement in actively hydrating cementitious samples. Unique to this testing methodology is the ability to provide active temperature control through heated or cooled liquid which runs through formwork surrounding both frames as well as water that is circulated around samples that are match-cured to the same time-temperature history as samples in the rigid and free frames. This chapter presents some of the most interesting findings from this dissertation research related to the early-age volume change of metastable and stable hydrates. It also provides further development of the innovative testing technique involving the use of rigid cracking and free deformation frames.

Chapter 6 evaluates the drying shrinkage of calcium aluminate cement concrete and micro-concrete, both in restrained (rings) and unrestrained test set-ups. Comparisons are made between CAC- and OPC-based systems, both in terms of short- and long-term shrinkage behavior.

In Chapter 7 a study investigating temperature rise, strain generation and relative humidity rise in outdoor calcium aluminate cement concrete slabs is presented. In total,

six slabs were cast measuring 0.9 x 0.9 m with varying depth of 0.1, 0.2 and 0.3 m. This study was launched to evaluate in-situ properties of realistic CAC concrete slabs and to generate realistic time temperature histories to drive the rigid cracking and free deformation frame tests to investigate stress and strain generation in actual hydrating samples going through a real heat signature.

Chapter 8 summarizes the key findings of this overall research program and recommends several technical areas that deserve further attention in future research.

2 Literature Review

2.1 INTRODUCTION

Calcium aluminate cements are characterized by their high alumina contents (32-45% Al_2O_3) when compared to ordinary portland cements (1-12% Al_2O_3). Consequently, the main hydrate phases of these cements are calcium aluminates. These cements have been in use since the 1910s. Although calcium aluminate cements are produced at much lower quantities when compared to ordinary portland cements, they offer several distinct advantages over portland cement when used in concrete applications, including:[1]

- Rapid strength development, even at low temperatures
- High temperature resistance/refractory performance
- Resistance to a wide range of chemically aggressive conditions

While calcium aluminate cement concretes (CACC) offer specific advantages over ordinary portland cement concretes, the unique properties of this material require special attention in applications. Specifically, CACCs are highly sensitive to variations in microstructural development based on the temperature history to which they are subjected, especially the temperatures attained during the initial curing and hydration phases just after placement. CACCs ultimately (either in the short- or long-term, depending on thermal history) undergo a process referred to as conversion, during which low density hydration products convert to higher density products while subsequently releasing water. This microstructural transformation in an already hardened concrete will lead to an increase in porosity and, as a result, a decrease in strength. Therefore, it is critical that the design strength for CACCs be based on fully converted strengths. Current practice typically recommends a maximum w/cm (water to cement) ratio of 0.40

and a minimum cement content of 400 kg/m^3. Early in the life of commercial application of CACC their misuse and lack of clear understanding behind the conversion process and other intricacies of dealing with such cementitious systems resulted in several structural failures[1-3]. Unfortunately this precluded the use of CACC in many markets and resulted in a less than favorable background for future use.

The following section of the dissertation provides an in-depth literature review to familiarize the reader with a brief history of calcium aluminate cements, the mechanisms underlying conversion, inherent advantages and disadvantages associated with the use of CACC and to set the framework for investigation into the early age volume change of concretes made with calcium aluminate cements. Currently a large body of work exists regarding early-age volume change in ordinary portland cement concrete (OPCC); however little published literature exists with respect to the same phenomena in calcium aluminate cement systems. As a result much of the early work for this study investigated the possibility of applying testing techniques that work well for OPCC to CACC systems. Ultimately it was born out that more advanced techniques and/or modifications to existing techniques were necessary to accurately characterize CACC systems. In this review section some of the fundamental aspects behind volume change in OPCC systems will be outlined with extrapolations to potential issues with CACC. Throughout the dissertation OPCC is used as a reference for observations in CACC testing. This literature review fits into the overall framework of this dissertation that will specifically delve into the issues of early-age volume change in calcium aluminate cement concrete.

2.2 HISTORY

In the mid 19th century it was reported that alumina-rich cements had inherently excellent cementing properties.[1] In 1888, the first patent for limestone-bauxite cement was granted. However, most of the development of what is today considered to be CAC was performed by Bied through work at the J. & A. Pavin de Lafarge Company in Le Teil, France. His work arose out of issues dealing with deterioration of mortars and concretes that were placed in soils high in sulfate, specifically gypsum and anhydrite. There was a need for a concrete system better able to resist these aggressive agents. In the 1840s Vicat investigated the production of cements with a ratio of silica plus alumina to lime plus magnesia that was greater than unity and was thought to provide suitable sulfate resistance. Meanwhile, Bied concentrated his research on developing cements with high alumina contents for similar purposes to Vicat. In 1908 Bied received a patent for a manufacturing process which fused bauxite and/or other materials containing alumina or ferruginous material of low silica content with limestone. This took several years to develop on an industrial production scale. After five subsequent years of trial development at Lafarge, Ciment Fondu Lafarge (CFL) was placed on the market in 1918 and is one of the many calcium aluminate cements still produced today.[1] In 2006 Lafarge Aluminates was sold and became a wholly-owned company called Kerneos Aluminate Technologies. Many of the calcium aluminate cements produced under this new company name have retained their trademark names such as Ciment Fondu and the range of products in the Secar family.

One of the first documented uses of calcium aluminate cements was in the P.L.M. Railway (Paris-Lyon-Marseille) for the reconstruction of a railway tunnel passing through a solid mass of anhydrite (calcium sulfate or $CaSO_4$). At about the same time in the United States (U.S.) a patent was issued on aluminate compounds intended as mineral additives to concretes (presumably portland cement concretes) by Spackman. These were

termed Alca natural cements, but their production was later abandoned. The U.S. Bureau of Standards carried out a study on CAC in the early 1920s.[1]

Calcium aluminate cements were introduced to the United Kingdom (UK) shortly after World War I (WWI) and were distinguished from ordinary portland cement by their high alumina content of roughly 32-45% (Al_2O_3). Initially, these cements were named "high-alumina cements"; even today they may be referred to as such. Since WWI, CAC with alumina contents ranging from 50-90% have been produced.[1]

2.2.1 Issues Associated with Early Use of CACC

When CAC increased in popularity just after WWI in Europe, minimum w/cm such as 0.40, were adopted owing to the ability of metastable hydrates to combine large amounts of water. In the 1930s poor performance of CACCs with high w/cm after conversion was recognized, but w/cm typical of OPC (~0.6) continued to be used. After subsequent failures in 1943 the French government placed prohibitive restrictions on the use of CAC in the public sector. Other failures in the 1960s in Bavaria, Germany occurred due to corrosion of prestressing wires in a type of CAC concrete produced as a blast furnace by-product. CAC concrete was no longer used in Germany as a result. However, investigations into this issue in other parts of Europe concluded that reinforcement performed well in normal CAC and these failures were owed to the type of blast furnace by-product CAC used in Bavaria. After extensive research in France, the restrictions placed on CAC concrete were removed in the 1970s and new guidance recommended a maximum w/cm of 0.40 and cement contents greater 400 kg/m^3 to ensure good performance.[1]

In the United Kingdom (U.K.) an extensive market using CAC in prestressed concrete developed in the 1950s through the 1960s. It is evident from codes of practice that the issues of conversion were well known; however, advice in codes was "aimed at

limiting or preventing conversion, i.e. trying to avoid the inevitable".[1] Even though a maximum w/cm of 0.40 was recommended in practice, this would have been hard to achieve since mixture designs often had aggregate to cement ratios upwards of 9:1. To place concrete at this high of an aggregate to cement ratio would likely require a w/cm greater than 0.5.[1] In 1973 two structures composed of CAC concrete collapsed: Camden School for Girls (built in 1955) and the Bennett Building on the campus of the University of Leicester (built in 1965). While reduced strength in CACC roof beams was found in each collapse, these were of minor consequence according to the failure reports. Instead, the main cause was "inadequate resistance of support nibs to the roof beams against horizontal tensile forces due to thermal movements".[1] Investigations into one of the roof beams at the Bennett Building revealed adequate strength for design despite conversion occurring in the beam. Another collapse of roof beams over a swimming pool in 1974 implicated conversion of CACC aggravated by subsequent chemical attack by sulfates. There was also evidence that the concrete did not fully meet code requirements for w/cm and cement content. These collapses led to eventual removal of CACC for use in buildings in the UK Building Regulation.[2]

In December of 1990 collapse of a roof of an apartment building in Spain occurred. The roof was made from prestressed beams made of both CAC and OPC concrete. The concrete did not meet current guidelines for w/cm and cement concrete. In addition the use of aggregates with soluble alkalies may have led to alkaline hydrolysis combined with water leakage and/or a warm humid environment in parts of the structure.[3] In its almost 100 years of use, calcium aluminate cement concretes have performed well. However, instances of failure have hindered widespread use and it has been learned that CACCs are much more sensitive to misuse than their OPCC counterparts. Correct usage must be based on good construction practices and design based on converted strengths.

Furthermore a maximum w/cm of 0.40 and a minimum cement content of 400 kg/m^3 should be used.[1]

2.3 COMPOSITION OF CALCIUM ALUMINATE CEMENTS

Calcium aluminate cements are produced mainly from two material sources: limestone and bauxite. While other materials may contain alumina, bauxite is the only suitable material from which CACs may produce on an industrial scale. Standard grades of CAC (38-40 % Al_2O_3) may be produced with ferruginous bauxites containing up to 20% Fe_2O_3; silica contents should remain low (<6%). For CACs with higher alumina contents more pure forms of raw materials may be required.[1]

While several methods have been used to manufacture calcium aluminate cements the most common process today involves the use of a reverberatory open-hearth furnace. This furnace type has a long vertical stack into which bauxite and limestone are introduced. It may be fired by pulverized coal or oil with hot-air blast. Water and carbon dioxide are driven off as the hot gases pass through the raw materials. As the material passes from the vertical stack into the hearth of the furnace, the melting process occurs. The "cement" is maintained in the molten state while in the hearth and then pours out continuously from a tap hole where it runs into molds and is subsequently cooled. The temperatures attained in the furnace may be in excess of 1450 °C. Once cooled, the clinker resembles a dark fine grained rock such as basalt. These are referred to as clinker ingots and are then crushed and ground in ball mills. Energy consumption and wear on grinding equipment is quite high with calcium aluminate cements. In contrast to portland cement, nothing is added during grinding (gypsum in the case of OPC); setting is controlled mainly by cement composition. High grades of CAC may be white in color as they contain few impurities. Lower CAC grades may contain significant quantities of

iron oxide and are often very dark grey to almost black in color. CACs are produced throughout the world, including France, UK, Spain, USA, Japan, Croatia, China, Poland, Brazil, India and to some lesser extents in the countries of the former USSR.[1]

Table 2.1 outlines typical chemical characteristics of calcium aluminate cements (adopted from Scrivener and Capmas).[1]

Table 2.1: CAC Typical Properties

Property	Value
Specific Gravity (kg/m^3)	3200-3250
Loose bulk Density (kg/m^3)	1100-1400
Consolidated Buld Density (kg/m	1850-1950
Specific Surface (Blaine) (m^2/kg)	250-400
Residue (on 100 μm sieve)	5%
High Fineness CAC S.S. (m^2/kg)	1000
Autoclave Expansion	<1 mm
Soundness	Irrelevant

Table 2.2 is also adapted from Scrivener and Capmas and gives the chemical compositions for several grades of CAC.[1]

Table 2.2: Composition Ranges for Calcium Aluminate Cements

Grade	Color	Al_2O_3	CaO	SiO_2	FE_2O_3 + FeO	TiO_2	MgO	Na_2O	K_2O	Countries of Manufacture
Standard (low alumina)	Grey or buff to black	36-42	36-42	3-8	12-20	<2	~1	~0.1	~0.15	France, Spain, Croatia, USA, India, Eastern Europe
Low alumina, low iron	Light buff or grey to white	48-60	36-42	3-8	1-3	<2	~0.1	~0.1	~0.05	France, USA, India, Korea, Japan
Medium Alumina	White	65-75	25-35	<0.5	<0.5	<0.05	~0.1	<0.3	~0.05	France, UK, USA, Japan, China, India, Korea, Brazil
High Alumina	White	=80	<20	<0.2	<0.2	<0.05	<0.1	<0.2	~0.05	USA, France, Japan, Brazil, Korea

All CACs contain monocalcium aluminate (CA or $CaAl_2O_4$) as the main hydraulic phase. While other phases may be present based on the type of CAC it is important to note that C_3A is not a normal constituent of CACs and CA_6 is rarely found. Phase compositions are complicated by the presence of silica and iron oxide. Iron oxide

may be present in both the ferric and ferrous form (Fe_2O_3 and FeO, respectively). Silica is usually present as C_2S, C_2AS (gehlenite) or in both forms. Other oxide forms may also be present: TiO_2, SiO_2 and MgO.[1]

Of particular interest is the presence of $C_{12}A_7$. It is almost always present in CACs and was long mis-identified as C_5A_3. This phase is cubic and has triangular morphology. The ratios of CA to $C_{12}A_7$ play an important role in hydration and long-term performance of CACC and this will be discussed later in this review.[1]

Petrographic examination of thin sections by transmitted light microscopy combined with X-ray diffraction may provide the best means for determining the phase compositions of calcium aluminate cement. Additionally, use of backscattered electron imaging (BSE) in a scanning electron microscope is a good technique for phase distribution determination and characterization.[1]

2.4 HYDRATION

Hydration of calcium aluminate cements is complicated and highly temperature dependent. The mechanisms of hydration are referred to as "through solution", meaning dissolution of the anhydrous phases upon contact with water is followed by precipitation of the hydrated phases. The types of hydrates that are formed, based on thermal history, are most commonly divided into two categories: stable and metastable hydrates. The stable hydrates from 5 °C (possibly lower) are C_3AH_6 (a form of hydrogarnet) and γAH_3 (gibbsite); they also have the lowest solubility.[1, 4] The morphology of C_3AH_6 is that of equidimensional crystals, whereas γAH_3 is often referred to as an amorphous gel. However, the formation of the stable hydrates is *usually* preceded by the formation of metastable hydrates: CAH_{10} and C_2AH_8 and other amorphous phases. CAH_{10} is characterized by fine needles while C_2AH_8 is found in hexagonal plates.[4]

At ambient temperatures the metastable hydrates may exist for many years. However, there is an inevitable thermodynamic driving force for conversion. Poorly crystalline or amorphous hydrates may be present in addition to the stable and/or metastable hydrates. It is also important to note that while conversion is occurring both stable and metastable hydrates may exist within the same microstructure. At early ages the AH_3 "gel" may have a composition more closely resembling CAH_{10}.[1] Other research has suggested the presence of amorphous material with Al in fivefold coordination through NMR studies. For example, Kirkpatrick and Cong for the first time showed that at temperatures above 25 °C hydration products of CA contained tetrahedrally coordinated aluminum and, at 4 °C, a possible four or fivefold coordinated Al.[5] Other authors postulate that the induction period may be related to quality and type of alumina in the CAC system.[6]

The main hydration reactions are noted as follows:[1]

$$CA + 10\ H \rightarrow CAH_{10}$$

$$2\ CA + 11\ H \rightarrow C_2AH_8 + AH_3$$

$$3\ CA + 12\ H \rightarrow C_3AH_6 + 2\ AH_3$$

Conversion Reactions

$$2\ CAH_{10} \rightarrow C_2AH_8 + AH_3 + 9\ H$$

$$3\ C_2AH_8 \rightarrow 2\ C_3AH_6 + AH_3 + 9\ H$$

The last two reactions labeled "conversion reactions" are highly dependent upon temperature, moisture state (availability) and w/cm. The reactions presented are for monocalcium aluminate (CA) but may be written similarly for $C_{12}A_7$. At temperatures

less than 10 °C the formation of CAH_{10} is predominant, while between 10 °C and 27 °C CAH_{10} and C_2AH_8 will both form. At higher temperatures CAH_{10} no longer forms and the stable phase of C_3AH_6 occurs early in the processes of hydration. It is claimed that the formation of C_3AH_6 is always preceded by some formation of C_2AH_8, even up to 90 °C. The direct formation of C_3AH_6 from CA can take place after the nucleation of some C_3AH_6.[1] Once nucleation of C_3AH_6 has occurred, further hydration will lead to direct formation of stable hydrates since there is no nucleation barrier to overcome.[4] When temperatures remain above 50 °C, C_3AH_6 rapidly becomes the only hydrated phase. Crystallization of AH_3 gel to gibbsite is highly temperature dependent and is sluggish at ambient temperatures.[1]

A review paper in 2001 by Gessner and Moehmel highlighted some of the most important research to date on calcium aluminate cements.[7] Of particular interest was the characterization of the structure of the crystalline hydration of "CAH_{10}" by Guirado and co-workers. Using XRD powder methods to characterize this hydration product they were able to show that the crystalline part of this first hydrate product may not actually have the literature assumed value of "10 waters", where in fact it is on the order of $CAH_{7.8}$.[8]

The higher calcium-to-alumina ratio in $C_{12}A_7$ favors the formation of C_2AH_8 over CAH_{10}, this combined with the highly exothermic hydration of $C_{12}A_7$ leads to more rapid formation of stable hydrates compared to hydration of CA.[1] Interestingly, at temperatures below 15 °C, despite the presence of small amounts of $C_{12}A_7$; CAH_{10} is the predominant hydrate at these lower temperatures. It is also important to note that the solubility of the hydrates changes greatly with small perturbations in temperature. CAH_{10} is especially sensitive and as the temperature increases up to roughly 27 °C, nucleation of this phase is increasingly disfavored relative to C_2AH_8.[1] As a result, setting time

actually increases as curing temperatures (isothermal) approach 30 °C as observed by Banfill.[9] Bushnell-Watson and Sharp attribute this retardation to the inability of calcium aluminate cement hydrates to form in the range of 25-30 °C. They state that the nucleation of CAH_{10} is no longer thermodynamically favored and that the formation of C_2AH_8 is very slow. Because formation of C_3AH_6 is at least initially preceded by formation of meta-stable hydrates (especially in this temperature range), neither of which can easily form at these temperatures, progression of the hydration reactions for all phases is severely limited.[10] However, Capmas and co-workers found no evidence that C_2AH_8 was difficult to nucleate. They did however conclude that CAH_{10} was difficult to nucleate in these ranges, with nucleation becoming impossible above 29 °C. They postulated that the formation of a gel phase hinders dissolution and precipitation at that temperature. They also noted that commercial CACs which contain varying amounts of $C_{12}A_7$ could explain anomalies in setting time in these systems.[11] Other work by Fryda and co-workers confirmed by differential thermogravimetric analysis (DTA) that the predominant hydrates formed between 36 °C and 64 °C were C_2AH_8 and AH_3. Above 64 °C the predominant hydrate phases were C_3AH_6 and AH_3. Work by these researchers helped to elucidate the profound effect of temperature during curing of CACC and will be discussed in more detail in the section on strength development of CACC.[4]

2.5 SETTING AND STRENGTH DEVELOPMENT

The setting time of CACC (without accelerator and/or other admixtures) is similar to that for OPC in terms of initial set; however the time between initial set and final set for CAC systems is much more rapid. Table 2.3 adapted from Scrivener and Capmas, shows typical initial and final set times for calcium aluminate cement (CAC) pastes (without admixtures e.g.,, accelerator or superplasticizers), rapid-hardening portland cement and ordinary portland cement (OPC) pastes.[1]

Table 2.3: Setting times of CAC and OPC Cement Pastes[1]

	Initial, h:min (SD)	Final, h:min (SD)
Calcium Aluminate Cement	3:55 (±0:35)	4:10 (±0:35)
Rapid-hardening Portland Cement	2:10 (±1:30)	2:50 (±1:40)
Ordinary Portland Cement	3:00 (±1:20)	4:00 (±1:10)

Interestingly for CAC systems there is a decrease in setting time between temperatures of 0 and 10 °C with a steady increase in setting time up to a maximum somewhere in the range of 25 to 30 °C owing to the transition between formation of CAH_{10} and $C_2AH_8 + AH_3$. The temperature at which the maximum setting time occurs depends on the ratio of $C_{12}A_7$/CA in the cement. Setting time then decreases at temperatures above 30 °C. These changes are most readily observed under isothermal curing regimes and in normal concrete these changes may not be observed due to continual temperature rise owing to heat of hydration of the cement.[1] However, because calcium aluminate cement concrete, like ordinary portland cement concrete, is placed in a wide range of ambient temperatures it is probable that during the rapid hydration of CACC a range of hydrates may be formed while the concrete passes through different temperature "thresholds". This plays an important role in determining short and long-term strength and impacts the eventual conversion processes.

Long-term strength development is attributed to formation of C_3AH_6 and gibbsite. The metastable phases of CAH_{10} and C_2AH_8 are of low density but occupy a large volume due to high amounts of combined water. These help occupy much of the space filled by water during early hydration and account for rapid early strength gain. During conversion the overall porosity of the system increases and strength decreases. It is important to keep the w/cm low as this has a profound effect on ultimate strength. The critical w/cm is around 0.35 for formation of stable hydrates in mortars and pastes and corresponds to roughly a 0.40 w/cm for concretes. If the w/cm is kept low, unreacted

cement may be available to combine with released water and a subsequent gain in strength is observed after conversion. Ultimately the long-term converted strength should be used for design of calcium aluminate cement concretes. At an equivalent w/cm, OPCC strength is generally higher than that of CACC after conversion. As a result CACCs are desirable when rapid hardening properties, good resistance to chemical attack and abrasion resistance are desired. It is interesting that the "intrinsic" strength of the stable hydrates may be higher than that of the lower temperature hydrates. However, their inclusion in a hardened matrix with increased porosity leads to lower converted strengths.[1]

2.6 CONVERSION PROCESSES AND CURING REGIMES

The temperature to which CAC concrete is exposed during its lifespan affects the rate of conversion. In relation to the expected lifetime of most applications, the duration of the conversion process is typically short and on the order of 5-10 years. As a result the design strength of CAC concrete must be based on long-term stable (i.e., fully converted) strengths. To this end much work has been carried out to characterize fully-converted strengths, but also to capture the typically high early strengths as the range of strengths a structure may undergo is certainly important for design purposes. The three most common testing curing regimes to characterize strength development in CAC systems are outlined next with specific reference to recent work using CAC formulations most applicable to today's market.

2.6.1 Ambient Temperatures

Curing laboratory concrete in ambient temperatures (e.g.,, 20 ± 3 °C) inside either plastic or cardboard molds will encourage only moderate self-heating of the concrete with temperatures typically not exceeding 40 °C. The resulting microstructure will be

unconverted and strengths will therefore be high. This is, of course, dependent upon the size of sample cast and these values would be for concrete cylinders no greater than 150 mm (diameter) x 300 mm (length). For larger sample sizes higher temperatures and thus higher degrees of conversion may be obtained. The conversion of metastable hydrates to stable hydrates will ultimately pass through a minimum with strength gain thereafter due to continuing hydration of unreacted cement. This type of testing may only represent long-term unconverted strengths experienced in extreme cases. For instance CAC concrete in the UK that was continuously immersed in sea water (average temperature = 8 °C) showed little difference from unconverted strengths after 30 years. For the majority of studies on concretes that have been exposed to temperate climates or laboratory conditions of 18-25 °C show that substantial conversion has occurred after 5-10 years. Effects of conversion on strength may be significant even after as little as one year for these concretes.[1]

2.6.2 38 °C Curing

Significant data exist for curing CAC concrete at 38 °C as this temperature will accelerate formation of stable hydrates. Curing at 38 °C was used by Lafarge in the 1970s and 1980s as a quality control measure. It was found that pre-curing at lower temperatures (20 °C) greatly slowed the rate of conversion. For instance, concrete cured in a 38 °C bath immediately after casting showed a minimum in strength at 5 ± 1 day. However, if the same concrete mixture was cured at 18 °C for 1 day and then placed at 38 °C, the minimum in strength occurred after 3 months. The immediate exposure to 38 °C was thought to give the most conservative approach to design and qualification of mixtures for commercial application.[1, 2]

Current recommended practice is to immerse the sealed concrete, immediately after casting, into a water bath maintained at 38 °C. Strength is periodically monitored

over the next 5 days or until conversion has occurred. It is especially important to measure strength at 1, 3 and 5 days after casting for appropriate strength benchmarks. The minimum strength (converted strength) corresponds to a conservative design approach for that same mixture placed into service. However, there have recently been efforts made to more accurately cure concrete in a regime more closely resembling that of the field. In larger concrete elements rapid hydration of CACC leads to heat gains which may be much higher than 38 °C and therefore isothermal curing at this temperature may not accurately reflect true in-situ performance.[4]

2.6.3 Higher Temperatures

In relatively thick sections (thickness > 200 mm), the self-heating effects of CAC hydration may result in a temperature rise in excess of 80 °C. Depending on the length of time that the concrete remains at high temperature formation of stable hydrates may occur within the first 24 hours. While metastable hydrates will always form first, conversion can occur very rapidly during hardening in thicker sections or in CAC concrete applications which remain at high temperature for long enough duration.

2.6.4 Other Methods

Current practice to evaluate how conversion affects strength by immersing samples at 38 °C immediately after casting was discussed in-depth in section 2.6.2; Fryda and co-workers followed this recommended practice referred to as method (a) as well as two other testing methods with micro-concrete (essentially a CAC mortar).[4] The second method (b) involved casting partially insulated samples to encourage self-heating with a maximum temperature rise of ~50 °C during the first 8 hours after casting. These specimens were then demolded, coated with plastic film and placed in water at 38 °C up to 24 hours. In the third method (c) samples were fully insulated and a maximum

temperature of ~ 100 °C was attained after about 6 hours. At 8 hours after casting the samples were coated with plastic film and placed in water at 38 °C. Then at 24 hours samples in all methods were demolded or the protective plastic film was removed and placed back into water at 38 °C. Strength was monitored and reported up to 14 days. Figure 2.1 shows the compressive strength development of CAC micro-concrete in these methods to aid in discussion of results.

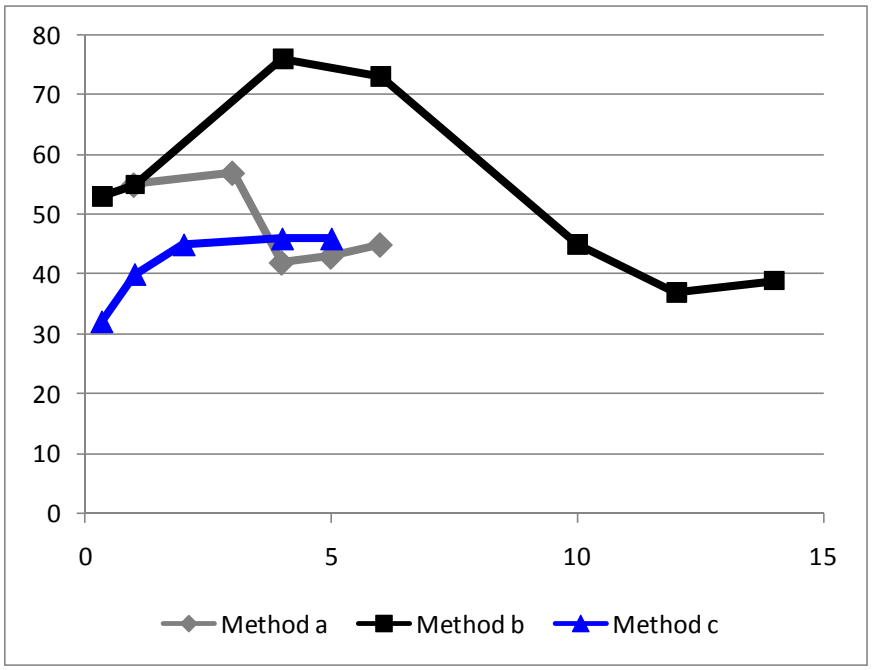

Figure 2.1: Impact of self heating on conversion, adapted from Fryda et al., 2001[4]

For curve (a) (micro-concrete immersed immediately at 38 °C), a minimum in strength occurs approximately four days after casting. In contrast to this, the minimum strength for curve (b) - (maximum temperature of ~50 °C in the first 8 hours) occurs at twelve days. The micro-concrete shown in curve (c) (maximum temperature of ~100 °C in the first 8 hours) shows no minimum in strength and only an increase due to continued

hydration after rapid initial conversion. What is most important to observe is that the micro-concrete in method (b) only experienced temperatures above 38 °C for about 1 hour of the first 8 hours with a maximum temperature of ~ 50 °C.[4] Therefore, the thermal activation (one driving force) of conversion was not imposed on this concrete for a duration long enough to enable complete conversion. As a result the predominant hydrates formed were metastable (likely lesser amounts of CAH_{10} and greater amounts of C_2AH_8 due to elevated with only minor amounts of C_3AH_6. After exposure to 38 °C and water, the conversion process occurred more slowly (compared to method (a)) owing to the slow nucleation of C_3AH_6 and the presence of more metastable phase necessary to convert than in method a. In contrast micro-concrete in method a was subjected to 38 °C water immediately after casting and remained there for the duration of curing and testing period. While C_2AH_8 was likely formed initially (possibly with small amounts of CAH_{10}) continued exposure to 38 °C favored more rapid formation of C_3AH_6 in a concrete where temperature remained high, particularly at early-age, compared to method (b). It may also be that the process of converting from CAH_{10} to stable hydrates (potentially going through C_2AH_8 as an intermediary step) is a longer process for any CAC concrete where temperatures have not remained high enough during initial curing (e.g., less than 24 hours after casting in). This would be in contrast to converting from C_2AH_8 to C_3AH_6 at a constant higher temperature (e.g.,, 38 °C). Micro-concrete in method (c) experienced much higher temperatures initially and thus formation of C_3AH_6 - occurred much earlier in the lifetime of these samples as evidenced by the minimum strength just above 30 MPa at one day after casting followed by subsequent strength gain thereafter.[4]

These data demonstrate the profound effect that temperature has on microstructural formation, mechanical property development and conversion for CAC

concrete which is essential to understanding much of the research presented in this dissertation. Small deviations in temperature within the first 12 (and possibly 24 hours) after casting can have a significant effect on conversion processes.

Method (b) is likely the most representative of what actually occurs in the majority of field applications of CAC. It is important to note that although converted strengths in method (a) and (b) are similar (roughly 40 MPa), there is an almost 20 MPa difference in maximum strength, with the highest maximum strength occurring in method (b) after 4 days.[4] This is important as an in-service concrete would likely experience a more significant microstructural variation due to conversion than laboratory concrete cured at 38 °C. The result may in fact be a microstructural gradient that develops as a result of temperature rise and fall in a hydrating element. In contrast to ordinary portland cement concrete, where the hottest part of the element develops strength the most rapidly, the hottest portion of a CAC concrete element may in fact be the weakest (due to conversion). This has important implications for volume change, creep and strength loss (design strength parameters).

Fryda and co-workers also developed a computer model to simulate self-heating and to aid in prediction of the hydrate assemblages formed.[4] This predictive model using various insulation conditions, heat flux parameters and equations combined with semi-adiabatic calorimetry provided good prediction for self-heating when compared to laboratory values. One of the other important findings from this study was that the immersion of concrete immediately after casting in a 38 °C bath provided minimum strength prediction that correlated well with their predicted results and is thus confirmed as a useful predictive tool.[4]

2.6.5 Other Factors Influencing Conversion

The rate of conversion is significantly reduced at low relative humidities. Additionally, aggregate type may have an effect on conversion. Pure or relatively pure limestones may exhibit strengths about 20% higher than CAC concretes containing silico-calcareous aggregates. Limestones may effectively "poison" the conversion process.[1] In the presence of limestone, C_2AH_8 may transform into $C_4A(CaCO_3)H_{11}$ (monocarboaluminate). This phase is stable below about 60 °C and its density is similar to that of C_2AH_8. Therefore, even with an accelerated test at 38°C, the presence of reactive limestone may lead to the observation that there is no strength reduction.[12]

Purely siliceous aggregate sources may exhibit strengths about 20% lower than CAC concretes with silico-calcareous aggregates upon conversion. Some of these variations in strength may be due to the rate and extent of absorption of water by the aggregates and also due to the paste/aggregate bond. Limestone aggregates with high absorption capacities may effectively lower the w/cm ratio (free water) resulting in an inherently higher strength concrete, more by coincidence than by any real interaction between the aggregate and the paste matrix. The use of synthetic aggregates with compositions close to that of CACs will result in very high strengths. It is important to avoid aggregates with soluble alkalis as alkali hydrolysis may occur.[1]

Provided that the w/cm remains at or below 0.40, the stable converted strengths are typically satisfactory for typical CAC usage, predominantly flat-work including pavements, bridge-deck overlays, sidewalks, etc.[1] However, it is best to actually measure strength and converted strength on the mixture design for intended use to ensure it meets the requirements for any CAC concrete placed into service. Curing concretes in a water bath at 38 °C will likely provide a good prediction of minimum in-situ strength. It may also be useful to cure the concrete under a method that will best replicate in-situ

hydration temperatures. In this way the advantages of CAC concrete associated with rapid setting and strength gain may be fully realized.

2.6.6 Conversion Inhibitors

While inhibitors to eliminate or reduce conversion may be available it is likely that these products will only reduce the rate of conversion. Studies do show that above 38 °C C_3AH_6 may still form very rapidly. These systems also show a rate of strength development that is similar to a much cheaper system incorporating OPC. While addition of sodium salts was mentioned earlier to improve strength development, their incorporation may lead to alkaline hydrolysis in the long-term.[1] As outlined in section 2.6.5 it is best to test the CAC concrete to ensure it will meet minimum design requirements for a particular job so that it may be used to its fullest extent.[1]

2.6.7 Volume Change

There exists a critical w/cm for the complete hydration of the various reaction products dependent upon temperature and composition of cement. For a standard grade CAC with roughly 50% CA and 30% ferrite at low temperatures (predominant hydrate – CAH_{10}) the critical w/cm is roughly 0.7. At higher temperatures where C_3AH_6 and AH_3 are formed the critical w/cm is around 0.35.[1]

In terms of relative volumes of anhydrous materials and their subsequent hydrates the following depicts the relationship:

$$V_{anhydrous} + V_{water} > V_{hydrates} > V_{anhydrous}$$

The overall decrease in volume or "chemical shrinkage" for the hydration of monocalcium aluminate is around 16% for the formation of CAH_{10} and around 25% for the formation of C_3AH_6 and AH_3. This results in an average volume decrease for standard grade CACs of 10-12%, which is on the order of that for portland cements. This

does not correspond, however, to the macroscopic shrinkage of concrete which is on the order of two magnitudes lower. This is similar to macroscopic shrinkage of OPCC.[1]

The volume change during conversion of metastable hydrates to stable hydrates may also be calculated.

$$3\ CAH_{10} \longrightarrow C_3AH_6 + 2\ AH_3 + 18\ H \qquad 2.1$$

$$3\ C_2AH_8 \longrightarrow 2\ C_3AH_6 + AH_3 + 9\ H \qquad 2.2$$

In equation 2.1 the volume of solids as a result of conversion is reduced to just about 1/2 of the original metastable product. In equation 2.2 the resulting volume is ~2/3 of the original volume. It is important to note that during conversion water is released which may then be available to react with anhydrous cement which may lead to a further increase in solid volume. It is more straightforward to consider long-term volume changes in terms of direct reaction to C_3AH_6 and AH_3.[1]

If one actually does consider the conversion reactions by taking into account the release of water, interesting results are obtained. Table 2.4 summarizes work previously presented as well as the calculations to show the change in hydrate volume including the release of water.[1, 4]

Table 2.4: Theoretical volume change in calcium aluminate cement systems

Hydration Reactions	CA to CAH_{10}	CA to C_2AH_8	CA to C_3AH_6
Δ V Hydrates	-15.5%	-18.23%	-25.3%
Conversion Reactions	CAH_{10} to C_2AH_8	C_2AH_8 to C_3AH_6	CAH_{10} to C_3AH_6
Δ V Hydrates	-36.8%	-33.7%	-52.5%
Δ V Hydrates + Water	+4.4%	-4.2%	+2.4%

The formation of any of the hydrate phases from unreacted CA would predict chemical shrinkage. The overall volume change taking into account the release of water, only shows a prediction of shrinkage by 4.2% in the case of C_2AH_8 converting to C_3AH_6. However, when CAH_{10} converts to C_2AH_8 or CAH_{10} converts to C_3AH_6 volume increases of 4.4% and 2.4%, respectively would be expected. While this is a very slight increase in volume it more accurately represents what is occurring during conversion and this will be looked at more in-depth within chapters 5 and 6.

2.6.8 Drying Shrinkage

Macroscopic shrinkage of calcium aluminate cement concretes in air (i.e. drying shrinkage) is similar to that of ordinary portland cement concretes; however, it occurs much more rapidly. Nearly half of the total drying shrinkage will occur within one day for CACC compared to 7 days for OPCC (Scrivener and Capmas, 1998). As a result, it has been proposed that shrinkage measurements for CACC begin at 6 hours as compared to 24 hours for OPCC. During conversion no macroscopic change in dimension is observed.[1] However, this may be a result of conversion occurring over a relatively long-duration compared to macroscopic volume change associated with conversion occurring on a shorter time scale (e.g., within the first 24 hours). Further detail regarding macroscopic dimension change of CAC systems is discussed in further depth chapters 6, 7 and 8. Due to apparent rapid shrinkage of CACCs; it may be recommended to keep the bay size of unreinforced slabs to approximately 3 m square. Formation of stable hydrates through heating will result in a concrete less susceptible to cracking.[1] Other volume change mechanisms such as chemical and autogenous will be discussed in further depth within the dissertation (chapters 5, 6 and 7) as very little prior work exists for inclusion in this literature review.

2.7 HYDRATES FORMED IN THE PRESENCE OF OTHER MATERIALS

2.7.1 Silica

The main hydrate formed in the presence of siliceous phases is C_2ASH_8. This phase is often called gehlenite hydrate or strätlingite. It is an AFm phase closely related to C_2AH_8. Strätlingite is stable in comparison at ambient temperatures. This may be a result of the hydration of C_2S in the alumina-rich solution formed by the cement. It may also form due to interaction with certain supplementary cementing materials (SCMs) such as ground granulated blast furnace slag and silica fume. The hydrogarnet phase (C_3AH_6) may also contain significant amounts of silica existing in solid solution.[1]

2.7.2 Ferrites

At temperatures around 20 °C the reaction of ferrite solid solution (F_{ss}) is negligible at early ages. As temperatures increase to 30-38 °C, over 80% of this phase may react after several months. The influence of temperature was confirmed by research performed on Ciment Fondu by Scrivener and Houghton as reported by Scrivener and Capmas.[1] They saw little evidence of reaction at 20-40 °C, whereas at 70-90 °C substantial reaction had occurred even after several hours. The extent to which the iron can enter the hydrogarnet phase is controversial and may be influenced by silica presence.[1]

2.7.3 Slag

Slag as a replacement for CAC up to 50% and for curing temperatures up to 40 °C results in formation of C_2ASH_8 as the predominant phase (strätlingite), although significant amounts of C_3AH_6 still form at temperatures greater than 40 °C. Strength of 50/50 blends of slag and CAC are on the order of half that of their 100% CAC counterparts, this is *without* a minimum in strength due to conversion. Work by Ding, Fu

and Beaudoin, as reported by Scrivener and Capmas, investigated a wide range of SCMs at temperatures up to 38 °C and found that strätlingite was formed in all cases. They also saw that initial strengths were lower compared to pure CAC systems. However, additions of sodium salts, which increase pH, increased the rate of formation of strätlingite and strength gain.[1]

2.7.4 CAC + OPC

The replacement of CAC by OPC may result in rapid or even flash set over a wide range of replacement levels (nominally 20 up to 90%). This is highly dependent on the composition of the portland cement and the combined amounts of each respective material. This rapid or flash set may be due to the uncontrolled reaction of C_3A in the OPC after depletion of sulfate by the reaction of OPC with CAC. The early formation of ettringite and acceleration of the reaction of CAC may also be "co-conspirators". Hydrates that form vary depending on the relative amounts of CAC or OPC. When amounts of OPC are much greater than CAC predominant hydrates are C-S-H and CH. When amounts of CAC are much greater than OPC, C_2AH_8 and CAH_{10} are formed (at ambient temperatures). In between these ranges a large and complex variation in the type of hydrates formed is found.[1]

2.7.5 CAC + Calcium Sulfate

Normal conversion reactions in these systems do not occur. The first product usually formed is ettringite ($C_3A(C\overline{S})_3H_{32}$). The ability of ettringite to bind large amounts of water can be advantageous to produce rapid drying and rapid hardening concretes. Further development of hydrates depends on the mechanical properties of the relative amounts of the system components and the type of sulfate used (hemihydrate, gypsum or anhydrite).[1]

2.7.6 Admixtures

In general many admixtures including air entraining agents, superplasticizers, retarders and accelerators are used with calcium aluminate cement concretes. The most common type of accelerator for CAC systems are lithium salt-based. Incorporation of lithium salt additives is thought to precipitate a lithium aluminate hydrate which can act as a heterogeneous nucleation substrate. Common types of retarders for CAC include hydroxycarboxylic acids (citric, tartaric and gluconic). Superplasticizers used for CAC may include sodium nitrate and sodium citrate and essentially function more as retarders than as superplastisizers. The primary function of a superplasticizer in CACC is to retain workability during placement. Typically an accelerator and superplastisizer are used in conjunction with trial batching done to ensure a balance between desired setting time and placeability and finishability for a particular CAC application. Newer, proprietary formulations based on polycarboxylate technology are currently used. The disodium salt of ethylenediamene tetraacetic acid (EDTA) has strong fluidifying effects and while it is also a retarder, its effects are less marked than sodium citrate.[1] Air entraining agents based on vinsol resins are not as effective in CACs as in OPCs.

However, the reaction with admixtures specifically designed for portland cement concretes may not produce the desired results when incorporated in calcium aluminate cement systems. Therefore, procurement and knowledge of products specifically designed for CACC must be sought and utilized.

2.7.7 Heat of hydration of CACC

While the total heat evolved during curing of calcium aluminate cement concretes is on the same order of that for ordinary portland cement systems, its evolution occurs on a much more rapid time scale. Total heats evolved for CACC are typically on the order

of 500 kJ/kg and this may be reached within 5-7 days of curing; whereas the same values for OPC systems may take more than 28 days to reach total evolutions of ~400 kJ/kg.[1]

2.8 DURABILITY OF CAC CONCRETE

The durability of CAC concrete is generally thought to be very high. However, the construction of a quality concrete, with a low w/cm ratio, low porosity (<12%) and good finishing practices are all precursors to producing a durable material. Originally CACCs were developed for good resistance to sulfate attack and in fact a large database exists on the successful performance of these concretes in such environments as well as CACCs subjected to other deleterious forms of attack.

A possible reason for the durability of CAC concretes may be the formation of a dense outer-layer with low porosity that limits or greatly reduces the ingress of aggressive agents. While it may be thought that this outer layer could contain predominantly metastable hydrates, and that through eventual conversion this seemingly dense microstructure may be lost, investigation into 60-year-old concrete subjected to seawater showed the same formation of a dense outer-layer.[1]

2.9 GENERAL PRACTICES

Calcium aluminate cement concretes should be made with a w/cm of 0.40 or lower and a minimum cement content of 400 kg/m^3. One practice that has shown promise is to demold these concretes as soon as possible (after final set) and to apply water to the surface continuously.[1] This has been done in the past to avoid surface dusting due to dehydration. Interestingly, hydration in the interior sections (at higher temperatures) may lead to more rapid development of stable phases, while the exterior portions of the same concrete may contain the metastable hydrates and this practice of applying water at the surface continuously may in fact promote the formation of

metastable hydrates through artificial cooling of a several millimeter thick layer (skin) of the concrete.[1]

2.10 CRACKING IN OPCC AND CACC SYSTEMS

A more thorough understanding of CAC systems has developed in recent years and it has thus lead to more frequent usage of this material. However, there have been reports in the field of instances of early-age cracking (e.g.,, in the first 24 hours).[13] While a large database of research exists detailing the intricacies of cracking in ordinary portland cement concrete, there exists relatively little knowledge behind calcium aluminate cement concrete. Subsequently a major focus of the current research program will be to delve into the issues associated with volume change and cracking risk in such systems. While it is expected that there will be some synergy between cracking phenomena in OPCC systems and CACC systems it is also realized that the hydration mechanisms and products formed in the two systems are vastly different. Certainly the large amount of heat generated in such a short time period for CACC systems suggests a potential risk of thermal cracking. Furthermore, rapid hydration in these systems may lead to significantly more drying shrinkage at early ages when compared to OPCC systems. It is likely that there are also other types of volume change (chemical shrinkage, autogenous deformation, creep etc.) that may lead to cracking susceptibility with calcium aluminate cement concretes. In CACC's favor, rapid strength gain may help to provide earlier resistance to cracking where tensile strength is gained at a much more rapid rate than in OPCC. As a result it may be inherently more resistant to cracking than OPCC for shrinkage related volume change phenomena. A brief synopsis of cracking and the current knowledge for OPCC will be presented herein. Limited examples, extrapolation and knowledge of calcium aluminate cement concrete will be included.

While concrete is a material traditionally thought to be very strong in compression, it is relatively weak in tension. In simple terms cracking occurs when the tensile stress exerted on the concrete exceeds its tensile strength. This is, however, a gross simplification of the complex processes occurring, which may lead to cracking. Since cracking may be structurally related there may be as many reasons for cracking as there are structures. Other reasons for cracking may be due to deleterious internal reactions such as sulfate attack, alkali-silica reaction, freezing and thawing cycles or corrosion. For CACC, alkali-silica reaction sulfate attack may be considered less probable reasons for cracking than that for OPCC. The lower pH of the pore solution inside CACC (pH~10 as reported by Scrivener and Capmas[1]), precludes the formation of alkali-silica reaction.[1] However, it is foreseeable that externally applied chemicals such as deicing salts which may lead to elevated pH could provide conditions favorable for ASR, however no testing to date has been done to ascertain the susceptibility of CACC to this type of attack.

While CACC is traditionally thought of as a more durable material, its misuse may still lead to durability problems which may exacerbate or even initiate cracking in such systems. Certainly external effects such as structural impact and earthquakes may also lead to cracking. One of the largest reasons linked to cracking in CACC systems may be linked to shrinkage or development of thermal stresses. Figure 2.2 shows a flow-chart for potential cracking in OPC concrete; in fact many of these may also be applicable to CACC.

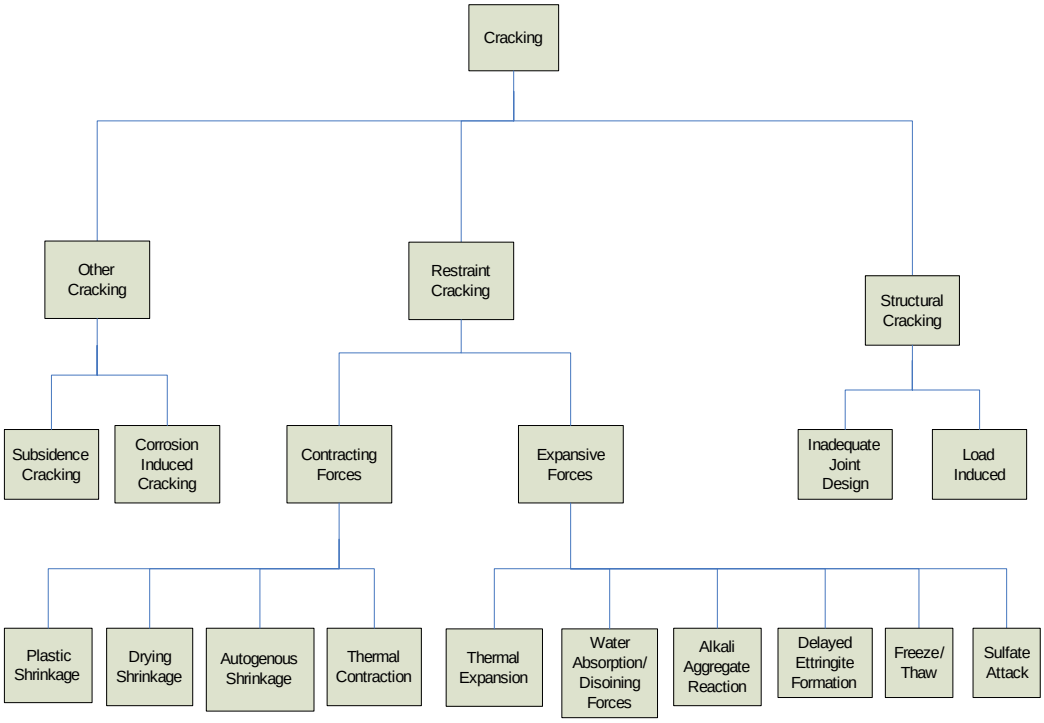

Figure 2.2: Flow chart for causes of cracking in OPCC from Riding and Poole[14]

Several codes exist for designing reinforced concrete structures; in the U.S. the primary source is ACI 318.[15] Other sources regarding cracking and its prevention in concrete structures: ACI 224R-01 (*Control of Cracking in Concrete Structures*) and ACI 209R (*Prediction of Creep, Shrinkage, and Temperature Effects in Concrete Structures*).[16, 17] A full discussion of design codes is beyond the scope of this literature review. However, references such as ACI 209R may provide valuable insight into the mechanisms behind cracking in concrete.

2.11 DISTRESS MECHANISMS LEADING TO CRACKING

2.11.1 Restraint

Cracking may be the first outward manifestation of distress in a concrete member. In a completely unrestrained state concrete will shrink and swell and presumably lead to no cracking as the volume changes. In actuality most, if not all concrete is restrained in some manner. Structural members may be anchored in footings or slabs providing restraint. Pavement sections are restrained by adjoining pavement sections and more importantly by the friction from the subbase on which they are placed. As the concrete begins to change in volume from any number of reasons, the present restraint causes a rise in stress in the affected concrete. When this stress exceeds the available strength, the concrete will crack. Expanding concrete will produce a compressive stress, when restrained, whereas shrinkage results in the development of tensile stresses. Additionally internal restraint may occur due to differential cooling, different coefficients of thermal expansion between different materials (especially aggregates), differential drying shrinkage (surface to bulk effects) or creep in the affected member.[14]

Quantification of this stress development is complicated by different parts of the concrete member or element experiencing different levels of restraint and response to the underlying mechanisms leading to cracking. While equations to deal with these effects are readily available for ordinary portland cement concrete mixtures, the same equations may not apply for calcium aluminate cement systems. Extensive testing on modulus, creep, long-term creep etc, would need to be performed to begin to develop the necessary information to apply to CACC. Gajda and McGee investigated the changes in elastic modulus, shear modulus and Poisson's ratio at elevated temperatures for CACC, concluding that physical properties are highly temperature dependent and further complicated by the hydration and dehydration reactions in CACC systems.[18]

2.11.2 Temperature

The time and temperature history of a concrete element may be the two most influential factors affecting cement hydration and further development of the mechanical properties of concrete. Cement hydration is an exothermic process that results in temperature rise in the concrete specimen and subsequent hardening. In calcium aluminate cement concrete this exothermic process occurs on a much shorter time scale (~1 day) than for ordinary portland cement concrete (~28 days).

The Arrhenius theory for rate processes is often the preferred equation for use in chemical kinetics. It is the most commonly used relationship to characterize the temperature sensitivity of portland cement.[14] Estimation of temperature in concrete is a complex mathematical process complicated by its dependency on a host of factors not limited to: environmental surrounding (weather, sunlight exposure, insulation from surroundings), construction environment (formwork, time of form removal, member/element size) and concrete materials properties (fresh temperature, admixtures, aggregate, etc.).[14] Compared to OPC systems changes in all of these variables may have much more dramatic effects in CACC systems due to the sensitivity of the mixture and the different types of hydrates that form based on the concrete temperature history.

2.11.3 Thermal Effects

In CACC systems it is reasonable to expect that the large amounts of heat generated during hydration may be one of the most influential factors affecting early-age volume change. However, other mechanisms are likely to be at least partially responsible for early-age volume change. In fact many of these realized properties may be a direct result of the temperature gain seen in such systems. Usually an increase in temperature

leads to expansion, whereas a decrease in temperature leads to contraction. It is these changes that may be more pronounced in CAC concrete at early ages when hydration produces temperatures greater than traditional OPC concrete. Researchers have suggested the coefficient of thermal expansion (CTE), which may help to partly explain tendencies toward cracking, may be significantly different in early age concrete than in concrete in the hardened state. Certainly with CACC the different types of hydrates formed depending on temperature may have inherently different CTEs that could lead to or exacerbate cracking tendencies.

2.11.4 Drying Shrinkage, Creep, Relaxation

The underlying mechanisms for drying shrinkage, creep and stress relaxation, are essentially related to the movement of water in and out of the pore structure of a concrete matrix. Processes such as diffusion, capillary suction, surface tension and disjoining pressures are all a result of water movement. Changes in the pore structure of CACC systems, especially during the conversion from metastable hydrates to stable hydrates, may make these systems more susceptible to such phenomena. It is important to note that the pore structure of CAC systems after conversion is much coarser than the pore structure for a mature OPC concrete, thus making extrapolation of existing prediction models for drying shrinkage, creep and stress relaxation to CAC result in inaccurate prediction of such phenomena.

Loss of water from concrete occurs when concrete is stored in unsaturated air. Drying shrinkage results from a loss of adsorbed water on the surface of cement hydrates. Loss of "free water" and water from capillary pores greater than 50 nm is not associated with drying shrinkage. It is possible also that shrinkage is related to the removal of intercrystalline water and or adsorbed water from the hydrated cement paste (especially in the case of calcium silicate hydrate (C-S-H)). Pastes made with both ordinary portland

cement and high-alumina cement, and also pure calcium monoaluminate exhibit essentially similar shrinkage.[19] While this is generally thought to be more of a long-term process in mature concrete, a form of this type of drying may occur during the rapid hydration of CACC systems. It is noted that during curing it is important to keep the surface wet to prevent dusting. This "dusting" of the surface may be due to dehydration from the rapid consumption of water into the rapidly forming hydration products within the bulk of the concrete. While this may be more traditionally thought of as autogenous shrinkage there is nonetheless, sacrificial drying at the surface of the concrete for interior bulk hydration due to rapid hydration in CAC systems.

Creep is also related to movement of water within the pore structure of concrete. While certain applied loads create instantaneous deformation, their removal within the elastic range will result in theoretical full recovery of the element. However, in the case of creep a continuously applied load will result in deformation that for a large part is irrecoverable. Creep occurs over a relatively slow timescale (months to years) for OPC. With CAC, a microstructural change can occur rapidly due to conversion with temperature and could lead to more short-term creep. Under constant load water will move within the capillary and gel pores of the concrete microstructure. Water may move due to applied loads and/or due to drying forces. Therefore two types of creep are further delineated: basic creep and drying creep. Basic creep will only occur due to applied external loading whereas drying creep occurs as a result of moisture loss. As moisture moves from certain capillary pores to and/or from gel pores and visa versa the resulting void may be such that the force exerted by the water (surface tension) is overcome and these pores actually close, resulting in a local densification of the microstructure. Over the long-term this will eventually lead to deformation of the element.[19]

Relaxation is often related to creep and results from a reduction in stress over time. Similar equations may be used to describe both phenomena. Figure 2.3 shows a graphical description of relaxation. Accurate modeling of creep and relaxation requires extensive knowledge of concrete strength and maturity. Creep in mature concretes differs significantly from creep in early age concrete.[14]

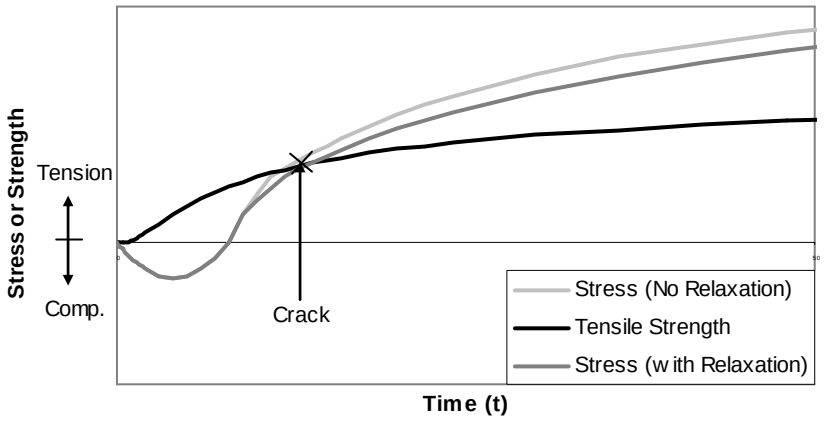

Figure 2.3: Reduction in concrete stress due to relaxation, adapted from Riding and Poole[14]

2.11.5 Plastic Shrinkage

While concrete is still in the fresh or "plastic" state a form of shrinkage related to moisture loss, specifically in the surface layer is referred to as plastic shrinkage. Evaporation at the surface results in loss of volume in the mortar-rich upper layer of concrete. Additionally, bleed water that rises to the surface during finishing to replace lost water may help to protect against cracking in the surface due to plastic shrinkage. When the cumulative evaporation exceeds the cumulative bleeding, cracking may occur. This may allow the evaporation rate to take over in the battle between bleeding and loss of moisture, resulting in increased susceptibility to cracking. The bleeding rate may be

reduced with additions of certain SCMs, specifically silica fume. Additionally, finishing options may affect plastic shrinkage cracking. Increasing the aggregate content and decreasing paste content generally leads to a reduction in plastic shrinkage cracking.[20] However, due to current recommendations regarding minimum cement contents, lowering paste volume may be challenging with CACC.

2.11.6 Autogenous Shrinkage

Internal self-desiccation, which results in autogenous shrinkage of concrete, combined with thermal deformation is a driving force behind cracking in concrete structures.[21] At high w/cm (water-to-cement ratio) this type of shrinkage is generally not considered problematic. It is usually associated with concretes having a w/cm less than 0.40.[22] As a result of hydration throughout the lifespan of concrete a chemical shrinkage may occur due to densification of the microstructure. This may occur in CACC when the metastable hydrates proceed through conversion and release chemically combined water which is then free to react with anhydrous cement grains resulting in further hydration. At higher w/cm free water is available for further hydration. However, as the w/cm is lowered, solution from smaller and smaller pores is accessed providing a threshold limit to the w/cm above which autogenous shrinkage will not occur. Autogenous shrinkage may be exacerbated by the incorporation of SCMs such as silica fume which may result in a more refined pore structure, thus making the concrete more susceptible to this type of shrinkage. Additionally, it is likely that that calcium hydroxide crystals restrain shrinkage and when they are consumed in the pozzolanic reaction with silica fume (to form C-S-H) they are no longer able to provide restraint to shrinkage.[23] While the hydrates for CAC are vastly different from OPC, there may be similar intrinsic differences in the amount of restraint provided based on the hydration products formed.

Regardless of the mechanism of shrinkage, concrete at early ages is more susceptible to autogenous shrinkage due to the lack of tensile strength developed.

2.11.7 Cracking Prevention

Current methods to prevent cracking in ordinary portland cement concrete are well-known and often used, however their application may not transfer directly to calcium aluminate cements. The overall key to eliminating cracks in any concrete is to provide good curing and create low elastic modulus, low coefficient of thermal expansion, low heat generation, and high creep materials. In addition, the relevant causes of shrinkage must be assessed and subsequently mitigated to produce crack-free concrete. Good curing practices to eliminate loss of moisture from evaporation and to produce the densest possible microstructure are likely applicable to CACC. Plastic shrinkage cracking may be avoided by monitoring evaporation rates during curing and providing liquid evaporative retarders or foggers. The addition of fibers may also be very beneficial in the case of CACC to provide increased early age tensile strength. Adding excess water to aid in finishing should be avoided as this creates a locally higher w/cm and may exacerbate plastic shrinkage cracking. Internal curing may be accomplished by providing an internal supply of moisture that can be accessed past the phases of initial curing. However, high heats attained in CACC systems may make this approach problematic as the methods used to provide internal curing (e.g., polymers) may degrade under higher heat applications.

One of the most viable and common ways to avoid issues with thermal-induced stresses and subsequent cracking is to use low heat generating materials. This is clearly not an option with CACC and limiting early temperatures may delay setting/hydration and more importantly strength gain, thereby eliminating most of the major benefits of

CACC. There is likely a center ground that can be reached between temperature generation, benefits of early strength gain, mixture proportioning and design, and producing the desired hydrates to take full advantage of calcium aluminate cement concretes while still providing a crack-free concrete.

2.12 CRACKING TEST METHODS

2.12.1 Ring Tests

In 1942 Carlson developed the shrinkage ring test to investigate the effects of concrete curing on its extensibility. Originally it was only used as a qualitative measure with a longer time to cracking indicating a mix less prone to cracking.[24] The current version of this test has been adopted by both AASHTO and more recently in ASTM in 2004.[25, 26] There are small differences between the test methods depending on the specifying agency. It is claimed that these devices can measure the cracking sensitivity of concrete due to drying and autogenous shrinkage; the test method also claims it can be used for thermal cracking due to heat of hydration. Due to the small size and lack of insulation it is not thought this will give very much useful data related to thermal effects in OPC systems.[14] However, in CACC this may not be an issue. Certainly additional modifications to the test to either encourage self-heating or maintain isothermal conditions could be made to potentially qualify this as a valid test option.

In theory the steel shrinkage ring around which fresh concrete is cast provides restraint for the concrete. The strain in the inner steel ring is measured with surface mounted strain gages. Once the specimen is demolded it is sealed on the top surface so that drying is only allowed in one direction. It is then placed in a temperature and humidity controlled environment. When the specimen cracks the stress is relieved in the

concrete and the strain in the steel ring will decrease significantly. The stress rate can be calculated based on the strain rate in the steel.

ASTM C 1581 utilizes a ring with a concrete specimen measuring 38 mm thick which subsequently limits aggregate size in the test to 12.5 mm. On the other hand the AASHTO version of the test (AASHTO PP34-98) uses a 76.2 mm thick specimen. While the thinner specimen in ASTM C 1581 dries more quickly and cracks sooner, the larger specimen size in the AASHTO version may provide more reliable results due to greater heat generation and the larger specimen size.[25, 26]

2.12.2 ASTM C 157

Drying shrinkage may be characterized utilizing ASTM C 157. This test is performed on concrete prisms measuring 76 x 76 with a 285 mm length. Two metal reference studs are cast into the ends of the prisms to allow for measurement. One day after casting the prisms are demolded, measured and placed in a lime-water bath at 23 ± 2 °C. After a 28-day curing period the prisms are removed, measured for initial length and placed in a temperature and humidity controlled humidity room at 23 ± 2 °C and a relative humidity of 50 ± 4%. As the prisms are exposed to the lower humidity of this environment they begin to shrink. The shrinkage is measured daily for one week, then once a week for one month and at monthly intervals thereafter. Three prisms are traditionally cast for each mixture.[27] Similar tests have been used for CACC, however due to the interest in early age properties, prisms are often measured beginning at 6 hours after casting.[1]

2.12.3 Rigid Cracking Frame

Problems associated with cracking on the Salzburg-Vienna (Austria) Autobahn prompted the development of a cracking frame at the Institute of Building Materials,

Munich Technical University.[28] Figure 2.4 shows a schematic of the rigid cracking frame.

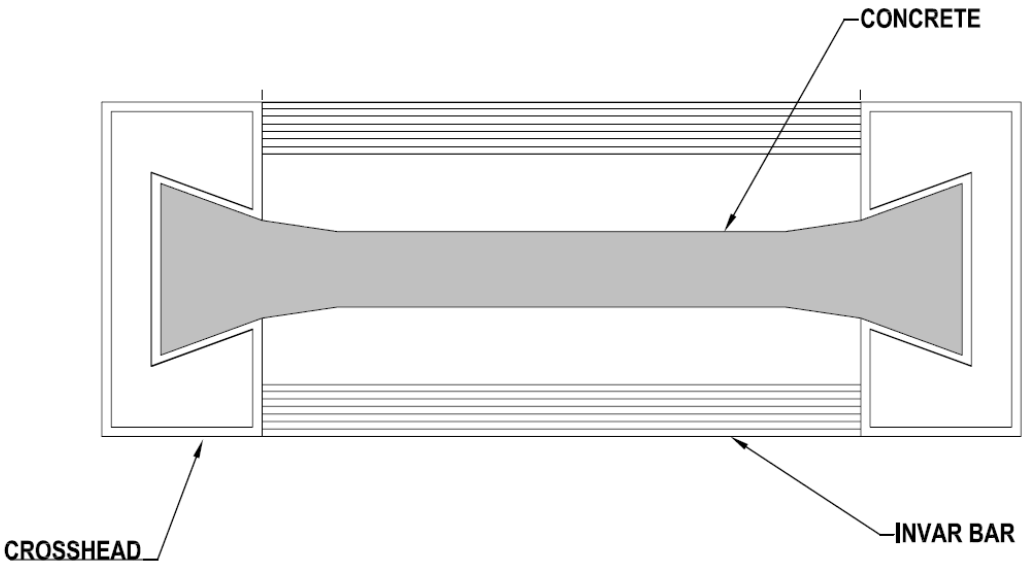

Figure 2.4: Schematic of Rigid Cracking Frame

In contrast to other tests, the cracking frame combines measurements of thermal effects, autogenous shrinkage, creep, relaxation, strength and modulus development (all from time of initial placement) into one test. The stress in the concrete specimen is measured over time throughout the duration of the test. The specimen is cast into the frame and therefore measurement begins immediately. Two large steel crossheads hold the ends of the beam. Stress is also uniform over the cross-section of the specimen. Once a crack forms the stress drops immediately. The concrete in the frame is restrained at about 80%, which is not theoretically ideal, but practically in line with restraint amounts seen in real structures. The specimen is also temperature controlled and insulated by formwork with pipes that allow temperature-controlled liquid to be

circulated completely around the specimen. This would allow for the test to be run at various isothermal conditions to eliminate temperature effects if so desired. Two long bars of Invar steel (DN 17 007, code no. 1.3912) connect the crossheads. As the bars deform with the movement of the concrete specimen, strain is subsequently measured. Through knowledge of the steel properties and strain measurements the stress in the concrete can be calculated.[14]

The test is usually run for five days. If at this point the concrete is not cracked, water is run through the frame and the temperature is reduced at a rate of 1 °C/hour until it cracks. The temperature at which the specimen cracks is referred to as the cracking temperature. Lower cracking temperatures indicate a lower risk of cracking in the field. The overall approach to using rigid cracking frames has been advanced in recent years, and the data generated have been used to model and predict early-age cracking in mass concrete elements.[29]

2.12.4 TST Machine

The ability to provide full restraint is provided in the temperature-stress-testing (TST) machine. This machine fully restrains the sample and measures the time, temperature and stress at cracking.[28] In the rigid frame both crossheads are fixed, whereas in the TST machine one of the heads is adjustable. As the concrete deforms, a stepper motor adjusts one moveable cross-head (the other is fixed) to maintain the sample at its original length. While the results are similar to that for the rigid frame, the TST allows for determination of early age modulus. While many successful tests have been performed with the rigid frame, tests with the TST have a high failure rate due to the number of factors which much be presicley controlled.[14]

2.13 SUMMARY

Calcium aluminate cements have been used successfully since their introduction after WWI. However, their misuse and a general lack of understanding behind the complexities associated with hydration, curing and time-temperature history have lead to issues in the field. Some of these issues, such as structural failures have hindered mainstream use of CACs. A recent resurgence in their use has prompted more thorough investigations to characterize early-age volume change of this unique material. The aim of this literature review was to familiarize the reader with calcium aluminate cement basics: manufacture, chemistry, hydration, conversion, property development, and durability. In addition a brief review of volume change and cracking susceptibility was given as it relates to ordinary portland cement concrete. The remainder of the dissertation will focus on the testing methods that were performed to characterize calcium aluminate cement concrete. While some of these testing methods are modifications of well-established methods to characterize volume change in OPC systems others have been developed specifically to test CAC systems and their unique properties.

3 Materials and Mixture Proportions

In this research project, a relatively small range of materials was investigated as the focus centered on investigations into inherent material properties of calcium aluminate cement. Two calcium aluminate cements, provided by the manufacturer were investigated. In addition, two reference ordinary portland cements were investigated for comparative testing. A local siliceous river sand and gravel from the same area along the Colorado River bed were used in all concrete, micro-concrete and mortar testing. A class C fly ash (as per ASTM C 618) from a manufacturer in Dallas, Texas was used in selected mixtures.[30] Ground granulated blast furnace slag, provided by the calcium aluminate cement manufacturer (Kerneos Aluminate Technologies), was also used. Admixtures also provided by Kerneos were used to ensure compatibility with calcium aluminate cement systems.

3.1 CEMENTS

Two calcium aluminate cements were used in this dissertation research: Ciment Fondu and GCX Binder. Ciment Fondu was received in 43 kg bags for each of three shipments and GCX Binder was received in 25 kg bags for each of two shipments. Calcium aluminate cement is more susceptible to aging than ordinary portland cement and as a result, each bag was individually wrapped twice in heavy plastic bags and stored in enclosed outdoor storage units. The final shipment of GCX Binder was received in a 450 kg “big bag” or “super sack”. This cement was placed inside large plastic barrels (200 L) that were double lined with heavy duty plastic bags and stored in the same outdoor storage units outlined above. Both calcium aluminate cements were replaced on a yearly basis to ensure that material remained consistent and fresh. The two ordinary portland cements used were standard laboratory cements at The University of Texas at

Austin. These cements were stored in the same manner as the final GCX Binder outlined above. Table 3.1 shows the chemical composition (oxide analyses) for the four cements used in this research.

Table 3.1: Cement oxide analysis

Oxide	GCX Binder	Ciment Fondu	OPC C	OPC
Al_2O_3	50.75	39.90	5.28	5.27
CaO	35.26	36.28	65.77	60.06
SiO_2	5.17	4.68	20.26	19.46
Fe_2O_3	3.06	14.77	1.91	3.37
Mg0	0.59	0.81	1.26	2.94
Na_2O	0.08	0.12	0.09	0.28
K_2O	0.28	0.12	0.66	0.82
TiO_2	2.13	1.79	0.26	0.21
MnO_2	0.07	0.35	-	-
P_2O_5	0.16	0.14	0.14	0.13
SrO	0.05	0.03	0.11	0.21
BaO	0.02	0.02	0.03	0.03
SO_3	0.00	0.05	3.09	4.11
LOI	2.39	1.94	1.1	2.96

3.2 AGGREGATE

The aggregates used in this research project were a siliceous river sand and a siliceous river gravel from Austin, Texas. These aggregates were procured from two sand and gravel pits located along the Colorado River, approximately 7 km to the south east of the center of Austin, Texas, USA. The river sand had a bulk specific gravity (oven dry) of 2.60 and an absorption capacity of 0.55%. The river gravel had a bulk specific gravity (oven dry) of 2.56 and an absorption capacity of 1.83%. The maximum size for the coarse aggregate was 25 mm.

3.3 SUPPLEMENTARY CEMENTING MATERIALS

Two different supplementary cementing materials (SCMs) were used for this project. A Class C fly ash from Dallas, Texas was used as it was a locally available fly ash for potential use by a mobile-mix concrete producer in Dallas, Texas in combination with calcium aluminate cement. Ground granulated blast furnace slag (Grade 120) was provided by the calcium aluminate cement manufacturer and was only used in chemical shrinkage testing. Table 3.2 shows the chemical composition of these two SCMs.

Table 3.2: Oxide analysis for fly ash and slag

Oxide	Class C Fly Ash	GGBFS
Al_2O_3	17.75	11.04
CaO	28.98	41.95
SiO_2	30.76	35.28
Fe_2O_3	5.98	0.97
MgO	6.55	7.82
Na_2O	2.15	0.23
K_2O	0.30	0.37
TiO_2	-	0.55
MnO_2	-	0.26
P_2O_5	-	0.00
SrO	-	-
BaO	-	-
SO_3	-	2.14
LOI	0.44	-

3.4 ADMIXTURES

Two admixtures were provided by Kerneos Aluminate Technologies to ensure compatibility with the calcium aluminate cement. A superplasticizer and a lithium-based accelerator were provided. Typical dosage for the superplasticizer in the field is 1.0-

1.5% (by mass of cement in the mixture). The accelerator is typically dosed up to a maximum of 1.0%, again by mass of cement. In this research project, typical dosages of accelerator ranged from 0.3-0.6% and for superplasticizer from 0.2-0.4%. The dosages (particularly the accelerator) were reduced to provide slightly longer working time in the laboratory before setting and to ensure the mixtures were workable enough for placement in the various testing methods.

3.5 MIXTURE PROPORTIONING

Micro-concrete mixture proportions for the majority of the mixtures in this dissertation were based on mix proportions from Fryda and coworkers.[4] A concrete mixture proportion is scaled to micro-concrete mixture proportions by removing the coarse aggregate. The sum of the percentage of fine aggregate, cement and water (55.9% in this case) is scaled to 100% by multiplying by 1.79. Each individual component is then multiplied by this scaling factor to obtain new relative mixture proportions for each of the constituents. The cement content is then increased to retain a heat signature closer to that of calcium aluminate cement concrete in the field. This cement content of 696.0 kg/m^3 becomes the reference for the remaining percentages of fine aggregate and water. These mixture proportions are shown in Table 3.3.

Table 3.3: Concrete and micro-concrete mixture proportions, Fryda et al.[4]

Mixture Component	Concrete (wt%)	kg/m^3	Micro-concrete 2 (wt%)	kg/m^3
Coarse Aggregate (4.75-20 mm)	44.8	1054.0		
Fine Aggregate (0-4.75 mm)	31.4	739.8	56.9	1144.2
Cement content	17.0	400.0	30.8	618.7
Water	6.8	160.0	12.3	247.5
Total	100.0	2353.8	100.0	2010.3
scale factor = 1.81	*cement wt.*	400.0	*cement wt.*	618.7

Concrete mixture proportions for larger scale testing followed the mixture proportions in Table 3.4. The scaled micro-concrete mixture proportions from this concrete mixture are shown as "Micro-concrete 2". This micro-concrete mixture proportion was used for the realistic time-temperature history mixtures cast in the rigid cracking and free deformation frames.

Table 3.4: Concrete and micro-concrete mixture proportions, UT Austin

Mixture Component	Concrete (wt%)	kg/m^3	Micro-concrete 2 (wt%)	kg/m^3
Coarse Aggregate (4.75-20 mm)	44.8	1054.0		
Fine Aggregate (0-4.75 mm)	31.4	739.8	56.9	1144.2
Cement content	17.0	400.0	30.8	618.7
Water	6.8	160.0	12.3	247.5
Total	100.0	2353.8	100.0	2010.3
scale factor = 1.81	*cement wt.*	400.0	*cement wt.*	618.7

3.6 NOMENCLATURE

A simple naming system for the concrete and micro-concrete mixtures tested in this research project was adopted with a prefix in reference to the type of cement used: GCX, Fondu or OPC, followed by a numerical designator following in chronological order. For instance the mixture GCX 54 is the 54th mixture evaluated in this research

project and was made with GCX cement. The majority of mixtures cast followed micro-concrete mixture proportions. However, concrete mixtures and sieved mortar were also tested. The specific material type will be specified when discussing that particular test within the appropriate chapters in this dissertation. In addition, all figures contain two legends. One legend provides the specifics of the mixture designs including the mixture identification (e.g.,, GCX 54). This same legend also includes the w/cm, admixture dosages (in percent) and the date cast for that particular mixture.

4 Chemical Shrinkage

The volume of cement and water when separate is greater than when they are combined, and this reduction in volume is commonly referred to as chemical shrinkage. Chemical shrinkage was first investigated by Le Chatelier and used a measurement of the degree of chemical reaction that had occurred in a hydrating cement paste.[31] Since this early work, chemical shrinkage has been utilized extensively as a tool to monitor the progression of reactions. Chemical shrinkage was related to compressive strength by Knudsen and Geiker.[32, 33] More recent work has centered on the use of chemical shrinkage as a predictive tool for the amount of autogenous shrinkage that may occur in concrete.[34, 35] In 2006 Sant and co-workers compared various testing approaches to characterize autogenous deformation and chemical shrinkage at early-age for ordinary portland cement systems. They used an automated set-up for chemical shrinkage testing based on buoyancy of a suspended sample in a water-bath and showed good correlation to measurements by other well-established methods.[36] They also highlighted the importance of sample thickness and composition of solution above the hydrating sample.[36] In 2005 ASTM adopted a standard version of this testing procedure and it is on this standardized test method that chemical shrinkage performed as part of this study is based.[37] In short the standard way to measure this reduction in volume involves casting a small volume of cement paste in a rigid vial. Water is placed above the sample almost immediately after mixing the paste and the quantity of water "absorbed" by the paste is monitored over the course of time

Over 150 chemical shrinkage tests were performed to characterize the chemical shrinkage of calcium aluminate cements. Tests were performed with and without an accelerator and on binary systems with replacements of either 30% high calcium oxide

fly ash (ASTM C 618 Class C) or 30% slag (ASTM C 989 Grade 120) for the cement portion of the test.[30, 38] Two standard reference ASTM C 150 Type I portland cements were also included in the study.[39] Measurements were taken manually and with the aid of an automated test set-up at École Polytechnic Féderalé de Lausanne in Switzerland (EPFL), which was then fabricated and utilized for testing at The University of Texas at Austin (UT Austin). In addition to the traditional temperatures investigated (20 °C) a range of isothermal temperatures were investigated: 15, 20, 25, 30, 34, 38, 45, 55 and 70 °C. The goal was to investigate the chemical shrinkage characteristics of metastable versus stable hydrates and to determine chemical shrinkage during conversion as a possible link to observed volume change in other testing presented in this dissertation. A small set of experiments performed at 20 °C investigated the effect of a lower w/cm (0.3) and on a variation in sample heights in the 50 mm vials (2.5, 5, 10 and 20 mm) in the standard test vial to determine the effect of sample volume.

4.1 TESTING PROCEDURE

The standard testing procedure outlined in ASTM C 1608 was used to evaluate chemical shrinkage, with certain modifications made for working with calcium aluminate cement pastes.[37] Temperatures outside the standard 20 °C were investigated to determine chemical shrinkage characteristics of the different CAC hydrates, as well as the chemical shrinkage evolution during conversion (temperatures investigated above 30 °C). In addition, an accelerator was used with the calcium aluminate cement paste since neat CAC paste with no admixture cured isothermally at 20 °C may take 9-12 hours to set because there are no nucleation sites to promote deposition of hydration products. The critical nucleation sites must slowly build during this period before massive precipitation of hydrates can occur. The incorporation of a relatively small amount of accelerator (< 1.0% by weight of cement) provides the nucleation sites necessary to promote hydrate

precipitation on a time scale commensurate with portland cement pastes (e.g.,, several hours).

Results are presented for manual measurements collected during early trials, followed by results from an automated set-up that was originally developed at EPFL in Lausanne, Switzerland and later fabricated and used for testing at UT Austin in Texas, USA. The procedure for mixing and placing the pastes/water in the vials is identical for either method and that will be briefly outlined before a description of the two testing methods is given. Cement paste of desired w/cm was mixed according to ASTM C 305.[40] The paste is mixed with ultra-pure water (18 megaohm resistivity) that has also been de-aired. The paste is then carefully placed in a vial that measures nominally 50 mm in height and 25 mm in diameter. The paste is usually placed at a height of no more than 20 mm in the vial. De-aired water is carefully placed above the sample with a ~3 ml disposable syringe. Then a rubber stopper, through which an inverted glass pipette passes (1 ml), is placed carefully into the top of the vial. Additional de-aired water is added to the top of the pipette so it is close to full and a few drops of paraffin oil are added to the top of the pipette to prevent evaporation. For testing of calcium aluminate cement pastes a larger pipette (2 ml) was used. The vial/pipette combination is placed in a water bath in an appropriate holder immediately after casting and addition of water to the vial. The level of de-aired water in the pipette is measured for a period of at least 24 hours and chemical shrinkage is usually reported as a normalized value of ml water absorbed to grams of cement in the vial for this 24 hour period (according to ASTM). Modifications to this testing protocol are enumerated in the specific section describing the two testing methodologies utilized for this dissertation.

4.2 MEASUREMENTS TAKEN BY HAND

When chemical shrinkage testing first began at UT Austin the vials with cement paste and deaired water were placed in a small wire sample holder (10 samples maximum) that was immersed in a circulating refrigerating/heating type high capacity water bath. For this testing the recommended glass vials to hold the paste samples and 1 ml glass pipettes were used. After the first trial test at 20 °C all of the water had left the 1 ml pipette for the calcium aluminate cement pastes while the water remained at a reasonable height within the vial for the portland cement pastes investigated. A 2 ml pipette was found to be adequate for chemical shrinkage measurements on calcium aluminate cement pastes and was thus the standard size used for the remainder of testing. The predominant w/cm investigated was 0.4 as that is the typical (and maximum) w/cm recommended for CACC in the field. Samples are referred to as "GCX" for the GCX Binder without any admixtures, GCX + ACC or GCX A for mixtures made with the GCX Binder plus accelerator, OPC or OPC C depending on the type of OPC investigated. Blue lines and symbols are used to represent GCX pastes without accelerator while orange lines and symbols are used to delineate GCX pastes with accelerator. Green lines and symbols are used for OPC pastes.

4.2.1 Results of 23 °C Testing

Testing was first performed at 23 °C in accordance with ASTM C 1608-05. The results of this test are shown in Figure 4.1.

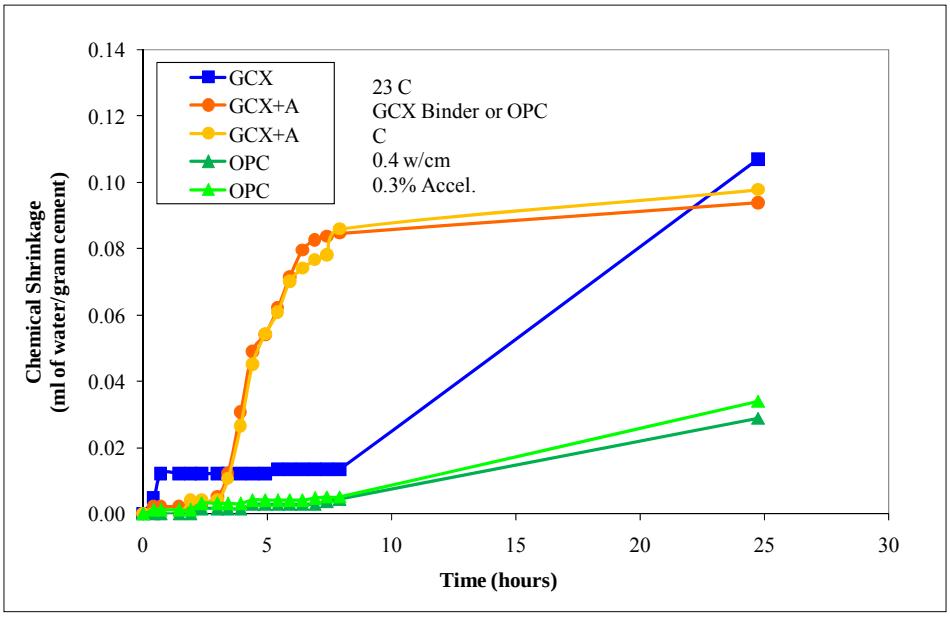

Figure 4.1: Chemical shrinkage testing at 23 °C isothermal

The first successful results utilizing a larger glass pipette (2 ml for CAC pastes) confirmed in fact that the chemical shrinkage for a CAC paste with or without accelerator was much greater (~ 3 x) than that of OPC (ASTM C 150 Type I) and that utilizing a larger than standard size pipette was necessary to provide enough available water for the rapidly hydrating CAC pastes. While it is important to note that due to the rapid hydration of CAC the equivalent maturity between the CAC paste and OPC paste is quite different, the fact that hydration is occurring on a much shorter time period has important implications on how rapidly water is consumed in the hydration reactions. This is evidenced by a chemical shrinkage of 0.107 ml/g (water/cement) for GCX cement with no admixture compared to 0.031 ml/g for the OPC paste. GCX binder with 0.3% accelerator has a chemical shrinkage of 0.098 ml/g. It can be seen that with no accelerator addition to the GCX binder (blue line) chemical shrinkage is delayed, commensurate with setting of the cement, nominally 8 hours after casting. However, ultimate chemical shrinkage values for GCX Binder with or without accelerator are quite

similar. One of the drawbacks to this testing procedure is that unless measurements are taken continuously there is a gap in the data during the second half of each 24 hour period after mixing. This is one of the advantages possible with the utilization of an automated set-up which would allow for continual monitoring of water uptake by the cement paste.

According to literature the predominant CAC hydrate formed below roughly 27 °C is CAH_{10}. To ensure that the chemical shrinkage of this hydrate phase was isolated chemical shrinkage was performed at 15 °C and those results are shown in Figure 4.2. In addition the test was carried out for 48 hours to provide more "long-term" results.

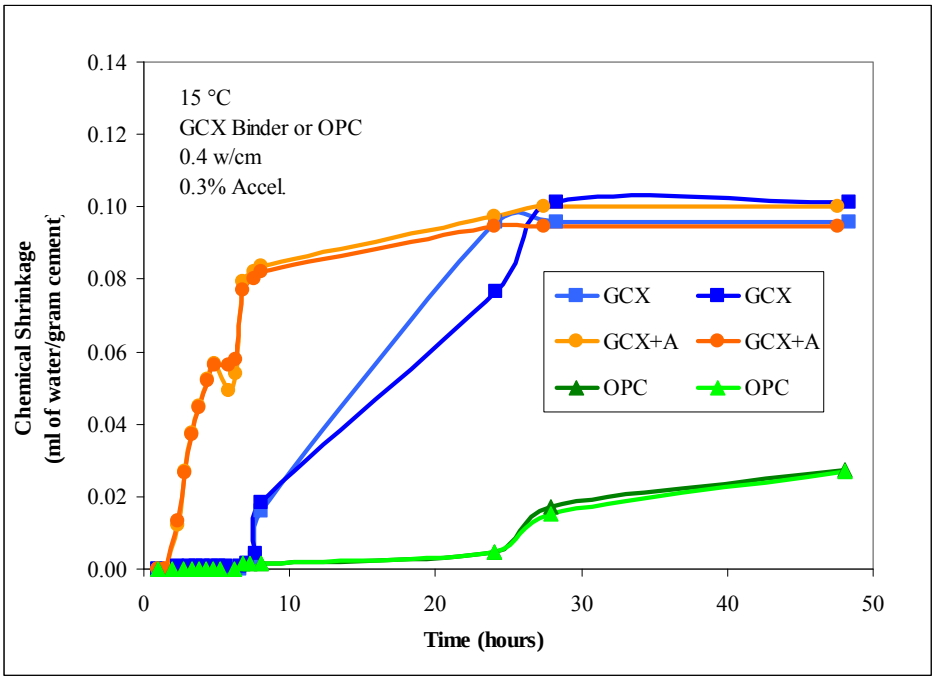

Figure 4.2: Chemical shrinkage at 15 °C isothermal

The chemical shrinkage for CAC paste at 15 °C was very similar to that at 23 °C. Values for GCX Binder with and without accelerator were roughly 0.1 ml/g (water/cement) at 48 hours after mixing. OPC had a chemical shrinkage of 0.027 ml/g.

In Figure 4.2 the time to initiation of chemical shrinkage (e.g.,, setting) for portland cement is more than twice that observed at 23 °C, as one would be expect for OPC cured at lower temperature. In contrast, the GCX Binder without accelerator seems unaffected by this temperature; in fact the GCX Binder with accelerator begins to exhibit chemical shrinkage more quickly than at 23 °C. It is well established that setting time for CAC pastes decreases as temperature approaches approximately 30 °C from either higher or lower temperatures.[9]

To determine the amount of chemical shrinkage for metastable hydrates and to potentially capture chemical shrinkage during conversion, testing was performed at 38 °C with quite surprising results, as shown in Figure 4.3 and Figure 4.4. These two figures show chemical shrinkage testing performed at 38 °C isothermally. This was done in an effort to promote the formation of metastable hydrates initially (predominantly C_2AH_8 according to literature) followed by stable hydrate formation after conversion. As a result the projected timeline for the test was 120 hours based on literature and results from present research which showed that samples cured isothermally at 38 °C convert by approximately 5 days (after 4 days of exposure to water). Due to the continual exposure to water for these paste samples it was thought that conversion may occur on a more rapid time scale. However, as shown in Figure 4.3and Figure 4.4 the data collection stops at 8 and 12 hours, respectively, for GCX Binder paste (no accelerator) and at roughly 24 and 83 hours, respectively, for GCX Binder paste with 0.3% accelerator. It was observed that the glass vials containing the calcium aluminate cement samples actually cracked and in most cases fully ruptured at some point throughout the testing period at 38 °C. Initially this result seemed rather surprising in that some inherent mechanism yielded expansion of the CAC paste resulting in rupture of the glass vials; however, the samples showed continued evidence of chemical “shrinkage”. This

mechanism was further investigated, as outlined in Chapter 5 of this dissertation, and a brief summary for this expansive behavior with continued chemical shrinkage will be given at the end of this chapter.

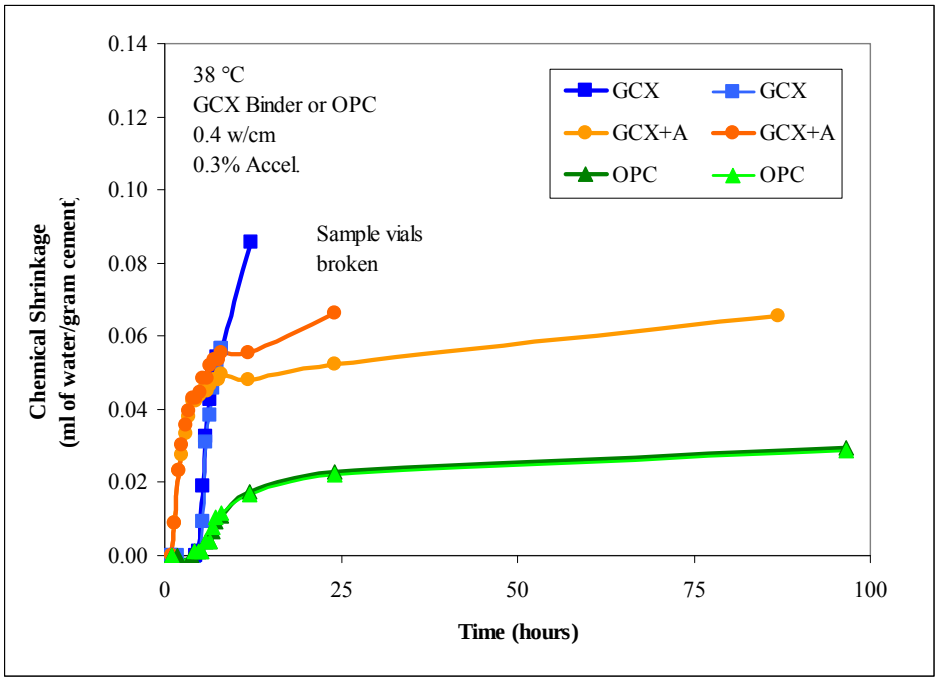

Figure 4.3: Chemical shrinkage at 38 °C isothermal (100 hours)

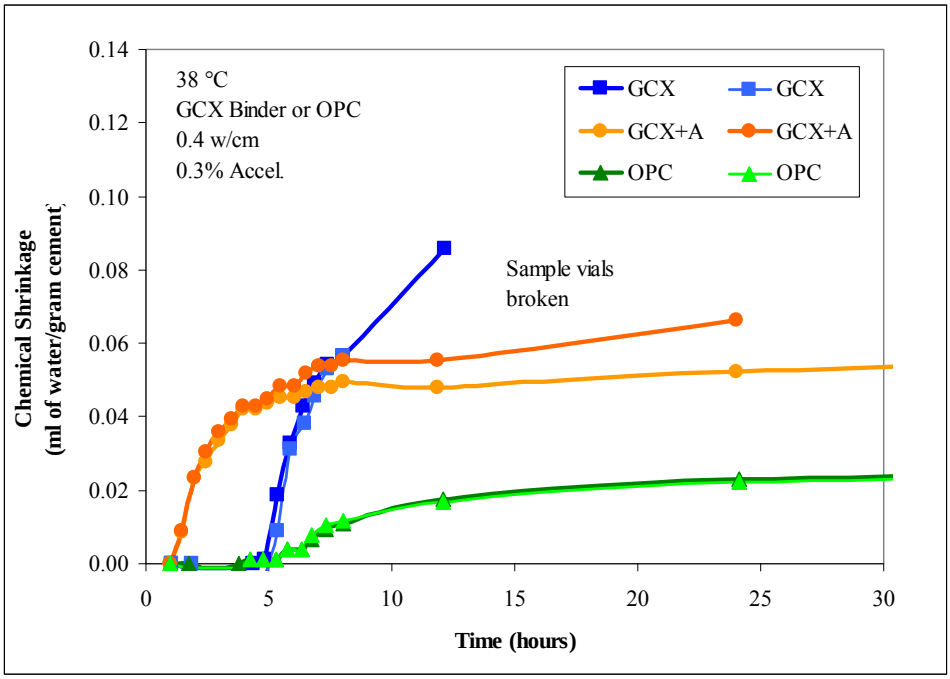

Figure 4.4: Chemical shrinkage at 38 °C isothermal (30 hours)

Testing at 38 °C was repeated and the same results (i.e., breakage of the glass vials) were observed; however the timing of breakage for the glass vials was highly variable and it was ultimately decided to investigate the possibility of utilizing plastic vials instead of the standard glass vial to avoid breakage of the brittle glass. Figure 4.5 and Figure 4.6 show the results of these investigations.

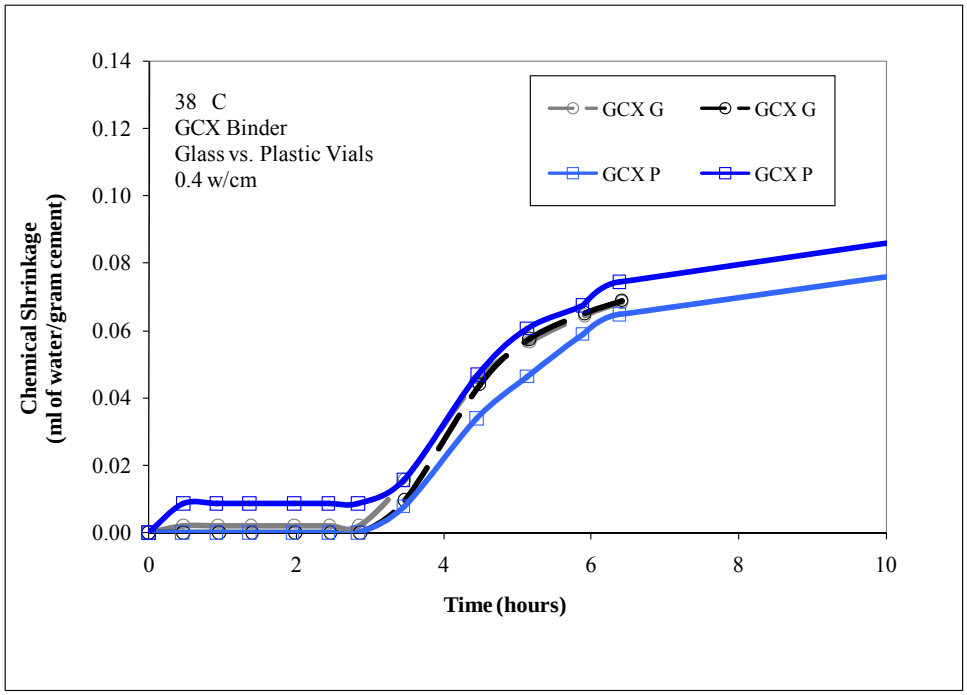

Figure 4.5: Chemical shrinkage at 38 °C, glass (G) or plastic vials (P)

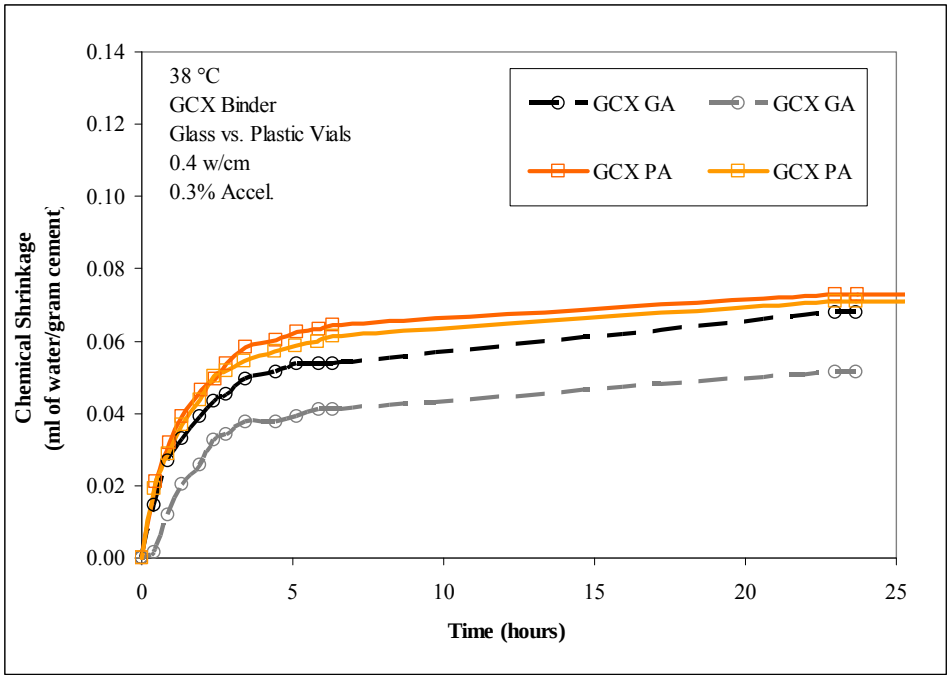

Figure 4.6: Chemical shrinkage at 38 °C, glass (G) or plastic vials (P)

Figure 4.5 shows the evolution of chemical shrinkage for four CAC paste samples without accelerator cast into two plastic and two glass vials. The results show that there is good agreement between the two testing apparatus up to the point of rupture of the glass vials (last measurement at 6.4 hours). Figure 4.6 shows that there is good agreement for CAC binder with 0.3% accelerator cast in plastic vials and one of the glass vials. The results for glass and plastic vials tracked each other up until the point that the glass vials fractured, providing confidence that the data generated were accurate (or as a minimum gave the same results). Using the plastic vials avoided fracture and allowed for data collection beyond the time that the glass vials would have otherwise failed. Plastic vials were used for all subsequent chemical shrinkage tests.

Figure 4.7 shows the long-term results from the chemical shrinkage testing at 38 °C using only plastic vials.

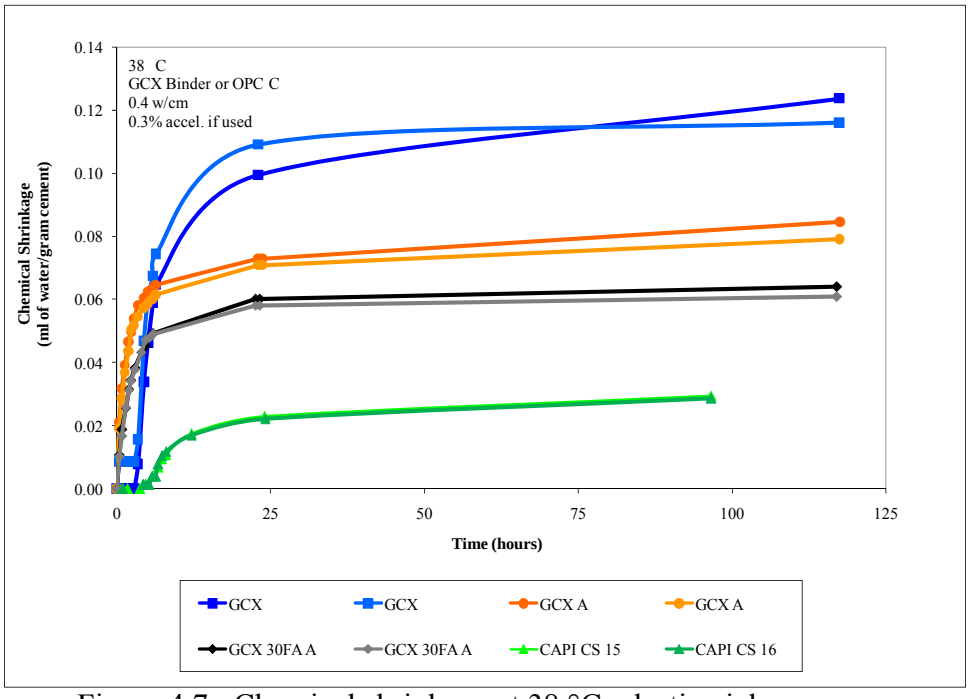

Figure 4.7: Chemical shrinkage at 38 °C, plastic vials

Figure 4.7 indicates that chemical shrinkage at 38 °C is highest for GCX Binder without accelerator with an average value of 0.12 ml/g (water/cement) after 117 hours of testing. Chemical shrinkage for GCX Binder with 0.3% accelerator is the next highest with an average value of 0.082 ml/g (117 hours). The replacement of 30% class C fly ash for GCX Binder further reduces chemical shrinkage in this testing environment to 0.06 ml/g (117 hours). The lowest chemical shrinkage is observed for OPC (C) with an average value of 0.03 ml/g at 96 hours (value not recorded at 117 hours). After 25 hours of testing the rate of chemical shrinkage decreases significantly for all samples tested, indicating for the CAC that the reaction rate is greatly slowing as well. In fact, for CAC pastes with accelerator the rate of chemical shrinkage drops significantly after approximately 6.5 hours. For CAC paste without accelerator the rate of chemical shrinkage does not decrease until approximately 18 hours (from first evidence of chemical shrinkage at 4.5 hours); this suggests that the accelerator increases early-age setting time and may also shorten the total time of the initial hydration of CAC, which has not previously been observed.

Despite the valuable information gained by following the hand measurement technique outlined in ASTM C 1608 for chemical shrinkage, the gap in measurements that occurs during each "overnight period" left questions as to when the progression of reaction really slowed down (i.e., more data points necessary) and long-term monitoring of samples was desired to more closely monitor chemical shrinkage during conversion.

4.2.2 Automated Chemical Shrinkage Test Set-up at EPFL

To monitor chemical shrinkage continuously and for a longer period of time than recommended by ASTM C 1608 (e.g.,, 2 weeks) an automated test set-up was developed at EPFL in Lausanne, Switzerland. The test set-up is shown in Figure 4.8 and Figure 4.9.

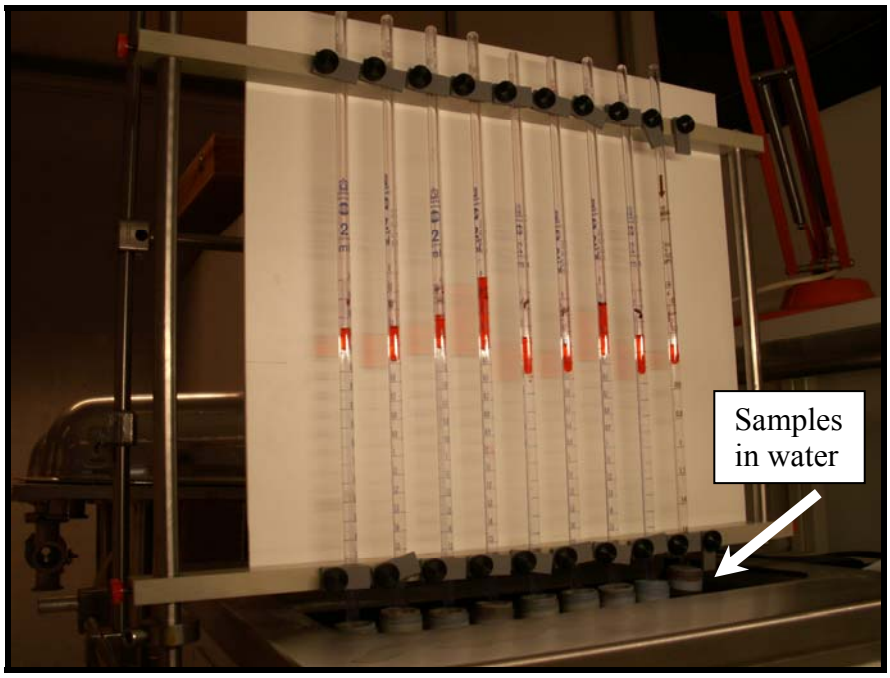

Figure 4.8: Automated chemical shrinkage test set-up at EPFL

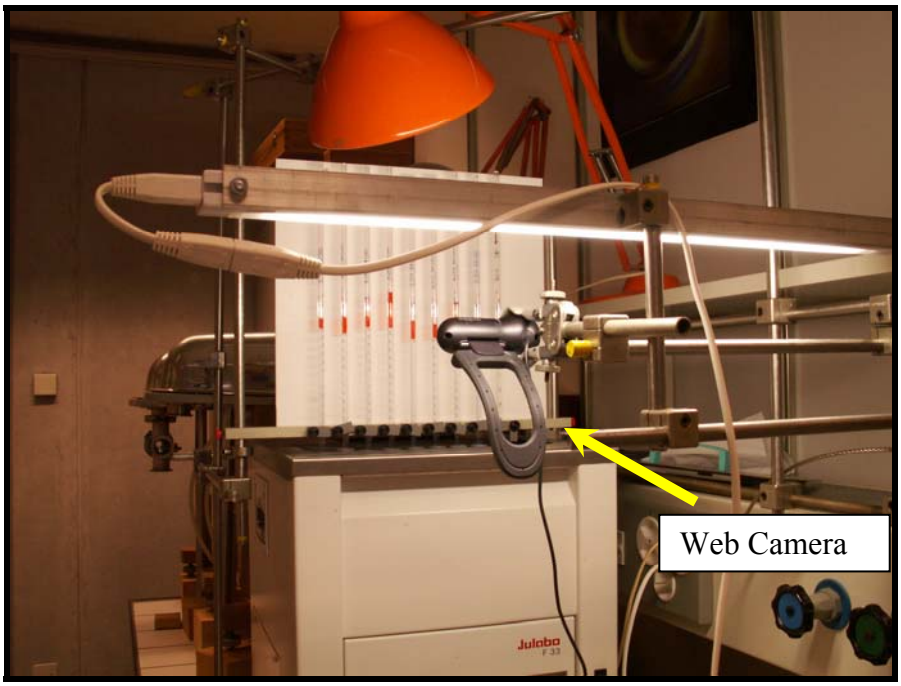

Figure 4.9: Automated chemical shrinkage test set-up, EPFL (2)

The mixing procedure and sample preparation are the same for chemical shrinkage measured by hand or automatically. Once the samples have been prepared a color indicating dye (typically a dyed oil of red or orange color) is placed above the water in the top of the pipette. The oil touches the top of the water so that as the water level in the pipette drops commensurate with chemical shrinkage, the level of the colored dye follows the movement of the water in the pipette. The samples are then placed in a rack as shown in Figure 4.8. There is a white background (opaque plastic) behind all of the samples and the sample vial itself sits in the water bath so that the top of the vial (with imbedded rubber stopper) sits just above the surface of the water in the bath. A web camera is located directly in front of the samples at a distance of approximately 0.5 m. Both fluorescent and incandescent lights are mounted in front of and over the top of the sample rack to provide adequate lighting for image acquisition. The web camera is linked to a computer which utilizes a commercially available software program to perform image acquisition at specified time intervals. Typically an image of the pipettes in the rack is acquired every four minutes. At the end of a 2-week testing period approximately 6000 images showing the decrease in water level in the pipettes were obtained. A computer program written at EPFL then analyzed the location of the dye in each pipette from image to image and returns a table of x and y pixel coordinates for the bottom meniscus of the dye for each pipette. A linear transformation can then be applied to each pixel height to determine the exact level of water in the pipette in milliliters as a function of time. In this way an exact curve showing the evolution of chemical shrinkage was developed with an appropriate graphing software program. Figure 4.10 shows a typical image for the chemical shrinkage specimens in the automated test set-up at EPFL.

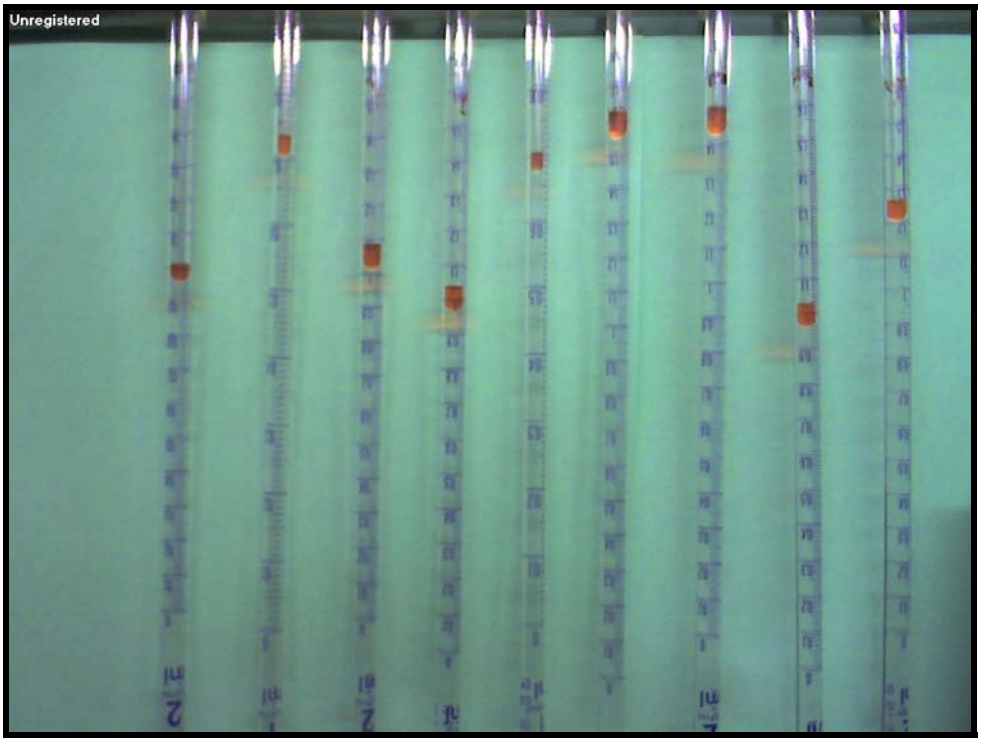

Figure 4.10: Typical image of specimens in automated set-up

The image shown in Figure 4.10 is of a lower resolution because it is from the first set-up that was developed and used in 2006. However, since that time the set-up has been updated with a 2.0 megapixel web camera and the image quality has improved. However, it is important to note that images of a quality around 1.3 megapixels are adequate for analysis by the EPFL software program.

4.2.3 Results from testing using automated set-up at EPFL

The following section examines results of chemical shrinkage testing using the automated test set-up at EPFL. The only temperature investigated at EPFL was 20 °C.

4.2.3.1 *20 °C Isothermal Testing: GCX Binder and OPC*

Figure 4.11 shows the chemical shrinkage results from the first test at EPFL in the automated test set-up for GCX Binder with and without accelerator and OPC (the same cement tested at UT Austin in later testing) at 20 °C.

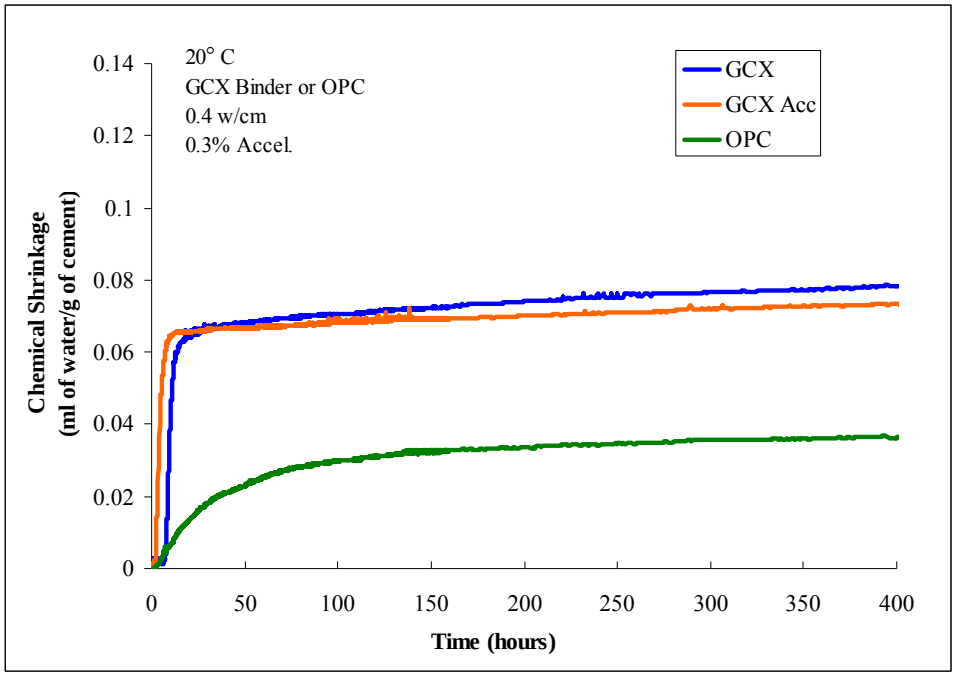

Figure 4.11: Chemical shrinkage testing, 20 °C isothermal, automated

The results shown in Figure 4.11 represent approximately 6,000 data points for each of the three chemical shrinkage curves shown over the course of 400 hours. The ultimate chemical shrinkage at 400 hours for both CAC paste samples (with and without accelerator) was very similar, 0.078 ml/g (no accelerator) and 0.037 ml/g with 0.3% accelerator. The amount of chemical shrinkage for the OPC paste sample was approximately half that of the CAC pastes at 0.036 ml/g at 400 hours of testing. Perhaps the most interesting observation from this testing is the sharp change in slope for both CAC pastes that occurs at roughly 10 hours after testing this is in profound contrast to the OPC paste which gradually reaches a plateau approximately 150 hours after mixing.

There is a steep slope in the initial hours after casting (~ 0 – 12 hr) where a high rate of chemical shrinkage is observed for CAC pastes. Then a clear inflection is observed with a sudden decrease in slope to an almost flat, but slightly increasing curve where chemical shrinkage continues at a markedly decreased rate up to about two weeks of continued testing (the longest duration tested). This dramatic change in chemical shrinkage around 10 hours may be caused by several factors (or a combination thereof). Due to the rapid hydration of CAC (as evidenced by rapid strength gain) it is not surprising that such a steep slope is evidence of a high rate of chemical shrinkage in the first 10 hours, with a change in slope indicative of the rate of reaction slowing down. In this case, this dramatic change in slope essentially indicates that reaction beyond this point is severely limited compared to reaction in the first 10 hours.

However, other work as part of this study (more details in chapter 5) show continued strength gain well beyond 10 hours for samples cured isothermally at 20 °C indicating that continued reaction and filling of microstructure leads to increased strength. In fact, the sharp change in slope may indicate the point at which the cement matrix becomes densified with hydration product such that continued infilling of void space by water is essentially blocked. This is supported by SEM analysis (Figure 4.12) on mortars cured at 20 °C isothermally for one day that show a large amount of unreacted calcium aluminate cement (potentially available for further reaction) and a very dense microstructure with discrete porosity (i.e., not well-connected porosity).

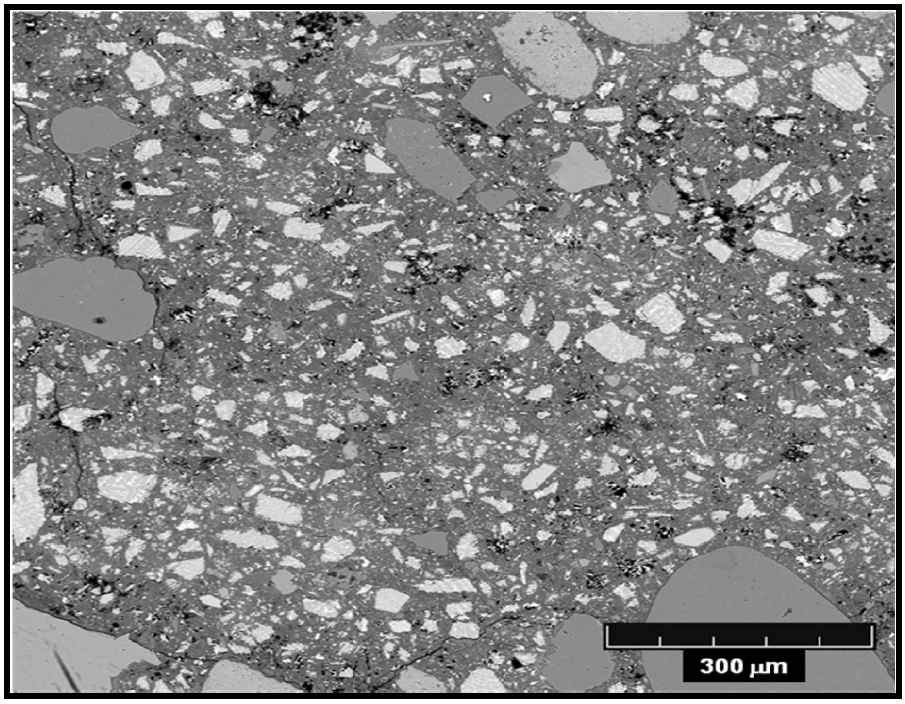

Figure 4.12: SEM Image of CAC Mortar, 24 hr 20 °C isothermal cure

The potential explanation for this dramatic reduction in chemical shrinkage at 20 °C may be that the metastable hydrate CAH_{10} fills space at such a high rate in the first 10 hours that:

- The pore space becomes essentially blocked with metastable hydrates before even a significant portion of cement can react, resulting in high amounts of unreacted CA
- This results in high strength, as observed at low temperature isothermal curing
- There is evident porosity, but it is discretely located and appears to be poorly connected. This may give rise to the idea that even though porosity exists in CAC systems cured at low temperature, if it is not well connected, the resulting permeability is low as the matrix "closes up" and

a significant reduction in the amount of chemical shrinkage is thus observed.

It is also important to mention that the degree of hydration between the calcium aluminate cement paste and the ordinary portland cement paste are not equivalent. Certainly there is more chemical shrinkage observed for the calcium aluminate cement paste with a lower degree of hydration as evidenced by the amount of unreacted calcium aluminate cement in Figure 4.12. Perhaps more chemical shrinkage could be observed in samples at a higher degree of hydration.

To further investigate the space-filling hypothesis, samples of varying height (2.5, 5, 10, and 20 mm) were tested to see if chemical shrinkage was higher for a smaller sample size (i.e., greater potential for access to fill pores with a smaller sample size, resulting smaller distance for infiltrating water front to reach open pores). These samples contained no accelerator. Two standard samples (20 mm height) are shown for reference: GCX Binder with 0.3% and OPC. These results are shown in Figure 4.13.

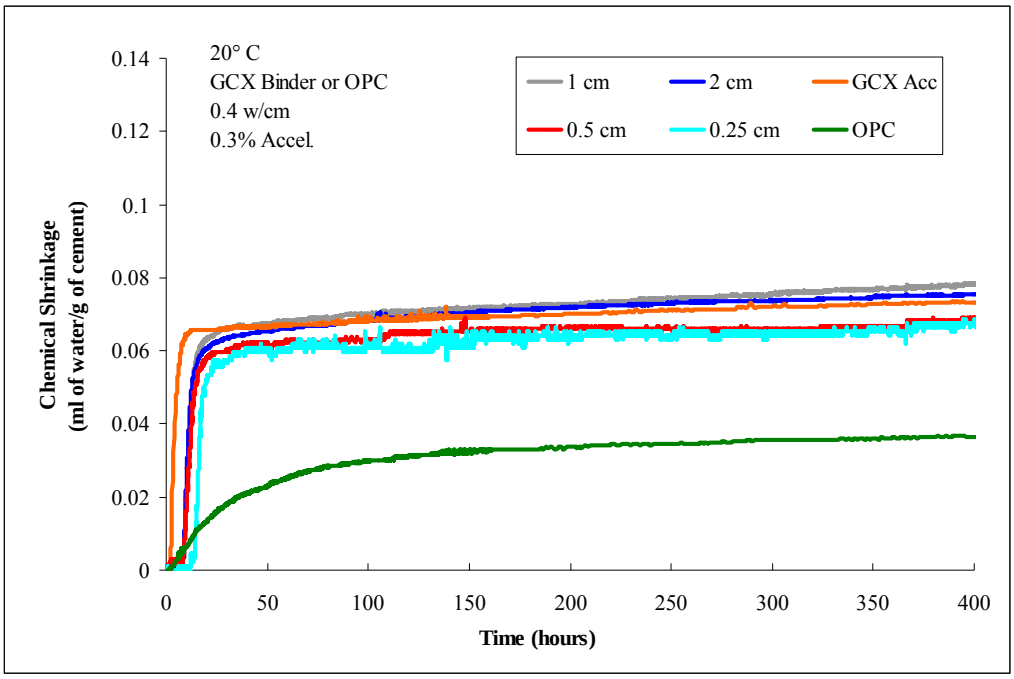

Figure 4.13: Varying sample heights in chemical shrinkage testing

Figure 5.13 shows that varying the sample height for CAC cement paste without accelerator has little effect on the normalized chemical shrinkage (ml water / g cement). In fact slightly less chemical shrinkage is observed for samples with heights of 5 and 2.5 mm. As a result the standard height of 20 mm was used for the remainder of chemical shrinkage testing.

The next figure shows chemical shrinkage for CAC pastes with either ground granulated blast furnace slag or class C fly ash as a 30% replacement of the GCX Binder. There is also a sample cast at a lower w/cm or 0.3 and OPC is shown as reference. All testing was performed isothermally at 20 °C.

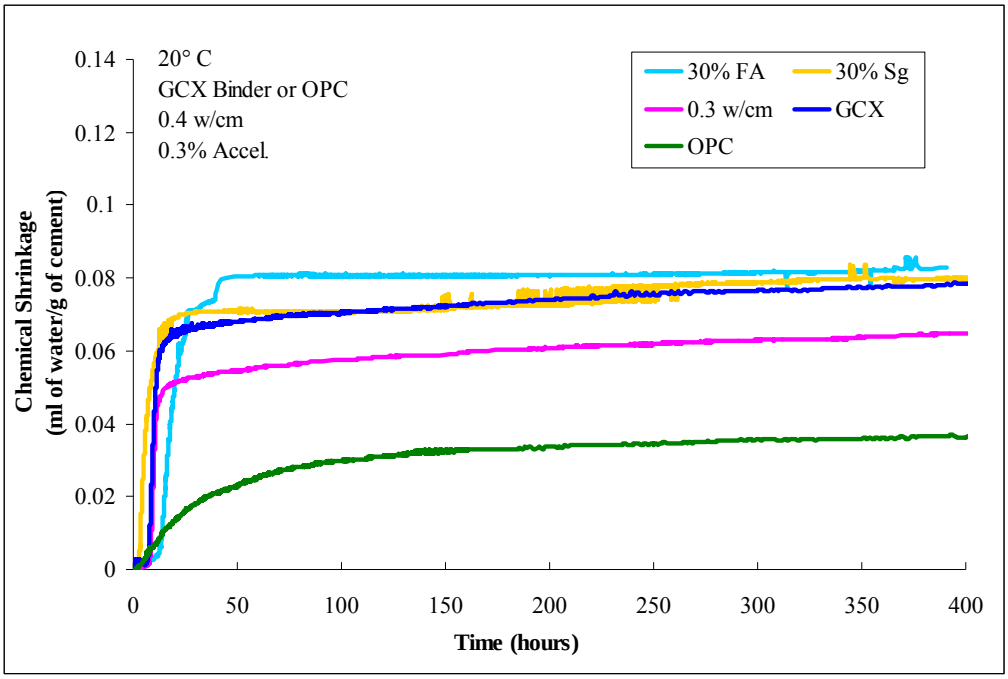

Figure 4.14: Chemical shrinkage testing with fly ash and slag, 20 °C isothermal

As expected, testing the GCX cement at a lower w/cm (less void space) resulted in a lower chemical shrinkage of 0.066 ml/g compared to 0.078 ml/g for a w/cm of 0.4. The replacement of slag or fly ash for CAC resulted in little change in the ultimate chemical shrinkage, 0.080 and 0.083 ml/g respectively, compared to the control at 0.078 ml/g. It is interesting to observe that the mixture cast with 30% fly ash shows initiation of chemical shrinkage is delayed compared to any of the other mixtures tested. However, the ultimate value for chemical shrinkage is essentially the same as that for 30% slag or the control GCX paste.

4.2.4 Results from testing using automated set-up at UT Austin

The remainder of chemical shrinkage testing was performed at UT Austin with an automated test set-up similar to that used at EPFL. This set-up currently holds only 6 samples due to the opening size of the water bath. It can be expanded to hold 6 more

samples on the opposite side if a second web camera is used. Figure 4.15 shows a picture of the automated test set-up at UT Austin.

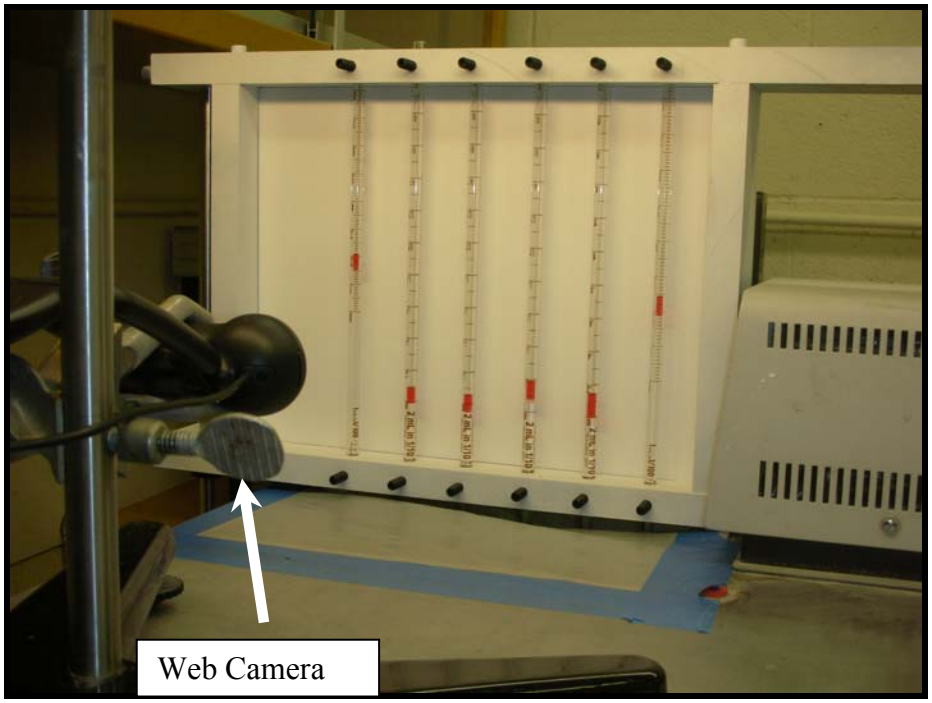

Figure 4.15: Chemical shrinkage test set-up at UT Austin

Testing has been performed at UT Austin through a wide range of isothermal temperatures (25, 30, 34, 38, 45 and 55 °C). To facilitate testing at higher temperatures, a plastic cover was taped over the top of the water bath to limit evaporation. The web camera, image acquisition, and data analysis are identical to that used for the automated set-up at EPFL. Testing as part of this series investigated the effects of temperature on chemical shrinkage of three cement pastes, two samples investigated for each paste for a total of six samples: GCX Binder, GCX Binder + 0.6% Accelerator and OPC all at a w/cm of 0.4. The OPC cement was the same cement used at EPFL and is the standard reference OPC cement shown in Table 3.1.

4.2.4.2 25 °C Isothermal Testing: GCX Binder and OPC

Figure 4.16 shows the results of chemical shrinkage testing at 25 °C. Similar to testing at 20 °C, a sharp inflection in the chemical shrinkage of the CAC paste with and without accelerator can be seen. The CAC paste with accelerator showed an initiation of chemical shrinkage about 10 hours before the CAC paste without accelerator. However, the ultimate chemical shrinkage for CAC paste with and without accelerator is effectively the same, with an average value of 0.066 ml/g for CAC paste without accelerator and 0.068 ml/g for CAC paste with accelerator. OPC has a chemical shrinkage of 0.032 ml/g in testing at 25 °C.

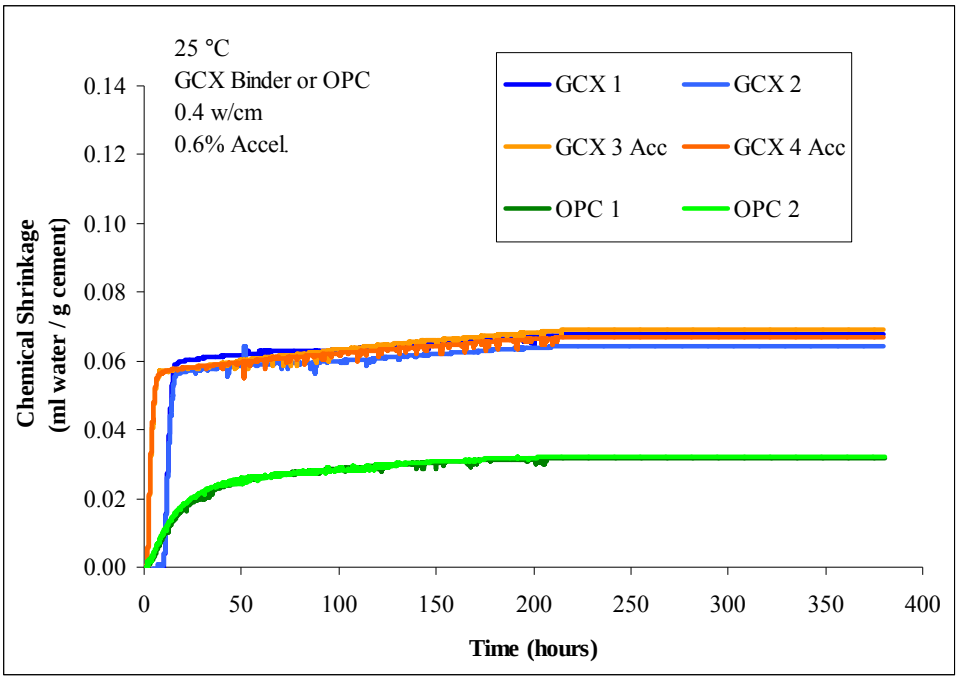

Figure 4.16: Chemical shrinkage testing at 25 °C, UT Austin

Figure 4.17 shows the results of chemical shrinkage testing at 30 °C. Under testing conditions at 30 °C it can be seen that there is a definitive difference between chemical shrinkage of GCX pastes with and without accelerator. After 380 hours the

chemical shrinkage for GCX Binder with and without 0.6% accelerator was 0.087 and 0.111 ml/g, respectively. It is purported in literature that incorporation of accelerator leads to an accelerated formation of C_2AH_8 compared to CAH_{10}.[1] It may be that if more C_2AH_8 is formed in the paste with accelerator that less water is combined in the system to produce hydrates with 8 water molecules versus one with 10 water molecules. However, this is not necessarily supported by chemical shrinkage data at from 20 or 25 °C where values are very similar between CAC pastes with and without accelerator. Curing at isothermal temperatures lower than 30 °C may favor formation of CAH_{10} over C_2AH_8 regardless of accelerator dosage (low temperature more influential on hydrate formation during isothermal curing than presence of accelerator). It may also be due to the slow formation of hydrates especially around 30 °C, without incorporation of accelerator that allows for incorporation of more water due to a more slowly hydrating microstructure. In 20 °C isothermal testing, an inflection in the slope of the chemical shrinkage is observed around 20 hours (0.08 ml/g) for GCX Binder with no accelerator. However at 30 °C this inflection occurs more gradually and can be estimated to begin around 50 hours for the same level of chemical shrinkage (0.08 ml/g), indicating a less steep slope (longer hydration time) as seen in Figure 4.17. Compared to testing at 20 and 25 °C the amount of chemical shrinkage for OPC paste is increased slightly to an average value between the two samples of 0.036 ml/g.

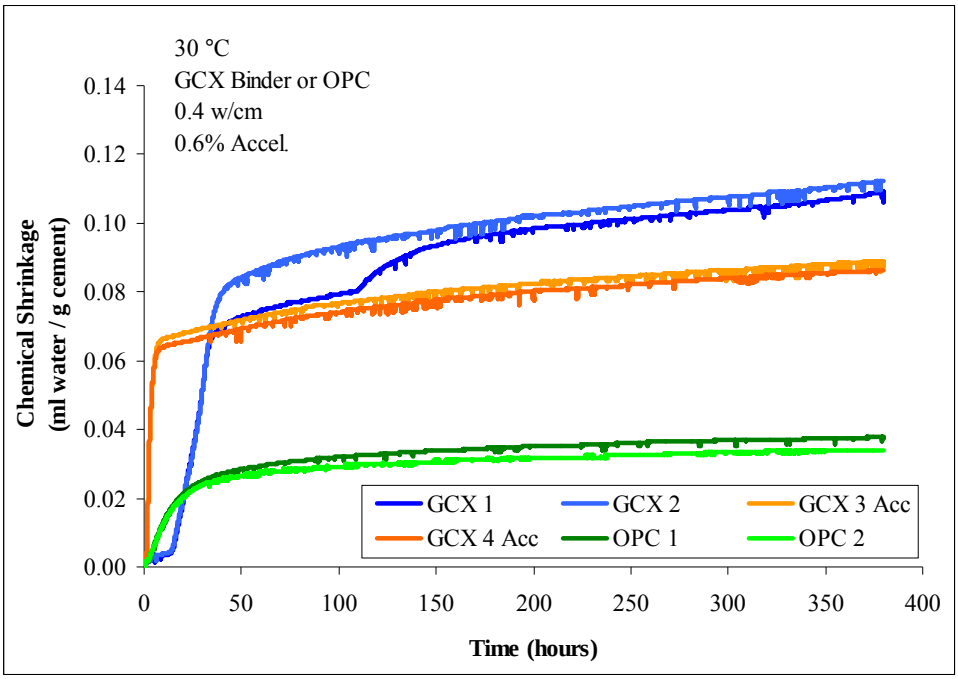

Figure 4.17: Chemical shrinkage testing at 30 °C isothermal, UT Austin

Figure 4.18 shows the results of chemical shrinkage testing at 34 °C. Results of testing at 34 °C are very similar to those at 30 °C where more chemical shrinkage is observed for GCX Binder without accelerator. This test was run for a shorter time period of 200 hours. The average chemical shrinkage at 200 hours for GCX Binder without accelerator was 0.114 ml/g. The average chemical shrinkage at 200 hours for GCX Binder with accelerator was 0.077 ml/g. At 200 hours chemical shrinkage for OPC 1 was 0.033 ml/g. Again the same trend of a slower hydration rate in the GCX Binder pastes without accelerator, commensurate with a higher amount of chemical shrinkage can be seen.

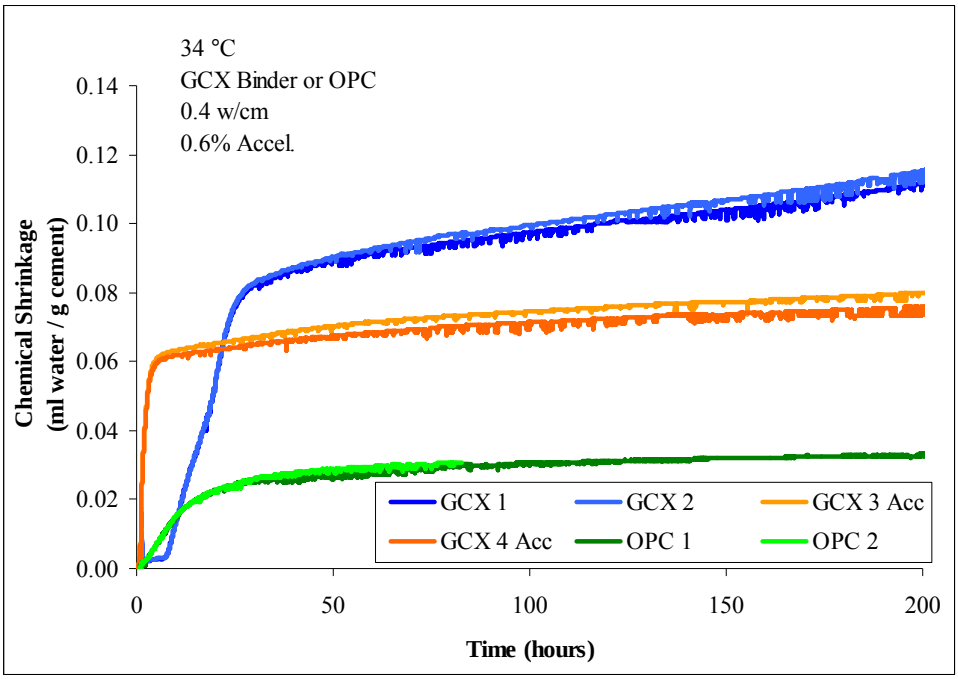

Figure 4.18: Chemical shrinkage testing at 34 °C, UT Austin

Results of testing at 38 °C are shown in Figure 4.19 and Figure 4.20. Figure 4.19 shows that at 38 °C chemical shrinkage at 329 hours (test duration) is very similar for GCX Binder samples with or without accelerator. These ultimate values are significantly higher than those at 20 or 25 °C. Average chemical shrinkage for all four samples is 0.117 ml/g compared to nominally 0.076 ml/g for testing at 20 °C. The average chemical shrinkage for OPC is 0.35 ml/g at 38 °C.

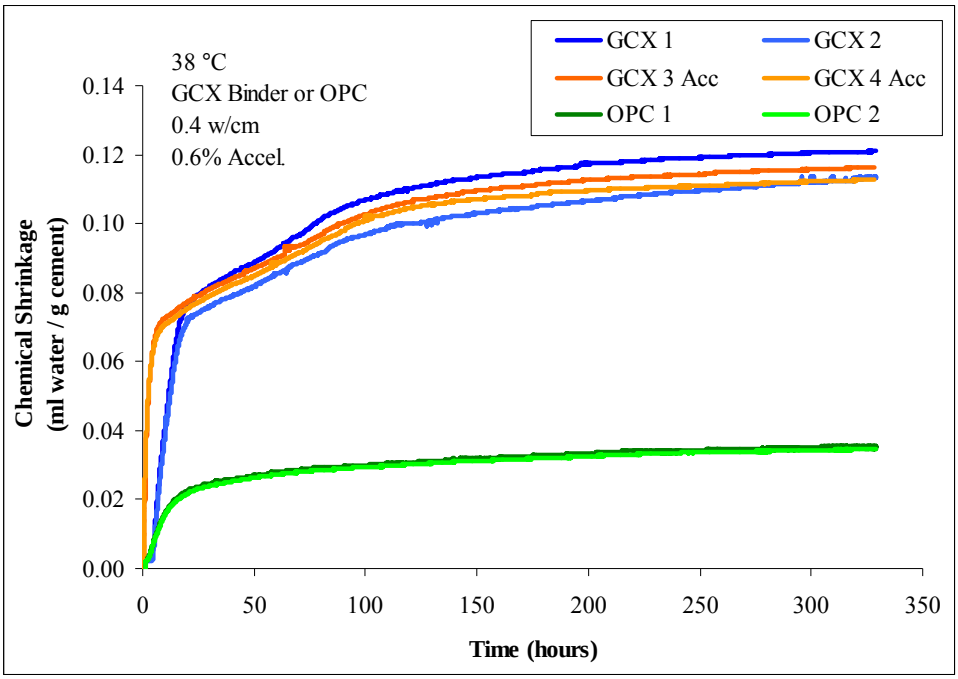

Figure 4.19: Chemical shrinkage testing at 38 °C

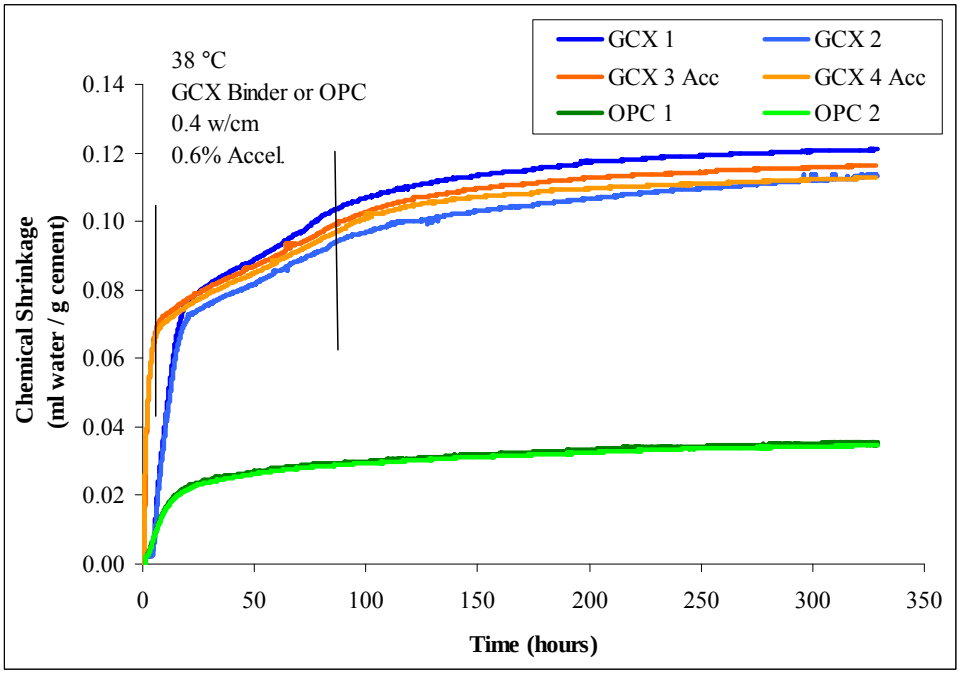

Figure 4.20: Chemical shrinkage testing at 38 °C, delineation of conversion

The most interesting result from testing at 38 °C is shown in Figure 4.20 where three distinctive portions of the graph can be seen. The initial rapid rate of chemical shrinkage in the first 10 hours is followed by a change in slope that continues for approximately the next 90 hours after testing, after which point the slope again changes and the chemical shrinkage real begins to reach a plateau. This time period of 90 hours to the end of the second phase of chemical shrinkage corresponds well to the time period for conversion to complete at 38 °C in literature. The slightly shortened time span of 90 hours (compared to 120 hours) is likely a result of continual exposure to water throughout the testing duration. Typically concrete that is cured isothermally at 38 °C in the laboratory remains in a mold for the first 24 hours and thus has no access to external water, one of the driving forces for conversion. In chemical shrinkage testing the continued exposure to water drives the reaction on a faster time scale. The first change in slope for chemical shrinkage occurs between 0.07 ml/g (GCX Binder + 0.6% accelerator) and 0.08 ml/g (GCX Binder with no accelerator). Interestingly these values correspond roughly to the ultimate chemical shrinkage seen at 20 °C where only metastable hydrates have formed throughout the duration of the test (i.e., no conversion). Then the slope changes for roughly the next 80 hours of the test corresponding with the progression of conversion until this phase ends roughly 90 hours after mixing the pastes.

Figure 4.21 and Figure 4.22 show chemical shrinkage for testing at 45 and 55 °C, respectively. Figure 4.21 and Figure 4.22 show that conversion takes roughly 40 hours to complete at 45 °C and approximately 20 hours at 55 °C. In testing at 55 °C, both of the OPC samples dropped off of the rubber stopper and fell into the bath within the first 24 hours of the testing period and as a result no data was recorded for OPC for this test. In this testing, the maximum chemical shrinkage attained was at 45 °C for GCX Binder without accelerator (0.118 ml/g) and GCX Binder with accelerator (0.117 ml/g). At 55

°C slightly lower values for chemicals shrinkage were obtained: 0.109 ml/g (GCX Binder no accelerator) and 0.110 ml/g (GCX Binder with accelerator). Average chemical shrinkage for OPC paste at 45 °C was 0.035 and showed little change over testing at 34 or 38 °C and was only slightly greater than OPC paste chemical shrinkage for testing at 20, 25 or 30 °C.

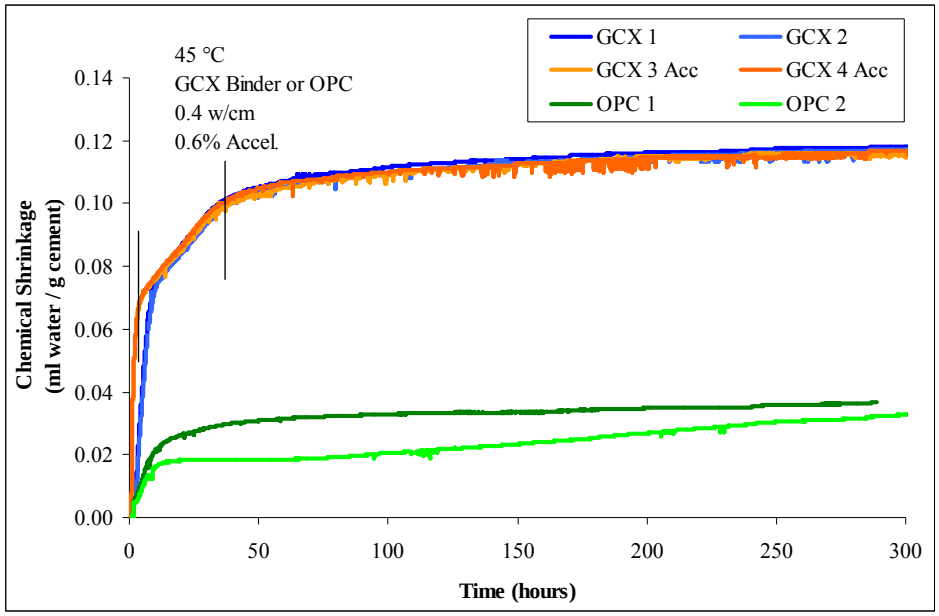

Figure 4.21: Chemical shrinkage at 45 °C, UT Austin

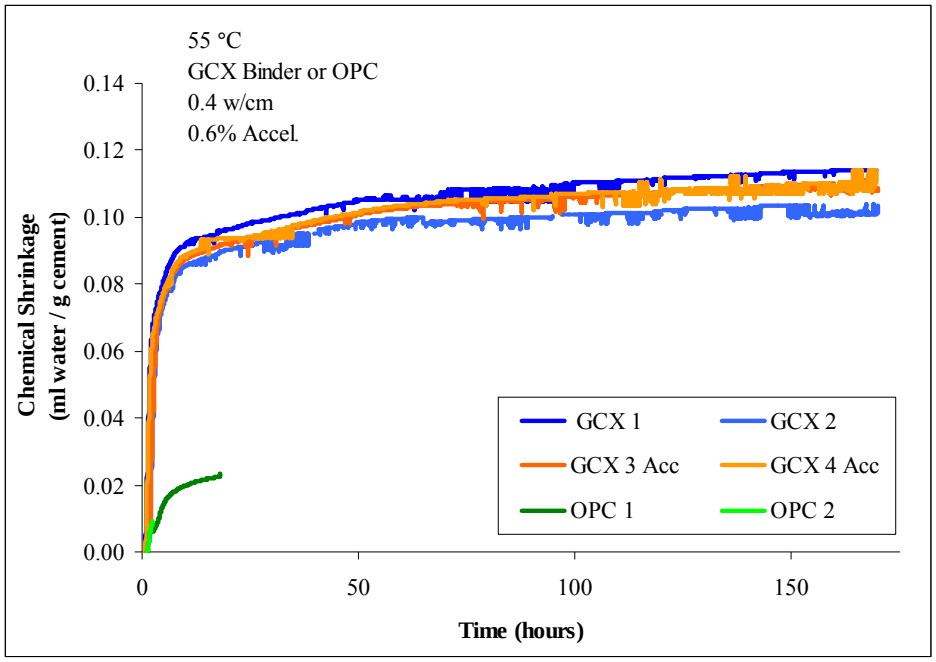

Figure 4.22: Chemical shrinkage at 55 °C, UT Austin

4.3 DISCUSSION

Table 4.1 summarizes the chemical shrinkage of GCX Binder with and without accelerator and OPC pastes through the range of isothermal temperatures investigated with the automated chemical shrinkage test set-ups at EPFL and UT Austin. The length of each test is indicated in the final column or adjacent to the chemical shrinkage value if it was taken a time other than the full duration of the test.

Table 4.1: Summary of results of chemical shrinkage testing (ml H_2O/g cement)

Temp.	GCX		GCX + Acc		OPC		Duration
(°C)	1	2	3	4	1	2	(hr)
20	0.078	-	0.073	-	0.036	-	400
25	0.068	0.064	0.069	0.067	0.032	0.032	380
30	0.112	0.110	0.088	0.086	0.038	0.034	380
34	0.115	0.112	0.080	0.074	0.033	0.031 (82 h)	200
38	0.121	0.113	0.116	0.113	0.035	0.035	329
45	0.118	0.117	0.116	0.117	0.037	0.033	300
55	0.114	0.103	0.109	0.110	0.023 (18 h)	NR	170

It was shown that chemical shrinkage for OPC through a range of isothermal testing (20 to 55 °C) exhibits chemical shrinkage between 0.03 and 0.04 ml water/g cement. No trend is evident for the effect of temperature on chemical shrinkage for OPC pastes as the values are consistently within the aforementioned range with slight increase and decrease likely more a result of the standard deviation of results for testing. In contrast chemical shrinkage testing for CAC cement pastes (GCX Binder) shows an increase from 20 °C isothermal to a maximum value at 45 °C with a slight decrease for testing at 55 °C. There was good agreement between chemical shrinkage values for CAC pastes with and without accelerator (i.e. ultimate chemical shrinkage values roughly the same) below 30 °C and at and above 38 °C. However, isothermal testing at 30 and 34 °C indicated increased chemical shrinkage for CAC paste samples without accelerator compared to paste samples with 0.6% accelerator. A potential explanation for this increase in chemical shrinkage for pastes without accelerator was explained by the higher amount of water combined in the metastable hydrate CAH_{10} compared to C_2AH_8 which may be formed in greater amounts for pastes without accelerator (incorporation of accelerator leads to predominant formation of C_2AH_8). It may also be that the slower rate of reaction that was shown in testing at 30 and 34 °C for pastes without accelerator

provides for a slower hydration which allows more water to be combined into a more slowly space-filled microstructure.

In isothermal testing at 20 and 25 °C two distinctive portions of the curve for chemical shrinkage were observed. After a high rate of chemical shrinkage to roughly 0.08 ml/g an abrupt change in slope is observed followed by a much slower rate of chemical shrinkage. While the reasons for this abrupt change in slope are yet to be fully elucidated potential reasons were briefly discussed. Due to the rapid space filling by metastable hydration products the porosity becomes essentially full of hydration product and discrete porosity (in contrast to the microstructure at 38 °C and above where chemical shrinkage continues through conversion). As a result the ability for any additional water to access the relatively small remaining void space is severely limited. This has important implications for autogenous shrinkage where a microstructure that has very small and discrete pores is likely to experience more autogenous shrinkage than a microstructure with larger pores and better connectivity between those pores. In fact autogenous testing in Chapter 5 provides further justification behind the dense pore structure created at isothermal curing at or below ~ 30 °C.

In contrast to curing at 20 or 25 °C, curing at 38 °C and above shows three distinct portions of the chemical shrinkage curves. The testing shown indicates that chemical shrinkage continues through conversion (despite rupture of glass vials). In fact there may be so much combined water in the system initially that there is in essence a competition during conversion between water that is released from dissolving metastable hydrates (and the subsequent need to accommodate this released water) and the resulting increase in porosity that may be filled by water coming from above the sample (i.e., further chemical shrinkage). The rupture of the glass vials may be due to the fact that if the cement porosity is full of water the escape path for any released water may be close to

non-existent and if the porosity is not well-connected (and even if it is the rate of conversion may be too great at elevated temperature to accommodate the rapid release of water) then the released water exerts a pressure on the matrix great enough to result in expansion of the material.

4.4 CONCLUSIONS

Chemical shrinkage for CAC pastes with and without accelerator is significantly greater than that of OPC systems. Even though there is a notion that CAC pastes are more "mature" at early-age than comparative OPC pastes due to the rapid hydration of CAC systems, it appears that long-term chemical shrinkage of OPC pastes will not reach the same value of CAC pastes as the slopes of the two chemical shrinkage curves at all isothermal temperatures are essentially parallel. Furthermore, the practical and real-world implication is that a high rate of chemical shrinkage in the first 24 hours (as seen for the CAC pastes in this study) indicates that water that is in the system from the original mixture proportions will be rapidly consumed in hydration products, significantly impacting short-term mechanical properties and volume stability and potentially long-term implications on pore structure and microstructure.

5 Evaluating Early-Age Properties of Calcium Aluminate Cement Concrete with Rigid Cracking and Free Deformation Frames

Compared to the knowledge base for ordinary portland cement concrete (OPCC), relatively little information exists for calcium aluminate cement concrete (CACC), despite its existence for over 100 years. There is particularly a lack of knowledge related to early-age behavior of CACC, specifically volume change and cracking potential. To assess these early-age properties, two unique pieces of equipment were developed and employed: a rigid cracking frame and free deformation frame, each which were scaled down (from previous sizes used to evaluate OPC concrete). These frames enable quantification of restrained stress generation and unrestrained autogenous deformation, respectively. These two pieces of equipment employ active temperature control, thereby allowing a wide range of isothermal and realistic temperature conditions to be imposed upon hydrating cementitious samples. Testing of match-cured samples (i.e. identical temperature curing to that in the frames) allows for the evaluation of mechanical property evolution.

Due to the general lack of knowledge and data related to early-age volume change in CAC systems, a majority of the mixtures (32 of 38) tested in the frames were done through a range of discrete isothermal temperatures from 20 to 70 °C. In addition, realistic time and temperature histories were imposed on 8 mixtures. These time and temperature histories were from a field trial in France (data supplied by the CAC manufacturer) and from actual large-scale samples cast the laboratory at The University of Texas at Austin.

5.1 INTRODUCTION

Due to the rapid hydration of calcium aluminate cement concrete (CACC), the temperature rise due to self-heating is significant, even in relatively small members. As a result, a testing approach with active temperature control was needed. The majority of standard testing strategies for characterizing early-age volumetric change of ordinary portland cement concrete (OPCC) were not adaptable to CACC systems due to their inherently high heat generation. In addition, most standard tests do not capture the behavior of concrete prior to or upon setting. To address these challenges, the research team modified an existing test set-up that had been used successfully to evaluate early-age behavior of OPCC by scaling down the apparatus to provide more accurate temperature control of test specimens, which is essential for CACC. The newly-developed apparatus (rigid cracking frame and free deformation frame), discussed in more detail later in this paper, were found to be ideal for controlling CACC hydration temperatures during the testing period, specifically isothermal testing and testing using imposed time-temperature histories typical of CACC applications.

5.2 BACKGROUND

Problems associated with OPCC cracking on the Salzburg-Vienna (Austria) autobahn prompted the development of a rigid cracking frame at the Institute of Building Materials, Munich Technical University, Munich, Germany in the early 1990s[28]. In contrast to other testing methods, the rigid cracking frame combines measurements of thermal effects, autogenous deformation, creep, relaxation, strength and modulus development (all from time of initial concrete placement) into one test. Autogenous deformation is measured in a companion free deformation frame (unrestrained). The rigid cracking frame and free deformation frame each have cross sections measuring 150 x 150 mm. The rigid cracking frame is 1.9 meters in total length; the length of the

concrete specimen is 1.65 meters. The length of the concrete in the free deformation frame is 600 mm with an effective gage length of 520 mm. The cross-section of the free deformation frame is the same as the rigid cracking frame (150 x 150 mm). Formwork with integrated piping allows for active temperature control of the specimens in both the rigid cracking and free deformation frames. This allows the test to be run at under isothermal conditions to eliminate thermal movement and subsequent stress generation due to that movement. Furthermore, real time-temperature histories may be imposed upon the material to simulate field curing conditions. Even today, however, in Germany the testing procedure is run without active temperature control so the thermal behavior of the mixture is evaluated and a cracking temperature is determined after artificially cooling the sample by 1 °C/hour until cracking if it remains uncracked at the end of the typically 4 day testing period. Fresh concrete is cast in cylinders of appropriate dimension and match-cured (i.e. same time-temperature history) to the concrete in the frames inside a thermally insulated box through which temperature controlled water is circulated (in between and around all of the match-cured specimens). This allows for characterization of mechanical property development on specimens subjected to the same time and temperature history of the concrete placed inside the frames. Computer-controlled data acquisition systems, coupled with water baths, are used to monitor and control the temperature of the specimens inside the rigid cracking frame, free deformation frame and match-cured insulated box.

Several rigid-cracking frames have been produced to enable similar testing in the United States (U.S.) at both The University of Texas at Austin in Austin, Texas and Auburn University in Auburn, Alabama, U.S. Through collaborative research (funded by Texas Department of Transportation), these two groups have been able to develop a heat generation model for mass concrete members (OPC)[29, 41, 42] and have developed a model

for predicting cracking risk for select mass concrete elements. Although a limited number of other testing agencies and universities employ the use such testing apparatus, their use is certainly not widespread. Figure 5.1 shows a schematic of the rigid cracking frame and Figure 5.2 shows a schematic of the free deformation frame.

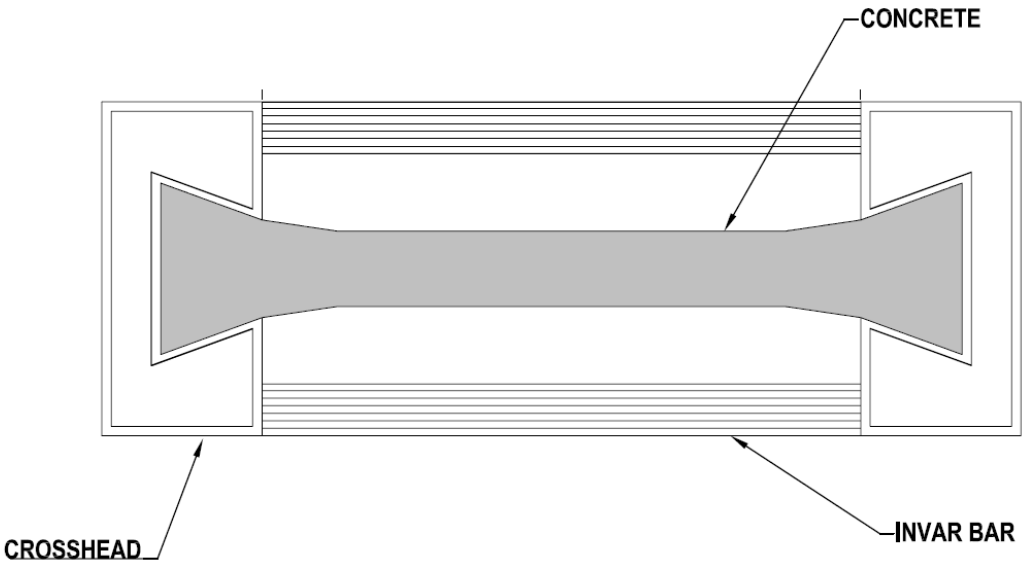

Figure 5.1: Schematic of rigid cracking frame (top view)

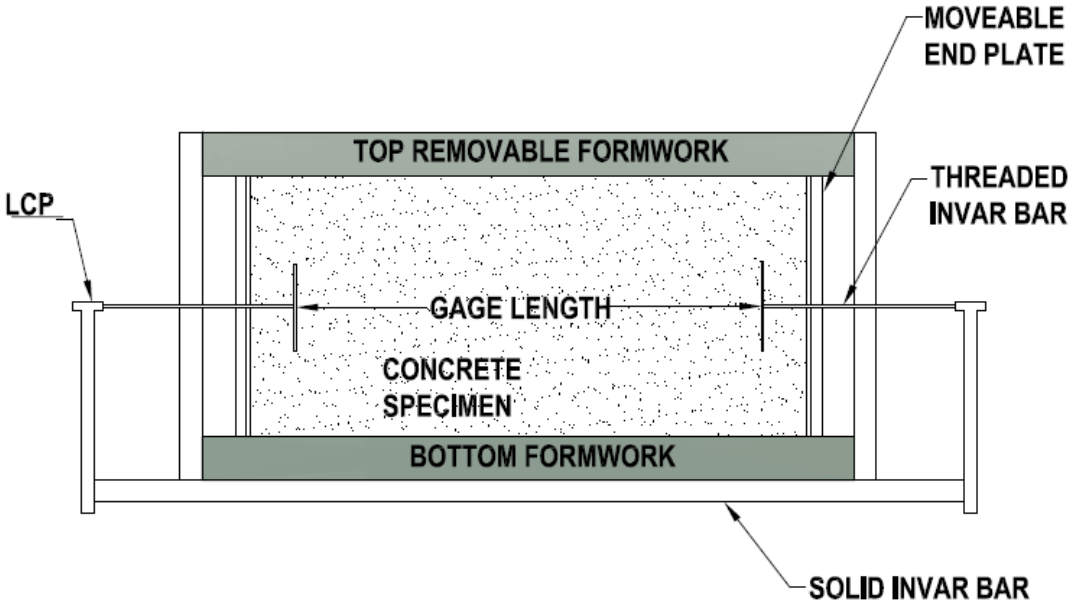

Figure 5.2: Schematic of free deformation frame (side view)

5.3 SCALING THE FRAMES

Due to the large amount of heat evolved in a shorter period of time with CAC systems compared to OPC systems, 1/3 scale versions of both frames were designed and constructed specifically to allow for better temperature control in rapidly hydrating CAC systems. Throughout this chapter the "scaled" or "mini" rigid cracking and free deformation frame will simply be referred to without the reference to their "scaled" or "mini" size. It is understood that the dimensions to which rigid cracking and free deformation frame refer in this chapter are for frames with a 50.8- x 50.8-mm cross section and a length of 546 mm for the rigid cracking frame and 175 mm for the free deformation frame. For a limited number of tests, the standard frames were employed for verification testing. For that testing the frames will be referred to as standard rigid cracking frame or standard free deformation frame. It is understood that standard frames have a cross sectional dimension of 150 x 150 mm concrete length of 1.65 m for the rigid

frame and 600 mm for the length of the concrete in the free deformation frame. The mixture proportions are also scaled to test a micro-concrete (aggregate < 8 mm) rather than a full-scale concrete when testing is performed in the smaller version of the frames. Examples of the mixture proportioning were given in Chapter 3. Specific mixture proportions for each mixture will be shown where appropriate for clarity.

5.4 TESTING PROCEDURE

The testing procedure is essentially identical, whether the standard size frames or scaled frames are used. The following descriptions (other than specimen dimensions) thus apply to both testing apparatus.

5.4.1 Rigid Cracking Frame

Uniaxial stress in the micro-concrete is measured using a scaled-rigid cracking frame[43]. The scaled rigid cracking frame tests a specimen measuring 50.8 x 50.8 x 546 mm. Micro-concrete is cast into the rigid cracking frame as a dog-bone type specimen. Two large steel crossheads grip the ends of the dog-bone specimen in the rigid frame[41]. Two longitudinal bars, constructed of Invar steel, connect these crossheads. These Invar bars are instrumented with strain gages so that as the bars deform, equal and opposite to the movement of the micro-concrete specimen, strain is subsequently measured. The restraint system is passive in the rigid cracking frame. Thus, if shrinkage occurs, tensile stresses develop in the micro-concrete and the stress state in the Invar side bars will become compressive in nature to resist the shrinkage movement. Conversely, if the micro-concrete expands, compressive stresses develop, and a subsequent tensile stress develops in the Invar side bars to maintain static equilibrium. Micro-concrete stresses are measured through use of strain recorded from the side Invar bars since the frame is a statically determinate structure. Through knowledge of the Invar steel properties (cross

sectional area, modulus) and strain measurements, the stress in the concrete can be back-calculated (with the aid of elastic modulus data from match-cured specimens). Further details outlining this testing apparatus, as well as the calibration of the frame, can be found in the Masters Thesis by J. Whigham[41].

The temperature in the rigid cracking frame is regulated using a programmable refrigerating/heating circulator (water bath) that circulates a 50/50 mixture of water and anti-freeze (ethylene glycol plus corrosion inhibitors) through the insulated formwork. The temperature of the specimen is recorded by the data acquisition system using three Type K thermocouples that are embedded into the fresh micro-concrete at the beginning of the test. One thermocouple is placed in the middle of the specimen and the other two are placed in the micro-concrete in each of the crosshead areas. The temperature in the water bath is controlled by the thermocouple embedded in the middle of the cracking frame. For example, if an isothermal test is conducted at 20 °C, the water bath reacts to the actual micro-concrete temperature in the middle of the specimen and appropriately cools or heats the circulating fluid to maintain an isothermal micro-concrete temperature of 20 °C. The bath does not simply circulate 20 °C fluid throughout the entire duration of the test.

The stress in the concrete specimen is measured immediately after placement by a data acquisition program that is started while the concrete is still in a plastic state and monitored throughout the duration of the test. Stress is assumed uniform over the cross-section of the specimen. If a crack forms, the stress drops immediately. The restraint provided by the cracking frame is 100% at the time of placement since the stiffness of the Invar steel bars is infinitely greater than that of the plastic micro-concrete. The restraint decreases with time as the concrete modulus increases[29]. At the end of the test the micro-

concrete in the frame is restrained at about 80%, which is not ideal, but is in line with levels of restraint observed in real structures.

5.4.2 Free Deformation Frame

The scaled free deformation frame (schematic in Figure 5.2) measures autogenous deformation in terms of linear movement of a micro-concrete test specimen measuring 50.8 x 50.8 x 175 mm in length with a 135 mm effective gage length. The bottom bars on which the framework rests are both made of Invar steel, as are the two threaded rods which are embedded into the micro-concrete specimen. The threaded rods are screwed onto one linear control potentiometer (LCP) at either end of the free deformation frame. The other end of the rod is threaded into a 13 x 13 mm aluminum plate which remains embedded into the concrete specimen once it has hardened. The movement of the LCPs is also calibrated using gage blocks of known dimension to develop a calibration curve to relate the measured output (voltage) to length change. Initially the concrete is held in place by two moveable steel plates at either end of the specimen. Upon final setting, as determined by ASTM C 403 (penetration resistance), these end plates are released to allow for free movement of the specimen for the remainder of the test.[44] This specimen can also be reclaimed at the end of the test for long-term drying shrinkage measurements (once placed in an appropriate environmental chamber with relative humidity at 50 ± 4% and a temperature of 23 ± 2 °C).

Initially the temperature in the free deformation frame was regulated using the same water bath that controlled temperature in the rigid cracking frame. After the fluid (50/50 v/v mixture of water and ethylene glycol plus corrosion inhibitors) had circulated through the rigid cracking frame, it then was circulated through the piping network surrounding the free deformation frame. However, difficulties with precise temperature control when conducting higher temperature isothermal mixtures (T > 50 °C) required the

use of a second water bath devoted to the free deformation frame. The temperature of the specimen is recorded by a data acquisition system using two thermocouples which are embedded into the fresh micro-concrete at the beginning of the test. The micro-concrete cast in the free deformation frame is subjected to the same time-temperature history as the micro-concrete in the rigid cracking frame. In other words the thermocouple embedded in the middle of the rigid cracking frames provides temperature information to the data acquisition system that then communicates with the water bath controlling the temperature of the free deformation frame so that it goes through the same time and temperature history as the micro-concrete in the rigid cracking frame.

5.4.3 Match-Cured Samples

In addition, specimens are cast and placed in a match-cured apparatus (essentially an insulated food-type cooler) through which water circulates from a third water bath, which is controlled by the same computer software program that controls the temperature of the concrete in the rigid cracking and free deformation frames. These cylindrical specimens (76 x 152 mm – for micro-concrete) are tested periodically through the duration of a cracking frame test to allow determination of mechanical property development (compressive strength, elastic modulus and splitting tensile strength). Specimens are also obtained for analysis by scanning electron micrcoscopy (SEM), x-ray diffraction (XRD) and/or thermogravimetric analysis (TGA) from selected match-cured specimens at specific ages. A selected number of samples will be included where appropriate for clarification of property development and hydrates present.

5.4.4 Control of the Frames

The entire test is typically conducted for four days. However, different testing lengths have been used for CAC systems, specifically at 38 °C, to monitor the effects of

conversion on stress development. If at the end of the testing period the specimen is not cracked, cooled liquid (50/50 by volume mixture of water and ethylene glycol with corrosion inhibitors) is circulated through the frames and the temperature is reduced at a rate of 1 °C/hour until the concrete cracks, or the temperature of the water bath essentially reaches 0 °C, the freezing point (lower limit of the water bath). The temperature at which the specimen cracks is referred to as the cracking temperature. Lower cracking temperatures indicate a lower risk of cracking in the field according to the developers of the testing regime. This measure is useful as a comparative tool between different mixtures, but the stress development, autogenous deformation and mechanical property development need to be looked at holistically to provide a more complete understanding of the material behavior and potential for volumetric change in field applications. These evaluated properties will be discussed in relation to volume change and the effects this will have on field performance of CACC.

5.5 RESULTS: ISOTHERMAL TESTING

Results in this section are presented from testing at isothermal temperatures of 20, 25, 30, 34, 38, 50, 55 and 70 °C. The majority of isothermal work focused on temperatures of 20 and 38 °C to investigate volume change with relation to metastable hydrates versus stable hydrates. In addition, testing at 38 °C allowed for characterization of volume change during the conversion process (i.e., initial formation of metastable hydrates then converting to stable hydrates over roughly a five day time period). Higher temperatures were investigated to determine volume change in CAC systems where stable hydrates formed more rapidly than in 38 °C testing. Isothermal testing at 25, 30 and 34 °C was performed to build on work by other researchers who investigated pastes under isothermal conditions approaching 30 °C from lower and higher temperatures. Interestingly, they observed that as isothermal temperatures approach 30 °C from either

upper or lower temperatures, anomalous (i.e., significantly retarded) setting time commensurate was observed.[9, 11, 45]

For each mixture and temperature investigated, three figures and one table are shown to clearly depict results. The first figure shows the temperature throughout the test from the thermocouple in the middle of the rigid cracking frame (RCF Mid T) and in one of the match cured samples (MCB T). Results for temperatures in the cross-heads of the rigid cracking frame are shown if there was a deviation of more than 3 °C from the middle of the rigid cracking frame for a significant portion of the test (e.g more than 1 hour). The second figure shows the stress generation in the rigid cracking frame. The final figure is a plot of the autogenous deformation from the free deformation frame also showing the temperature from one thermocouple in that test, labeled FS 1 T. Each figure contains the basic information for that test: mixture proportion (mixture identification number, mixture type, w/cm, admixture type and dosage, temperature investigated and date of test). Early trials of this overall testing methodology resulted in complications regarding the free deformation frame – problems with the data acquisition system were encountered. Ultimately a new data acquisition system was acquired to rectify this problem and essential data were then collected on subsequent trials. There are a number of tests for which free deformation data do not exist. Key mixtures (e.g.,, 20 and 38 °C) were repeated to obtain this vital data and to ensure repeatability. The table shown with each test will include mechanical property data obtained throughout the testing period and for selected mixtures up to 28 days including: compressive strength, elastic modulus and splitting tensile data. At the end of this section a table summarizing results with the appropriate figure and table numbers given to draw attention to specific results.

5.5.1 20 °C Isothermal Testing

5.5.1.1 GCX Binder, micro-concrete, trial testing

Figure 5.3 shows the temperature profile for the first mixture tested with GCX binder in the rigid cracking frame. This is one of several tests that were performed for "proof of concept" to ensure that the frames, water baths and data acquisition systems were working properly. As a result, mechanical properties are not be presented for the first three mixtures tested.

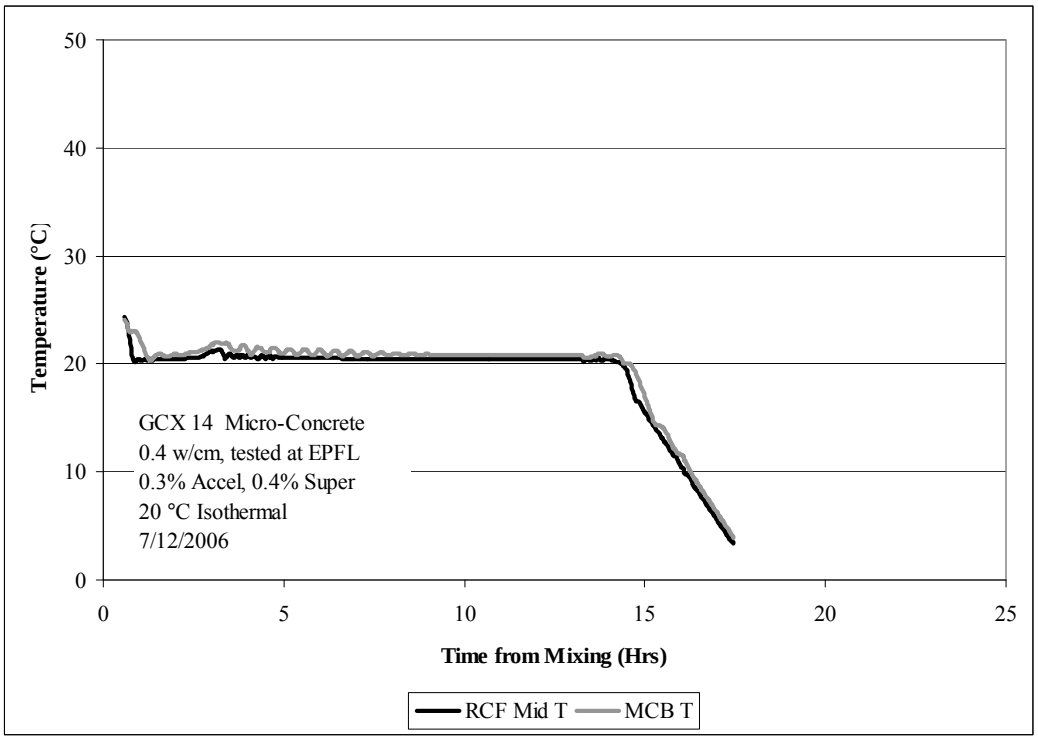

Figure 5.3: Temperature profile for 20 °C isothermal test, GCX 14

This test demonstrated that the water baths were able to maintain temperature within the frame extremely well even during hydration of the CAC micro-concrete. The mixture was cooled at 1 °C/hour after 14 hours to ensure this portion of the program was working correctly. Figure 5.4 shows the stress generation for this mixture.

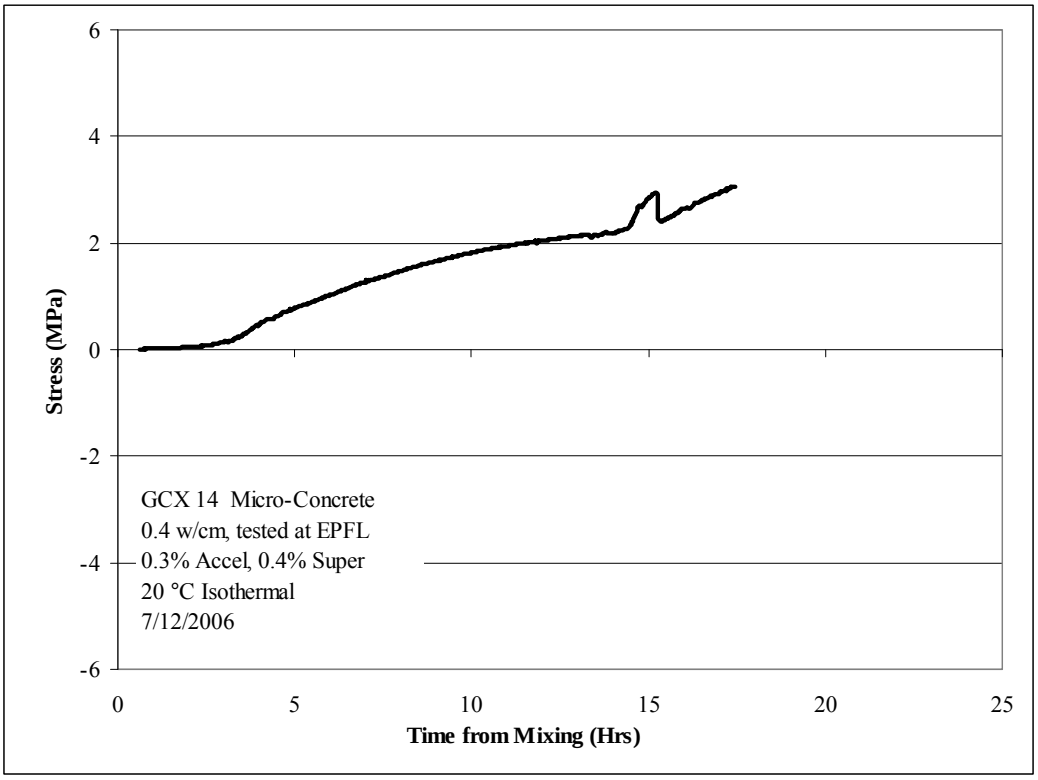

Figure 5.4: Stress generation for 20 °C isothermal test, GCX 14

These first results agreed reasonably well (in terms of general behavior) with the results for ordinary portland cement concrete (OPCC) with low w/cm, where isothermal testing around 20 °C (majority of testing at 23 °C isothermal) generated tensile stresses, mainly due to autogenous shrinkage of OPCC systems. However, the level of stress generated in just a short duration (14 hours) before cooling was somewhat surprising. Upon cooling it seems that a micro-crack developed in the concrete as evidenced by the brief drop in stress just after 15 hours in the test. However, a through-crack did not develop as tensile stress is seen to then increase commensurate with artificial cooling until the testing was stopped at 18 hours.

5.5.1.2 GCX Binder in Rigid Cracking and Free Deformation Frames: Standard and Smaller Size

Testing was performed at 20 °C isothermally, to compare results of stress generation and free deformation between the standard frames and the smaller frames used as part of this research. A concrete mixture according to the mixture proportions in Table 3.4 was cast in the standard frames; a portion of the concrete was sieved over a 9.5 mm sieve to obtain mortar for testing in the smaller frames used as part of this study. Results for the sieved mortar mixture tested at 20 °C in the smaller frames are shown first followed by results from the standard frames. Figure 5.5 and Figure 5.6 show the temperature profile and stress generation, respectively, for the sieved mortar tested at 20 °C isothermally in the smaller frames.

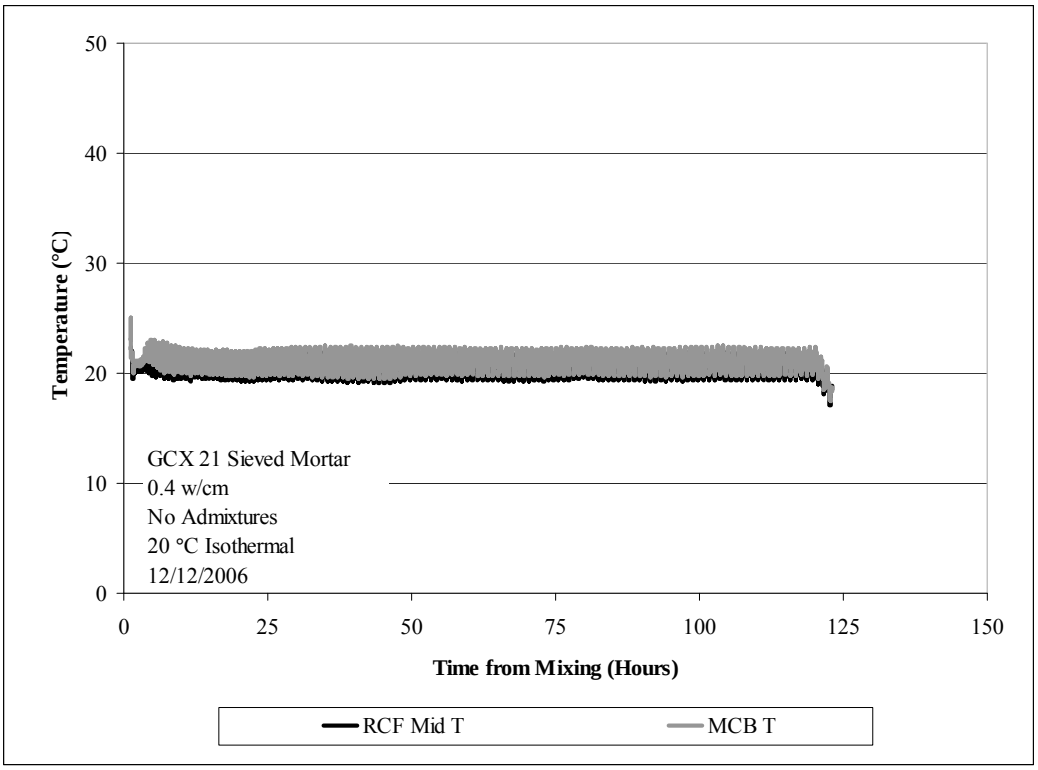

Figure 5.5: Temperature profile for 20 °C isothermal test, GCX 21

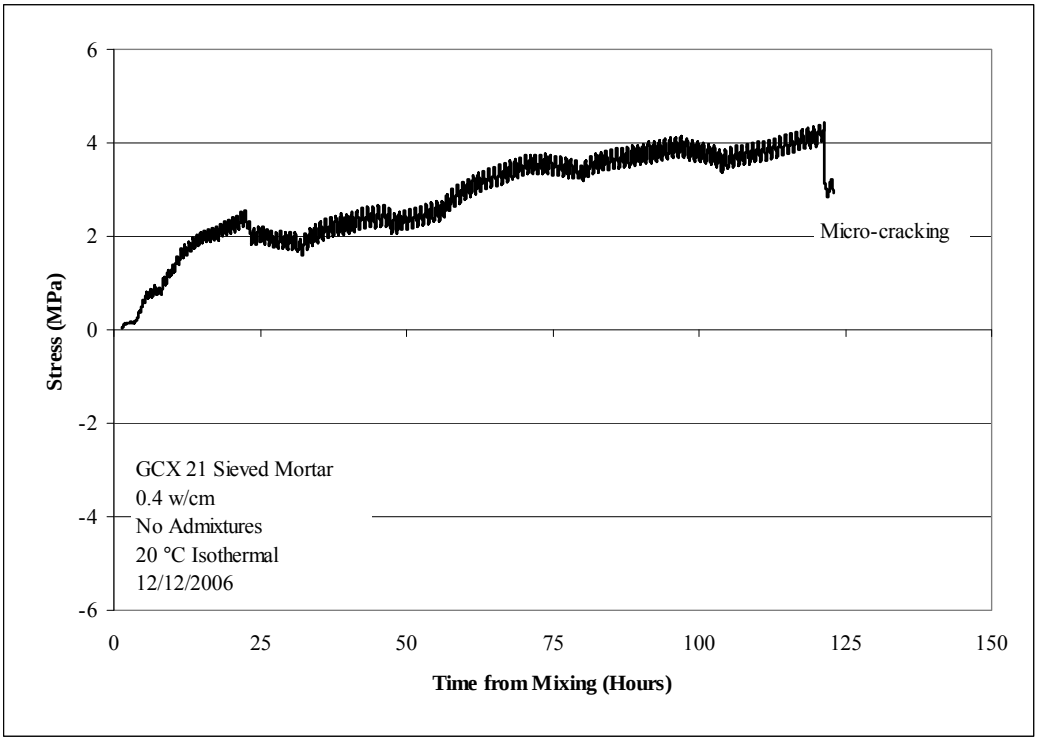

Figure 5.6: Stress generation for 20 °C isothermal test, GCX 21

As indicated in Figure 5.6 this mixture was a sieved mortar. This test was part of a concrete mixture cast in the standard rigid cracking frame and the smaller rigid cracking frame used for this research project. Due to the scaled size (1/3) of the rigid cracking frame, the concrete is sieved over a 9.5 mm sieve to obtain on the mortar fraction of the concrete for placement in the rigid cracking frame. From the temperature profile in Figure 5.5, and to a lesser extent, the stress generation in Figure 5.6, it can be seen that temperature control was still well-maintained for this test but there was much more fluctuation than in previous testing (e.g.,, 20 ± 2 °C). This was later corrected for in the software program, but the results definitely indicated the generation of tensile stress in this mixture. The level of tensile stress obtained is about twice as high as that obtained with micro-concrete at +4 MPa at 120 hours. Upon cooling the mortar rapidly exhibited micro-cracking after only a slight decrease in temperature (~17 °C). At this point, the

test was stopped to allow for the testing of other mixtures. Table 5.1 shows the mechanical property development for this test determined from match-cured cylinders also made of sieved mortar.

Table 5.1: Mechanical properties for 20 °C isothermal test, GCX 21, sieved mortar

Age (days)	Compressive Strength (MPa)	Elastic Modulus (GPa)	Tensile Strength (MPa)
0.2	5.2	-	-
0.3	24.9	29.3	-
0.4	35.8	39.8	-
1.1	56.1	45.8	-
3.3	59.9	48.5	8.0
6.2	64.2	47.6	-
28.3	67.4	55.5	8.3

Both compressive strength and the elastic modulus rapidly increased in the first several hours after casting the mixture. In fact by 10 hours the sieved mortar had already reached a compressive strength of 35.8 MPa. This increased to 56.1 MPa by 1 day after casting. The test ended after 6.2 days and the mortar was then placed into a moist cure chamber (fog room) at 23 ± 2 °C and 100% relative humidity (R.H.). No conversion was evident in this mixture after 22 days moist cure (28 days of age since mixing).

Figure 5.7 shows the temperature profile for the GCX 21 companion concrete mixture cured at 20 °C isothermally in the standard rigid cracking frame. The temperature of concrete cylinders in the match-cured box was not available for this test so the free deformation frame temperature is shown in this figure as FS T. Figure 5.8 shows the stress generation for the same mixture and Figure 5.9 shows the free deformation data for this test from the standard free deformation frame. Table 5.2 shows the mechanical property development for concrete cylinders (100 mm in diameter by 200 mm in length) cast from this mixture.

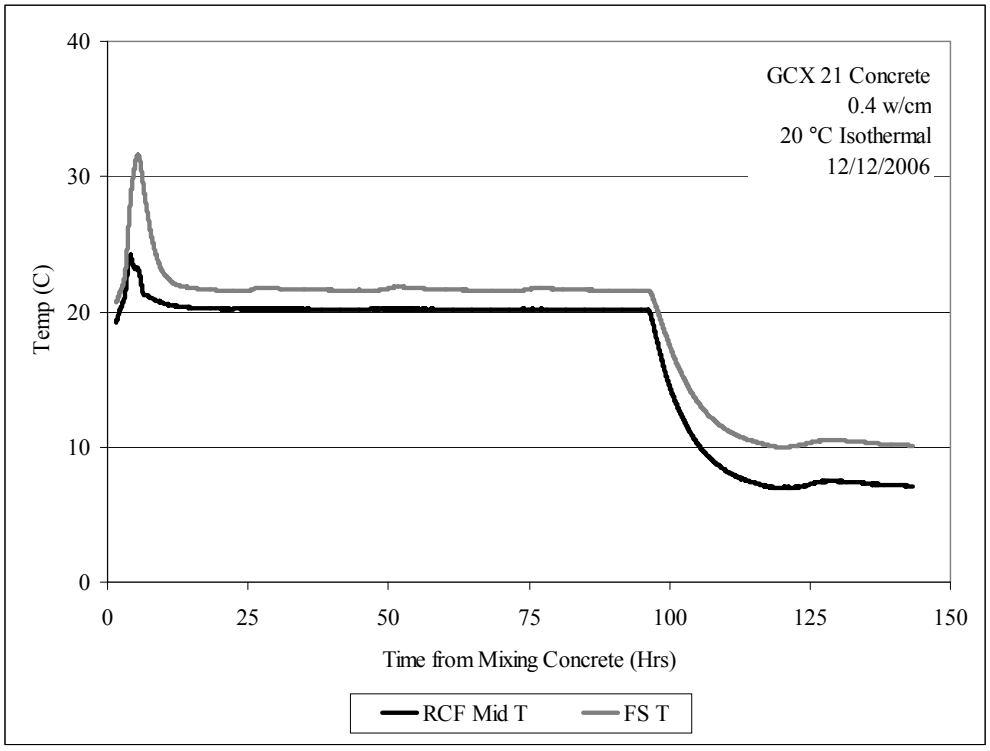

Figure 5.7: Temperature profile for 20 °C isothermal test, GCX 21 (concrete)

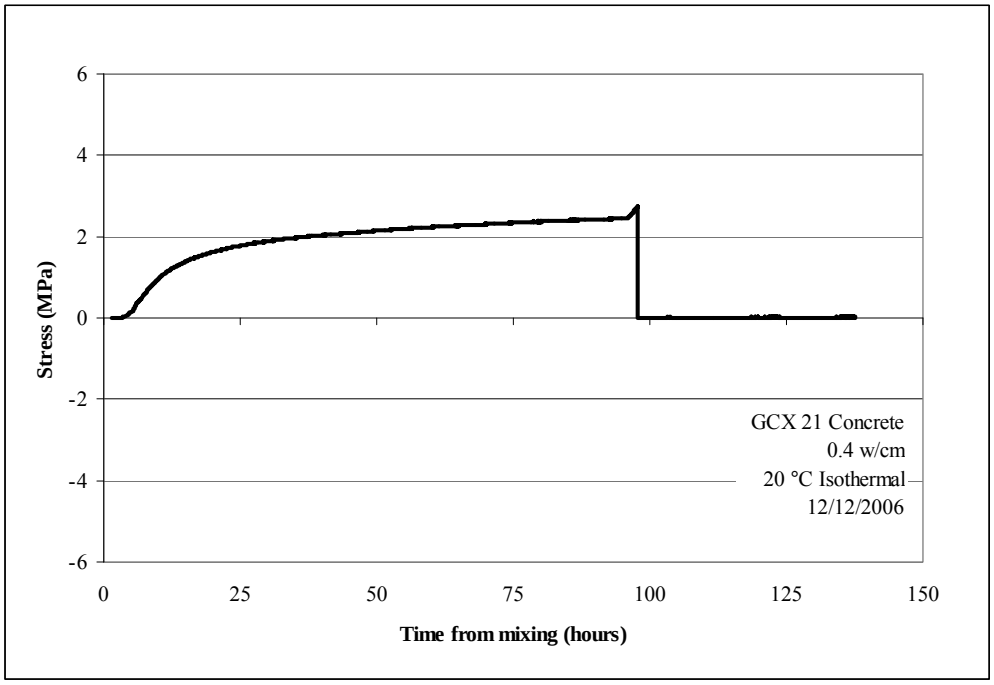

Figure 5.8: Stress generation for 20 °C isothermal test, GCX 21 (concrete)

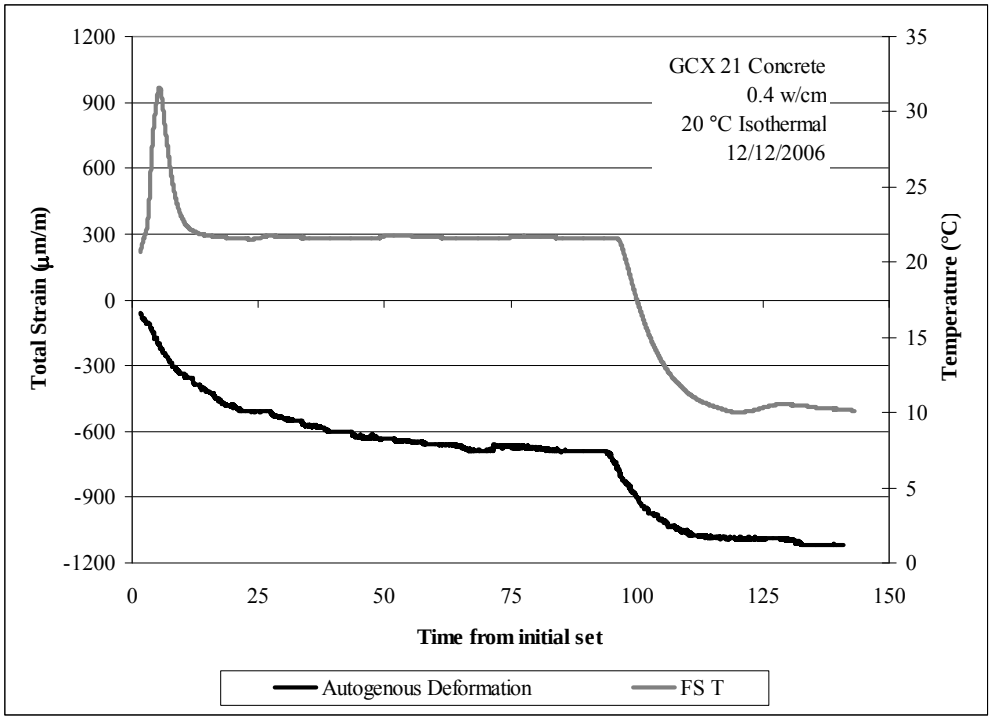

Figure 5.9: Free deformation for 20 °C isothermal test, GCX 21 (concrete)

Table 5.2: Mechanical properties for 20 °C isothermal test, GCX 21 (concrete)

Age (days)	Compressive Strength (MPa)	Elastic Modulus (GPa)	Tensile Strength (MPa)
0.3	37.1	27.5	3.7
0.4	40.7	33.9	4.7
1.1	49.4	31.0	6.8
3.2	54.3	33.1	6.2
6.2	52.3	33.1	6.9
28.3	61.5	37.9	6.8
66.3	51.2	42.3	-

Temperature control for this mixture as shown in Figure 5.7 was a greater challenge in the standard frames than it was in the smaller frames. The same piping size and circulating water bath is used to control the standard frames as the smaller frames, so it was expected that temperature control would be more difficult. The temperature of the concrete in the rigid cracking frame remained much closer to the desired 20 °C

isothermal temperature. However, the temperature in the free deformation frame rose by 12 °C just after final setting of the material. Within 8 hours this temperature was brought back to 20 °C, however five 5 kg bags of ice as well as cooled water were used to try and maintain temperature control of this mixture. The results from this comparison testing indicated that scaling the frames by one-third while keeping the same size for internal cooling pipes and the same circulating water baths was an important decision for testing calcium-aluminate cement micro-concrete and mortar. The stress generation for this mixture, shown in Figure 5.8 indicates the same behavior as that observed in the smaller rigid cracking frame. Tensile stress immediately develops in the sample after setting to a value just over +2 MPa after 100 hours in the rigid cracking frame. Upon cooling the mixture cracked almost immediately at a tensile stress of +2.7 MPa. This value was less than the tensile stress at cracking (+4.4 MPa) for the sieved mortar tested in the scaled frames at 20 °C isothermally.

Despite the 12 °C temperature rise to 32 °C during the initial hydration of this concrete mixture, the free deformation of the specimen shown in Figure 5.9 indicates that shrinkage behavior still dominated despite the temperature increase in this time period. This indicates that even though the temperature increased during this time period the formation of the metastable hydrates in this temperature range (predominantly CAH_{10}) promoted the development of shrinkage and resulted in tensile stress development in the rigid cracking frame. Shrinkage continued to a value of approximately 700 μm/m before artificial cooling at 100 hours.

Mechanical properties shown in Table 5.2 show a rapid strength gain in the first 24 hours after casting this concrete mixture. Strength increased to 61.5 MPa at an age of 28 days. At 66 days the strength had dropped to 51.2 MPa and was indicative of the initiation of conversion in this sample. Elastic modulus and splitting tensile strength

show a gradual increase throughout the testing period, although a splitting tensile test was not performed at 66 days of age, so the effects of conversion could not be evaluated on splitting tensile strength at this age. The ratio of splitting tensile stress to splitting tensile strength at the time of cracking was lower than would be expected for ordinary portland cement concrete at a value of 0.4.[29, 46]

5.5.1.3 GCX Binder, micro-concrete

Figure 5.10 and Figure 5.11 show the temperature profile and stress generation for a mixture tested at 20 °C isothermally in order to repeat this test for micro-concrete mixture proportions. In this figure the temperature in one of the cross-head regions is shown (RCF CH1 T) since it deviated from the desired isothermal temperature of 20 °C in the first 24 hours of this test. It is shown in bright blue to highlight this slight decrease to 18 °C.

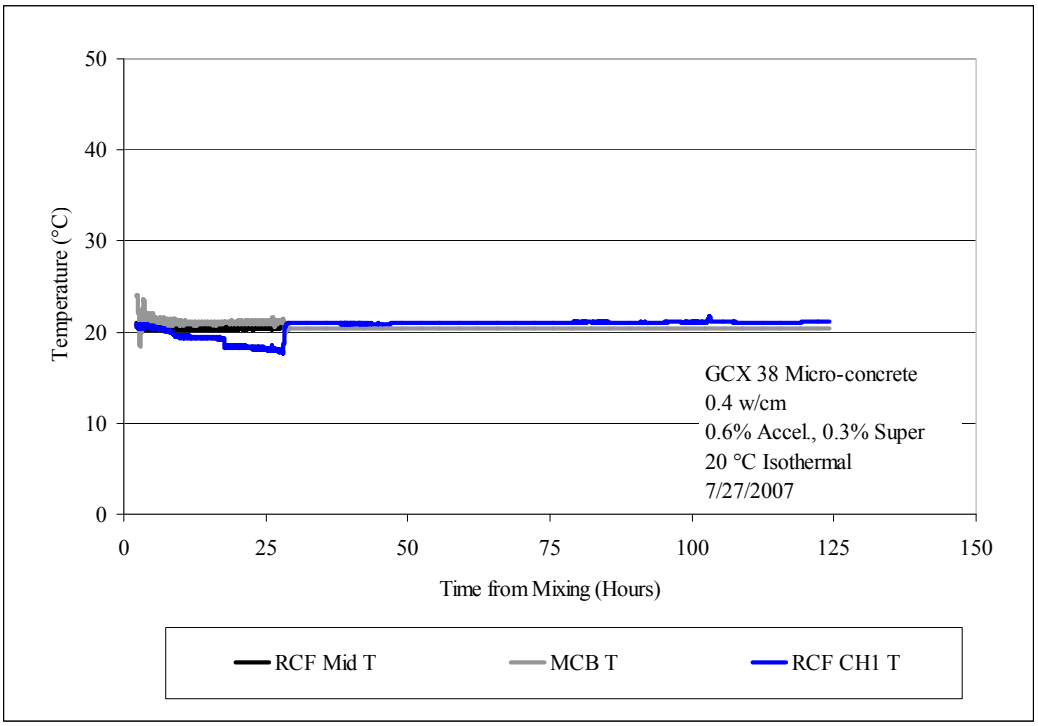

Figure 5.10: Temperature profile for 20 °C isothermal test, GCX 38

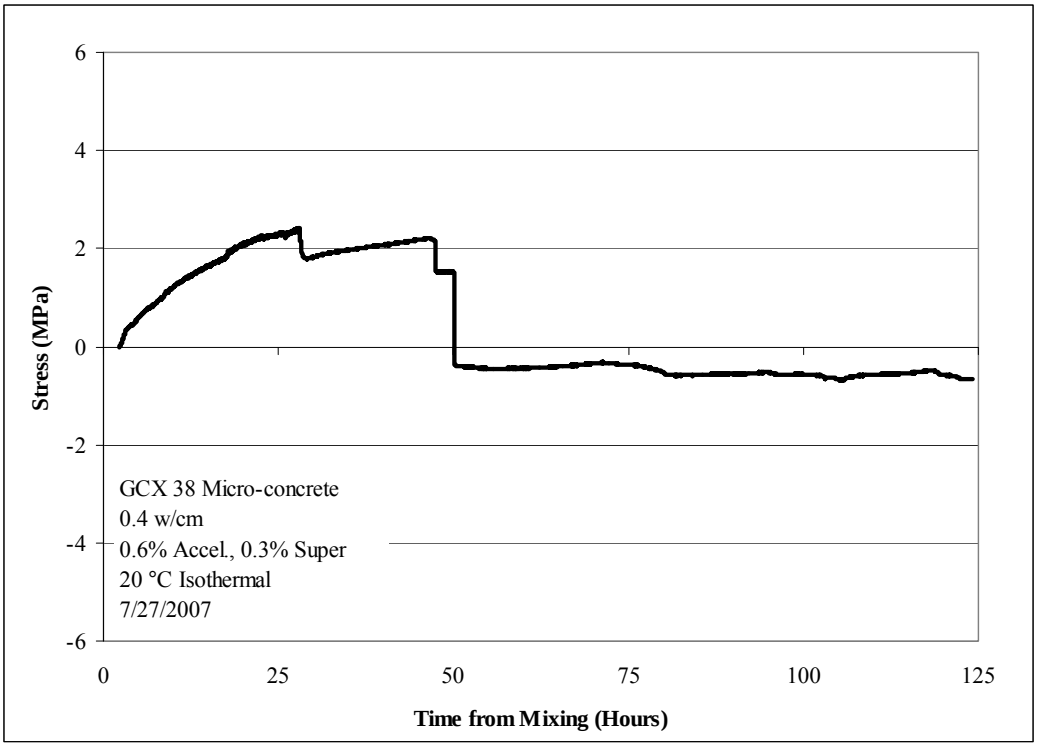

Figure 5.11: Stress generation for 20 °C isothermal test, GCX 38

Temperature control for this mixture was much more uniform than that for GCX 21 in that the oscillation within a 3 °C temperature range was not present in GCX 38. However, there was a slight decrease in temperature within the first 24 hours of the test to a minimum of 18 °C before cooling. However, this variation of 2 °C has little if any effect on the results of the testing. Since the isothermal temperature remained well below 30 °C, the predominant hydrate formed was CAH_{10}.[1] Tensile stress developed immediately in this mixture and increased to a value just over +2 MPa at about 28 hours after casting. At this point slight micro-cracking can be observed with the slight drop in stress to just below +2 MPa, however stress then increases again until more cracking is evident around 50 hours after casting of this mixture. The measured stress dropped immediately just after 50 hours and then no more tensile stress developed after this point due to the cracked state of the mixture. It is important to note that cracking and stress

relief are complex phenomena. For this mixture several cracks in the mid-section of the micro-concrete sample were observed upon demolding. However a complete separation or through-crack was not observed, likely explaining why the stress did not drop completely to 0 MPa as would be expected with a through-crack.

Autogenous deformation (labeled free strain) from the free deformation frame and temperature from one of the thermocouples is shown in Figure 5.12. The free strain confirms the generation of tensile stress in the rigid cracking frame with shrinkage to 1000 μm/m before artificial cooling at 120 hours after casting. This amount of shrinkage confirms the high level of tensile stress observed in the rigid cracking frame.

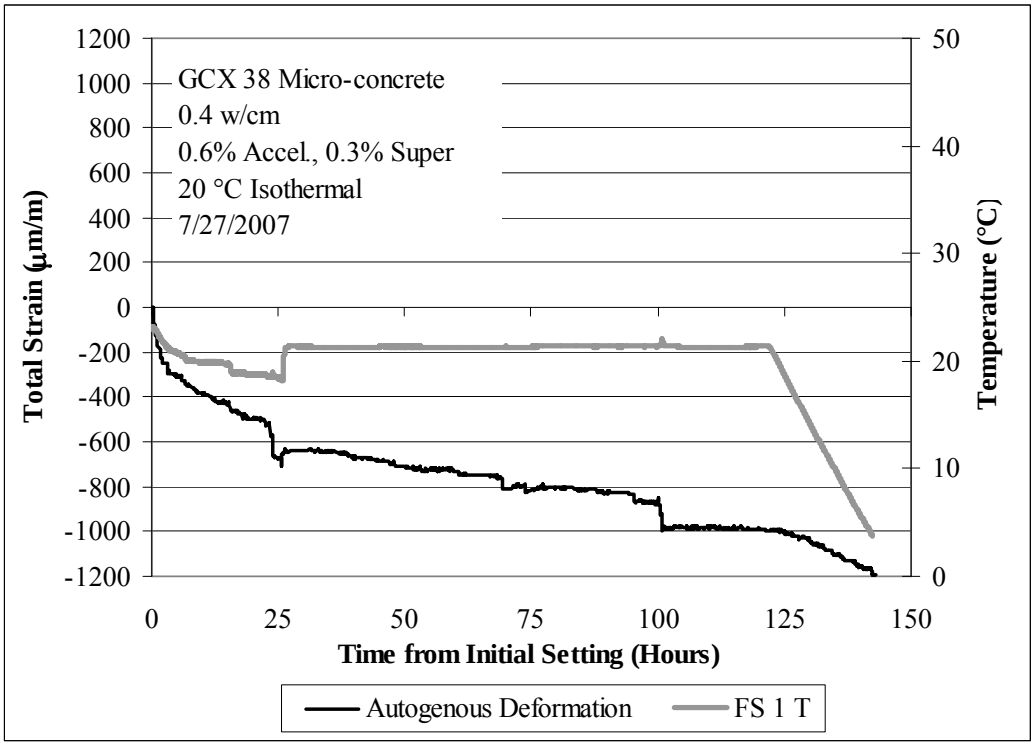

Figure 5.12: Free strain for 20 °C isothermal test, GCX 38

Table 5.3 shows the mechanical property development determined from match-cured cylinders for this mixture up to the end of the testing period.

Table 5.3: Mechanical properties for 20 °C isothermal test, GCX 38

Age (days)	Compressive Strength (MPa)	Elastic Modulus (GPa)	Tensile Strength (MPa)
0.2	34.1	22.9	4.2
1.2	40.2	26.8	6.6
3.2	35.0	33.6	7.0
5.2	39.7	34.5	6.1

Compressive strength increased to 40.2 MPa at one day after testing. However a slight reduction in compressive strength was observed after 3 days (35.0 MPa) and then it increased again slightly (39.7 MPa) at 5.2 days. The elastic modulus continued to increase to 34.5 GPa at 5.2 days while tensile strength decreased slightly to 6.1 MPa at 5 days. At the time of cracking in the rigid cracking frame (roughly 1 day) the ratio of tensile stress to splitting tensile strength at cracking was roughly 0.3. Concrete specimens are known to crack at ratios less than 1.0 (unity) for the following reasons:

- Splitting tensile strength overestimates direct tensile strength (as tested in the rigid cracking frame)[47]
- the rapid loading rate of the splitting tensile test gives a higher measured tensile strength than the true concrete tensile strength when loaded slowly as is the case with thermal stresses[46]

While splitting tensile strength is often higher than the stress required to induce a crack in essentially a direct tensile test (like the rigid cracking frame) this ratio of 0.3 is considerably less than that observed for OPCC systems.

The temperature profile and stress generated for the final mixture cast at 20 °C isothermally are shown, respectively, in Figure 5.13 and Figure 5.14.

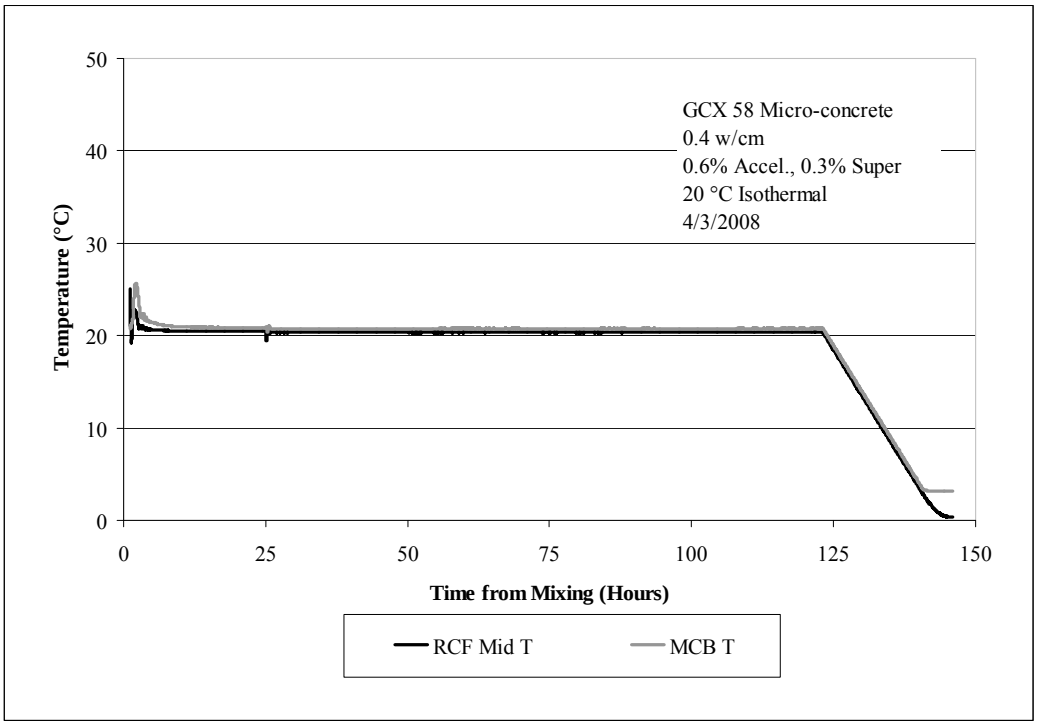

Figure 5.13: Temperature profile for 20 °C isothermal test, GCX 58

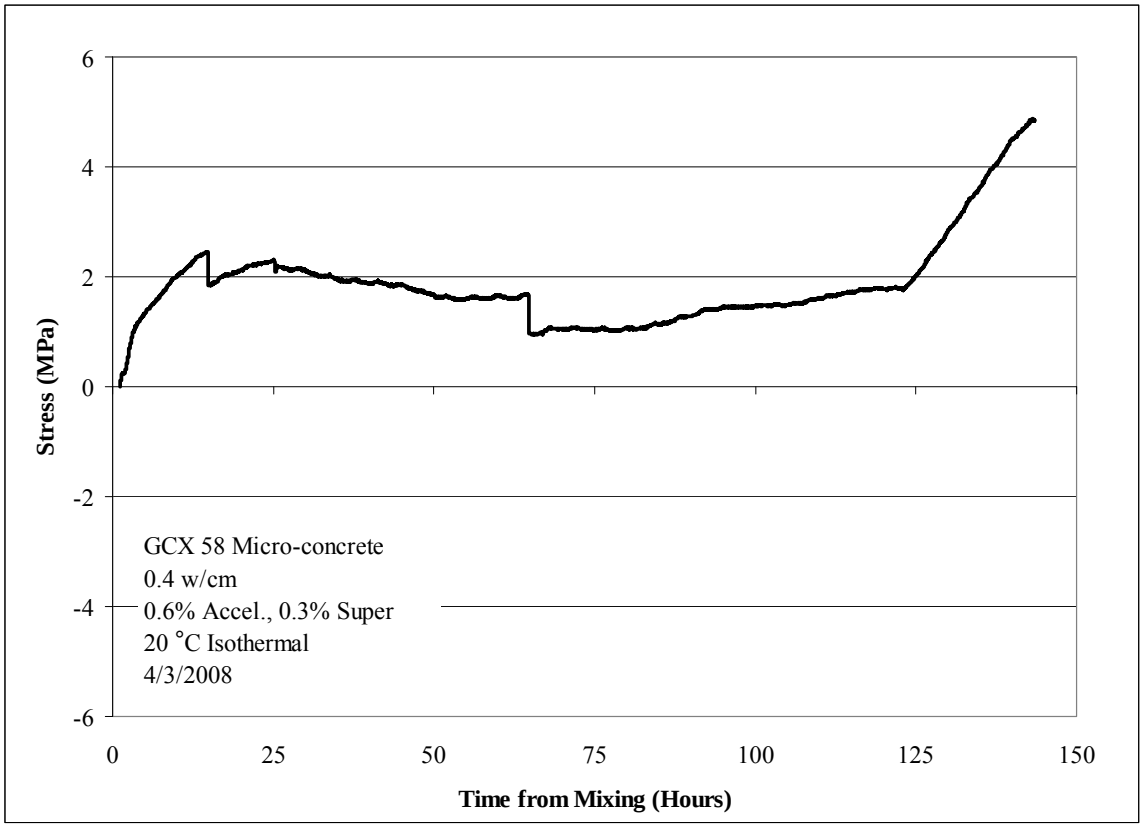

Figure 5.14: Stress generation for 20 °C isothermal test, GCX 58

Consistent temperature control was obtained for this mixture with an isothermal temperature of 20 ± 1 °C (until artificial cooling) as shown in Figure 5.14. Again this mixture exhibited tensile force generation immediately after measurement with micro-cracking evident at about 15, 25 and 60 hours. After removing the formwork, two cracks were observed in the micro-concrete and emanated from the first tooth in the cross-head on opposite ends and on opposite sides (i.e. diagonally) for about 25 mm inward to the micro-concrete before becoming invisible to the naked eye. A through-crack did not occur in this mixture and upon cooling tensile stress reached a maximum value of + 4.8 MPa at 143.5 hours after casting. Free strain results are shown in Figure 5.15.

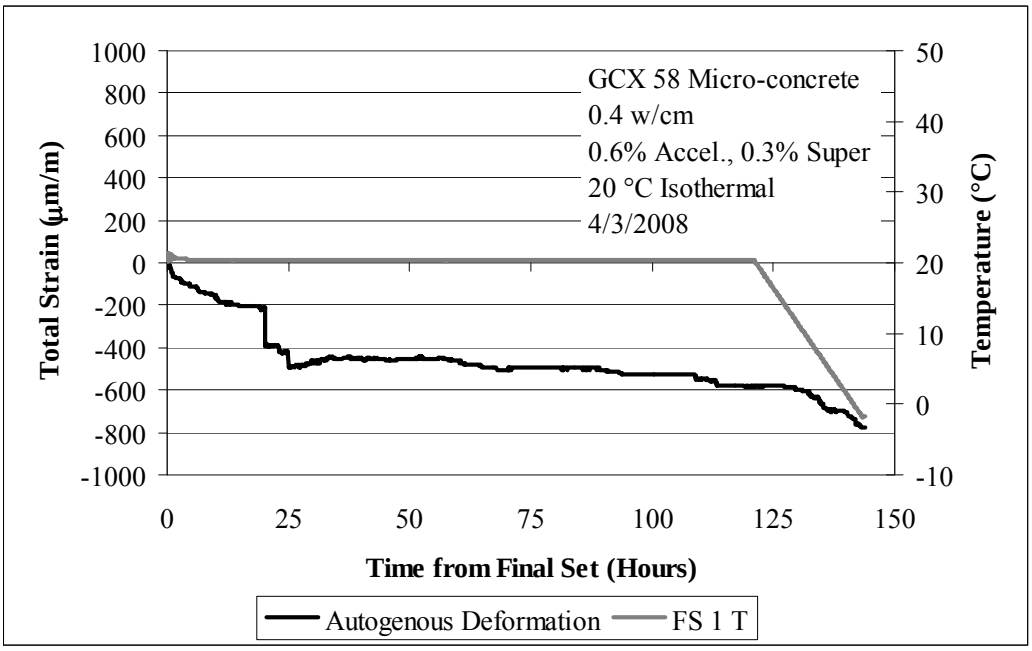

Figure 5.15: Free strain for 20 °C isothermal test, GCX 58

A shrinkage of 600 μm/m was observed in autogenous deformation testing for this mixture and again confirmed the development of tensile forces in the rigid cracking frame as a result of shrinkage. This mixture did shrink less than the same mixture, GCX 38 (1000 μm/m before artificial cooling), investigated previously. Table 5.4 shows the mechanical properties for this 20 °C isothermal mixture.

Table 5.4: Mechanical properties for 20 °C isothermal test, GCX 58

Age (days)	Compressive Strength (MPa)	Elastic Modulus (GPa)	Tensile Strength (MPa)
0.2	26.6	21.4	2.9
1.3	37.0	29.6	6.7
6.4	40.9	33.2	7.8

The ratio of tensile stress to splitting tensile strength was slightly higher for this mixture compared to GCX 38 with a value of 0.37.

5.5.1.4 OPC – ASTM C 150 Type I, micro-concrete

Testing performed in the rigid cracking and free deformation frame was also done with an ordinary portland cement binder as a reference to a more studied material. An ASTM C 150 Type I cement as described in Chapter 3 was used for this testing.[39] Mixtures were only cast and cured at 20 °C isothermally and the results are presented in this section.

Figure 5.16 and Figure 5.17 show the temperature profile and stress generation of an OPC micro-concrete tested at 20 °C isothermally in the rigid cracking frame. Figure 5.18 show the results of testing this same mixture in the free deformation. These are the same mixture proportions for the majority of the rigid cracking frame mixtures shown in chapter 2 with a w/cm of 0.40.

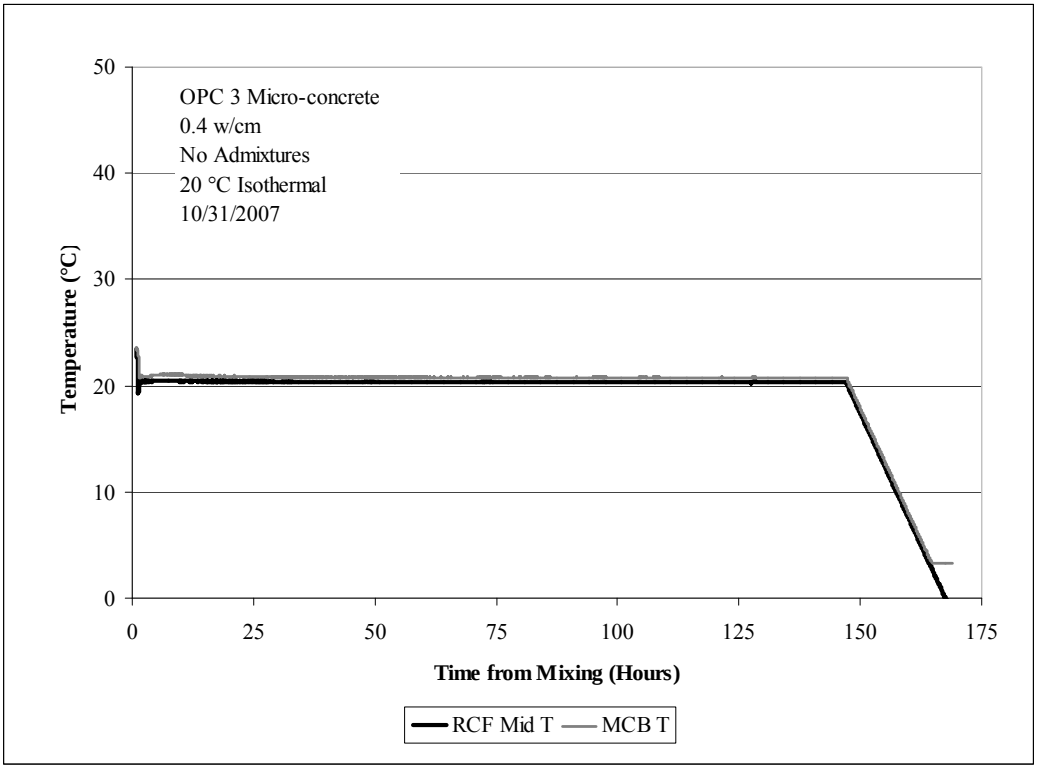

Figure 5.16: Temperature profile for 20 °C isothermal test, OPC 3

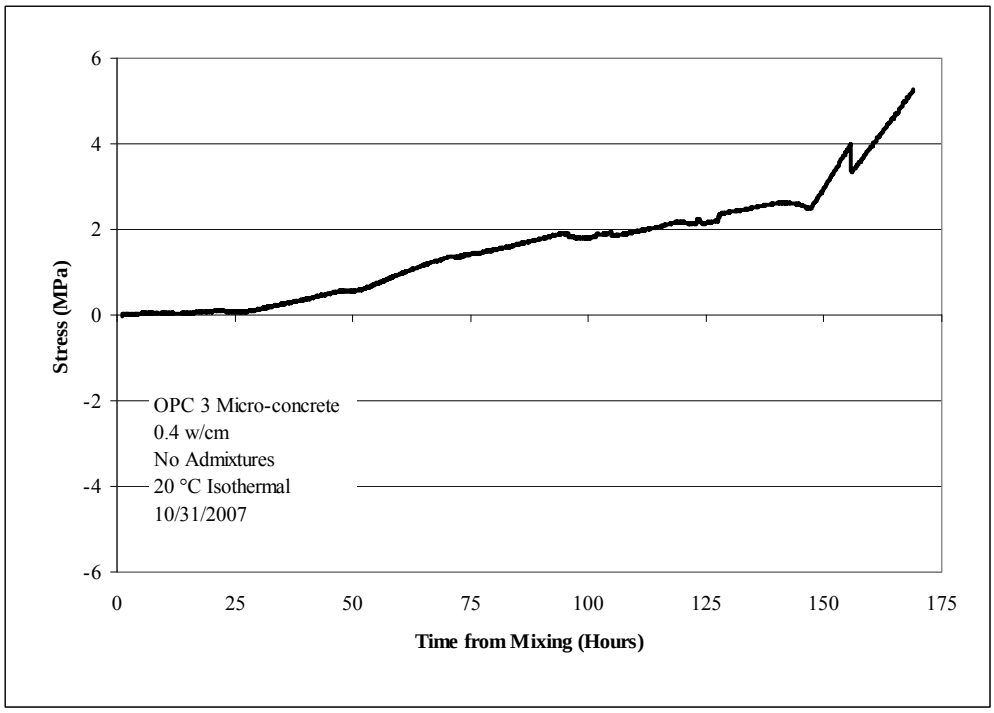

Figure 5.17: Stress generation for 20 °C isothermal test, OPC 3

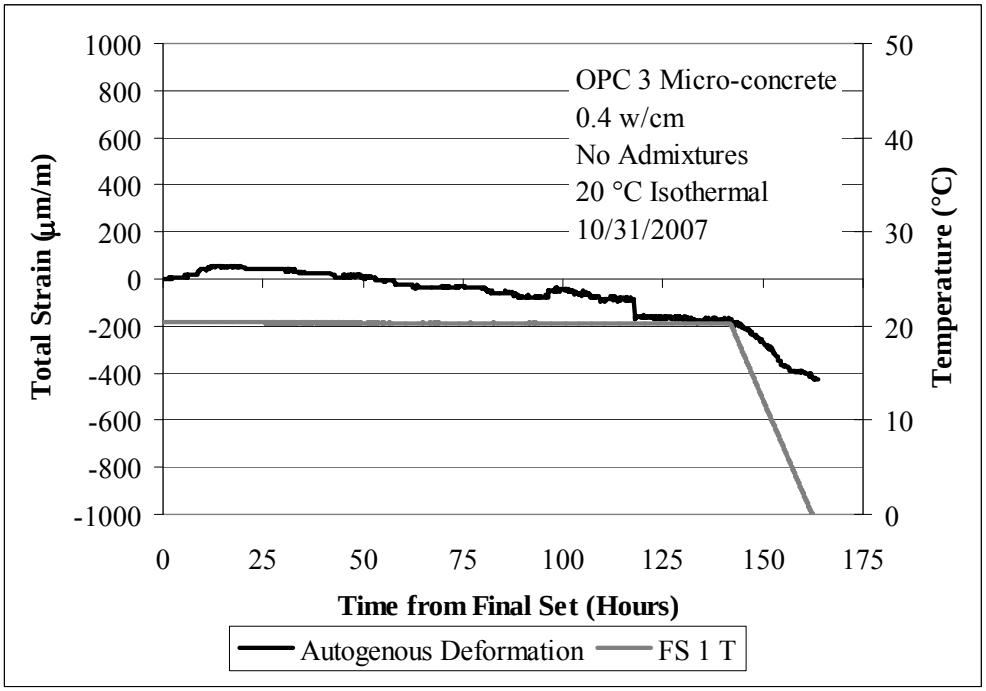

Figure 5.18: Free strain for 20 °C isothermal test, OPC 3

Tensile forces developed in isothermal testing at 20 °C where OPC was used as the binder in a micro-concrete. However, in comparison to the GCX binder, it took approximately three times as long to reach the same level of tensile stress in the OPC micro-concrete. In the first 24 hours of testing very little stress developed and this is substantiated by minor movement in free deformation testing as shown in Figure 5.18. In fact a slight increase in autogenous expansion, was observed for this mixture up to roughly 24 hours of testing commensurate with little stress development in the rigid cracking frame. After this point shrinkage was observed in the free deformation frame to 200 μm/m up to 150 hours of testing with more shrinkage observed upon artificial cooling to 400 μm/m. Tensile forces were observed to develop in the rigid cracking frame at about 24 hours after casting. Upon artificial cooling, minor cracking was observed when the temperature of the concrete was approximately 10 °C (160 hours after casting, 10 hours after artificial cooling). Table 5.5 shows the mechanical properties for this mixture. As expected the OPC mixture has little compressive strength at 10 hours after casting and as a result no elastic modulus testing was performed. Splitting tensile strength was also expectedly low at 0.8 MPa. The compressive strength and elastic modulus steadily increased to up to seven days of age. Tensile strength also increased up to 5.2 MPa at 2.3 days after casting but then decreased slightly to 4.2 MPa at 7.2 days. Interestingly, the mixture exhibited minor cracking at a tensile stress of +4 MPa at roughly the same age (6.6 days) so the ratio of tensile stress at cracking to tensile strength was 0.95 and is much closer than that for the CAC mixture cured under the same isothermal testing conditions.

Table 5.5: Mechanical Properties for 20 °C isothermal test, OPC 3

Age (days)	Compressive Strength (MPa)	Elastic Modulus (GPa)	Tensile Strength (MPa)
0.4	4.4	-	0.8
1.1	18.9	22.8	3.7
2.3	28.7	26.9	5.2
7.2	33.4	31.4	4.2
28.0	-	-	-

5.5.1.5 OPC – ASTM C 150 Type I, in Rigid Cracking and Free Deformation Frames: Standard and Smaller Size

As part of verification testing in the standard rigid cracking and free deformation frames OPC concrete mixtures were tested in both the standard and smaller frames with sieved mortar (material passed the 9.5 mm sieve) cured isothermally at 20 °C with a w/cm of 0.32 in the smaller frames used for this research. The lower w/cm ratio was used as testing was performed in conjunction with another ongoing project at the research laboratory and this was a mixture that we could test in both frames that would be beneficial to both projects. The results of testing in the smaller frames will be shown first. Due to an error with the data acquisition system for the standard frames two mixtures were cast successfully in the smaller frames. Only one mixture was tested successfully in the standard frames and those results will follow the two mortar mixture results. Figure 5.19 and Figure 5.20 show the temperature profile and stress generation for the first mixture in the smaller frames. Table 5.6 shows the mechanical properties for mixture OPC 1.

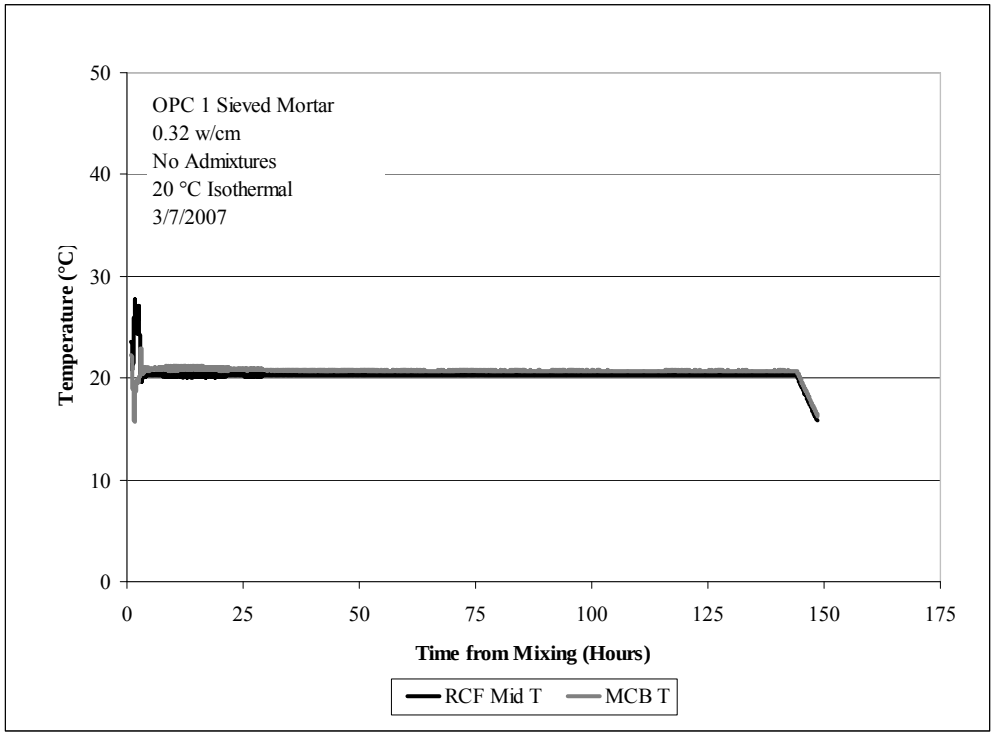

Figure 5.19: Temperature profile for 20 °C isothermal test, OPC 1

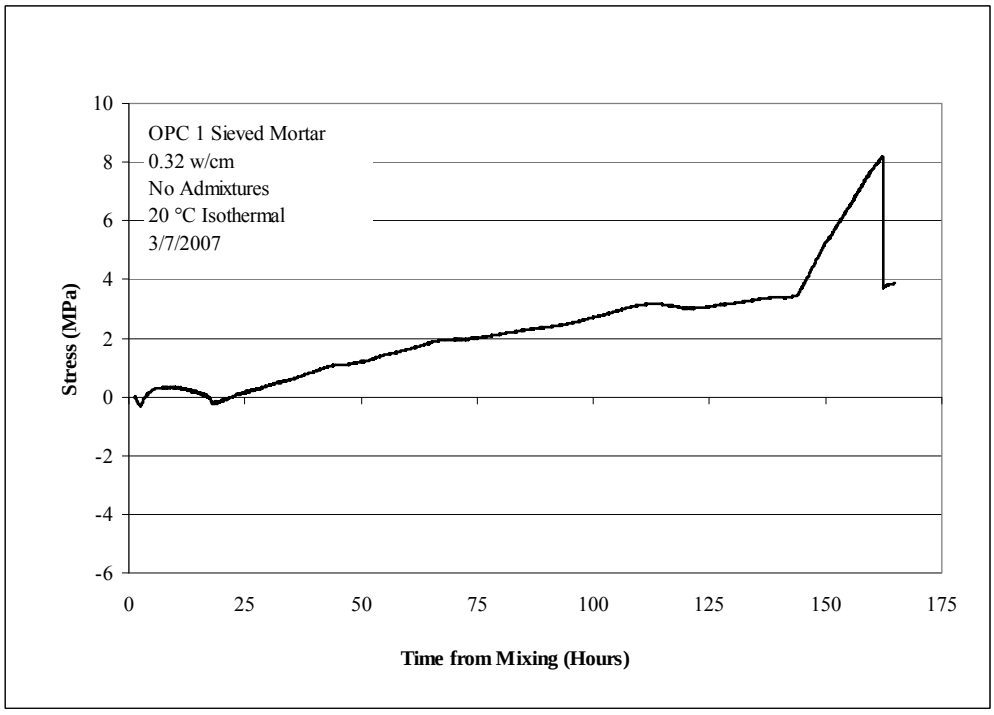

Figure 5.20: Stress generation for 20 °C isothermal test, OPC 1

Table 5.6: Mechanical properties for 20 °C isothermal test, OPC 1

Age (days)	Compressive Strength (MPa)	Elastic Modulus (GPa)	Tensile Strength (MPa)
1.3	37.3	33.8	5.4
5.3	55.3	45.0	7.6
7.2	57.4	42.6	8.5
189.3	57.9	-	-

The temperature profile for OPC 1 showed an initial rapid increase to almost 28 °C in the first five hours after casting, however, after this point temperature remained constant at 20 °C until artificial cooling. The mixture began to go into compression, possibly as a result of this initial increase in temperature and then it exhibited tensile forces in the rigid cracking frame with a slight decrease up to 24 hours. After this point, only tensile forces were observed with steady increase to just over +3 MPa before artificial cooling. As would be expected with a lower w/cm mixture, this mixture developed more tensile stress at an earlier age compared to OPC 3, the micro-concrete mixture. Upon cooling, tensile stress reached a value of approximately +8 MPa before cracking in this test. The ratio of tensile stress at cracking to tensile strength was very close to unity in this test at 0.94.

Figure 5.21 and Figure 5.22 show temperature evolution and stress generation for the second mixture which was a repetition of OPC 1 (results previously shown in Figure 5.19 and Figure 5.20). Table 5.7 shows the mechanical properties for mixture OPC 2 as determined on match-cured samples of the sieved mortar.

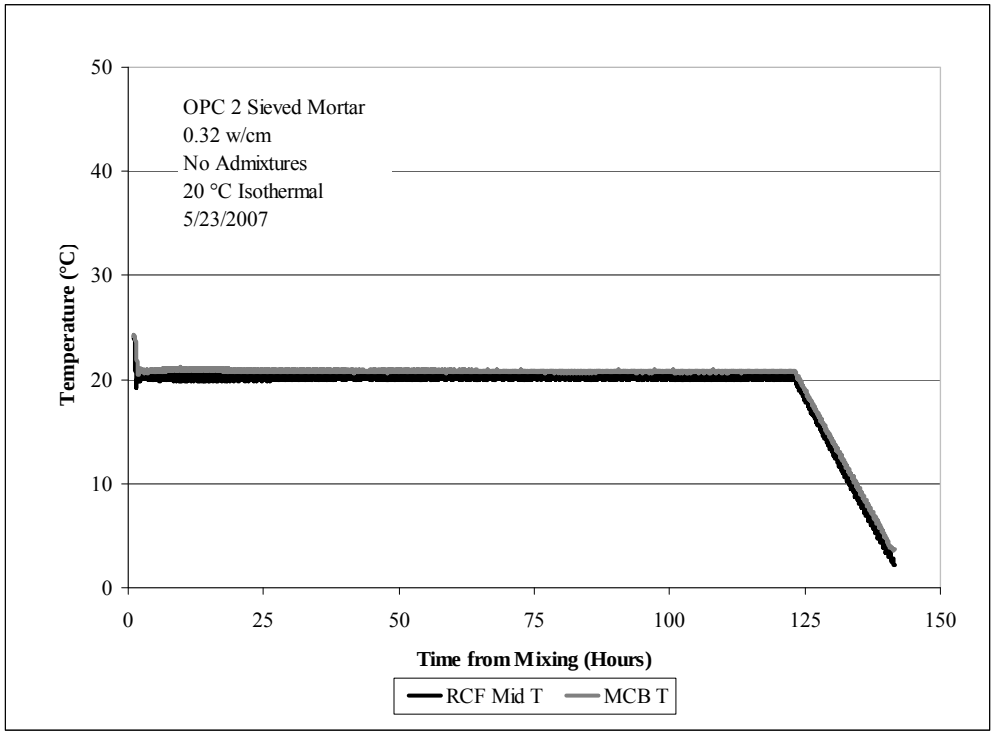

Figure 5.21: Temperature profile for 20 °C isothermal test, OPC 2

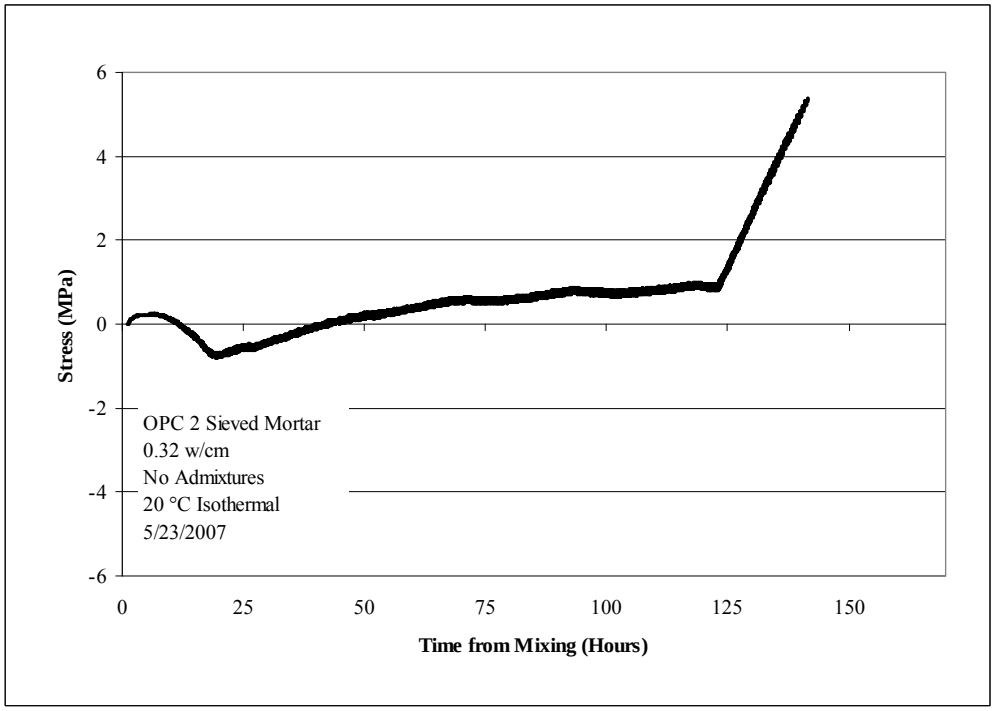

Figure 5.22: Stress generation for 20 °C isothermal test, OPC 2

Table 5.7: Mechanical properties for 20 °C isothermal test, OPC 2

Age (days)	Compressive Strength (MPa)	Elastic Modulus (GPa)	Tensile Strength (MPa)
1.0	30.8	36.2	5.1
6.2	47.1	41.4	7.3

Temperature control for the second sieved mortar mixture, OPC 2 was more consistent than the OPC 1 and there is still an initial development of tensile stress up to 6 hours in the testing regime. However, after this point the material went into compression over the next 14 hours until tensile stress developed again throughout the duration of the testing period. No free deformation data were available for this test to corroborate the development of shrinkage due problems with the data acquisition system. This behavior does have interesting implications in that the mixture did not crack upon cooling. The maximum tensile strength attained at 6.2 days was 7.3 MPa and the maximum tensile stress attained in the rigid cracking frame was just over 5 MPa. From previous strong correlation between tensile stress at cracking to tensile strength at time of failure in this testing apparatus and match-cured specimens this result is expected since the tensile strength of the material was not exceeded by the tensile stress. Since the material generated more compressive stress initially there was essentially more protection or pre-compression built-in to the system to resist the generation of tensile stress upon shrinkage and subsequent artificial cooling.

Concrete from this same mixture (OPC 2) was cast in the standard frames and tested at 20 °C isothermally. Figure 5.23 shows the temperature profile for this mixture in the standard rigid cracking frame and Figure 5.24 shows the resulting stress generation. Figure 5.25 shows the free deformation data and temperature of this specimen. Mechanical properties tested on match-cured concrete samples (100 mm diameter by 200 mm length cylinders) are shown in Table 5.8.

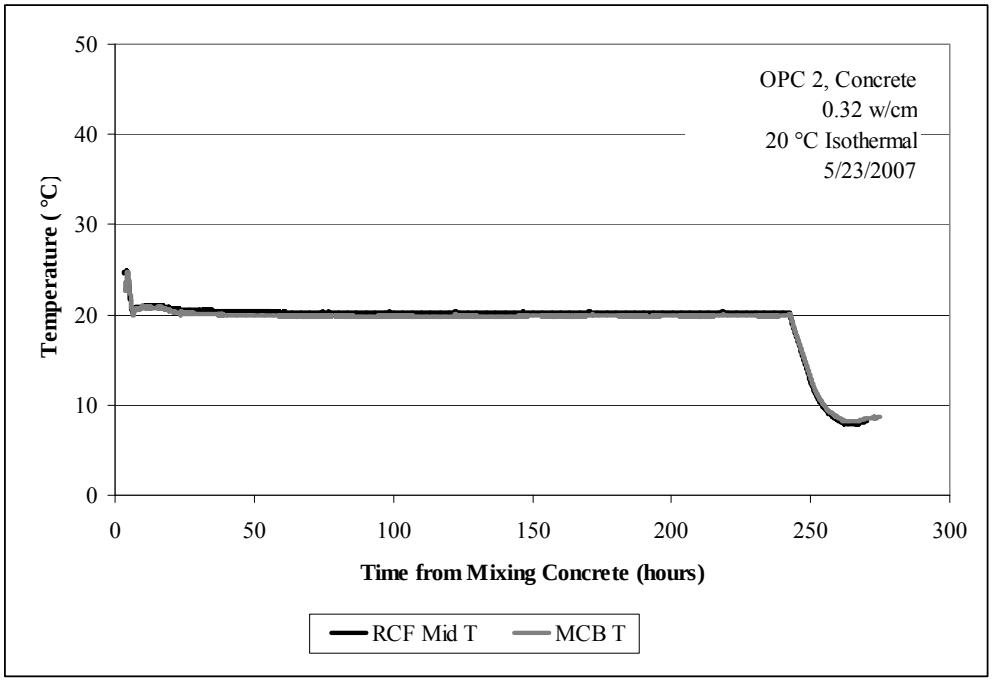

Figure 5.23: Temperature profile for 20 °C isothermal test, OPC 2 (concrete)

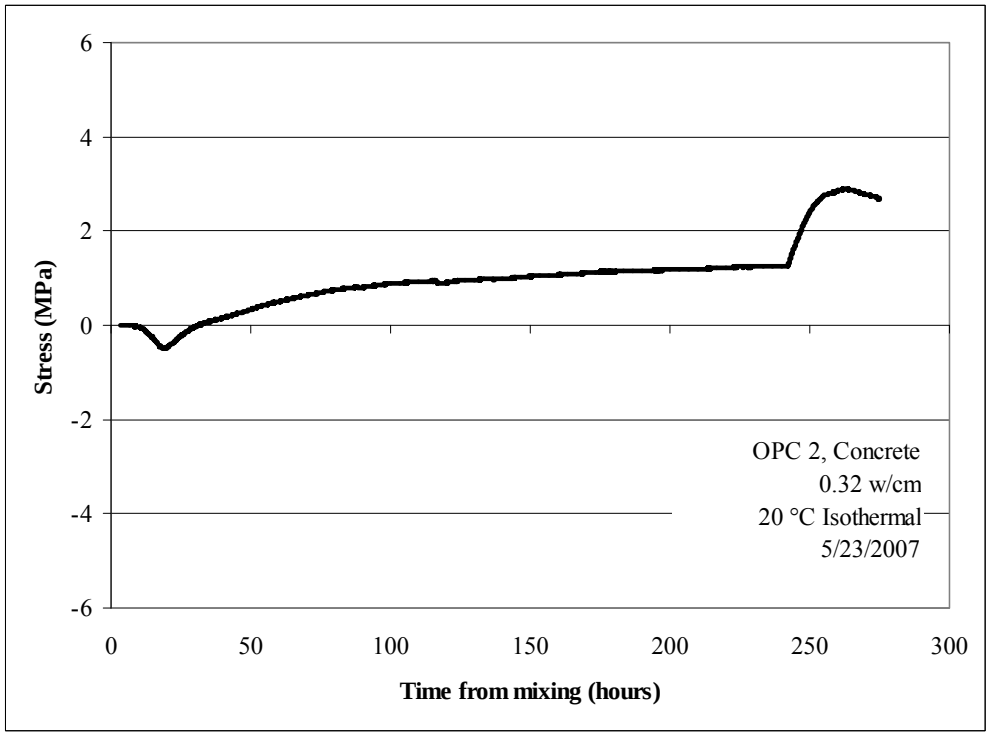

Figure 5.24: Stress generation for 20 °C isothermal test, OPC 2 (concrete)

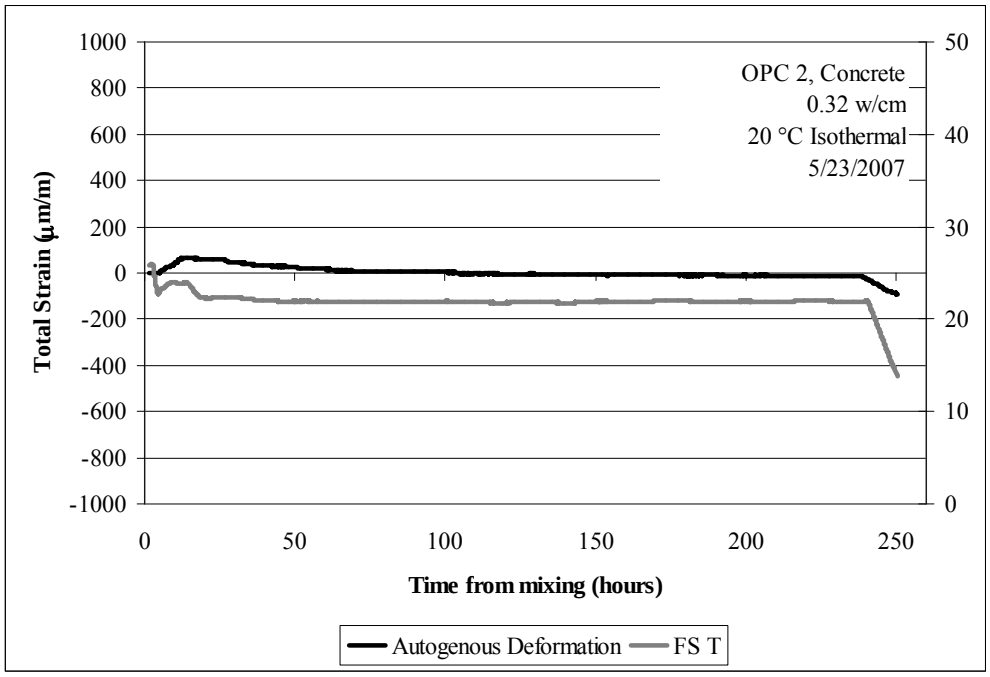

Figure 5.25: Free deformation for 20 °C isothermal test, OPC 2 (concrete)

Table 5.8: Mechanical properties for 20 °C isothermal test, OPC 2 (concrete)

Age (days)	Compressive Strength (MPa)	Elastic Modulus (GPa)	Tensile Strength (MPa)
0.4	1.7	6.2	0.2
0.9	28.8	30.9	3.9
2.2	45.7	37.3	5.2
3.1	48.0	38.0	6.0
7.1	54.2	40.6	5.8
35.2	62.5	41.6	6.3

The temperature profile shown in Figure 5.23 indicates excellent isothermal temperature control for this mixture throughout the isothermal portion of the test. The stress generation shown in Figure 5.24 indicates a slight amount of compressive stress initially developed in the rigid cracking frame followed by the development of tensile stress after 24 hours. Tensile stress continued to increase until artificial cooling after 250 hours of testing. Before cooling the tensile stress in the concrete was +1.3 MPa. Upon

cooling the mixture did not crack in the rigid cracking frame. Free deformation data shown in Figure 5.25 indicates very little movement compared to the calcium aluminate cement concrete shown in Figure 5.9. There is a slight amount of expansion initially followed by shrinkage but the value stays very close to 0 μm/m until artificial cooling where shrinkage to approximately 100 μm/m occurred. Mechanical properties shown in Table 5.8 show that compressive strength, elastic modulus and splitting tensile strength all increased up to 35 days after mixing, as expected for ordinary portland cement concrete. The splitting tensile strength at 7 days was 5.8 MPa and the tensile stress at the end of cooling in the frame was less than this value at just over 5 MPa, and is likely why the mixture did not crack in the rigid cracking frame.

5.5.2 38 °C Isothermal Testing

After several initial tests at 20 °C isothermal the next mixtures investigated were cast in the rigid cracking and free deformation frame and cured at 38 °C isothermally. Since this is well-established testing method used to capture both initial high early strengths associated with metastable hydrate formation (e.g.,, strength at 1 day after casting) and the ultimate low strength associated with conversion of metastable hydrates over the course of several days to stable hydrates it was thought this would be a very useful testing procedure for capturing volume change at early age through the full range of potential hydrate assemblages. The only variation of from the traditional testing method is that match-cured samples were not demolded until they were removed from the water bath for mechanical property testing. Since the micro-concrete in the frames is never in contact with an external moisture source, the micro-concrete samples must be cured in the same way to ensure that property development matches as closely and consistently as possible between the match-cured samples and the micro-concrete in the frames.

5.5.2.1 GCX Binder

The first two mixtures cast at 38 °C isothermal were done at EPFL in Lausanne, Switzerland. The temperature profiles for the first mixture is shown in Figure 5.26 and Figure 5.27 shows the same initial data up to 10 hours of testing. The stress generation for the first mixture is shown in Figure 5.28.

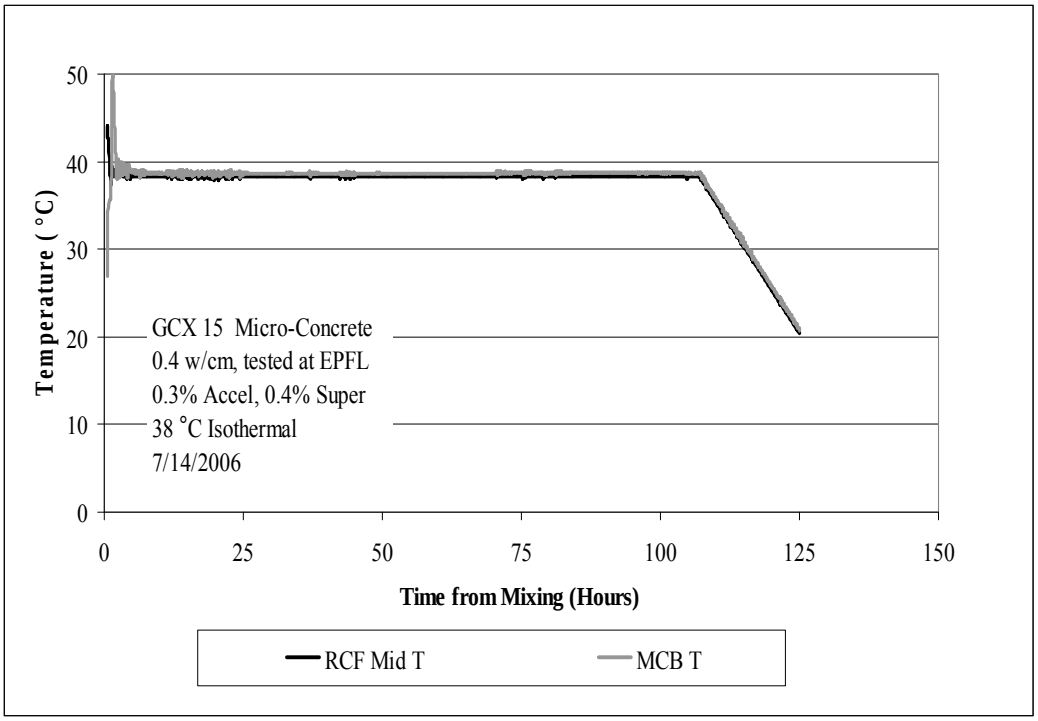

Figure 5.26: Temperature profile for 38 °C isothermal test, GCX 15

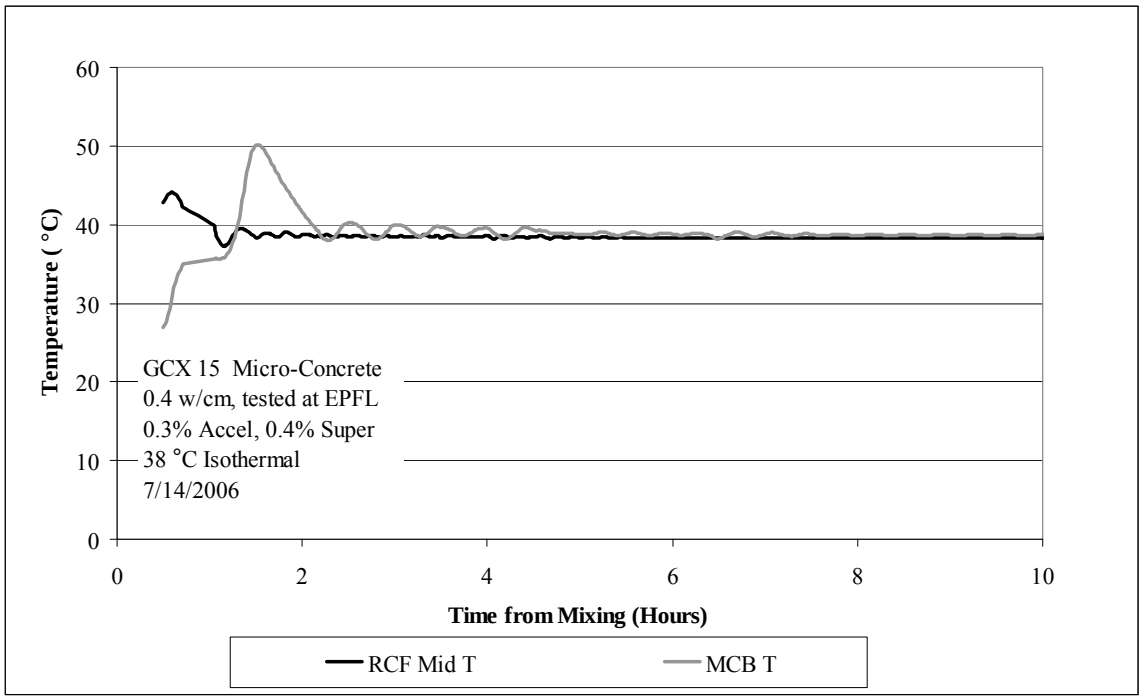

Figure 5.27: Temperature profile (2), for 38 °C isothermal test, GCX 15

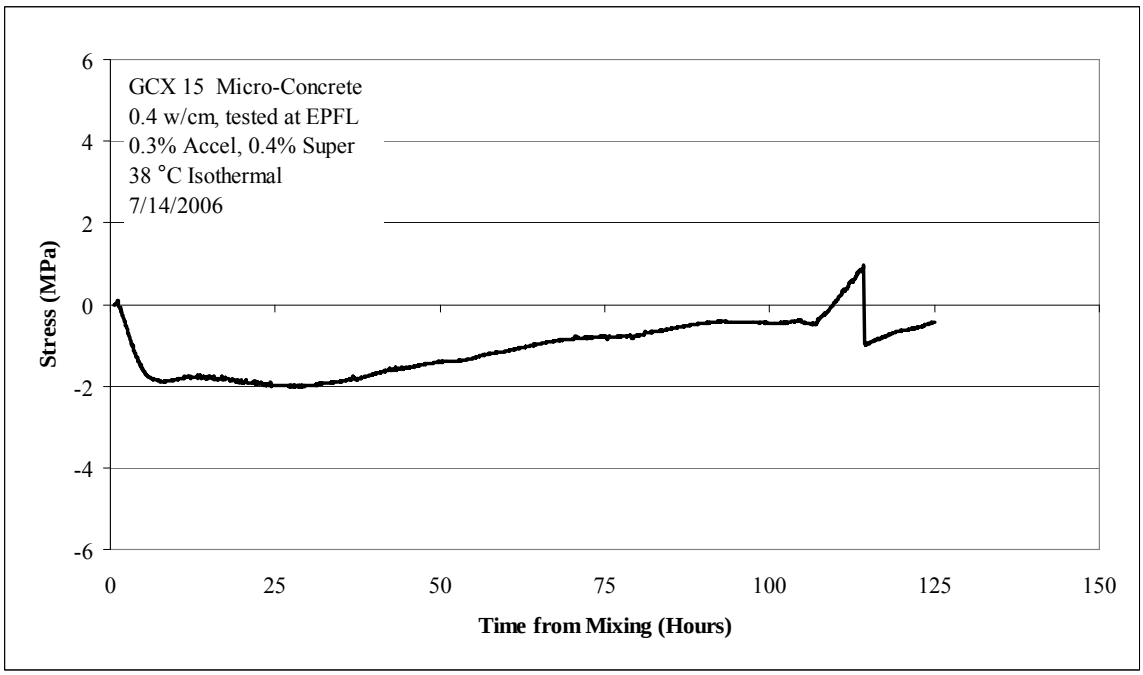

Figure 5.28: Stress generation for 38 °C isothermal test, GCX 15

While the temperature profile for the center of the rigid cracking frame was well-controlled at 38 °C the temperature of the match-cured samples rose to 50 °C as seen in Figure 5.27. After 2.5 hours the temperature control for the match-cured samples was much more consistent and stayed very close to 38 °C after this point as seen in the figure. What was extremely surprising was that this mixture generated compressive forces in the rigid cracking frame which was indicative of expansive phenomena, and since temperature control for the center of the frame was excellent at 38 °C, this was a somewhat unexpected result. The maximum compressive stress attained for this mixture was -2.0 MPa. It can also be seen that throughout the first 100 hours of the testing period that stress gradually reduced to -0.4 MPa until artificial cooling began at about 105 hours. This mixture did crack at a tensile stress of +1.0 MPa. Mechanical property data are not reported for this mixture as micro-concrete was only tested in the frame during the initial testing program.

The second mixture cast and tested at 38 °C isothermal was done immediately after the first mixture while still at EPFL to confirm the surprising results from the first test. The temperature profile for this mixture is shown in Figure 5.29 and with a shorter x-axis in Figure 5.30 . The stress generation for this mixture is shown in Figure 5.31 .

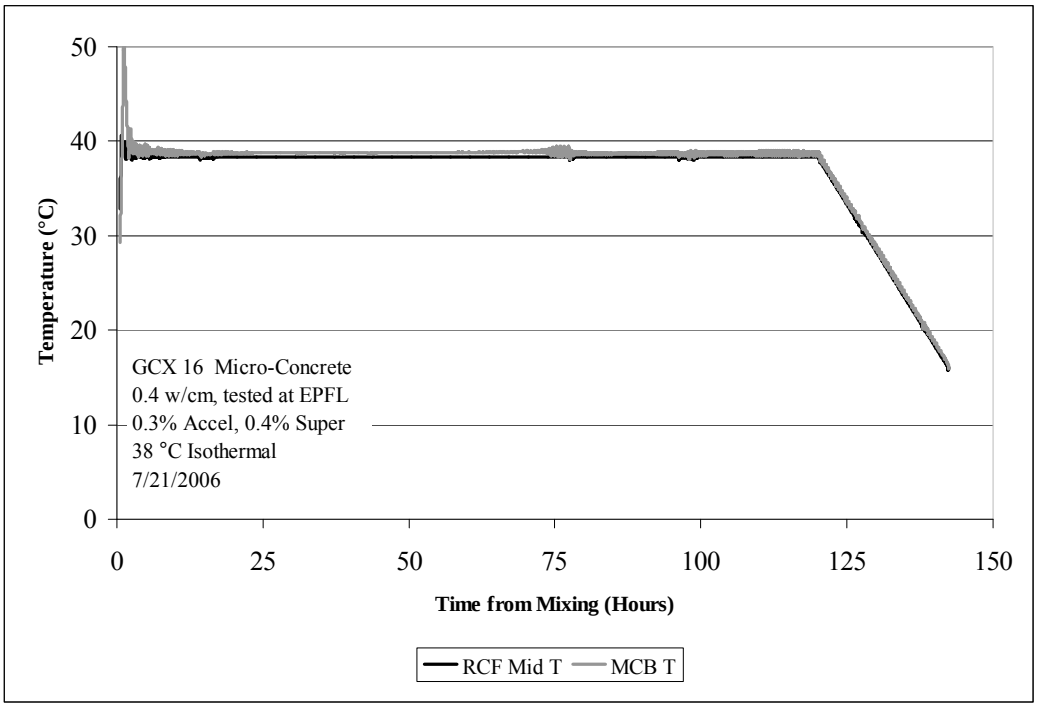

Figure 5.29: Temperature profile for 38 °C isothermal test, GCX 16

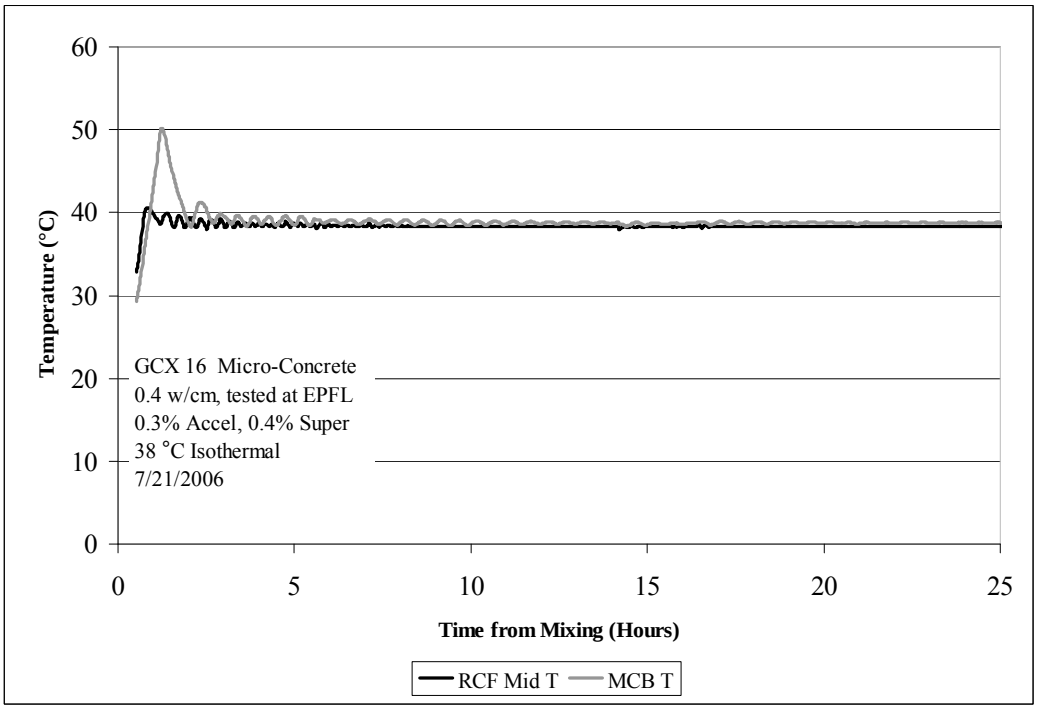

Figure 5.30: Temperature profile, first 25 hours only, for 38 °C isothermal

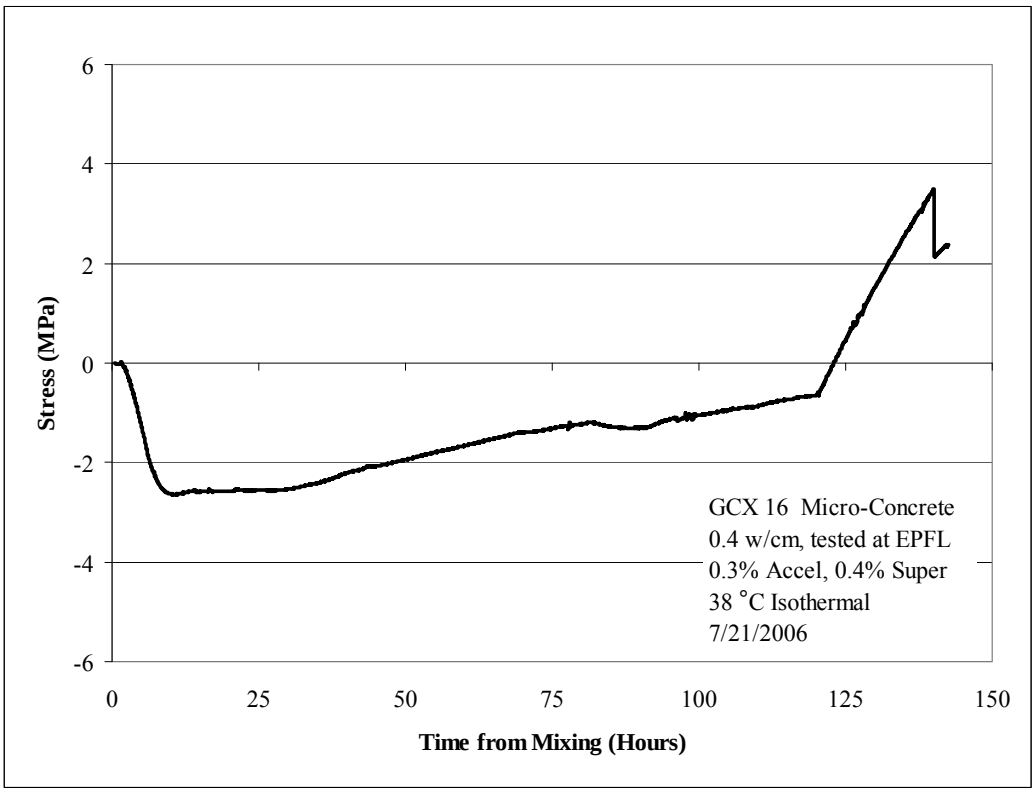

Figure 5.31: Stress generation for 38 °C isothermal test, GCX 16

As in previous testing temperature control was a challenge for the match-cured samples and it took about 2.5 hours to get the temperature under control and close to the isothermal target temperature of 38 °C. The temperature of the micro-concrete in the cracking frame was well-controlled at 38 °C. The stress generation confirmed the results from the first test that compressive stress developed immediately in the rigid cracking frame. The maximum level of stress obtained was slightly greater than GCX 15 at -2.6 MPa at 12 hours after casting. The stress in the frame gradually decreased to -0.5 MPa just before cooling at 120 hours. Upon cooling the mixture was forced further into a state of tensile stress and the mixture cracked at +3.5 MPa at 140 hours after cooling at a temperature of roughly 10 °C. At this point, it was hypothesized that the stress reduction

seen prior to artificial cooling may be a result of the conversion process and this was later tested through comparison to mechanical property development in subsequent mixtures.

The third mixture cast at 38 °C was done in the laboratory at the Concrete Durability Center in Austin, Texas. This was a trial mixture cast to ensure the frame was working properly and that similar results could be obtained without the use of any admixtures (e.g.,, no accelerator and no superplasticizer) as was done with GCX 15 and GCX 16. This mixture was cast prior to casting a full-scale concrete mixture in the standard rigid cracking and free deformation frames in a sense as a proof-of-concept test to make sure that behavior was similar to mixtures with admixtures. Due to the potential for rapid-setting of CACC (with accelerator) compared to OPCC the use of accelerator was avoided for the concrete mixture cast in the standard frames so that isothermal temperature could be better controlled. The temperature profile for this proof-of-concept test is shown in Figure 5.32. The stress generation for this mixture is shown in Figure 5.33. Mechanical properties are shown in Table 5.9.

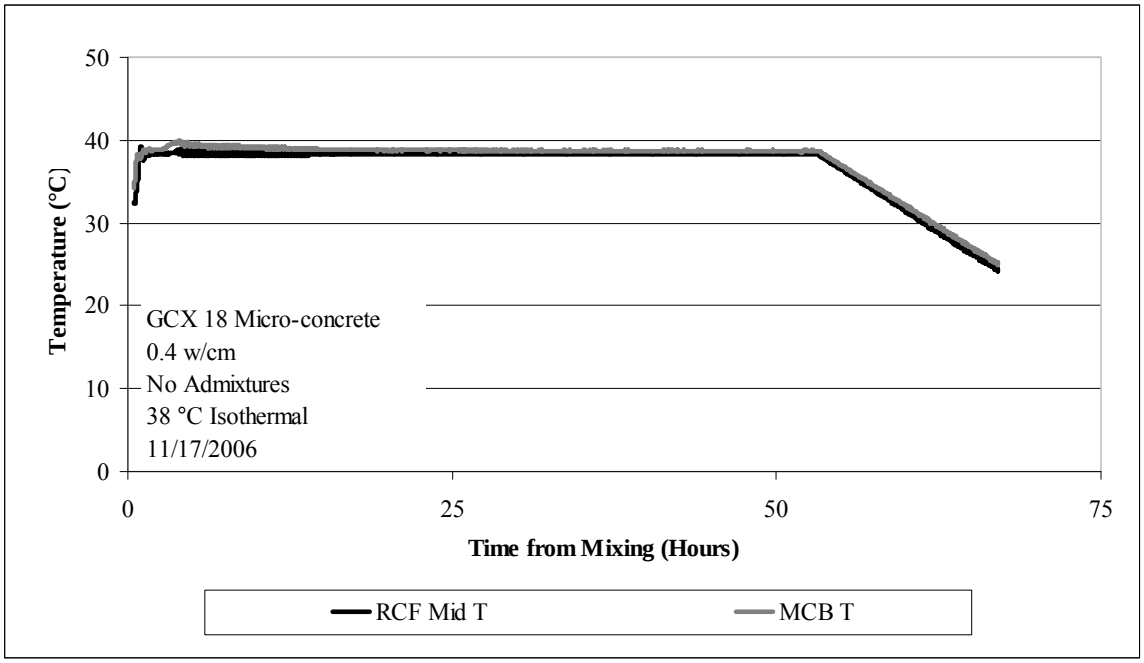

Figure 5.32: Temperature profile for isothermal test at 38 °C, GCX 18

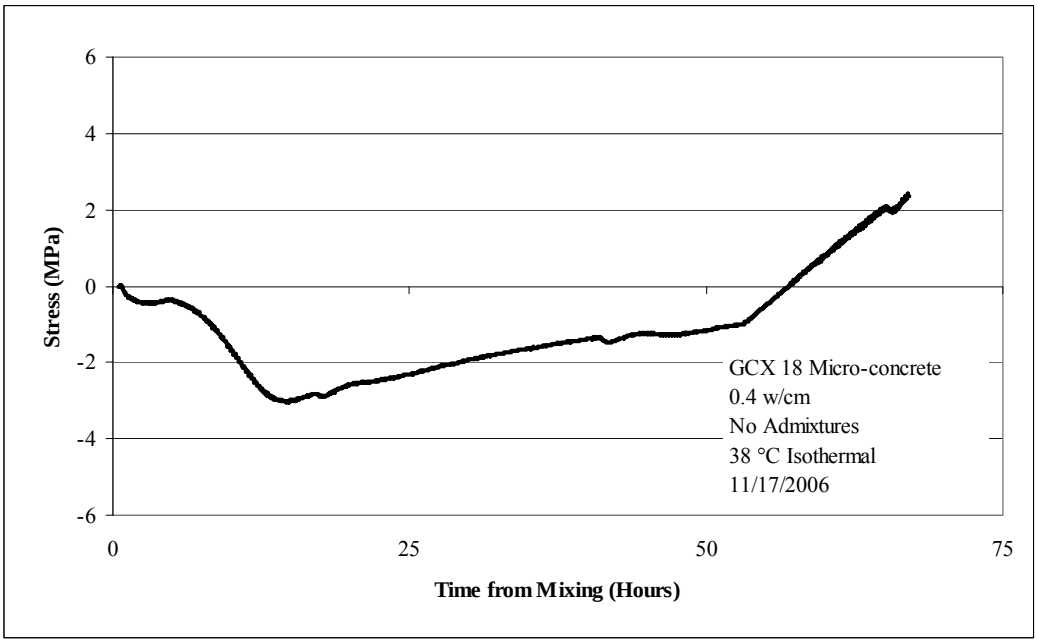

Figure 5.33: Stress generation for isothermal test at 38 °C, GCX 18

Table 5.9: Mechanical properties for 38 °C isothermal test, GCX 18

Age (days)	Compressive Strength (MPa)	Elastic Modulus (GPa)
0.3	10.6	21.5
0.8	37.7	29.6
2.2	38.2	30.6
3.0	47.1	35.5

Temperature control for this mixture was much improved over previous mixtures. A larger insulated food-type cooler was used for the match-cured samples cast from this mixture. The size of the cooler was approximately 142 L compared to the size used at EPFL of 70 L. The greater amount of insulation provided by a larger volume of circulating water may have been responsible for better temperature control in the UT-tested mixture. In addition the mixture contained no admixtures, therefore initial setting time (3.5 hrs) was slightly extended and may have provided additional time for the water baths to maintain 38 °C isothermal conditions before setting of the material (and rapid

heat rise). This may have resulted in a greater ability for the water baths to react to temperature rise due to hydration and subsequently maintain a more consistent 38 °C isothermal temperature. It is shown that compressive stress also developed in this mixture to a maximum value of -3.0 MPa at 15 hours after casting with gradual stress reduction, possibly due to conversion until artificial cooling at 50 hours after testing. A slight micro-crack was developed at a tensile stress of +2.1 MPa, 66 hours after casting or 12 hours after artificial cooling began. Mechanical properties were only monitored for the three-day duration of this proof-of-concept test and, as would be expected, compressive strength and modulus are relatively high (compared to an OPC system) at 1 day of testing at 37.7 MPa and 29.6 GPa, respectively. Both compressive strength and modulus gradually increased until 3 days at which point the testing was stopped. A more thorough description of mechanical property development will be given for future mixtures which were investigated for a longer duration.

5.5.2.2 38 °C Isothermal Testing, GCX Binder in Rigid Cracking and Free Deformation Frames: Standard and Smaller Size

Testing was performed at 38 °C isothermally, to compare results of stress generation and free deformation between the standard frames and the smaller frames used as part of this research. A concrete mixture according to the mixture proportions in Table 3.4 was cast in the standard frames, a portion of the concrete was sieved over a 9.5 mm sieve to obtain mortar for testing in the smaller frames used as part of this study. Results for two sieved mortar mixtures tested at 38 °C in the smaller frames will be shown first followed by results from the standard frames. Figure 5.34 shows the temperature profile for first 38 °C isothermal sieved mortar mixture. Figure 5.35 shows the stress generation for first 38 °C isothermal sieved mortar mixture and Table 5.10 shows mechanical properties for first 38 °C isothermal sieved mortar mixture. Figure 5.36 shows the

temperature profile for second 38 °C isothermal sieved mortar mixture. Figure 5.37 shows the stress generation for second 38 °C isothermal sieved mortar mixture and Table 5.11 shows the mechanical properties for the second 38 °C isothermal sieved mortar mixture.

These figures and tables are for two mixtures cast in the rigid cracking and free deformation frames as part of verification testing where companion mixtures were cast in the standard rigid cracking and free deformation frames. There was an error in the cooling rate for the first mixture which can be seen in the temperature profile. As a result this mixture was repeated. A discussion of these results will follow all four figures and two tables:

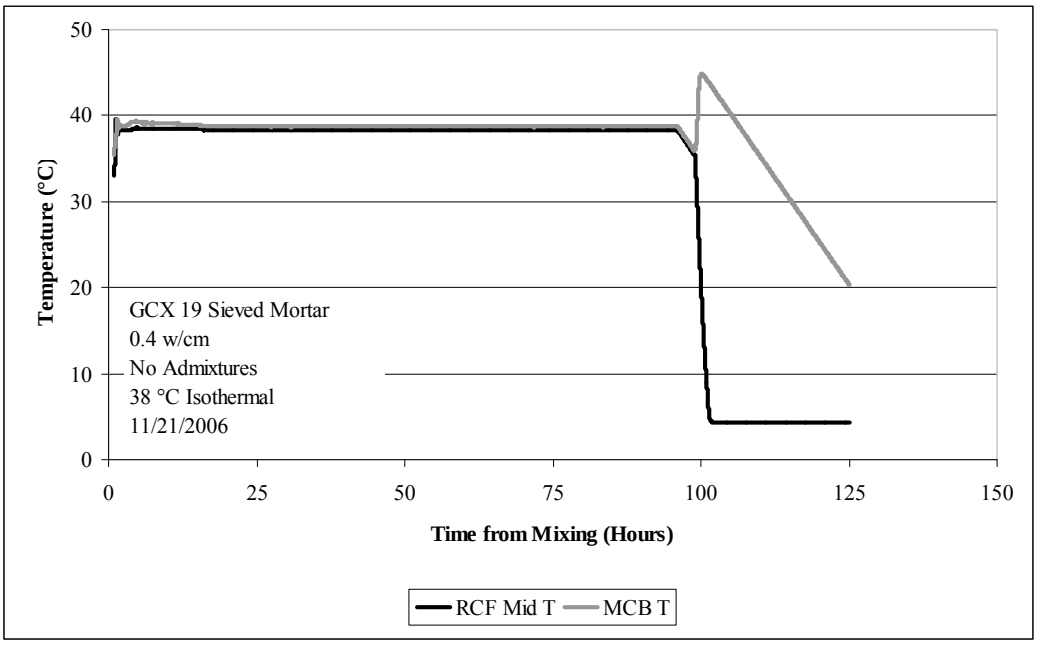

Figure 5.34: Temperature profile for 38 °C isothermal test, GCX 19

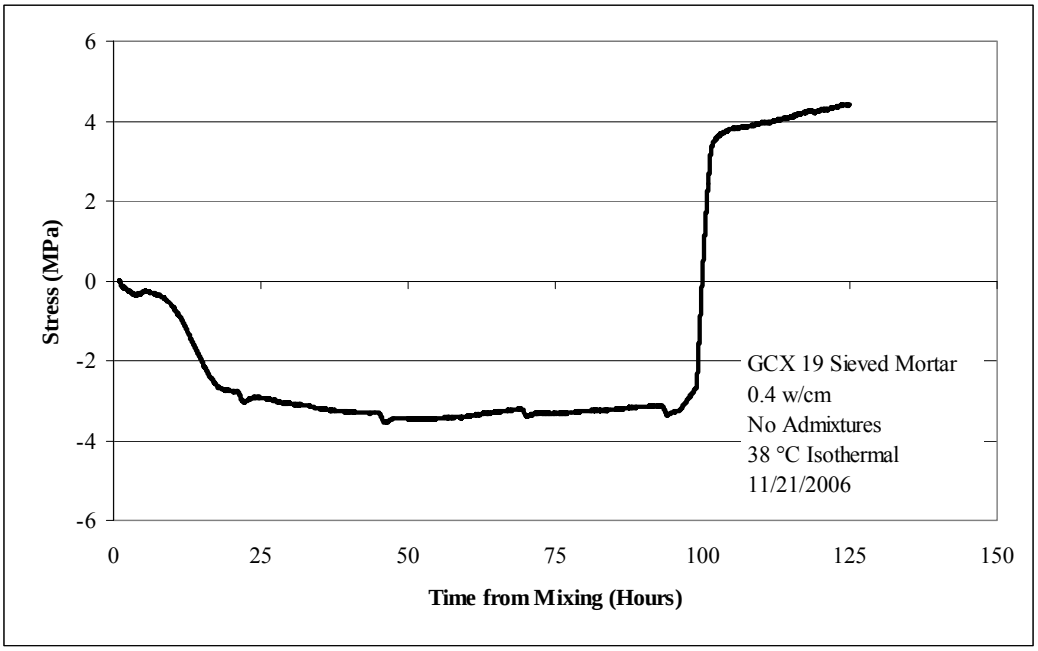

Figure 5.35: Stress generation for 38 °C isothermal test, GCX 19

Table 5.10: Mechanical properties for 38 °C isothermal test, GCX 19

Age (days)	Compressive Strength (MPa)	Elastic Modulus (GPa)	Tensile Strength (MPa)
0.3	11.4	-	-
1.2	41.5	37.7	5.5
4.1	*36.5*	-	-
5.2	*30.4*	-	-
6.3	34.5	38.8	5.9
8.1	35.3	44.5	-

Italics indicates only one test performed

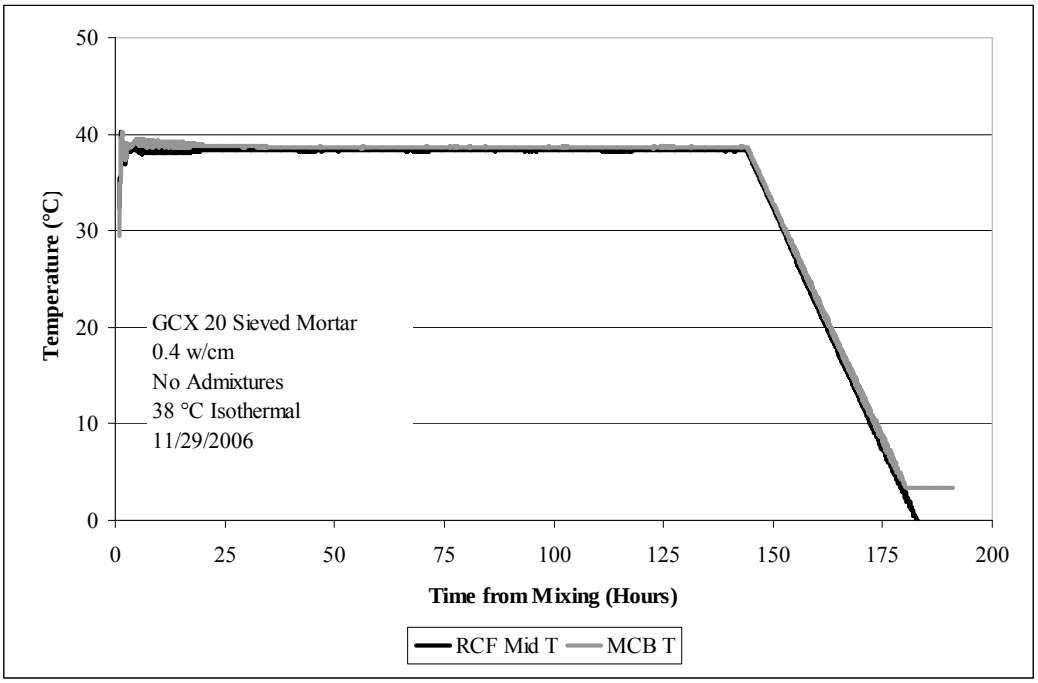

Figure 5.36: Temperature profile for 38 °C isothermal test, GCX 20

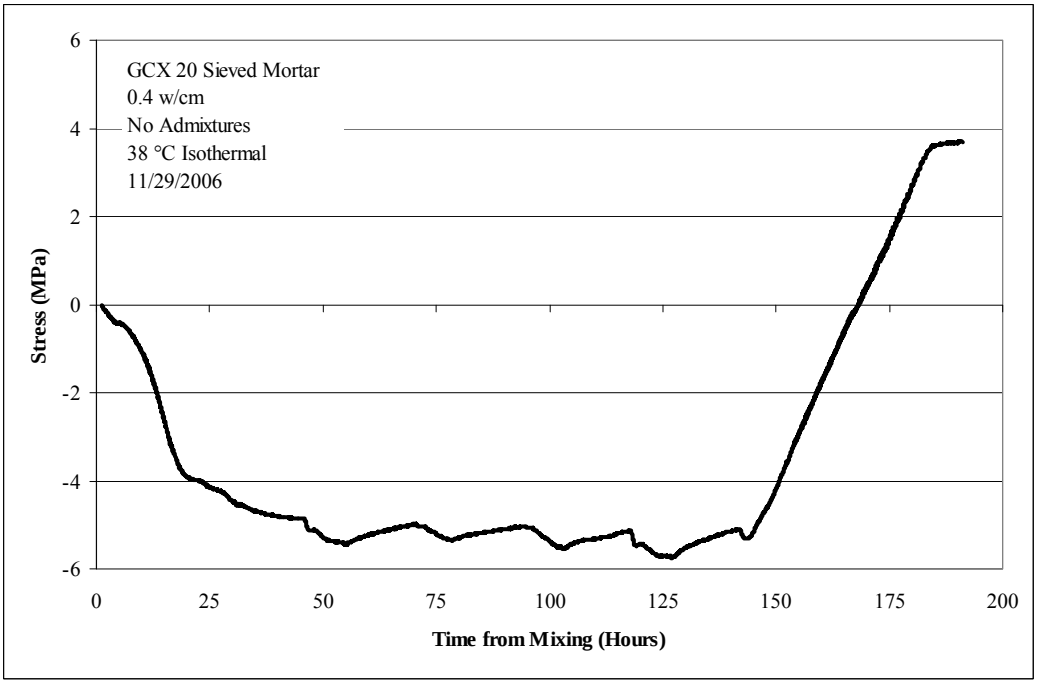

Figure 5.37: Stress generation for 38 °C isothermal test, GCX 20

Table 5.11: Mechanical properties for 38 °C isothermal test, GCX 20

Age (days)	Compressive Strength (MPa)	Elastic Modulus (GPa)
0.3	*3.77*	-
0.4	9.7	32.8
1.1	33.1	37.35
4.2	26.8	38.19
6.1	32.1	41.2

Italics indicates only one test performed

Isothermal temperature control for both mixtures was very close to the target temperature of 38 °C up until cooling. However, as mentioned previously, the cooling rate for the first mixture, GCX 19, was too rapid and was therefore repeated in GCX 20. What is interesting to note is that these are essentially two identical mixtures with the same materials, mixture proportioning and no admixtures. However, the first mixture developed compressive stress to a maximum value of -3.2 MPa during the isothermal range of the test. The second mixture developed compressive stress to a maximum value of almost -6.0 MPa during the isothermal range of the test which is almost twice as high as the first mixture. Upon cooling neither mixture cracked. Tensile strength measurements on match-cured samples from the first mixture were greater than the maximum tensile stress reached at the end of the artificial cooling period so cracking would not be expected in this mixture. Compressive strength results indicate for both mixtures that conversion occurred at approximately 4 days after casting with a gradual strength increase thereafter. In this testing the elastic modulus of the material does seem to be adversely impacted by the conversion process, which is an interesting and somewhat surprising result. It would be expected that a significant decrease in compressive strength would also result in a decrease in elastic modulus. It is important

to note that traditional testing at 38 °C for conversion would place samples in contact with the 38 °C water after 1 day of curing. In this regime the match-cured samples, like the counterpart micro-concrete, are never placed in direct contact with 38 °C water. This may be one factor leading to a less profound impact on compressive strength and the seemingly minimal effect on elastic modulus development.

Figure 5.38 shows the temperature profile for the GCX 19 companion concrete mixture cured at 38 °C isothermally in the standard rigid cracking frame. Figure 5.39 shows the stress generation for the same mixture and Figure 5.40 shows the free deformation data for this test from the standard free deformation frame. Table 5.12 shows the mechanical property development for this mixture.

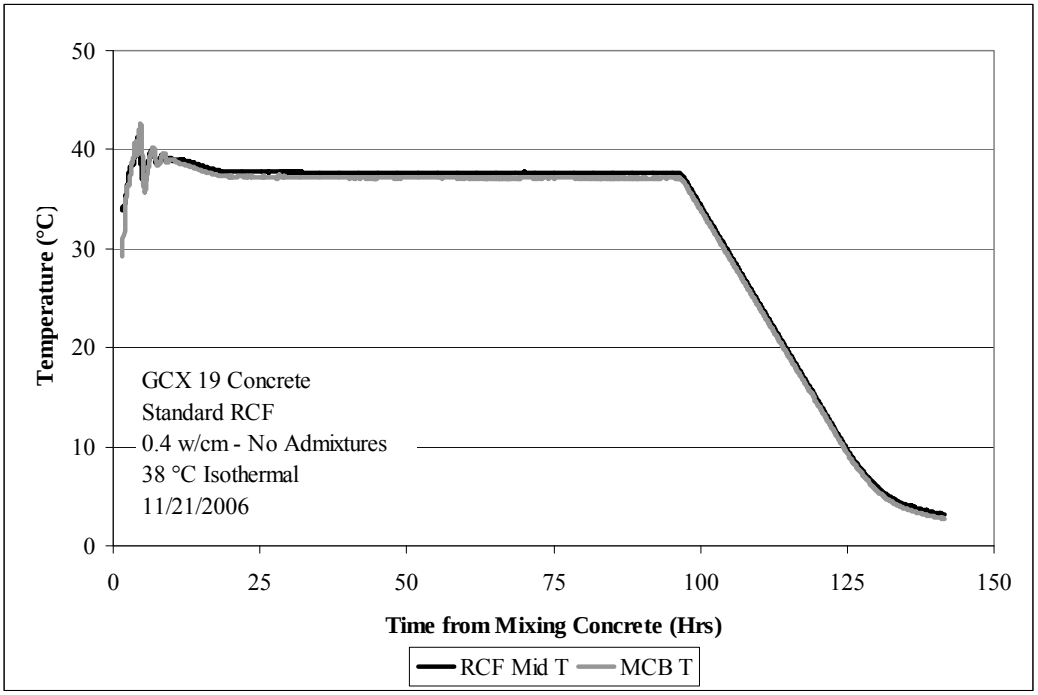

Figure 5.38: Temperature profile for 38 °C isothermal test GCX 19 (concrete)

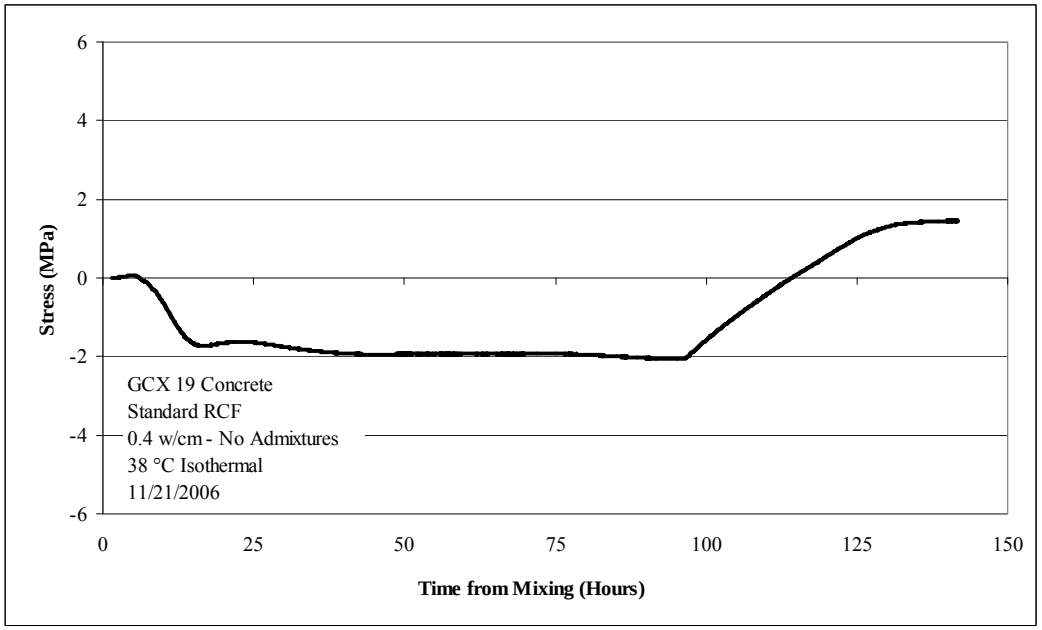

Figure 5.39: Stress generation for 38 °C isothermal test, GCX 19 (concrete)

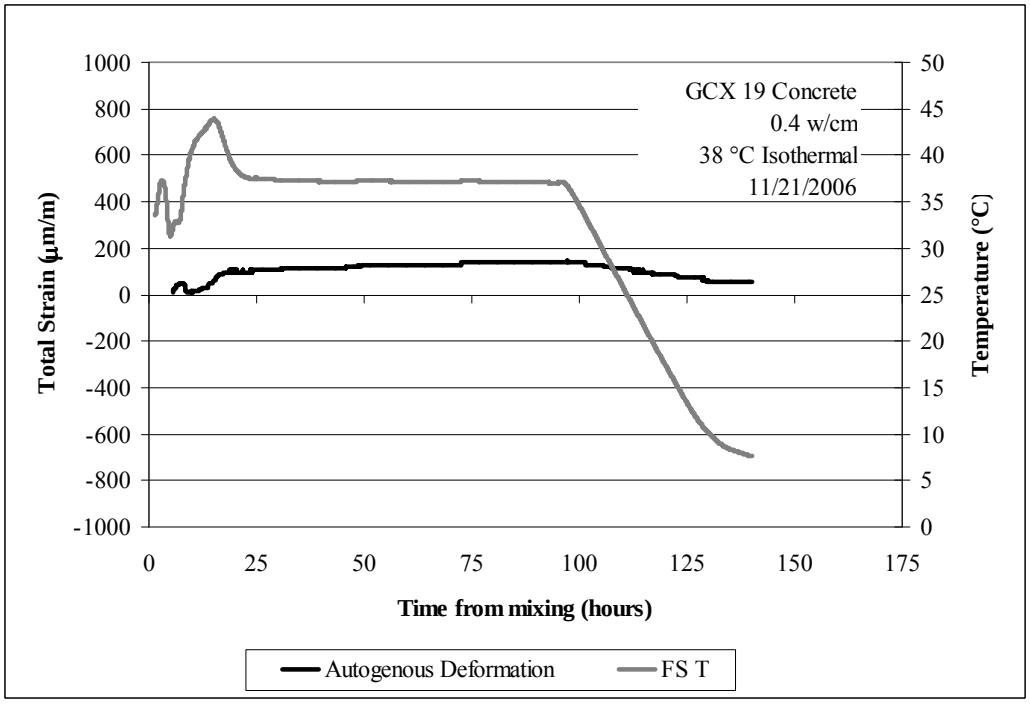

Figure 5.40: Free deformation for 38 °C isothermal test, GCX 19 (concrete)

Table 5.12: Mechanical properties for 38 °C isothermal test, GCX 19 concrete)

Age (days)	Compressive Strength (MPa)	Elastic Modulus (GPa)	Tensile Strength (MPa)
0.3	12.7	22.5	-
1.2	41.2	31.0	5.5
4.1	*44.9*	-	-
5.2	*50.0*	-	-
6.2	40.8	32.4	5.9
8.1	*40.8*	-	-
23.6*	42.4	-	-

Italics indicates only one test performed

Perhaps the most interesting outcome from this test performed in the standard frames was that temperature control in the first 10 hours of the testing period was extremely challenging. A total of six 5 kg bags of ice were used to keep the temperature as close to 38 °C as possible for the two water-baths controlling all the apparatus in this test. This was good confirmation that scaling the frames by 1/3 for the majority of testing of CAC was an important decision in providing the most accurate active temperature control. As was seen in testing with the sieved mortar, this mixture also developed compressive stresses of approximately -2 MPa prior to artificial cooling. This value was in strong agreement with the test run on sieved mortar. Upon cooling cracking was not observed in this sample. It does appear from the mechanical properties of match-cured concrete that conversion took slightly longer with the concrete, occurring at 6.2 days after casting. In fact the maximum strength observed occurred at 5.2 days at a value of 50.0 MPa. Due to the capacity of the system (maximum of 28 concrete cylinders), elastic modulus was not tested with every set of compressive strength breaks. Elastic modulus and splitting tensile strength did show a gradual increase throughout the testing period however, based on the limited results obtained.

After comparing the results of 38 °C testing between concrete in the standard frames and sieved mortar in the frames as part of this dissertation, 38 °C testing was performed on micro-concrete in several tests. Due to several problems with temperature control during the test, these mixtures were repeated to ensure reproducibility of results. Problems with temperature control typically occurred either just after placement and setting, when the water baths had difficulty maintaining isothermal temperatures or during the cooling phase if information fed from the thermocouples to the data acquisition system failed.

The following figures and tables show the results of two 38 °C isothermal micro-concrete mixtures. There were some problems with temperature control in both of these mixtures. In the first mixture the initial temperature in the rigid cracking frame rose to just above 50 °C and the temperature of the match-cured samples rose to just over 70 °C. As a result the test was repeated with the same mixture design. However the artificial cooling rate of the second mixture was too rapid due to an error with the data acquisition software. Subsequent mixtures at 38 °C (isothermal curing) have been repeated to remove both of these factors. The tests described in the following two figures and tables were performed once the free deformation frame was working properly and consistently producing sound results. Figure 5.41 shows the temperature profile for GCX 28. Figure 5.42 shows the temperature profile for GCX 28 but only for the first 25 hours. Figure 5.43 shows the stress generation and Figure 5.44 shows the free deformation for GCX 28. The mechanical properties tested on match-cured samples from GCX 28 are shown in Table 5.13. Figure 5.45 shows the temperature profile for GCX 29 which is a repetition of GCX 28. Figure 5.46 shows the stress generation and Figure 5.47 shows the free deformation for GCX 29. Table 5.14 shows the mechanical properties tested on match-cured samples cast from mixture GCX 29.

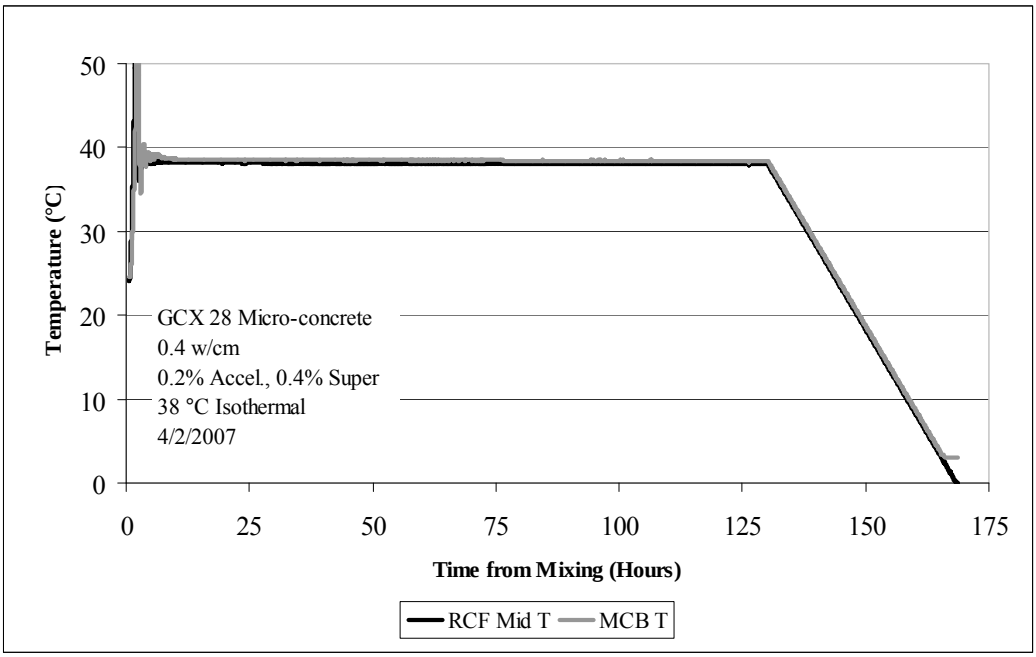

Figure 5.41: Temperature profile for 38 °C isothermal test, GCX 28

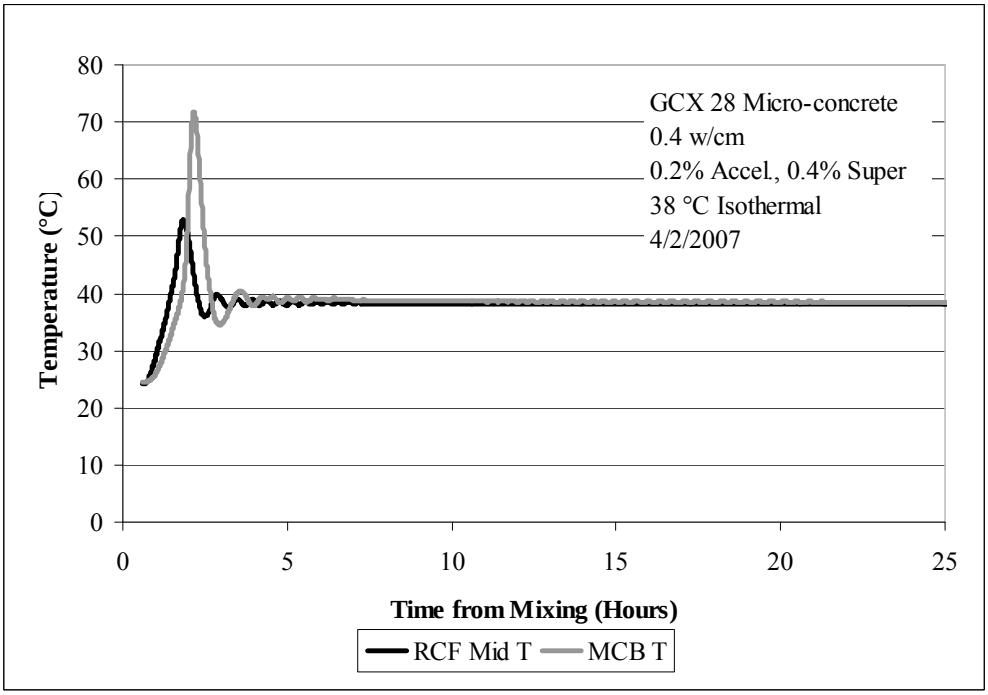

Figure 5.42: Temperature profile for 38 °C isothermal test, GCX 28, first 25

hours only

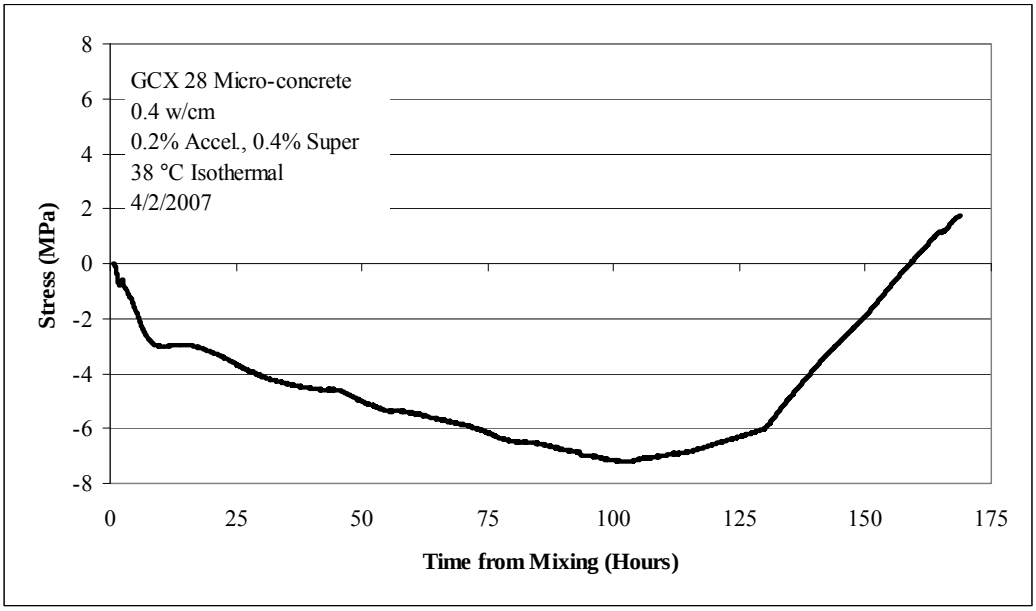

Figure 5.43: Stress generation for 38 °C isothermal test, GCX 28

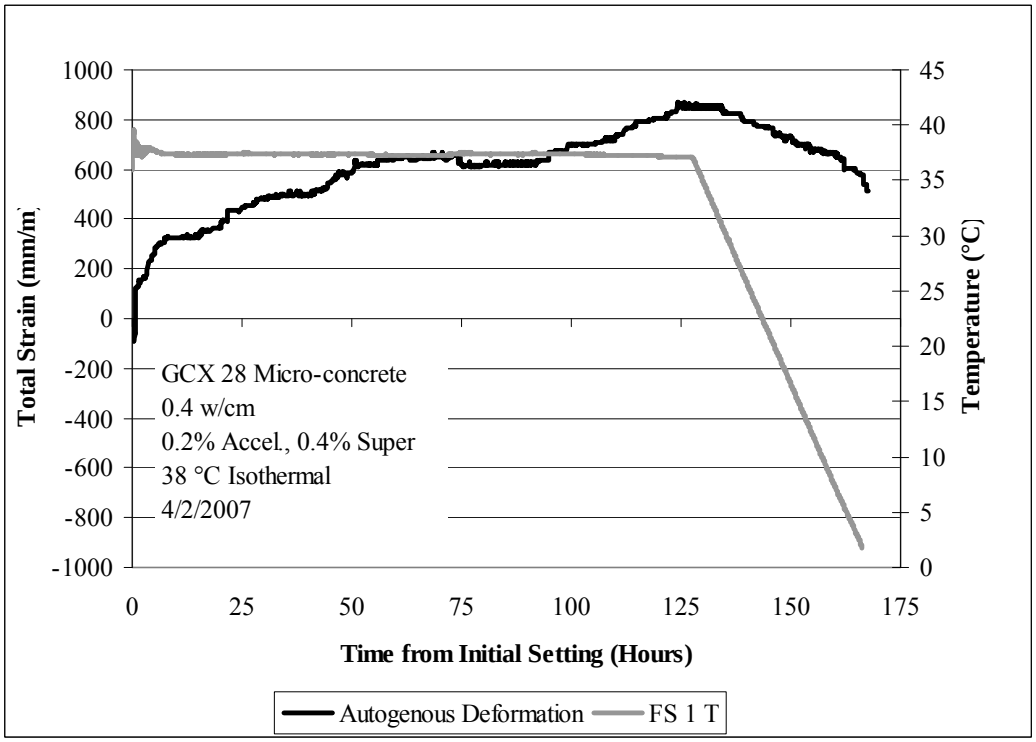

Figure 5.44: Free strain for 38 °C isothermal test, GCX 28

Table 5.13: Mechanical properties for 38 °C isothermal test, GCX 28

Age (days)	Compressive Strength (MPa)	Elastic Modulus (GPa)	Tensile Strength (MPa)
0.3	24.3	*25.3*	4.3
0.3	29.8	*28.3*	-
1.1	31.5	30.0	5.4
4.3	24.3	*27.9*	4.0
7.3	26.1	30.58	4.5

Italics indicates only one test performed

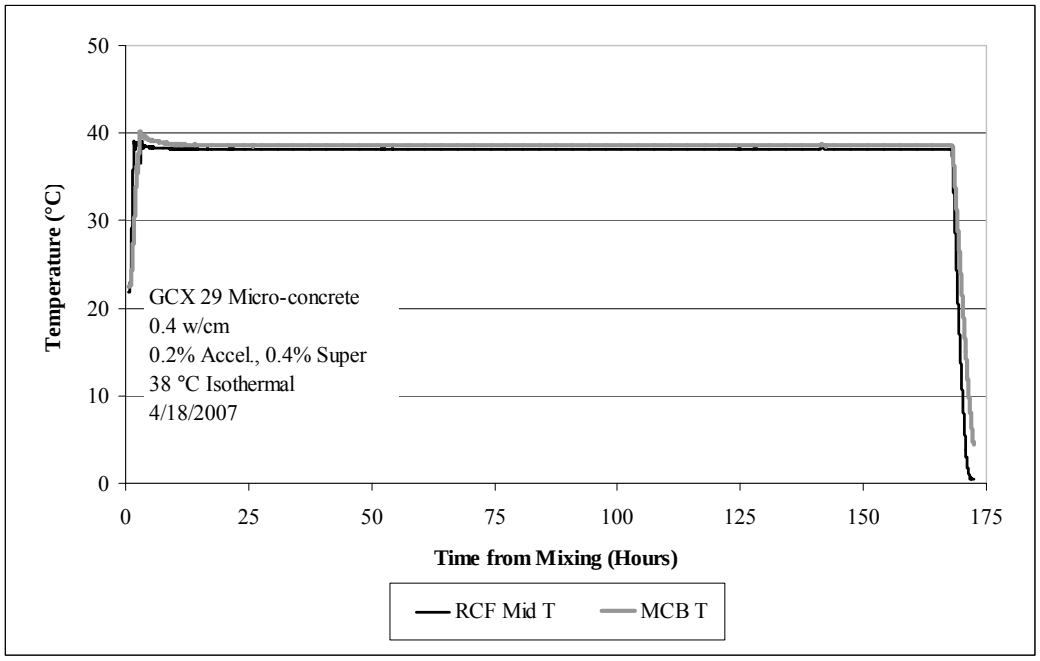

Figure 5.45: Temperature profile for 38 °C isothermal test GCX 29

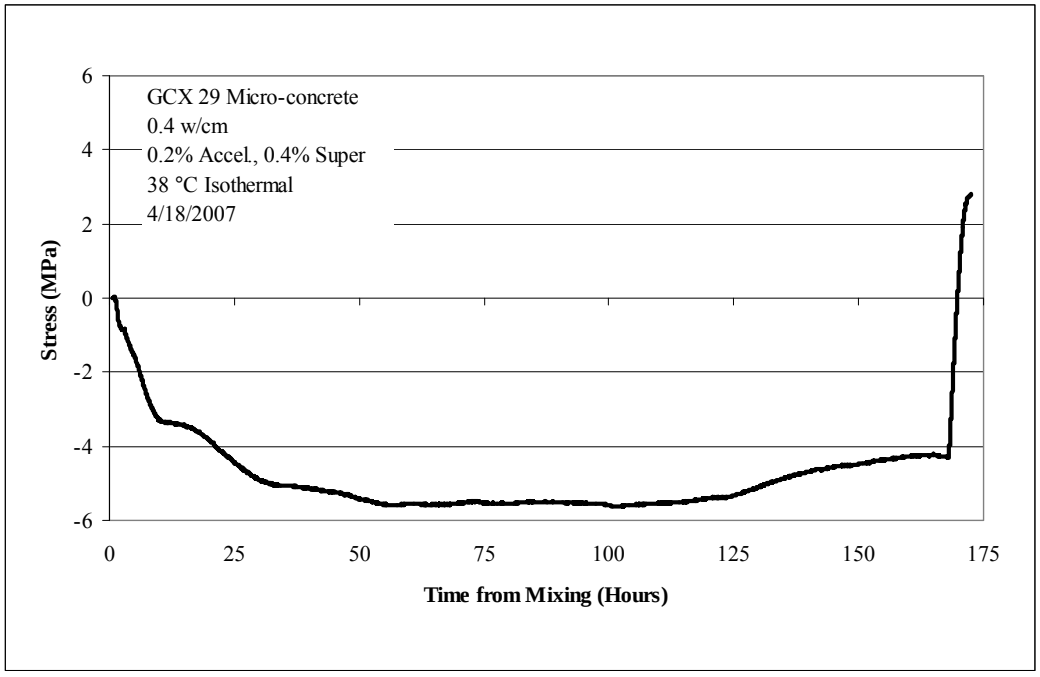

Figure 5.46: Stress generation for 38 °C isothermal test GCX 29

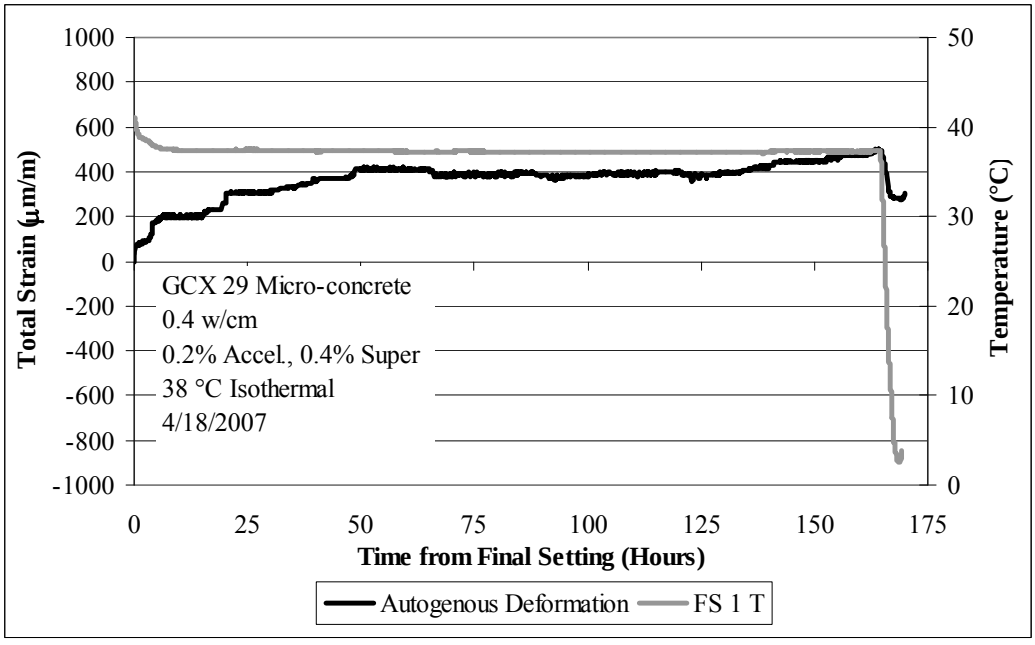

Figure 5.47: Free strain for 38 °C isothermal test, GCX 29

Table 5.14: Mechanical properties for 38 °C isothermal test, GCX 29

Age (days)	Compressive Strength (MPa)	Elastic Modulus (GPa)	Tensile Strength (MPa)
0.3	20.7	22.4	3.4
1.2	31.9	28.5	5.9
2.3	*37.9*	-	-
5.3	27.9	30.1	4.4
7.1	*27.1*		
9.4	28.6	31.2	4.9
12.3	*29.9*	-	-
16.2	28.7	32.4	5.4
44.2	33.0	33.9	5.1

Italics indicates only one test performed

GCX 28 and GCX 29 are both 38 °C isothermal tests conducted on micro-concrete with 0.2% accelerator and 0.4% superplasticizer by weight of cement. The temperature profile for GCX 28 shows that during initial hydration after setting that temperature rose to above 50 °C in the center of the rigid cracking frame and above 70 °C in the match-cured samples. By five hours the temperature was back under control but for at least 2 hours of the test the temperature for both the rigid frame and the match-cured samples was well above the desired temperature of 38 °C. The temperature of the free deformation specimen shown in Figure 5.44 was closer to 38 °C, however it still rose to 44 °C (results in figure are shown after final setting of the material). The cooling rate of this mixture was excellent and followed the desired 1 °C/hour cooling rate as desired as shown in Figure 5.41 and Figure 5.44. The temperature control for the repeated mixture, GCX 29, was excellent throughout the isothermal range of this test. However, when artificial cooling began the thermocouple in the middle of the frame began to produce erroneous data and thus the resulting cooling period took three hours to reach a temperature close to 0 °C for the various apparatus instead of the desired 38 hours to reach a 0 °C temperature (cooling rate of 1 °C/hour).

The impact of even a short period of time at high temperature for mixture GCX 28 produced a slightly higher maximum compressive stress of +7 MPa at 100 hours after casting compared to previous mixtures at 38 °C where slightly lower (from +3 to +6 MPa) compressive stresses were seen. Compressive stress for GCX 29 reached a lower maximum value of -5.6 MPa also at 103 hours after casting. Upon cooling neither mixture exhibited cracking due to the high level of compressive stress attained in the rigid cracking frame shown in Figure 5.43and Figure 5.46 (e.g.,, more tensile stress had to be induced upon cooling to force the micro-concrete into a high enough state of tensile stress to induce cracking).

GCX 28 also expanded more in free deformation testing compared to GCX 29 as shown in Figure 5.44. A maximum free deformation of 885 μm/m was measured for GCX 28 while a lower value of 485 μm/m was measured for GCX 29 (Figure 5.47). Although the temperature of the free deformation frame deviated by significantly less than the rigid cracking frame and match-cured samples, an increase in temperature up to 44 °C may have been enough to generate more converted hydrates and thus produced more expansion in the free deformation frame, even though temperature remained isothermal at 38 °C for the remainder of the test after the initial "spike" in temperature.

Mechanical properties for both mixtures indicated conversion at 4 days for GCX 28 and at 5 days for GCX 29 as shown in Table 5.13 and Table 5.14, respectively. This confirms the premise that even 2 hours spent above 38 °C in the case of GCX 28 resulted in the initial formation of more converted hydration products and as a result of prolonged isothermal temperature at 38 °C conversion occurred more rapidly in this mixture than for GCX 29 where isothermal temperatures remained at or close to 38 °C for the entire duration of the test (up to artificial cooling). This type of behavior for CAC further indicates the temperature sensitivity of the material and the direct impact on conversion.

This has important implications for concrete in the field which will be discussed in more depth at the end of this chapter and in the conclusion section of this dissertation.

The elastic modulus for GCX 28 did show a slight decrease to 27.9 GPa upon conversion. This decrease was not observed for GCX 29 where elastic modulus steadily increased throughout the course of the testing period. Recent work by Lamour and co-workers that investigated mechanical properties of CAC mortars with high paste contents (CAC=709 kg/m^3) and concretes with normal binder contents (477 kg/m^3).[48] They showed that for concrete samples, the elastic modulus (Young's Modulus) was less affected by conversion from metastable to stable hydrates than compressive and tensile strength in concrete. They also showed that other properties including resistance to crack propagation and ductility in mortars were also less affected by conversion compared to compressive strength.

One possible theory for the expansion of mixtures at 38 °C was that the release of water during the conversion process resulted in the generation of expansive forces as metastable hydration products dissolved and released water which was forced to occupy nearby space (or could combine with unhydrated cement, theoretically resulting in shrinkage). Theoretical volume change calculations shown in Chapter 2, Table 2.4 of this dissertation do indicate an increase in volume of 4.2% for the conversion of CAH_{10} to C_2AH_8. This volume change may be further magnified if the permeability of the material is such that rapidly released water during conversion cannot effectively find accommodating porosity nearby and a swelling pressure may then be exerted on the entire matrix.

To examine this theory further a micro-concrete mixture was air-entrained with a commercially available air-entraining agent. Trial mixtures were done to ensure that air-entrainment could be obtained with this particular agent and then the mixture was cured

isothermally at 38 °C in the rigid cracking and free deformation frames. The rationale behind this type of testing was that if the compressive stresses or expansion could be reduced with air-entraining this would indicate that presence of an air void system with adequate volume (and spacing) could at least in part accommodate the rapidly released water during conversion. However, if the results did not reduce compressive stress or free deformation, then this type of testing would be inconclusive; it could be that even an air-entrained micro-concrete with proper spacing may not provide necessary volume or access to accommodate the water released through conversion. The temperature profile and stress generation for this mixture are shown in Figure 5.48 and Figure 5.49. Free deformation is shown in Figure 5.50 and Table 5.15 shows the mechanical properties generated from testing the match-cured samples cast from this mixture.

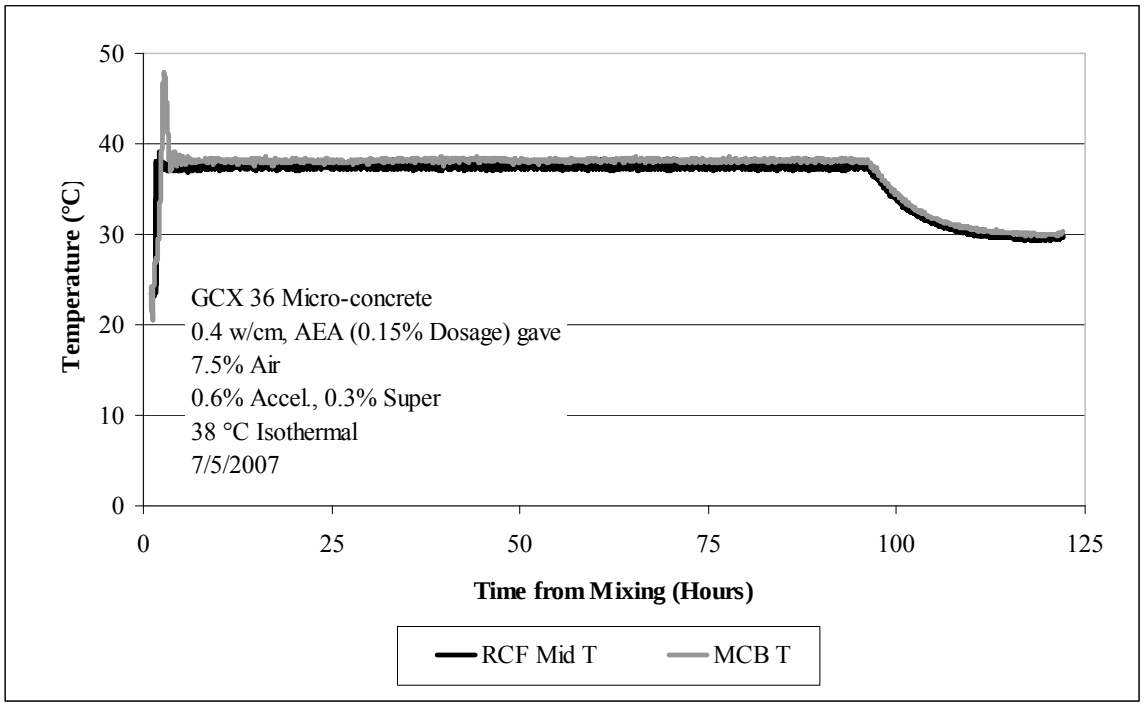

Figure 5.48: Temperature profile for 38 °C isothermal test, GCX 36

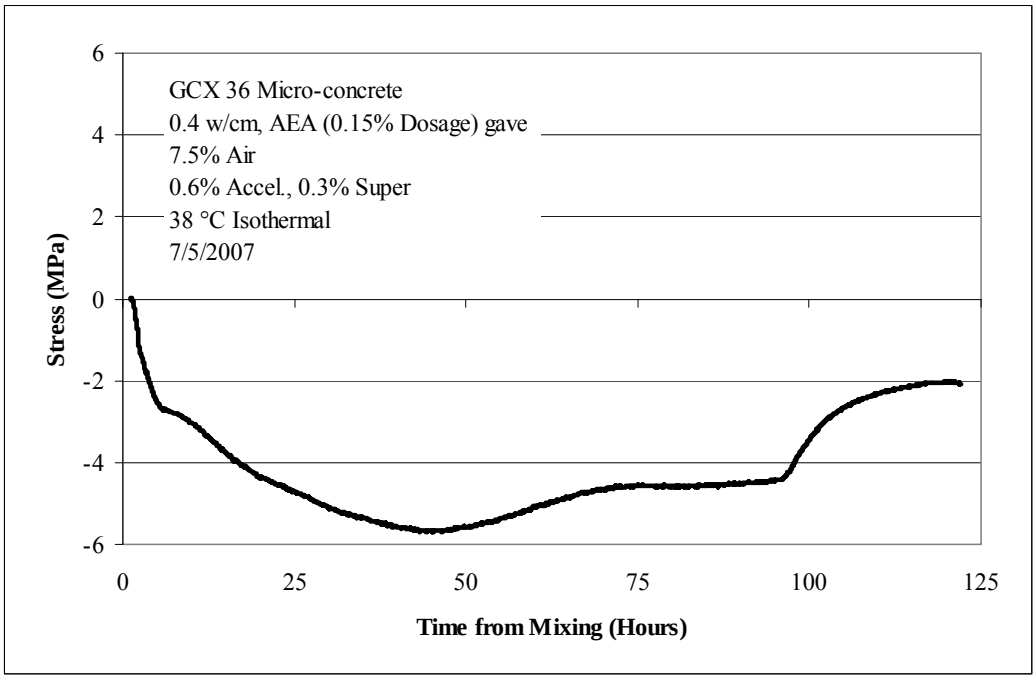

Figure 5.49: Stress generation for 38 °C isothermal test, GCX 36

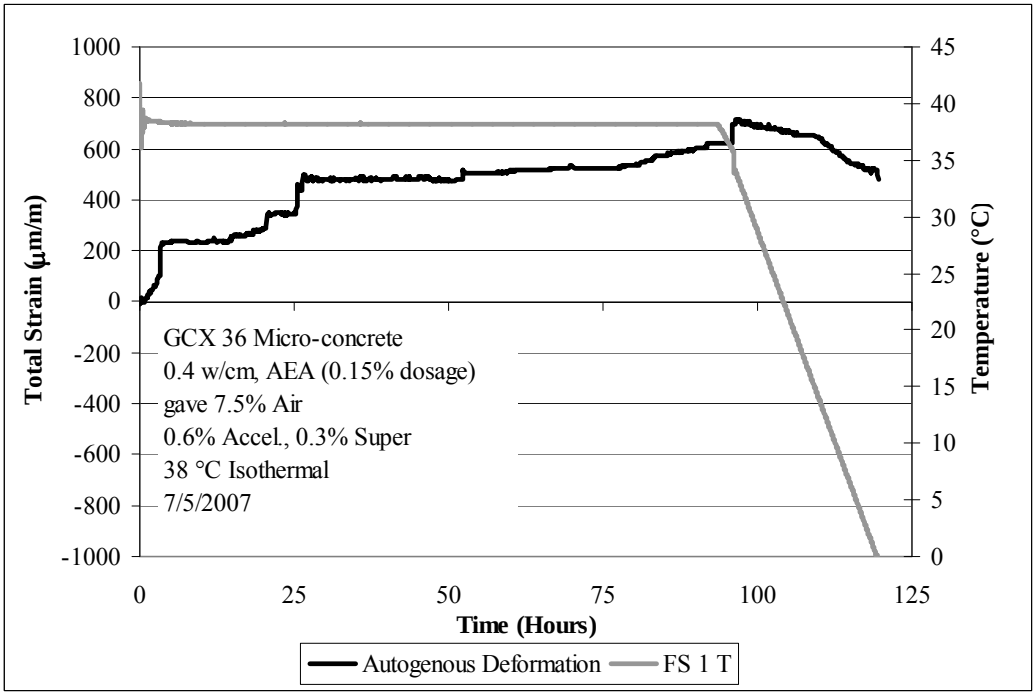

Figure 5.50: Free strain for 38 °C isothermal test, GCX 36

Table 5.15: Mechanical properties for 38 °C isothermal test, GCX 36

Age (days)	Compressive Strength (MPa)	Elastic Modulus (GPa)	Tensile Strength (MPa)
0.2	16.76	18.3	3.4
1.1	27.1	23.7	4.6
4.2	16.6	31.0	4.2
5.2	15.7	25.24	4.0
111.2	23.2	27.51	4.3

The temperature profile for this mixture indicated that 38 °C isothermal temperature was well-maintained in the rigid cracking frame. There was an initial increase in the temperature of the match-cured samples to 47 °C, but the temperature was quickly brought under control to 38 °C for the remainder of the isothermal portion of the testing period. It can also be seen that there was again another problem with the cooling portion of the test. Again the thermocouple in the middle of the frame began reading erroneous data after about 6 hours of artificial cooling. When this happened, the test could not continue to control temperature properly and as a result the program was stopped after this point.

However, the most important outcome of this test was the air-entrainment of 7.5% did not result in any reduction in the maximum compressive stress or free deformation of these specimens. A maximum compressive stress of -5.7 MPa was attained, however this maximum did occur earlier (47 hours after casting) than in previous mixtures with a slight reduction in compressive stress to -4.3 MPa at 96.5 hours after casting. This could be an indication that there was some limited ability of the air-entrainment during conversion to more adequately accommodate the release of water as this type of relaxation was typically not observed in previous mixtures until about 100-120 hours after casting, e.g.,, after conversion was mostly completed as shown by mechanical property testing on match-cured samples. Free deformation results showed continued

expansion throughout the isothermal range of the test to 623 μm/m until artificial cooling began.

Conversion occurred for this mixture by five days of continued exposure to 38 °C isothermal conditions and as evidenced by the low strength of 15.7 MPa attained at 5 days. It is important to note that the converted strength of this mixture was lower than that for GCX 28 or 29 and is likely a result of the increase porosity provided by the 7.5% air content in this mixture. Interestingly the elastic modulus also seemed to be affected by the conversion process for this mixture. Even though the air-entrainment may provide some accommodation for released water during the conversion process a 7.5% air content was not enough to significantly reduce expansion in the free deformation frame or the maximum compressive stress obtained in the rigid cracking frame. It is likely that other factors may be contributing to this interesting characteristic of CAC systems undergoing conversion. There could also be swelling associated with the formation of AH_3 gel and the further development of this material with the progress of conversion.

The final mixture investigated at 38 °C isothermal was a micro-concrete mixture with 0.6% accelerator and 0.3% superplasticizer with a w/cm maintained at 0.4. The purpose of this mixture was to perform isothermal calorimetry on the micro-concrete and to monitor the progressive heat signature through conversion. This would be compared to a mixture cured at 20 °C isothermally. Samples were taken from this mixture and the internal pore solution was expressed using a pore solution extraction device. This steel die utilizes high pressure to physically "squeeze" and remove the internal pore fluid of a cement paste or mortar. The solution is captured in the base of the device and is later analyzed using ion chromatography or inductively couple plasma optical emission spectrometry (ICP-OES). The pH of the pore solution was also measured. Samples were obtained for XRD analysis to confirm the presence of metastable and stable hydrates.

These results will be presented in future publications so that a comparison can be made between the same type of testing performed at 20 °C which was not complete by publication of this dissertation. The results from rigid cracking and free deformation testing are presented here. Figure 5.51 shows the temperature profile for this mixture and Figure 5.52 shows the stress generation. Free deformation and mechanical properties are shown in Figure 5.53 and Table 5.16, respectively.

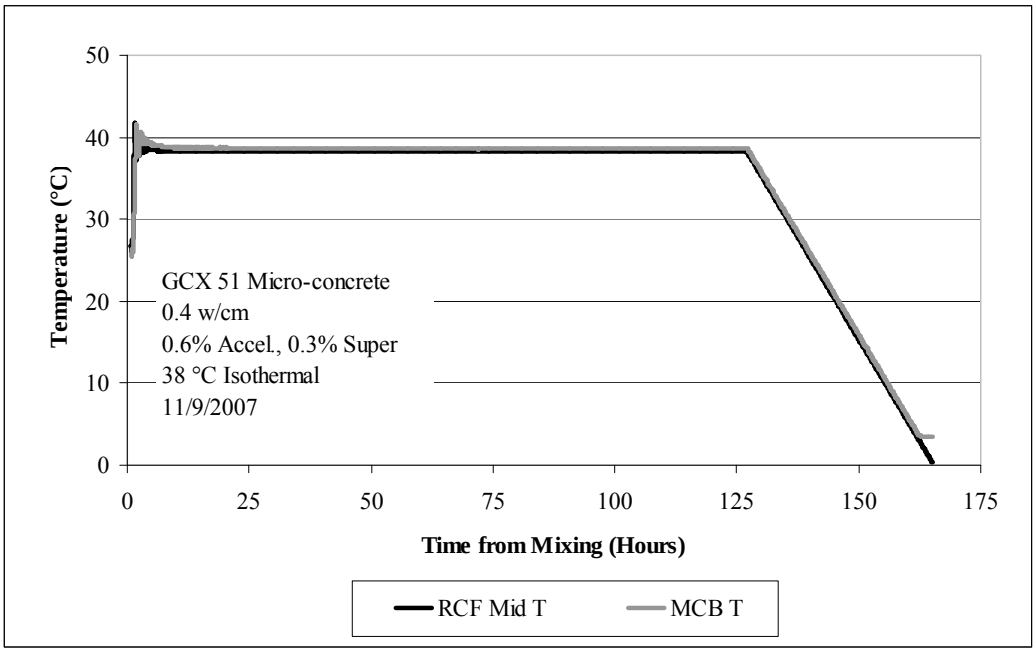

Figure 5.51: Temperature profile for 38 °C isothermal test, GCX 51

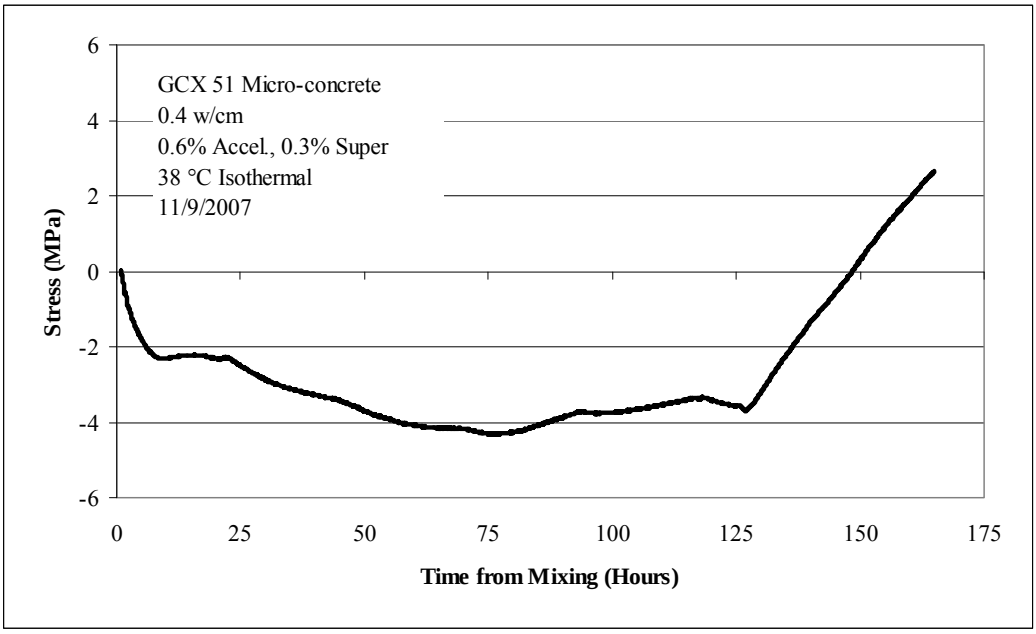

Figure 5.52: Stress generation for 38 °C isothermal test, GCX 51

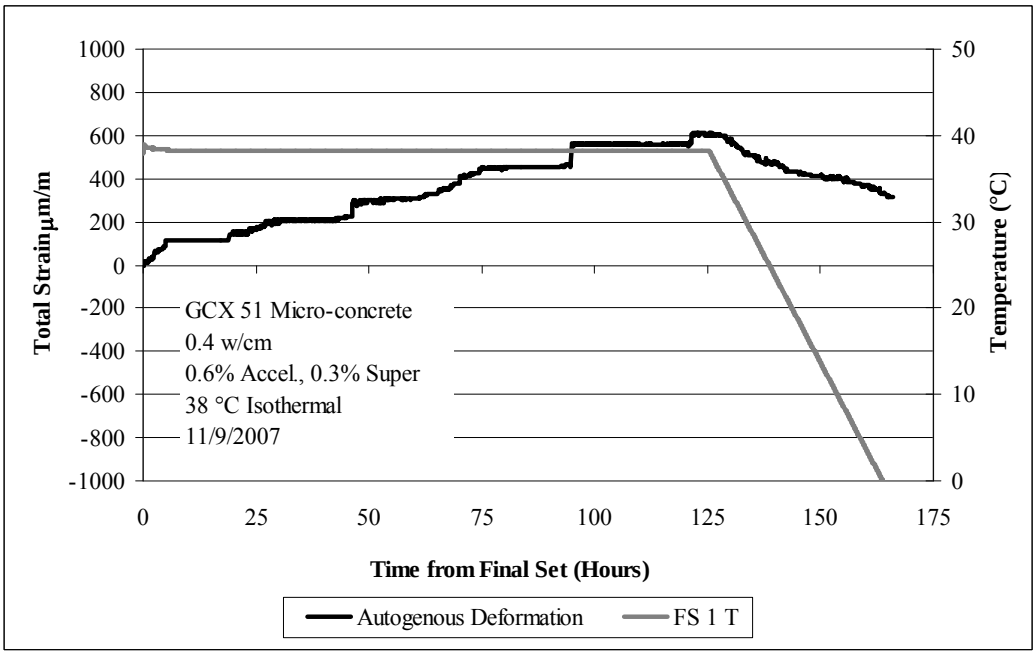

Figure 5.53: Free strain for 38 °C isothermal test, GCX 51

Table 5.16: Mechanical properties for 38 °C isothermal test, GCX 51

Age (days)	Compressive Strength (MPa)	Elastic Modulus (GPa)	Tensile Strength (MPa)
0.2	12.6	16.8	2.0
0.3	16.1	18.3	2.5
0.9	19.9	21.1	3.3
3.1	15.9	20.2	2.7
5.0	*14.0*	-	-
7.0	18.5	22.4	2.5

Italics indicates only one test performed

Isothermal temperature control at 38 °C was well-maintained throughout the isothermal portion of this test. The maximum compressive stress attained was -4.3 MPa at 78.9 hours after casting with a slight stress reduction thereafter until artificial cooling. Upon cooling this mixture did not exhibit cracking up to a maximum tensile stress of +2.7 MPa at 165 hours after casting. The maximum free deformation was 614 μm/m at 124 hours after final setting with shrinkage observed only during the artificial cooling portion of the test. The mechanical properties for this mixture show that compressive strength was quite low throughout the duration of the testing period with conversion occurring between 3 and 5 days. The reasons for this low strength are not well-understood but may be a result of cement aging as at this point the cement used in this test was approaching one year of age (the typical shelf life for GCX binder). There was not enough time to allow a repeat of this mixture with new cement obtained in February of 2008. However, for any published work this mixture will be repeated with the new cement, or previous results exhibiting higher strengths will be used.

5.5.2.3 Ciment Fondu, 38 °C

As another form of comparison, a mixture was cast with a different calcium aluminate cement binder, Ciment Fondu (mixture Fondu 37), and cured at 38 °C isothermally. The temperature profile for this mixture is shown in Figure 5.54 and stress generation is shown in Figure 5.55. Free deformation is shown in Figure 5.56. Table

5.17 shows the mechanical properties for this mixture from testing performed on match-cured samples cast from this mixture.

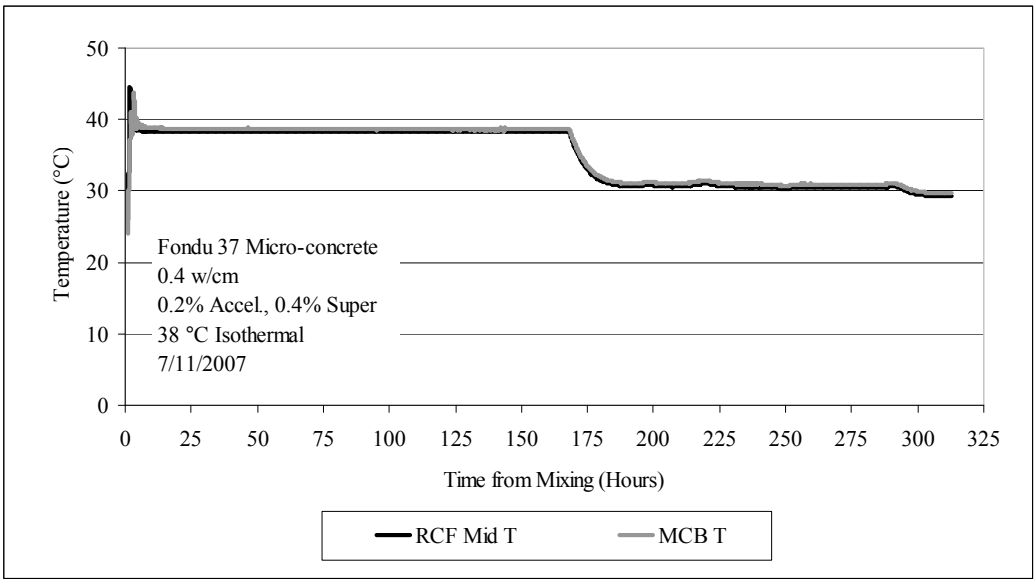

Figure 5.54: Temperature profile for 38 °C isothermal test, Fondu 37

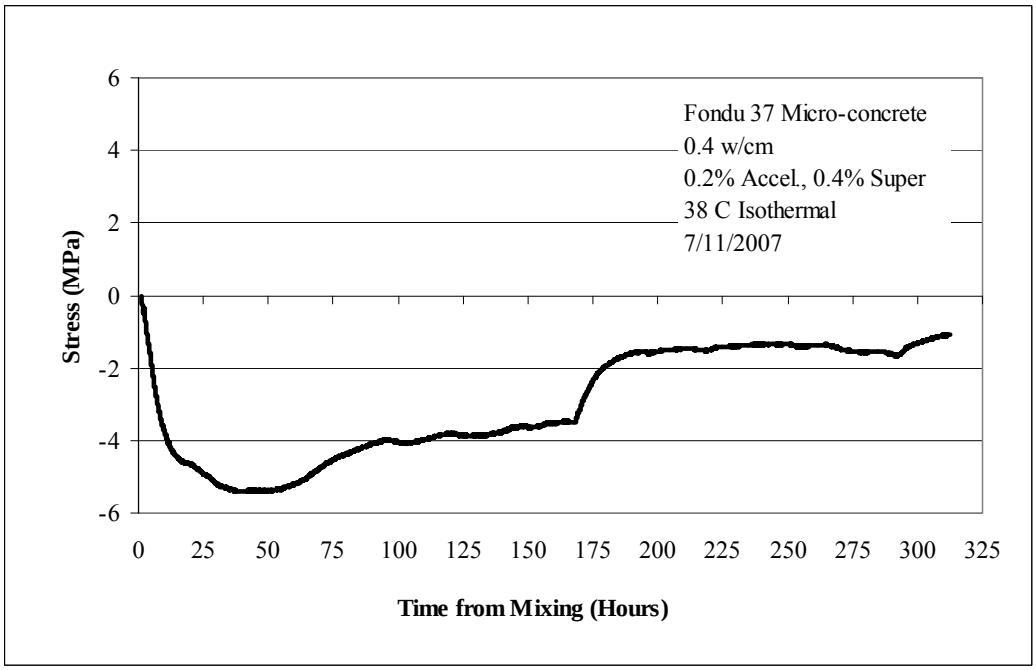

Figure 5.55: Stress generation for 38 °C isothermal test, Fondu 37

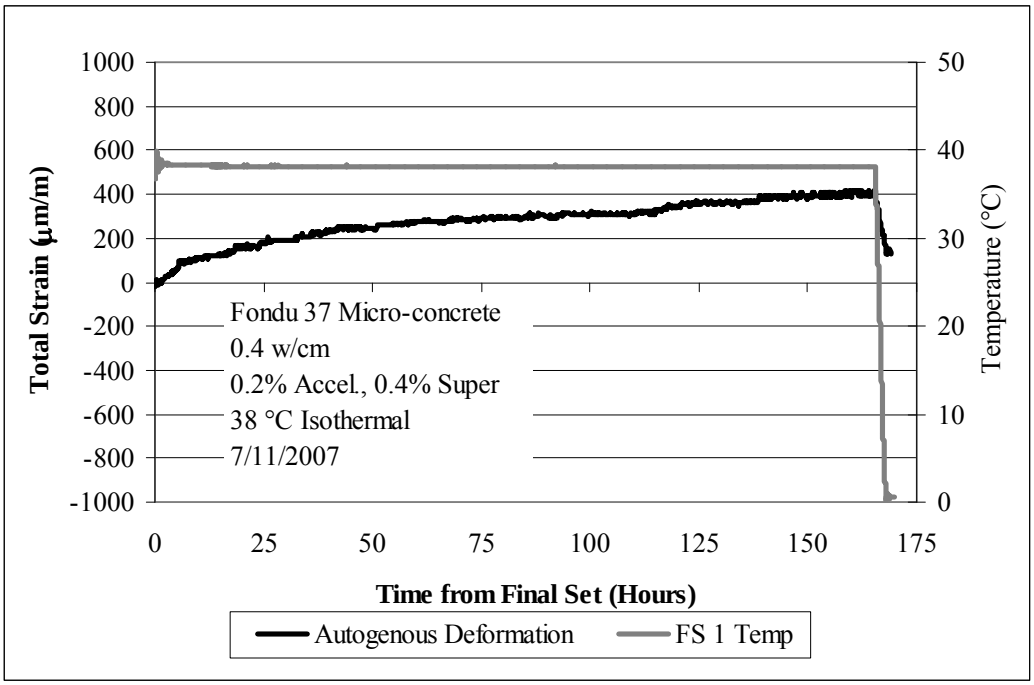

Figure 5.56: Free deformation for 38 °C isothermal test, Fondu 37

Table 5.17: Mechanical properties for 38 °C isothermal test, Fondu 37

Age (days)	Compressive Strength (MPa)	Elastic Modulus (GPa)	Tensile Strength (MPa)
0.2	12.35	18.6	2.0
1.2	25.9	29.5	4.9
2.3	28.7	*25.8*	4.6
5.2	27.0	25.90	4.6
7.2	29.2	-	-
9.3	31.7	-	-

Italics indicates only one test performed

Temperature control for this mixture was very good with only a slight elevation in temperature upon final setting as shown in Figure 5.54. The maximum compressive stress obtained for this mixture was -5.4 MPa at 44.3 hours after casting with a reduction in stress to -3.3 MPa until artificial cooling at 170 hours after casting. This reduction in stress may be related to the progression of conversion. These values are in good

agreement with the results from the GCX Binder presented in section 5.5.2. The cooling rate in the rigid cracking frame was not uniform at 1 °C/hour. However, the free deformation results show the proper cooling rate was attained for this mixture and a maximum expansion of 412 μm/m at 165 after final setting of the mixture. Mechanical property data indicate that conversion occurred by 5 days of exposure to 38 °C isothermal conditions. It does show that elastic modulus decreased from 29.5 GPa at 1.2 days to 25.90 GPa upon conversion. There was also a slight reduction in tensile strength from 4.9 MPa to 4.6 MPa upon conversion.

5.5.3 Isothermal Testing at Intermediate Temperatures (25, 30, 34): GCX Binder

The observation that volume change is highly dependent upon isothermal curing temperature prompted further investigation to determine at what isothermal temperature the behavior changed from that of generating tensile stress (shrinkage) to that of generating compressive stress (expansion). Other researchers have noticed anomalous behavior as isothermal temperature curing approaches 30 °C. Banfill observed retardation in setting time as isothermal curing temperatures approach 30 °C[9]. Bushnell-Watson and Sharp attribute this retardation to the inability of calcium aluminate cement hydrates to form in the range of 25-30 °C. They state that the nucleation of CAH_{10} is no longer thermodynamically favored and that the formation of C_2AH_8 is very slow. Since formation of C_3AH_6 is at least initially preceded by formation of meta-stable hydrates, neither of which can easily form at these temperatures, progression of the hydration reactions for all phases is severely limited[10]. However, Capmas and co-workers found no evidence that C_2AH_8 was difficult to nucleate. They did, however, conclude that CAH_{10} was difficult to nucleate in these ranges, with nucleation becoming impossible above 29

°C. They postulated that the formation of a gel phase hinders dissolution and precipitation at that temperature. They also note that commercial CACs which contain varying amounts of $C_{12}A_7$ could explain anomalies in setting time in these systems[11].

This research confirmed an increase in setting time within an isothermal range of 25-34 °C, with the most dramatic increase at 30 °C. Micro-concrete containing no accelerator was cured isothermally at 25, 30 and 34 °C in the rigid cracking and free deformation frames. Setting time was performed according to ASTM C 403, with initial set being indicated by a resistance of 3.4 MPa.[44] Initial set for the mixtures cured at 25, 30 and 34 °C were achieved at 6.6, 18 and 9.8 hours, respectively. One additional test was performed with micro-concrete and accelerator at 30 °C. The initial setting time for this mixture was dramatically reduced to 3.4 hours in comparison to the mixture without accelerator cured at 30°C isothermally. Results of testing at 25, 30 and 34 °C are presented in this section.

Figure 5.57 shows the temperature profile for the 25 °C isothermal test and Figure 5.58 shows the stress generation. Table 5.18 shows mechanical property development for this mixture.

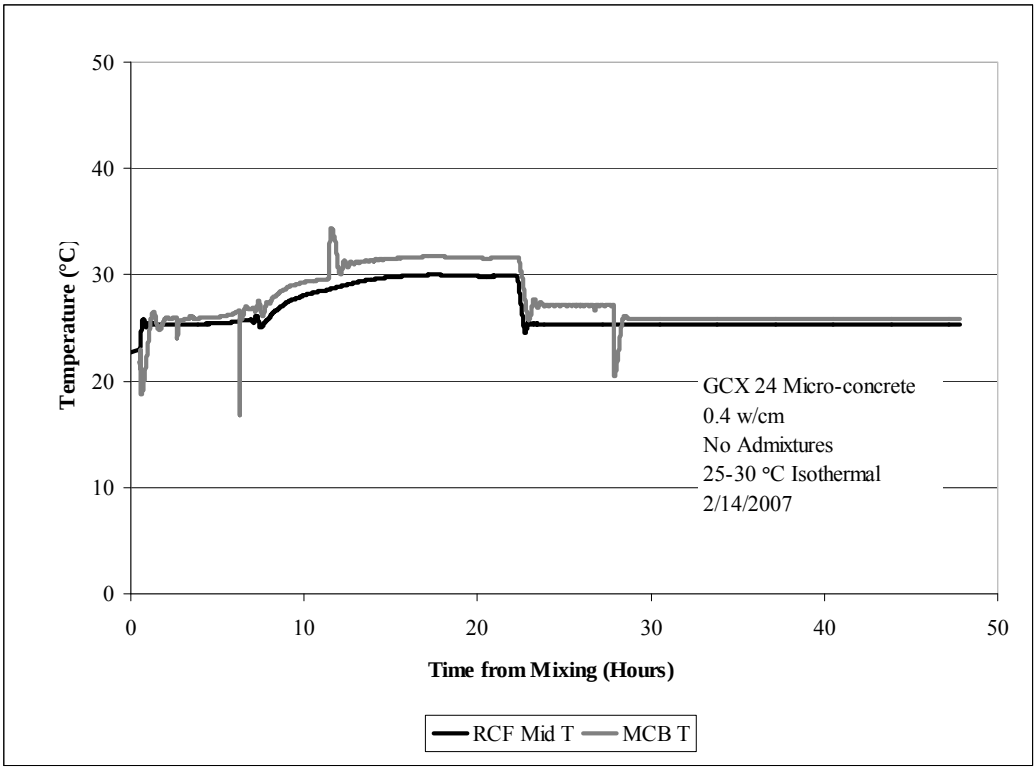

Figure 5.57: Temperature profile for 25-30 °C isothermal test, GCX 24

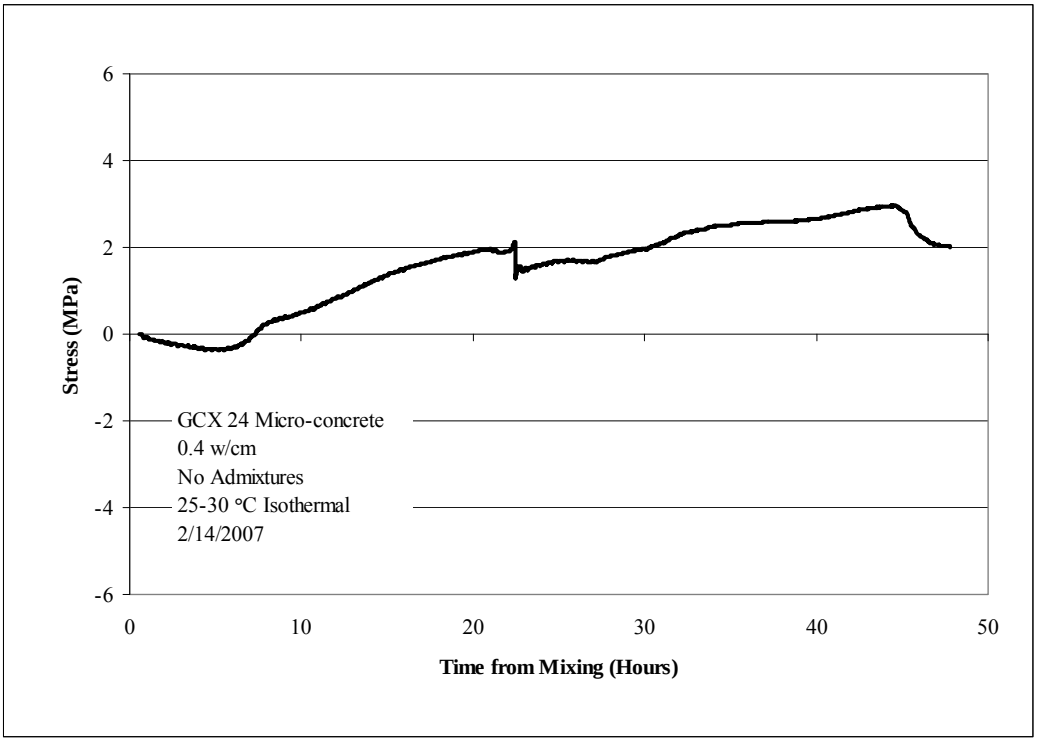

Figure 5.58: Stress generation for 25-30 °C isothermal test, GCX 24

Table 5.18: Mechanical properties for 25-30 °C isothermal test, GCX 24

Age (days)	Compressive Strength (MPa)	Elastic Modulus (GPa)	Tensile Strength (MPa)
1.2	65.0	39.8	10.2
240.1	48.4	47.4	6.2

Temperature control was problematic for this mixture within the first 24 hours of the testing period. For the first 8 hours the temperature remained isothermal, close to 25 °C. However, the temperature then gradually rose over the next 16 hours to 30 °C. The next day (first thing in the morning) when the mixture was checked, this deviation was realized and the program was restarted. The reason for this deviation was not apparent. The mixture reached initial set at 6.6 hours. What is most important to note from this mixture was that the stress generated almost immediately after setting was tensile in nature and as a result the mixture showed continual generation of tensile stress

throughout the 48 hour duration of this test. Once it was verified that stress was tensile within this isothermal temperature range the test was stopped to allow for investigation into other isothermal temperatures. The compressive strength and tensile strength of this mixture at 1 day were extremely high at 65.0 MPa and 10.2 MPa. Elastic modulus also was high at 39.8 GPa. Since this test was stopped early, there were enough match-cured samples to store and test at later age for possible conversion. A set of samples was tested at 240 days and the compressive strength has dropped to a value of 48.0 MPa commensurate with conversion. The tensile strength also decreased to a value of 6.2 MPa. However, what is somewhat surprising is that the elastic modulus has continued to increase to a value of 47.4 GPa. This result provides further evidence in support that conversion processes do not have a pronounced effect on elastic modulus. In fact this result shows that elastic modulus is essentially unaffected by conversion for this mixture.

Figure 5.59 shows the temperature profile for micro-concrete without accelerator tested at 30 °C isothermally (GCX 25) and Figure 5.60 shows the stress generation for this mixture. Table 5.19 shows the mechanical properties of match-cured samples from this mixture. Figure 5.61 shows the temperature profile for micro-concrete with accelerator tested at 30 °C isothermally (GCX 27) and Figure 5.62 shows the stress generation for this mixture. Figure 5.63 shows the free deformation for GCX 27 and the mechanical property data for this mixture is shown in Table 5.20.

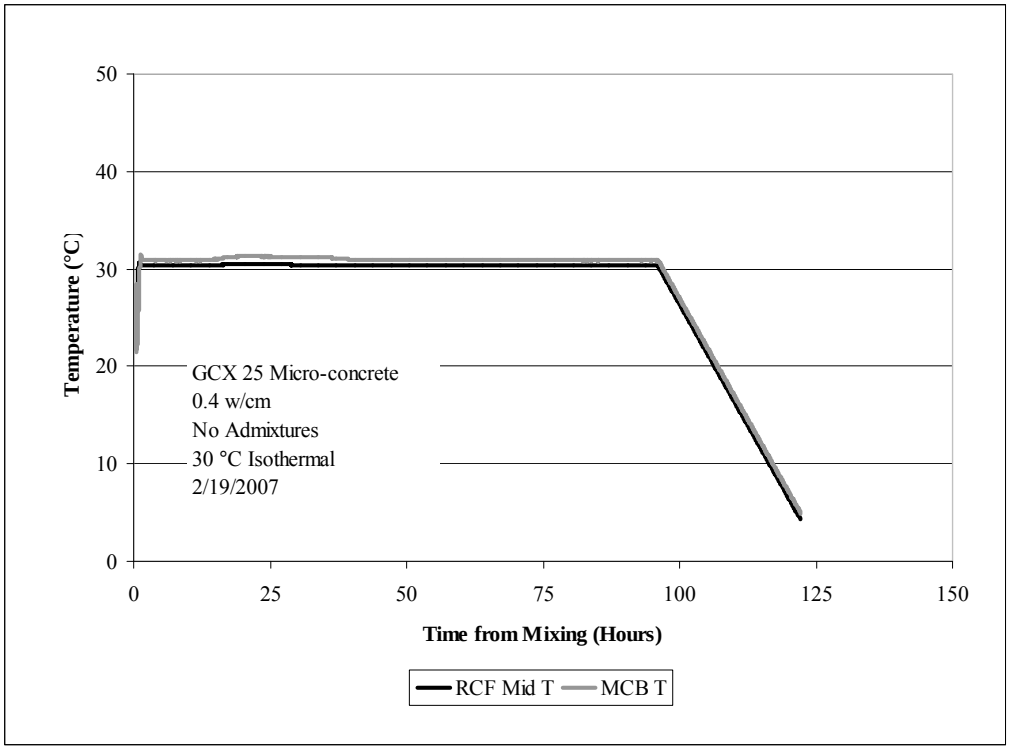

Figure 5.59: Temperature profile for isothermal test at 30 °C, GCX 25

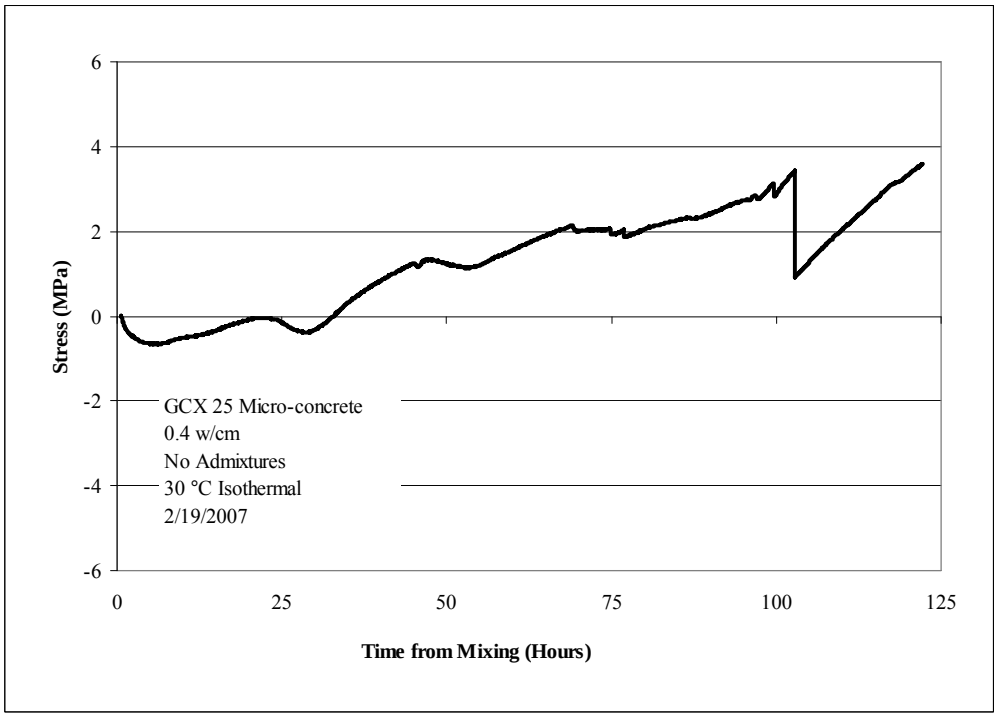

Figure 5.60: Stress generation for 30 °C isothermal mixture, GCX 25

Table 5.19: Mechanical properties for 30 °C isothermal test, GCX 25

Age (days)	Compressive Strength (MPa)	Elastic Modulus (GPa)	Tensile Strength (MPa)
1.0	3.0	9.6	0.5
2.1	43.6	*30.9*	7.3
6.3	48.8	33.8	8.4
28.3	37.9	*37.1*	8.1

Italics indicates only one test performed

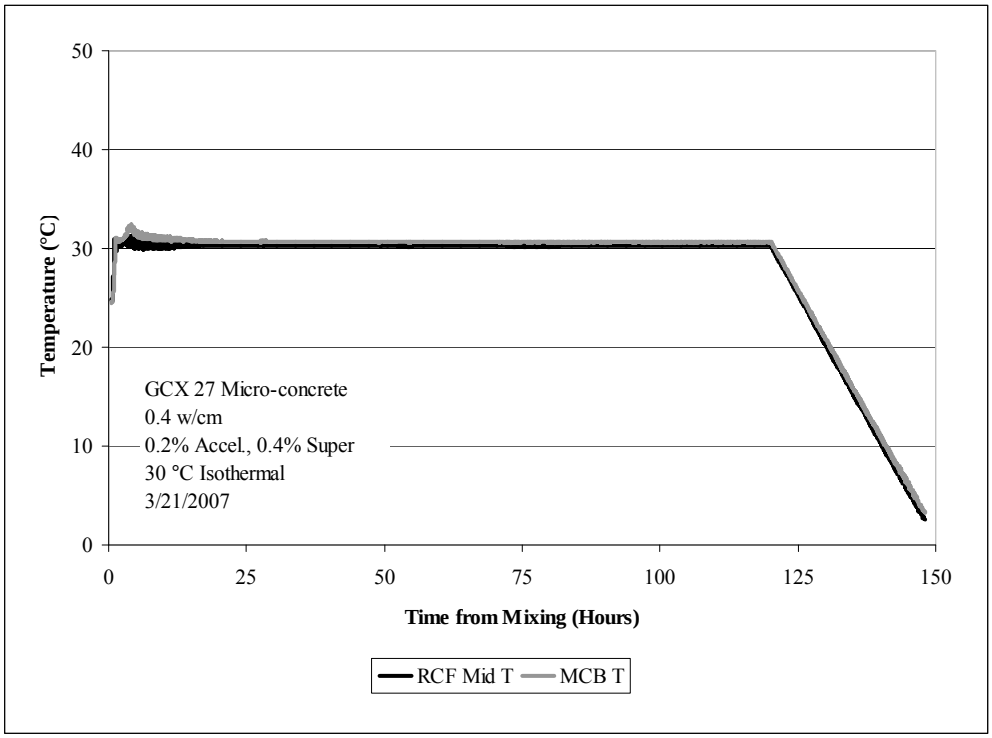

Figure 5.61: Temperature profile for 30 °C isothermal mixture, GCX 27

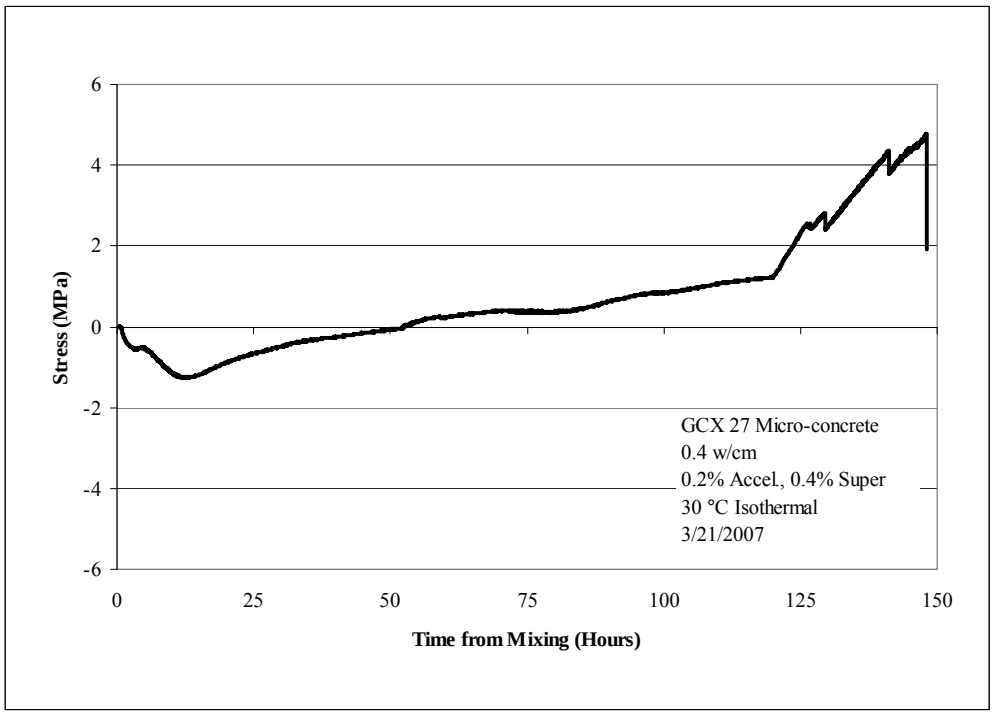

Figure 5.62: Stress generation for 30 °C isothermal test, GCX 27

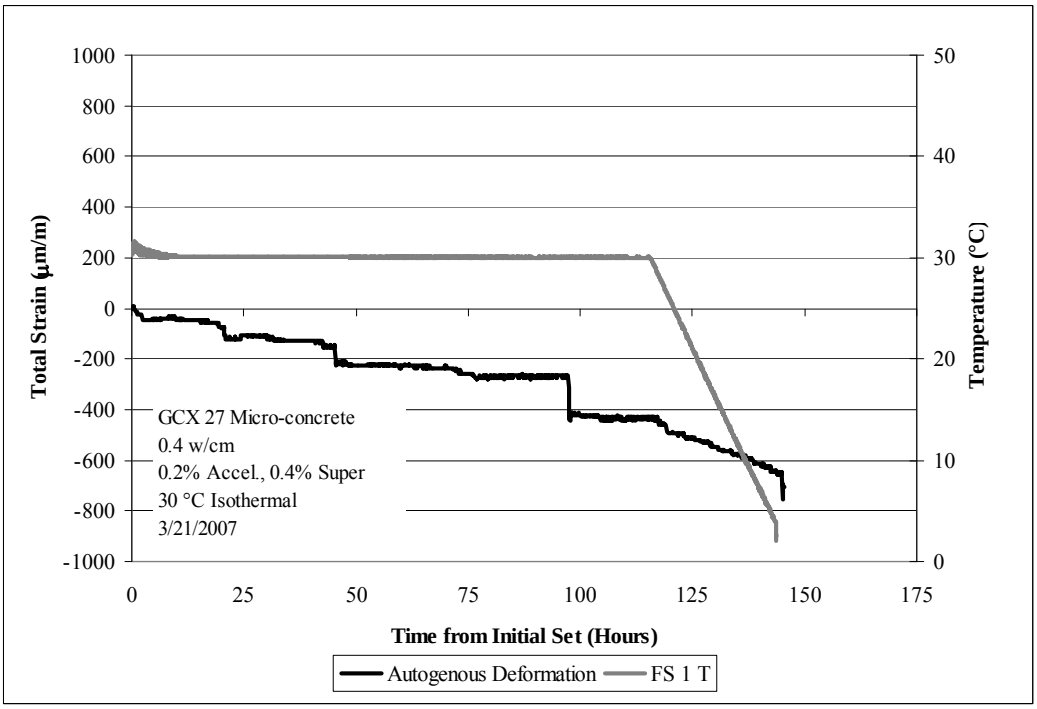

Figure 5.63: Free strain for 30 °C isothermal test, GCX 27

Table 5.20: Mechanical properties for 30 °C isothermal test, GCX 27

Age (days)	Compressive Strength (MPa)	Elastic Modulus (GPa)	Tensile Strength (MPa)
1.0	32.5	28.5	6.2
2.0	38.6	*27.3*	5.2
6.3	41.5	27.4	6.7
210.1	28.3	29.8	5.1

Italics indicates only one test performed

GCX 25 was a micro-concrete mixture with no admixtures, cured isothermally at 30 °C. This mixture had an exceedingly retarded setting time and it took 18 hours for the mixture to reach initial setting. During this time period the micro-concrete mixture developed a slight amount of compressive stress at 6 hours (- 0.6 MPa). However, after this point the mixture began to exhibit tensile stress development up to approximately 22 hours and then the mixture began to go into compression again for the next 5 hours until tensile stress was then generated continually up to + 3 MPa at 96 hours after casting. The mixture cracked 6 hours of the initiation of artificial cooling when the temperature was 24 °C at a tensile stress of + 3.5 MPa. Twenty-four hours after casting mechanical properties were measured and were found to be extremely low. This is not a surprising result since initial set had only occurred 6 hours prior to testing. At 2 days after casting compressive strength was 43.6 MPa, tensile strength was 7.3 MPa and the elastic modulus was 30.9 GPa. Strength continued to increase throughout the duration of the test with a maximum compressive strength of 48.8 MPa measured at 6 days after casting. By 28 days (22 days storage in a moist-cure room at 23 ± 2 °C and 100% relative humidity) the mixture appears to have converted with a compressive strength of 37.9 MPa.

When accelerator (0.2% by cement weight) and superplasticizer (0.4% by weight of cement) were used in a micro-concrete cured isothermally at 30 °C (Figure 5.62) initial setting time was dramatically reduced to 3.4 hours (compared to 18 hours with no admixtures). This mixture developed compressive stress to -1.3 MPa at 14 hours,

followed by the development of tensile stresses to a maximum of + 1.4 MPa at 120 hours after casting. Upon cooling this mixture also cracked but at higher stress than the mixture without accelerator at a value of + 4.9 MPa at 148 hours. Free strain for this mixture is seen as shrinkage up to a value of 650 μm/m before cooling at 122 hours after initial setting of the mixture. Mechanical property evaluation showed an increase in compressive (41.5 MPa) and tensile strength (6.5 MPa) as well as elastic modulus (27.4 GPa) up to 6 days of testing (duration of test). Later age samples measured at 210 days after casting showed conversion marked by a decrease in compressive strength to 28.3 MPa and a reduction in tensile strength to 5.1 MPa. No decrease in elastic modulus (29.8 GPa) was observed at 210 days after casting.

The results just described confirmed that isothermal curing of calcium aluminate cement micro-concrete, up to and including 30 °C, produced metastable hydrates that led to the development of shrinkage in free deformation testing and tensile stress development in the rigid cracking frame. The next isothermal temperature investigated was 34 °C. This mixture contained no admixtures. Figure 5.64 shows the temperature profile for this mixture and Figure 5.65 shows the stress generation. Mechanical properties are shown in Table 5.21.

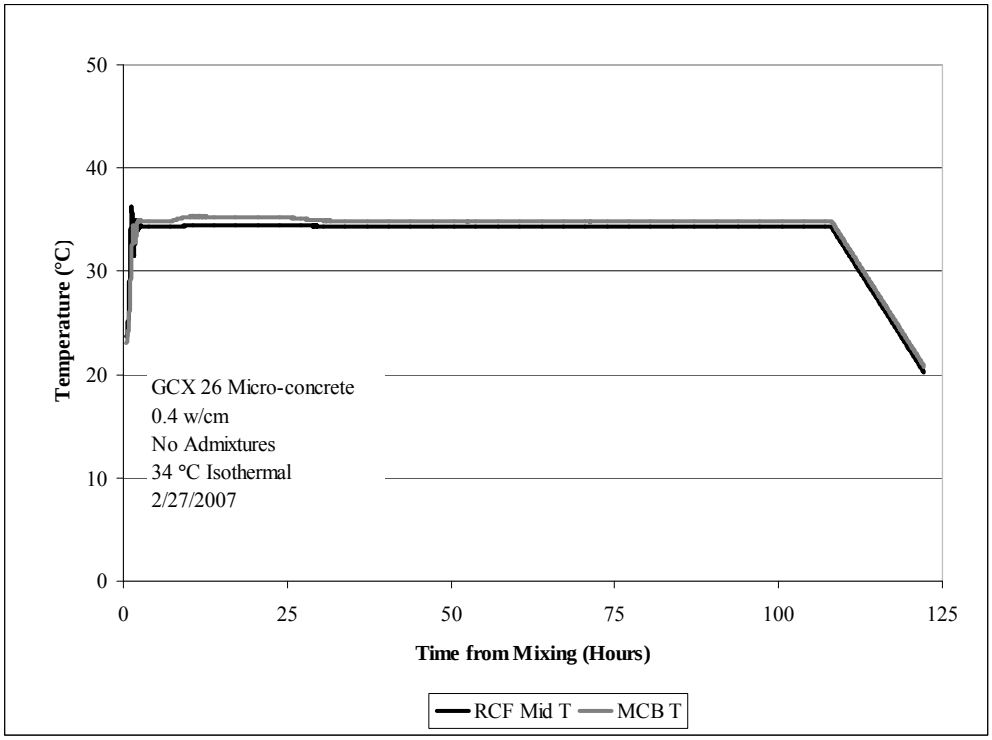

Figure 5.64: Temperature profile for 34 °C isothermal test, GCX 26

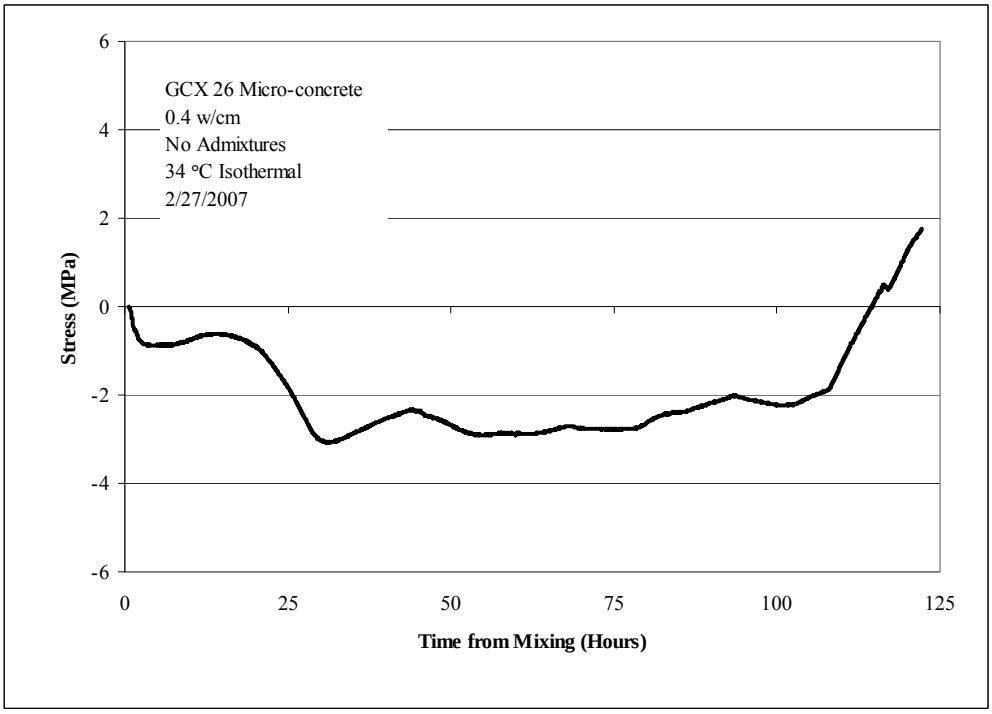

Figure 5.65: Stress generation for 34 °C isothermal test, GCX 26

Table 5.21: Mechanical properties for 34 °C isothermal test, GCX 26

Age (days)	Compressive Strength (MPa)	Elastic Modulus (GPa)	Tensile Strength (MPa)
1.0	30.0	24.7	7.0
3.2	33.9	*32.1*	6.7
6.2	36.8	30.3	6.5
28.2	30.5	30.4	-

Italics indicates only one test performed

The final mixture in this testing series was cured isothermally at 34 °C and did not contain accelerator. It also showed marked retardation in initial setting at 9.8 hours. This mixture developed compressive stress immediately to a maximum value of -3.1 MPa at 32.5 hours after casting and then showed a reduction in compressive stress to -1.7 MPa at 109 hours after casting. Upon cooling, this mixture reached an ultimate stress of +1.8 MPa at 148 hours but did not crack. Compressive strength gradually increased to 36.8 MPa at 6.2 days after casting. Tensile strength also increased to 6.7 MPa at 3.2 days and then decreased slightly to 6.5 MPa. Elastic modulus increased to 32.1 GPa at 3.2 days after casting and then decreased to 30.3 GPa at 6 days. Mechanical properties were evaluated at 28 days and the mixture showed evidence of conversion with a decrease in compressive strength to 30.5 MPa. Elastic modulus remained essentially unchanged from its value at 6.2 days, measuring 30.5 GPa.

This brief investigation into a range of intermediate isothermal testing elucidated the change in tensile stress development (shrinkage-related movement) to compressive stress development (expansive phenomena) as occurring above 30 °C. Mixtures cured isothermally at or below 30 °C developed tensile stress and shrinkage in free deformation testing. Mixtures cured at or above 34 °C developed compressive stress and expansion in free deformation testing.

5.5.4 High Isothermal Temperatures (50, 55 and 70 °C)

In an effort to determine the volume change of the stable hydrates, higher temperatures that would encourage rapid formation of stable hydrates were investigated. The first mixture investigated was 70 °C and the raw materials were preheated to 70 °C, in addition the water baths and formwork for the frames and match-cured samples were pre-heated to 70 °C. Unfortunately this mixture reached final set as it was being placed into the rigid cracking frame and the temperature rise was completely out of control. This approach was therefore abandoned and no results for this testing will be shown. Future mixtures were cast with materials at room temperature. Upon placement of the material into the frames and match-cured apparatus temperature was then increased to the desired temperature by control of the water baths. This process takes roughly 1 – 2 hours depending on the maximum temperature desired. Slightly lower temperatures of 50 and 55 °C were also investigated to allow more manageable control of the water baths and temperature of the match-cured specimens. Ultimately a third water bath was added to the testing set-up so that each apparatus (rigid cracking frame, free deformation frame and match-cured box) each had a separate high-capacity water bath to actively control temperature. This enabled the best possibility for active temperature control for future testing.

The first mixture tested at 50 °C are shown with two temperature profiles (Figure 5.66 and Figure 5.67) shown to enumerate the difficulty in temperature control at high temperature with just two water baths. Figure 5.68 shows the stress generation for this mixture and Table 5.23 shows the mechanical properties evaluated on match-cured samples tested from this mixture.

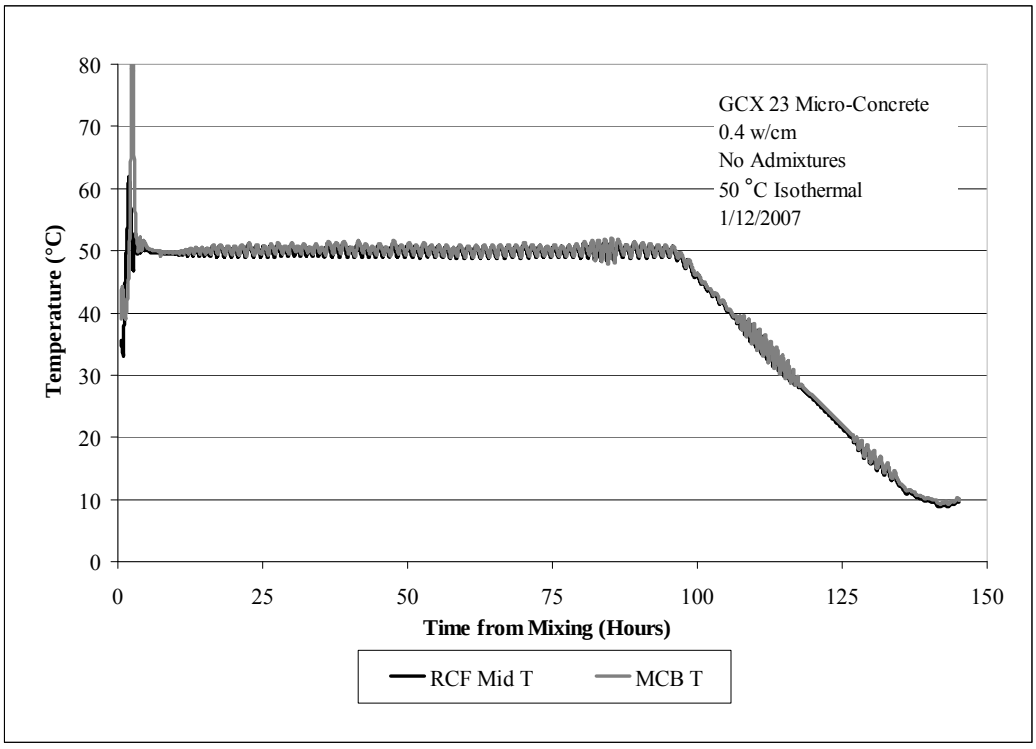

Figure 5.66: Temperature profile for 50 °C isothermal test, GCX 23

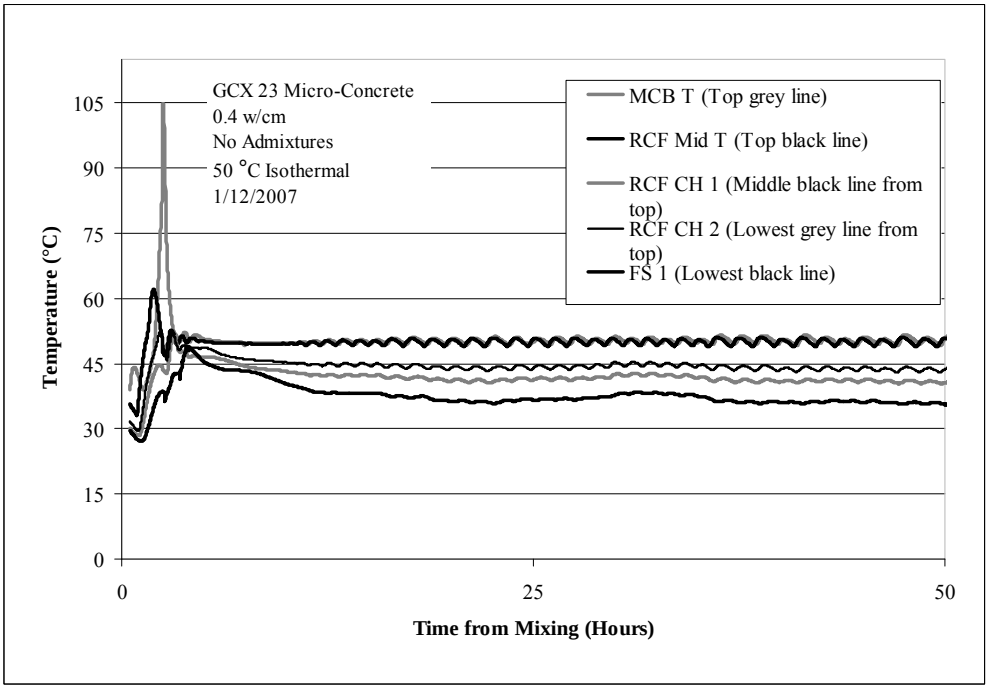

Figure 5.67: Temperature profile for 50 °C isothermal test, GCX 23, testing

up to 50 hours shown

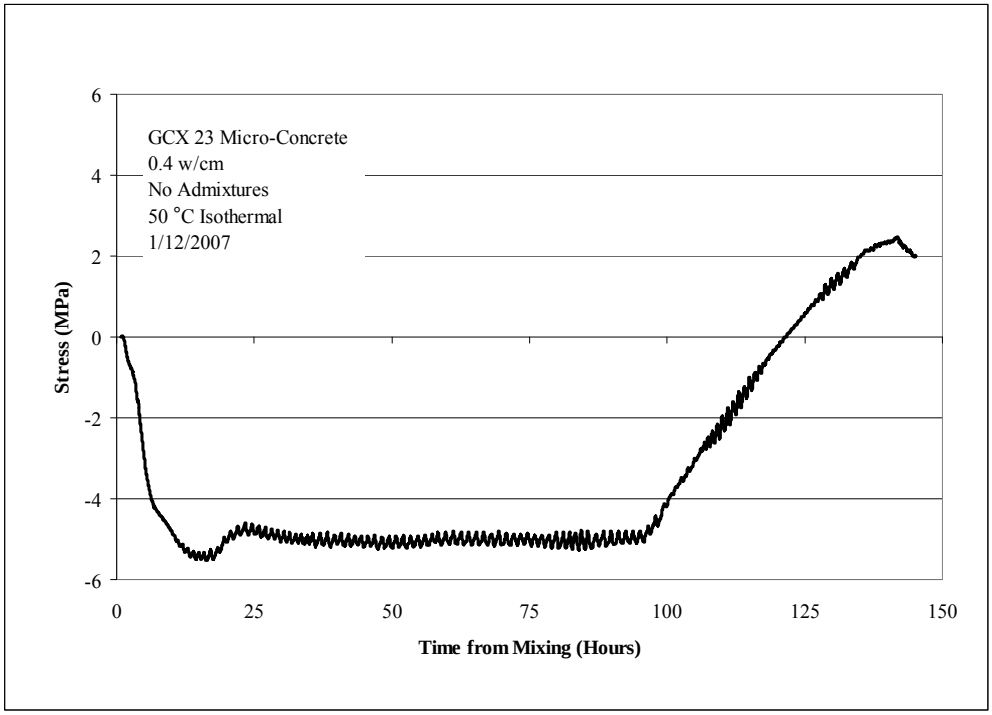

Figure 5.68: Stress generation for 50 °C isothermal test, GCX 23

Table 5.22: Mechanical properties for 50 °C isothermal test, GCX 23

Age (days)	Compressive Strength (MPa)	Elastic Modulus (GPa)	Tensile Strength (MPa)
0.3	31.3	34.0	5.2
1.1	35.2	34.2	5.7
6.3	41.3	37.7	6.3

From the temperature profiles it can be seen that while the temperature control for the rigid cracking and free deformation frame was relatively good with only a temperature increase to 60 °C upon setting, the temperature of the match-cured samples increased dramatically to 105 °C. Even with the use of two 5 kg bags of ice placed in the circulating water baths, the temperature of the match-cured samples was almost uncontrollable. What is important to observe is that the mixture did generate compressive stress up to a maximum value of -5.4 MPa at 16 hours after setting. There is

a slight decrease in compressive stress followed by a plateau in stress to -4.7 MPa up until the time of artificial cooling. The mechanical property development confirms that this mixture was already fully converted by testing at 1 day of age. Compressive strength, elastic modulus and tensile strength all increased throughout the 6 day duration of the test to respective values of: 41.3 MPa, 37.7 GPa and 6.3 MPa.

The next isothermal mixture investigated at high temperature was done at 55 °C and with the use of three water baths. The following is a summary of the figures and table that will be presented for this test. Figure 5.69and Figure 5.70 shows the temperature profile for this micro-concrete mixture cured at 55 °C isothermally (GCX 39). Figure 5.71 shows the stress generation for this mixture and Figure 5.72 shows the free deformation. Mechanical properties for this mixture are shown in Table 5.23.

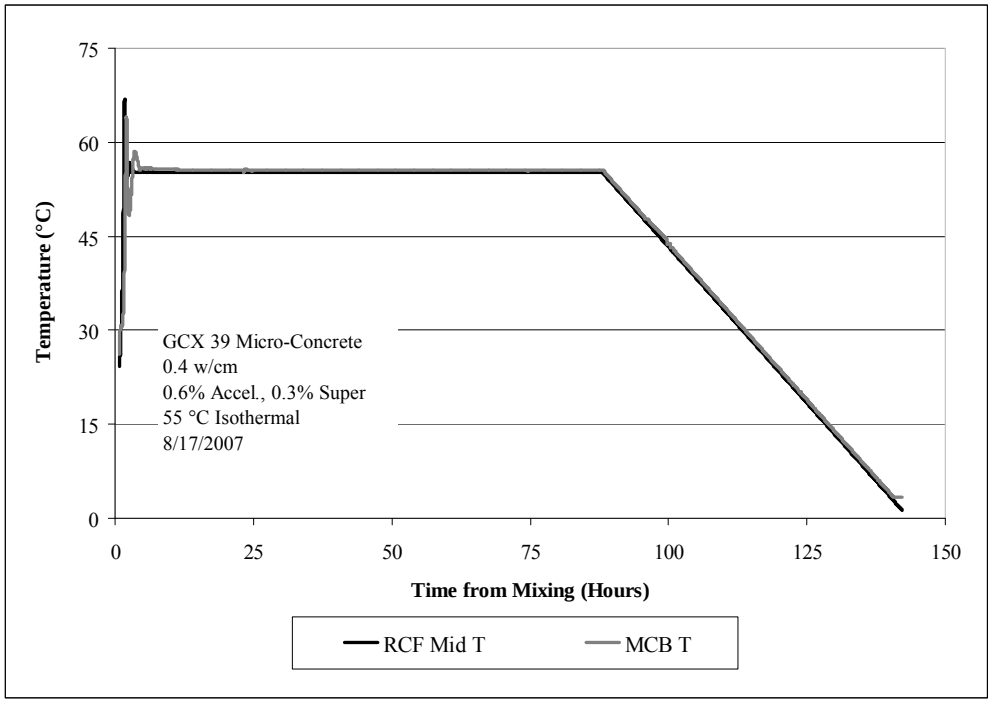

Figure 5.69: Temperature profile for 55 °C isothermal test, GCX 39

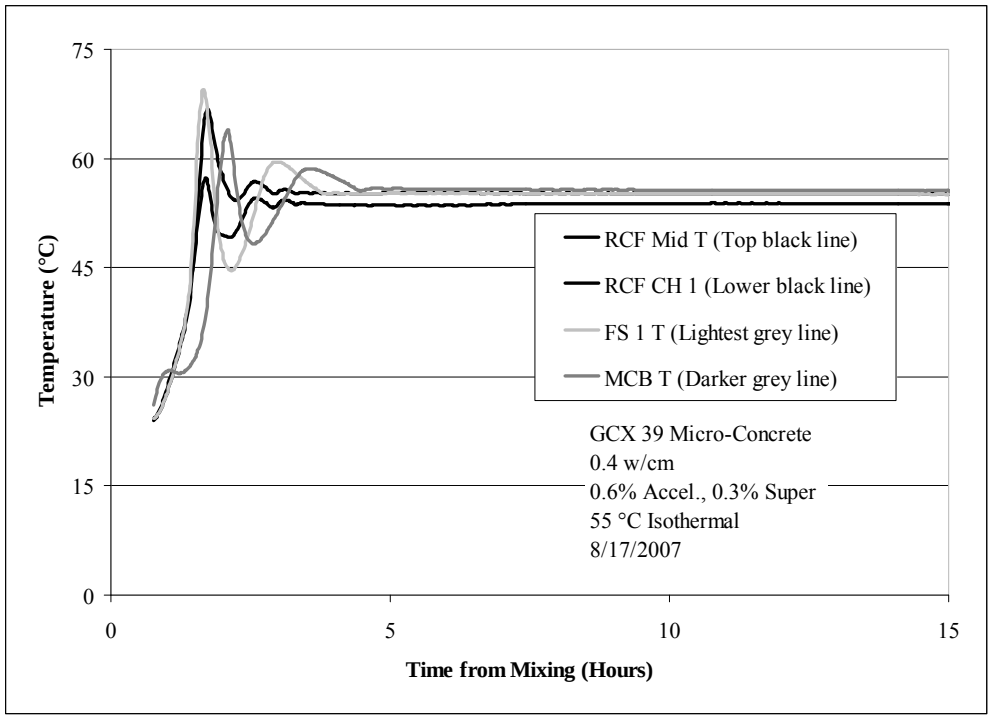

Figure 5.70: Temperature profile for 55 °C isothermal test, GCX 39, only 15 hours shown

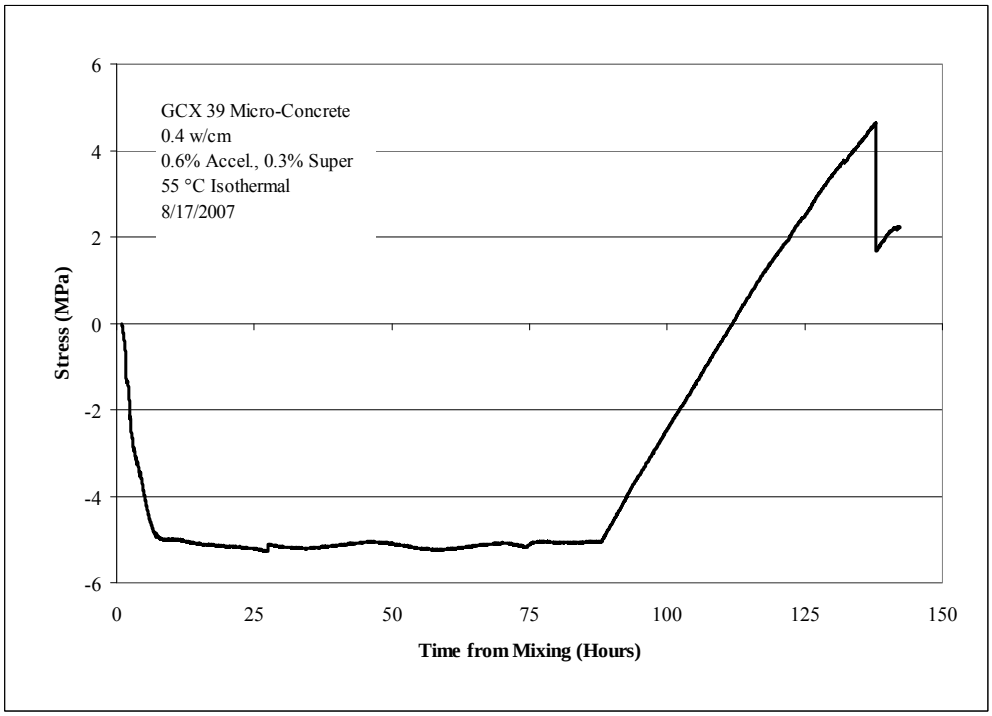

Figure 5.71: Stress generation for 55 °C isothermal test, GCX 39

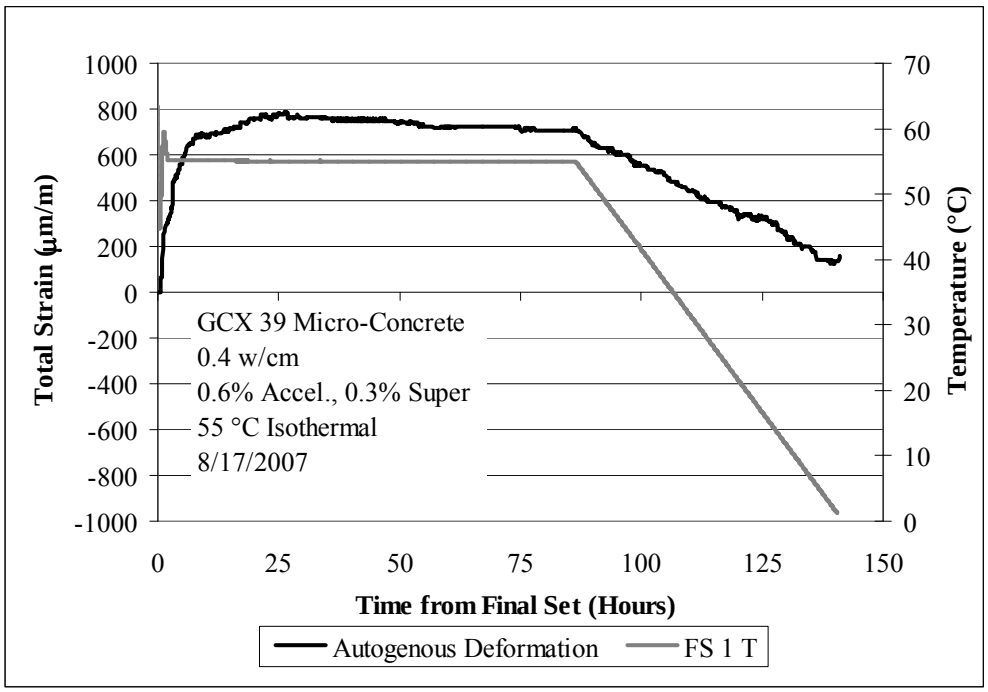

Figure 5.72: Free strain for 55 °C isothermal test, GCX 39

Table 5.23: Mechanical properties for 55 °C isothermal test, GCX 39

Age (days)	Compressive Strength (MPa)	Elastic Modulus (GPa)	Tensile Strength (MPa)
0.2	28.8	25.8	4.5
1.1	24.7	31.1	4.4
3.2	27.1	32.2	5.2
6.2	30.1	35.41	5.3

The use of three water baths enabled better temperature control; however, ice was still used to try and keep the temperature of the match-cured samples within a reasonable range. Nonetheless, there was still a temperature increase to 63 °C in the match-cured samples and to 65 °C in the middle of the rigid cracking frame. The micro-concrete in the free deformation frame experienced the highest temperature increase to 68 °C. Testing at high temperature was difficult and it is possible that even higher capacity water baths capable of rapidly cooling the circulating water, especially for the match-cured

samples may be necessary to ensure truly isothermal conditions, especially in the critical hours just after final setting of the material. This mixture generated compressive stresses to a maximum value of -5.0 MPa at 88.5 hours. The stress in the mixture reached a plateau within about 10 hours of the initial portion of the testing period. Upon cooling the mixture cracked at a tensile stress of +4.6 MPa at a temperature around 3 °C. Free deformation was indicative of a rapid phase of expansion within the first 25 hours of the testing period followed by a plateau in expansion, commensurate with compressive stress in the rigid cracking frame. Mechanical properties for this mixture indicate full conversion after 1 day with a gradual increase in compressive and splitting tensile strength and elastic modulus for the remainder of the testing period (6 days).

5.5.5 Isothermal Testing at 20 and 38 °C with 30 % Class C Fly Ash Replacement

Four mixtures were tested with a replacement of GCX Binder by a Class C fly ash (as per ASTM C 618) from a local source in northern Texas.[30] As the calcium aluminate cement manufacturer works to introduce their product to markets within the United States utilization of Class C fly ash has seen increasing popularity as it helps to reduce the overall cost of the material and it lessens the effects of the conversion process by production of the stable phase strätlingite. The following results demonstrate the effects of this fly ash replacement at 20 and 38 °C isothermal testing in rigid cracking and free deformation frames. These two isothermal temperatures have been proven to capture the difference in early-age volume change with metastable versus stable hydrate assemblages and were thus a logical choice to use for testing the replacement of Class C fly ash by 30% for GCX Binder.

5.5.5.1 20 °C Isothermal Testing

The following two tests were conducted at an isothermal temperature of 20 °C. Both mixtures were made from micro-concrete mixture proportions with 0.6% accelerator and 0.3% superplasticizer. The dosage of accelerator was increased in the summer of 2007 to 0.6% commensurate with a new shipment of admixtures (both accelerator and superplasticizer). This was done to retain workability similar to previous mixtures.

The temperature profiles shown for both GCX 43 (Figure 5.73) and GCX 46 (Figure 5.76) indicate excellent isothermal temperature control at 20 °C for the rigid cracking frame and free deformation specimens. The thermocouple in the middle of the rigid cracking frame stopped working after 13 hours into the testing for mixture GCX 43. However, this was realized quickly and the mixture was maintained at 20 °C throughout the isothermal duration of the test and cooling was done at the correct rate of 1 °C/hour as well. As a result of this error in testing this mixture was repeated in GCX 46. The stress generation from both mixtures, shown in Figure 5.74 and Figure 5.77 respectively, show that tensile stresses develop and both mixtures exhibit cracking within the first 24 hours of testing in the rigid cracking frame. At the initiation of cooling GCX 46 developed a full through crack with only a slight increase in tensile stress as seen in Figure 5.77.

Free deformation is shown for GCX 43 in Figure 5.75 and in Figure 5.78 for GCX 46. The results shown confirm the development of tensile stresses as shrinkage occurred for both mixtures. Ultimate shrinkage values prior to cooling were very similar for both mixtures at 680 and 632 μm/m for GCX 43 and GCX 46, respectively. Mechanical properties are shown in Table 5.24 for GCX 43 and in Table 5.25 for GCX 46. An increase in strength for both mixtures is shown throughout the duration of the testing period. Testing at 47 days for GCX 43 indicates that conversion is beginning to take

place as compressive strength and splitting tensile strength decrease slightly. The elastic modulus of this mixture (GCX 43) did not show a reduction at this testing time. The splitting tensile strength for GCX 46 dropped slightly at 2.3 days to 6.3 MPa. Overall the results are very similar to mixtures without 30 % class C fly ash, indicating that the calcium aluminate cement portion of the binder system predominates with respect to mechanical property development and early-age volume change (shrinkage at 20 °C).

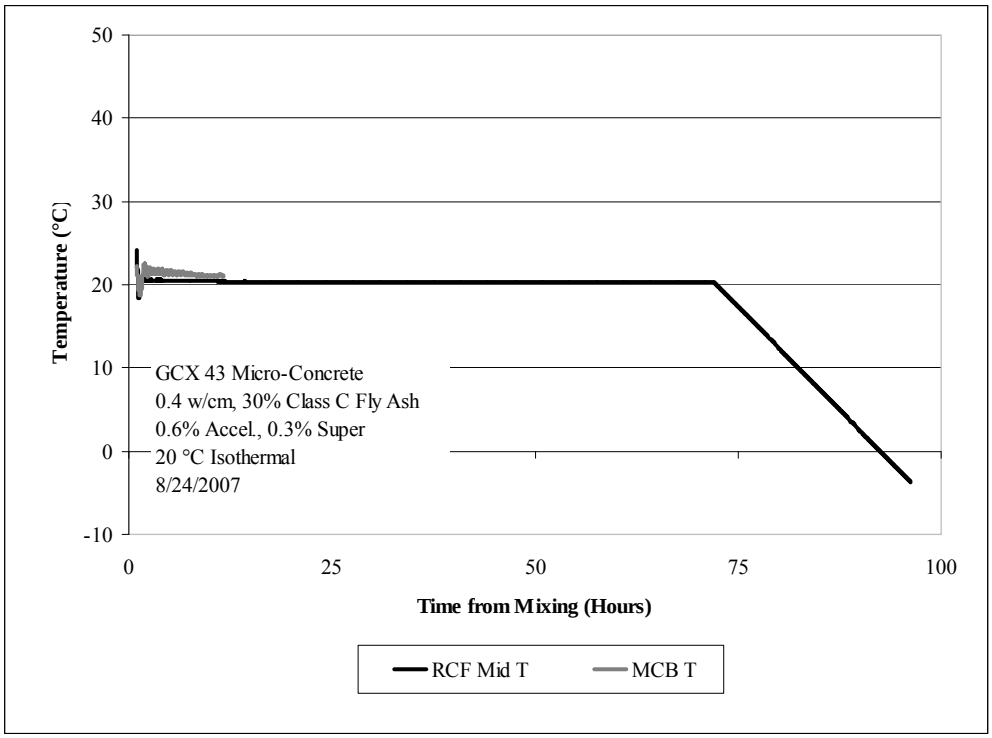

Figure 5.73: Temperature profile for 20 °C isothermal test, GCX 43

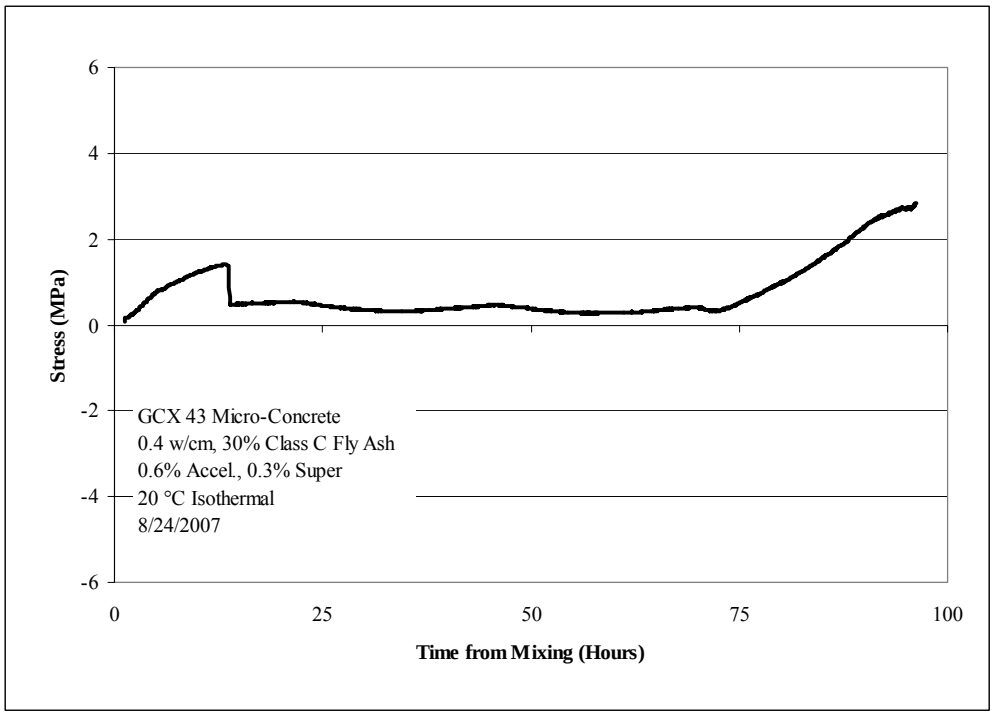

Figure 5.74: Stress generation for 20 °C isothermal test, GCX 43

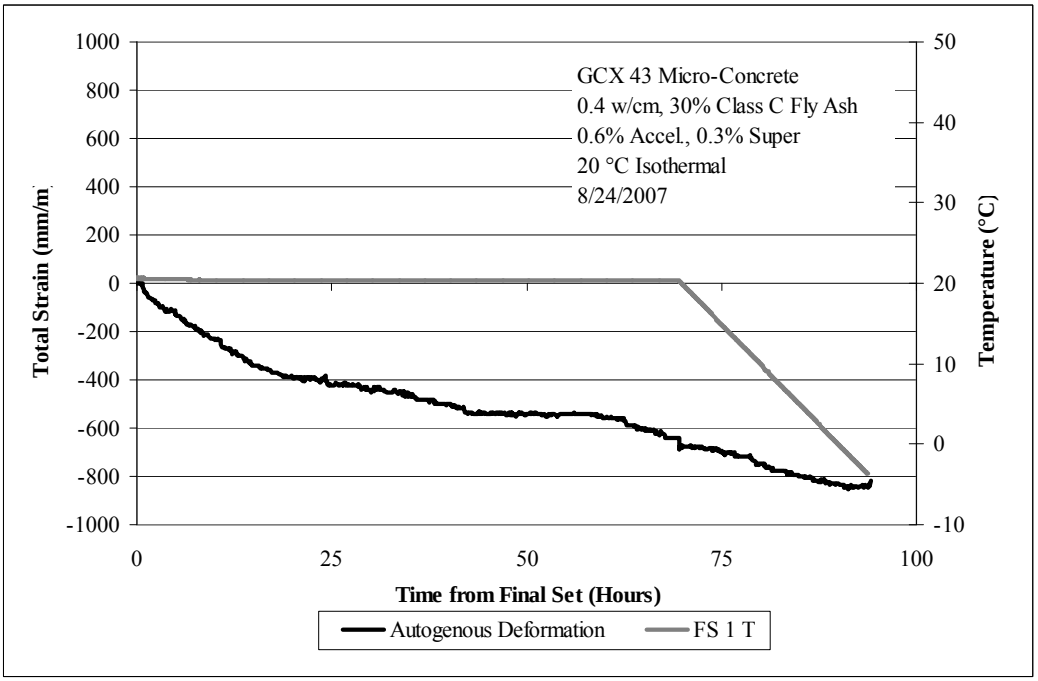

Figure 5.75: Free strain for 20 °C isothermal test, GCX 43

Table 5.24: Mechanical properties for 20 °C isothermal test, GCX 43

Age (days)	Compressive Strength (MPa)	Elastic Modulus (GPa)	Tensile Strength (MPa)
0.3	18.1	16.4	2.5
1.2	36.6	30.8	4.2
3.2	42.7	26.9	6.3
47.3	41.5	30.21	6.1

Italics indicates only one test performed

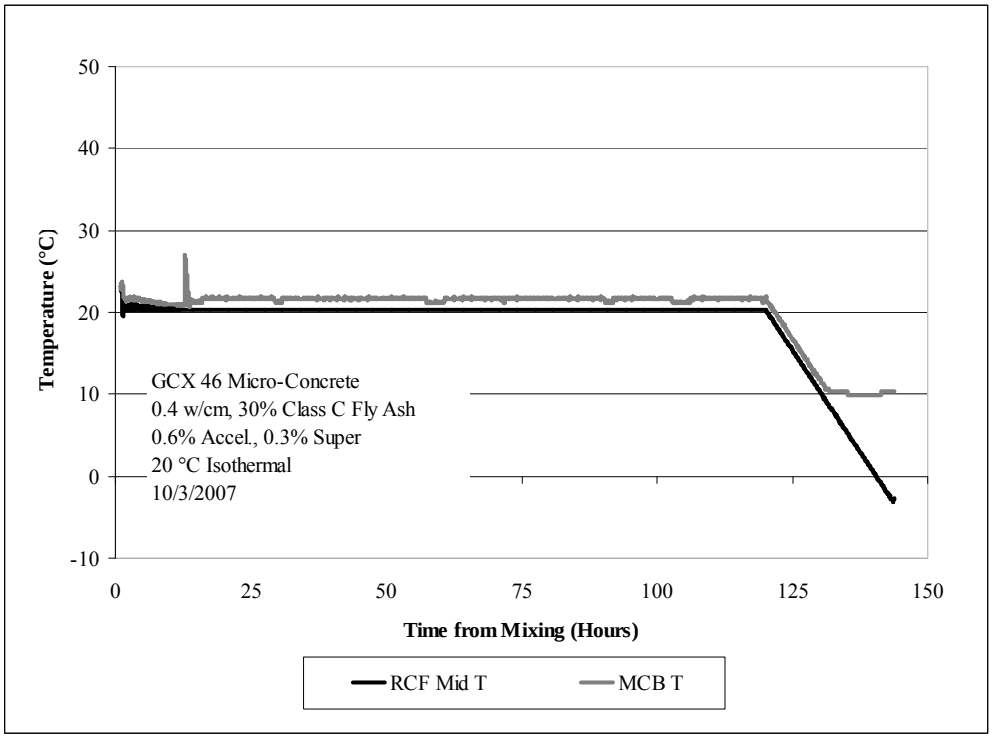

Figure 5.76: Temperature profile for 20 C isothermal test, GCX 46

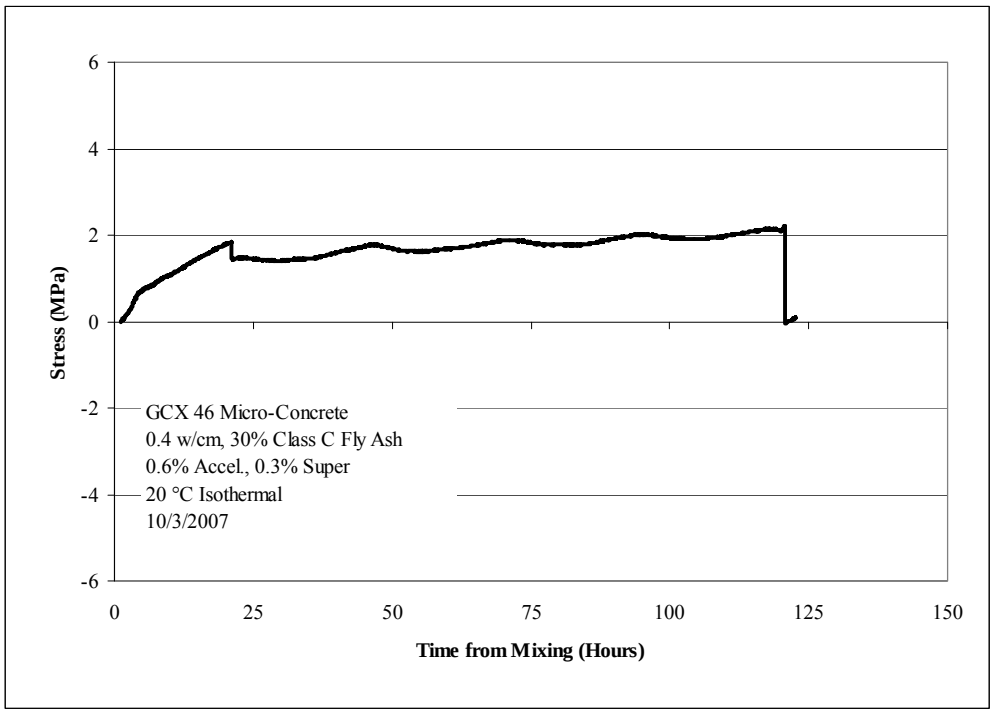

Figure 5.77: Stress generation for 20 °C isothermal test, GCX 46

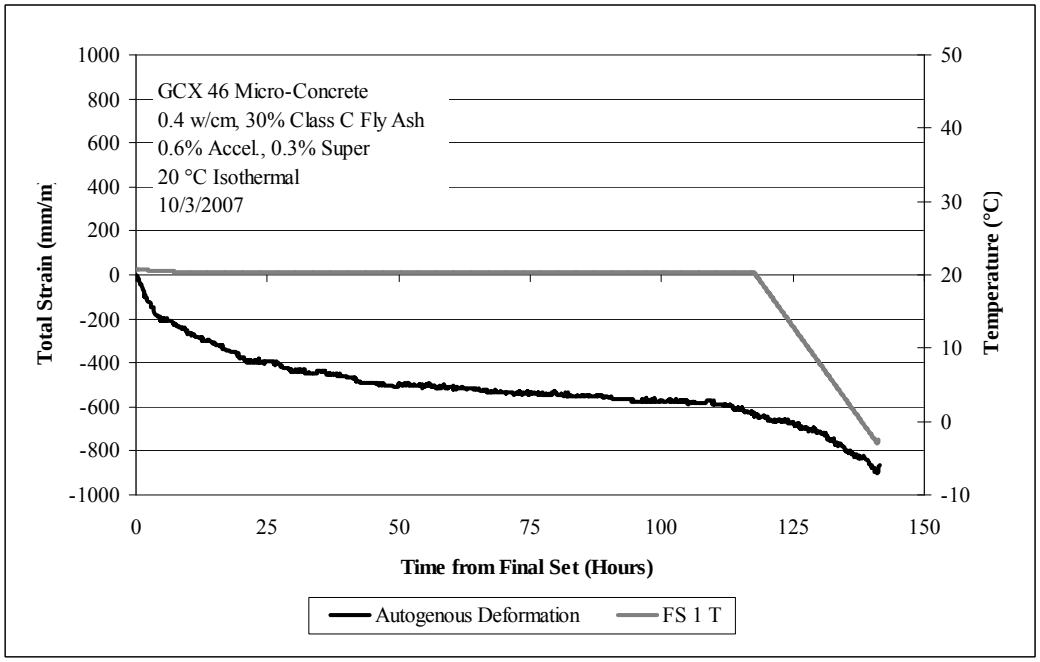

Figure 5.78: Free deformation for 20 °C isothermal test, GCX 46

Table 5.25: Mechanical properties for 38 °C isothermal test, GCX 46

Age (days)	Compressive Strength (MPa)	Elastic Modulus (GPa)	Tensile Strength (MPa)
0.3	26.9	22.5	2.9
1.0	35.9	29.8	6.8
2.3	38.6	30.7	6.3
5.3	41.0	30.96	7.1

5.5.5.2 38 °C Isothermal Testing

Testing was also conducted on the same mixture proportions (30% replacement of GCX Binder by class C fly ash) shown in section 5.5.5.1. The following two mixtures were cured at 38 °C isothermal in the rigid cracking and free deformation frame.

The temperature profiles for GCX 45 and GCX 47, shown in Figure 5.79 and Figure 5.82, respectively show good isothermal temperature control at 38 °C throughout the duration of the test. Artificial cooling was initiated at 120 hours for GCX 45 (Figure 5.79); it was then quickly decided to leave the mixture at 38 °C for an additional 5 days before cooling to ensure conversion had completed. This mixture was repeated for the same length of time shown in Figure 5.82 (GCX 47). The maximum compressive stress attained for GCX 45 (Figure 5.80) was -5.3 MPa at 134 hours after casting and the maximum compressive stress attained for GCX 47 (Figure 5.83) was -4.1 MPa at 225 hours after casting. Neither mixture cracked upon cooling.

Perhaps the most significant result from this series of testing was that the reduction in expansion in free deformation testing. Free deformation is shown for GCX 45 in Figure 5.81 and for GCX 47 in Figure 5.84. Compared to testing the GCX binder alone, the mixtures with 30 % Class C fly ash expanded by approximately 1/3 less (incidentally in line with the percent dilution of CAC by fly ash) with maximum expansion values just around 200 μm/m. This was the main reason for repeating this mixture (GCX 45 was repeated) and the results were almost identical for free

deformation (GCX 47). This was somewhat unexpected since the fly ash replacement seemed to have little impact on results of isothermal curing at 20 °C discussed in section 5.5.5.1. Furthermore, the amount of compressive stress that developed (Figure 5.80 and Figure 5.83) was in good agreement with 38 °C isothermal testing with a straight GCX binder micro-concrete.

Mechanical properties for GCX 45 (Table 5.26) show a steady increase up to 5.2 days of testing with a compressive strength of 34.7 MPa. After this age the compressive strength decreases to a value of 24.9 MPa at 28 days after testing (16 days of storage in a moist cure room). It seems that conversion occurred more slowly in this mixture compared to testing of straight GCX binder. The compressive strength at 2 days for GCX 47 (Table 5.27) was much lower than that for GCX 45 (30.4 MPa compared to 23.2 MPa). However, strengths at 9 days after casting were very similar between the two mixtures at 30.1 MPa (GCX 45) and 29.6 MPa (GCX 47).

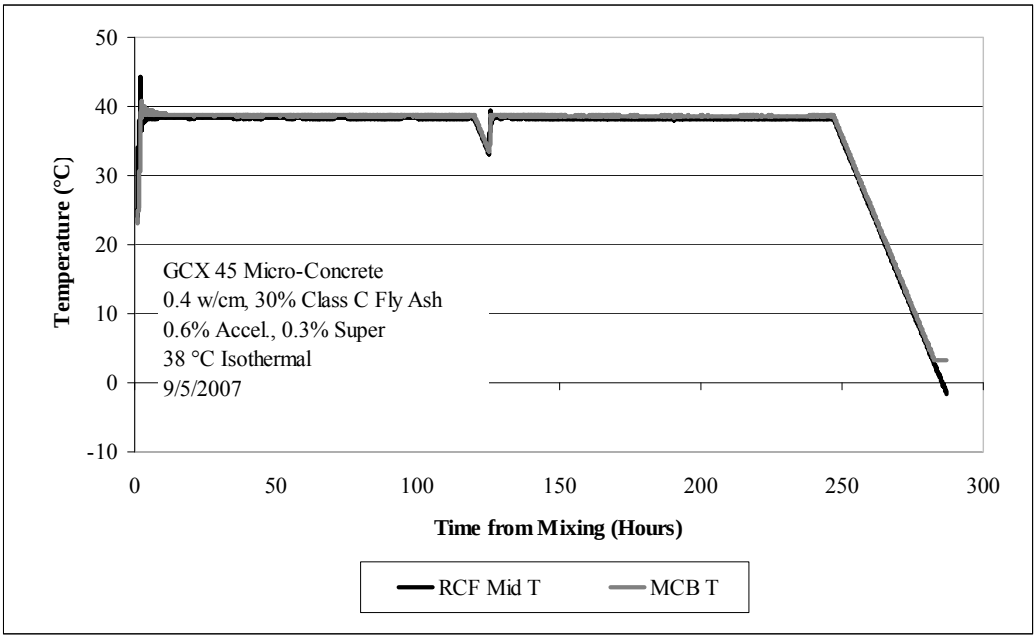

Figure 5.79: Temperature profile for 38 °C isothermal test, GCX 45

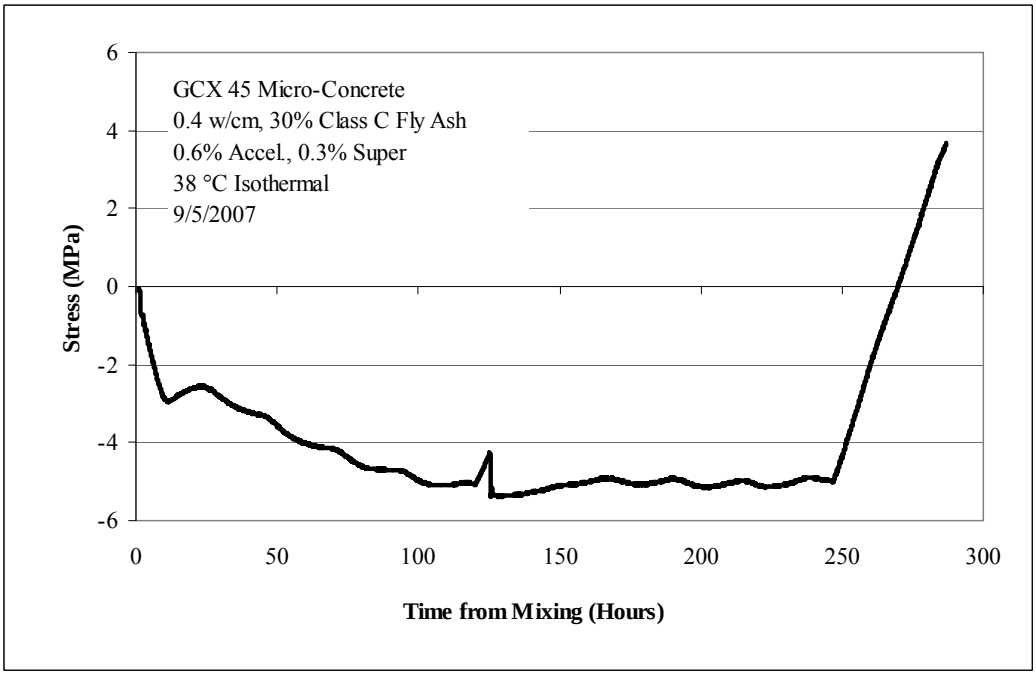

Figure 5.80: Stress generation for 38 °C isothermal test, GCX 45

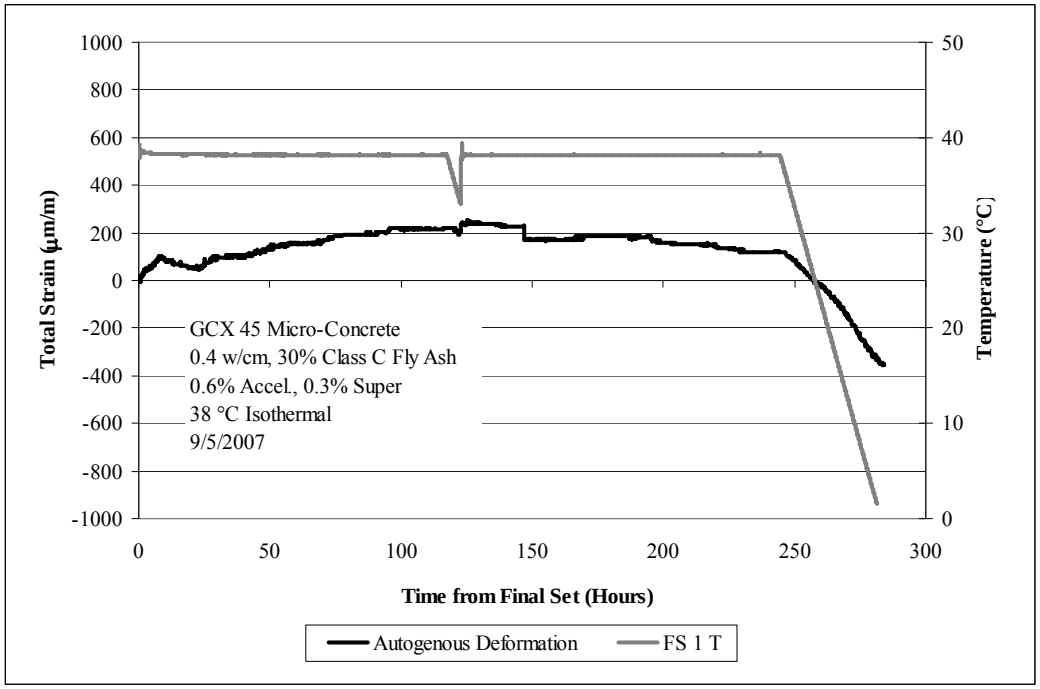

Figure 5.81: Free deformation for 38 °C isothermal test, GCX 45

Table 5.26: Mechanical properties for 38 °C isothermal test, GCX 45

Age (days)	Compressive Strength (MPa)	Elastic Modulus (GPa)	Tensile Strength (MPa)
0.3	12.6	20.0	2.1
1.2	25.6	25.6	4.1
2.1	*30.4*	-	-
5.2	34.7	24.69	5.2
7.2	*33.4*	-	-
9.3	*30.1*	-	-
14.2	27.4	25.94	3.8
23.2	*29.8*	-	-
28.3	24.9	26.8	4.2

Italics indicates only one test performed

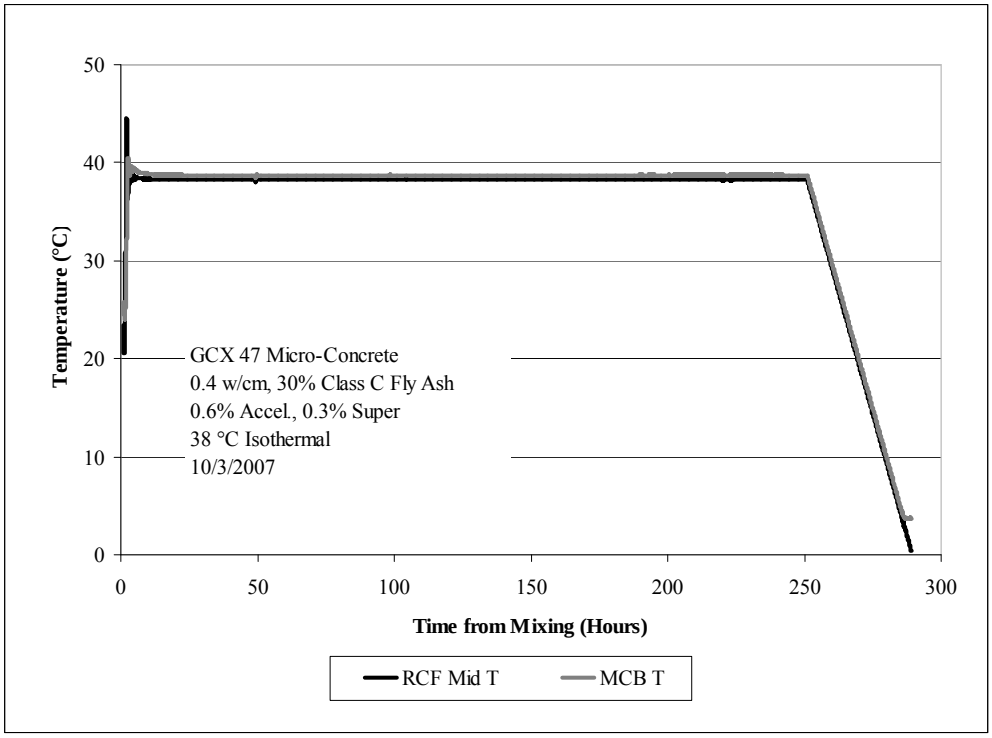

Figure 5.82: Temperature profile for 38 °C isothermal test, GCX 47

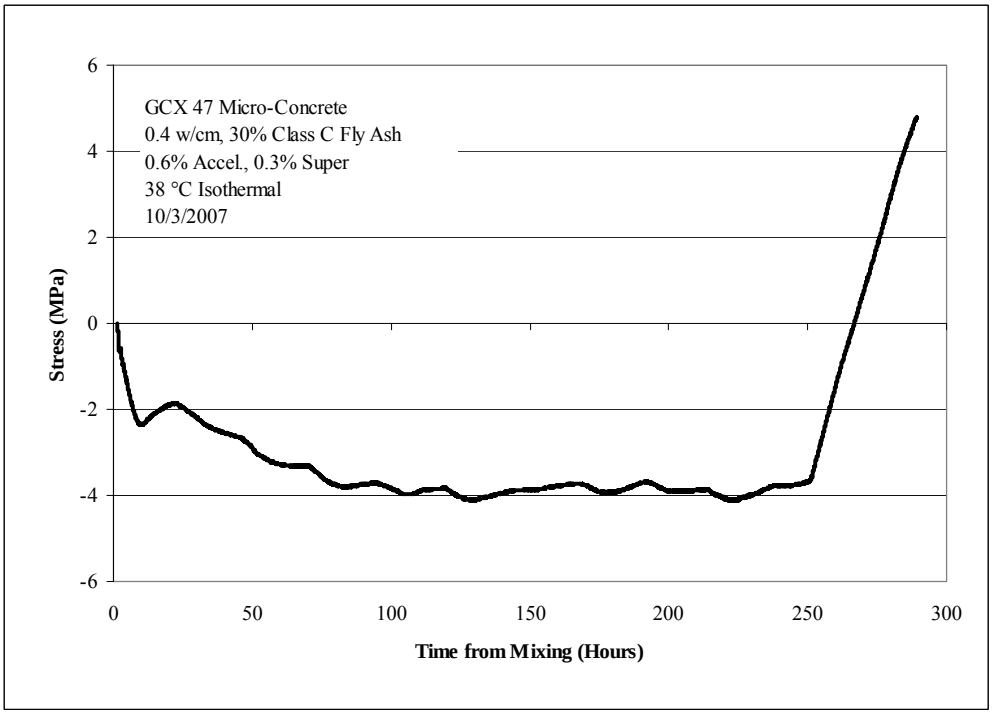

Figure 5.83: Stress generation for 38 °C isothermal test, GCX 47

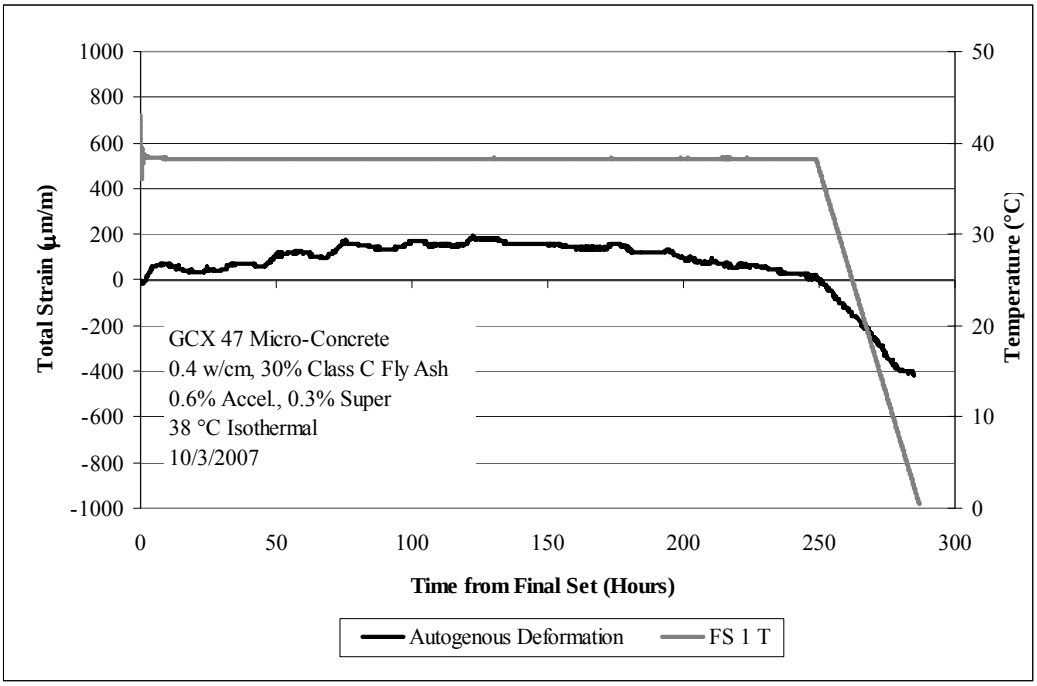

Figure 5.84: Free deformation for 38 °C isothermal test, GCX 47

Table 5.27: Mechanical properties for 38 °C isothermal test, GCX 47

Age (days)	Compressive Strength (MPa)	Elastic Modulus (GPa)	Tensile Strength (MPa)
0.2	11.7	16.3	1.9
2.0	*27.5*	25.2	5.1
2.2	23.2	23.6	4.8
9.4	29.6	29.92	5.4

Italics indicates average of 2 compression tests

5.5.6 Realistic Time-Temperature Histories

While investigating isothermal temperatures is necessary to isolate the early-age volume change resulting from micro-structural formation, no actual structures are cured isothermally in a real field application. As a result the final part of this study investigated realistic time-temperature histories from two field trials. The first realistic time-temperature history investigated was from a field trial in France in September of 2001. The second realistic time-temperature history investigated was taken from a small field

trial at The University of Texas at Austin which involved casting 6 slabs outdoors measuring 0.9 x 0.9 meter square. Four of the slabs were 100 mm in depth, one of the slabs 200 mm and the third slab 300 mm in depth. One of the 100 mm slabs was well-insulated to simulate self-heating typically of larger CACC elements. More details of this field trial can be found in Chapter 7 of this dissertation. The time-temperature histories used were from thermocouples placed in the center of the slabs in each field trial. The real time-temperature histories will be plotted with the temperature profile for the resulting rigid cracking frame mixtures. Several variations of temperature (e.g., maximum temperature reached, maintained at this temperature isothermally for various durations in each testing regime).

5.5.6.1 Realistic Time Temperature History: France, 2001

The first realistic time-temperature history was provided by the CAC manufacturer from a field trial that was performed in 2001. This was done to give a starting point for the investigations into realistic time and temperature histories prior to generation of this type of data at The University of Texas at Austin as part of this dissertation. Several variations using realistic time-temperature histories to drive the temperature in the rigid cracking and free deformation frames and match-cured apparatus were investigated. These included:

1) Following the actual temperature history
2) Following the actual temperature history to the maximum temperature attained during curing and holding it at that maximum temperature isothermally for varied amounts of time
3) Following the actual temperature history through roughly the first 24 hours (until the mixture had cooled in accordance with the real

temperature history) and then holding at an isothermal temperature of 20 °C.

The first trial mixture followed option 2 and this temperature history is shown in Figure 5.85. The stress generation for this mixture is shown in Figure 5.86. Free deformation is shown in Figure 5.87 and mechanical properties are shown in Table 5.28.

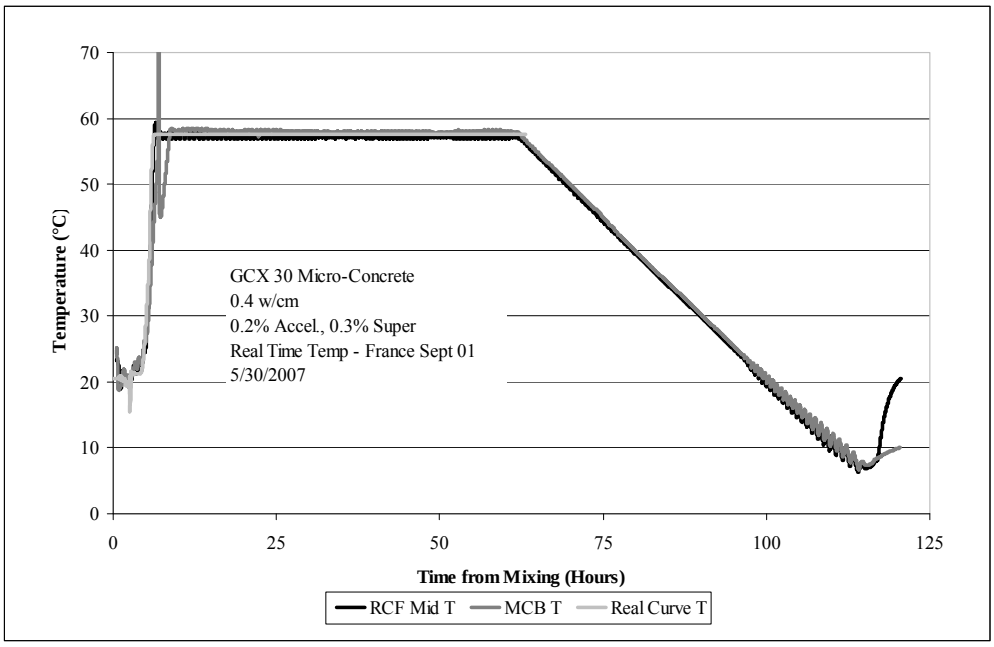

Figure 5.85: Temperature profile for real temperature history with hold, GCX 30

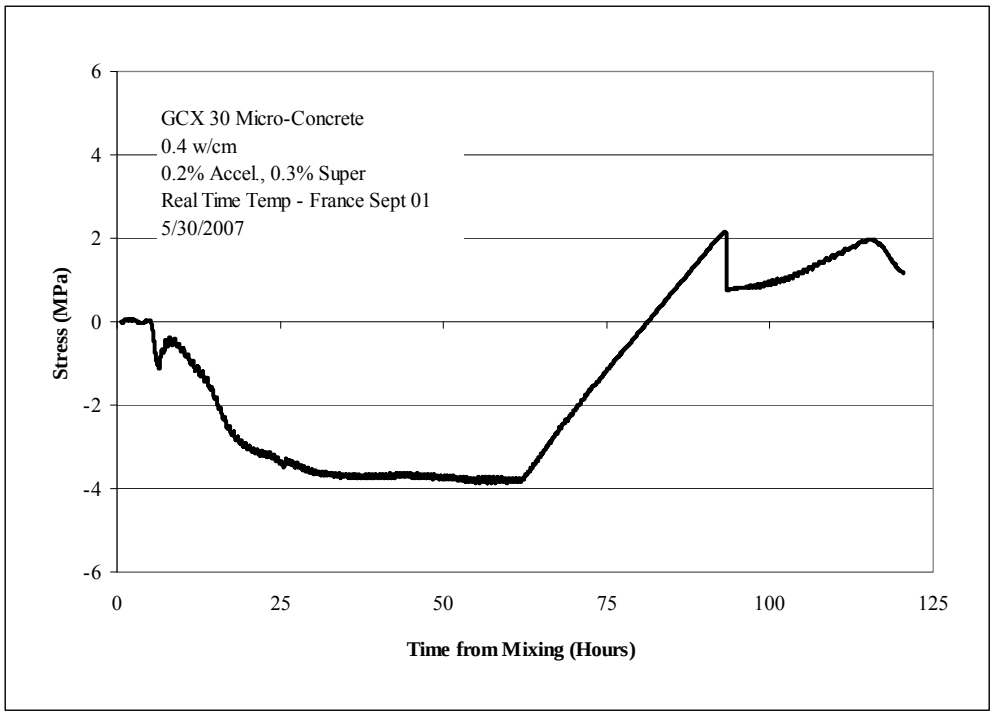

Figure 5.86: Stress generation real temperature history with hold, GCX 30

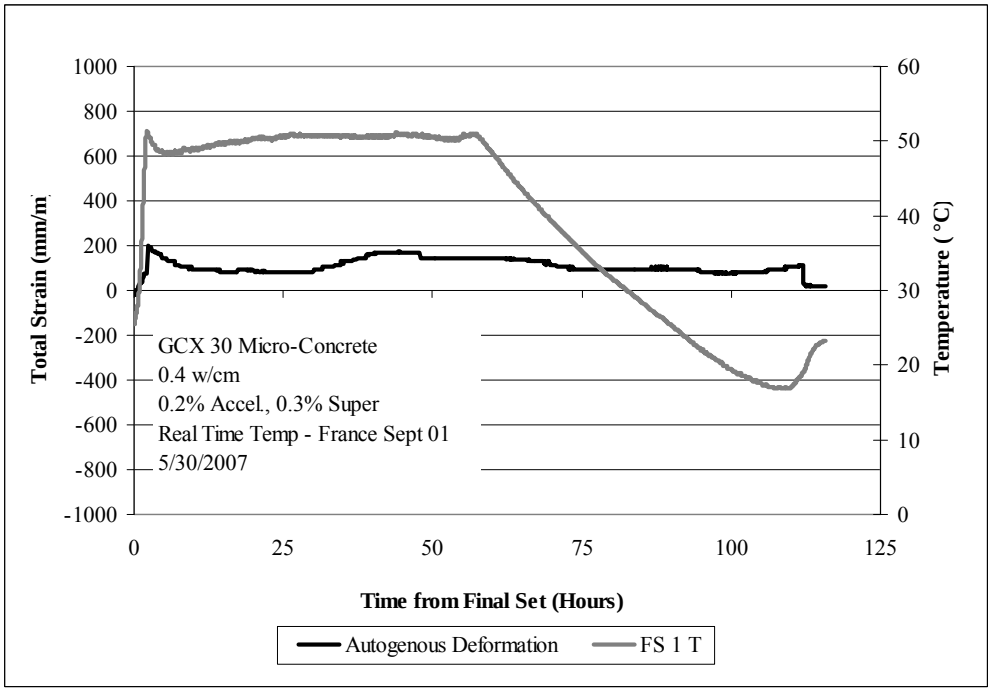

Figure 5.87: Free deformation for real temperature history with hold, GCX 30

Table 5.28: Mechanical properties for real temperature history, GCX 30

Age (days)	Compressive Strength (MPa)	Elastic Modulus (GPa)	Tensile Strength (MPa)
1.1	20.2	-	3.2
2.2	21.1	-	3.9
5.2	24.1	-	3.7

The temperature profile for this mixture shows excellent temperature control for the first realistic time-temperature history mixture cast in the frames and match-cured apparatus. This mixture was purposefully held at high temperature to force conversion to occur before artificially cooling at 62 hours after casting. The stress generation for this mixture shows an initial compressive stress development followed by a short decrease in compressive stress before finally going fully into compressive stress to a maximum value of -3.7 MPa at 62 hours (just before cooling). Upon cooling the mixture cracked at a tensile stress of +2.1 MPa at 93.3 hours after cooling when the temperature of the concrete was 26.5 °C. Mechanical property data indicated that the tensile strength of the mixture was close to 3.7 MPa. Compressive strength showed a steady increase after 1.1 day (20.2 MPa) to 24.1 MPa at 5.2 days into the test. Free deformation movement was only adequately recorded for movement of one of the LCPs. Assuming equal movement from both LCPs these values should essentially be doubled for this mixture.

The second mixture cast following the real time temperature histories from the field trial in France followed option 3 where the heating and cooling portion of the curve was followed and then the mixture was held isothermally at 20 °C for a long period of time (12 days). The temperature profile followed for this mixture is shown in Figure 5.88. Figure 5.89 and Figure 5.90 show the stress generation and free deformation, respectively. Mechanical properties are shown in Table 5.29.

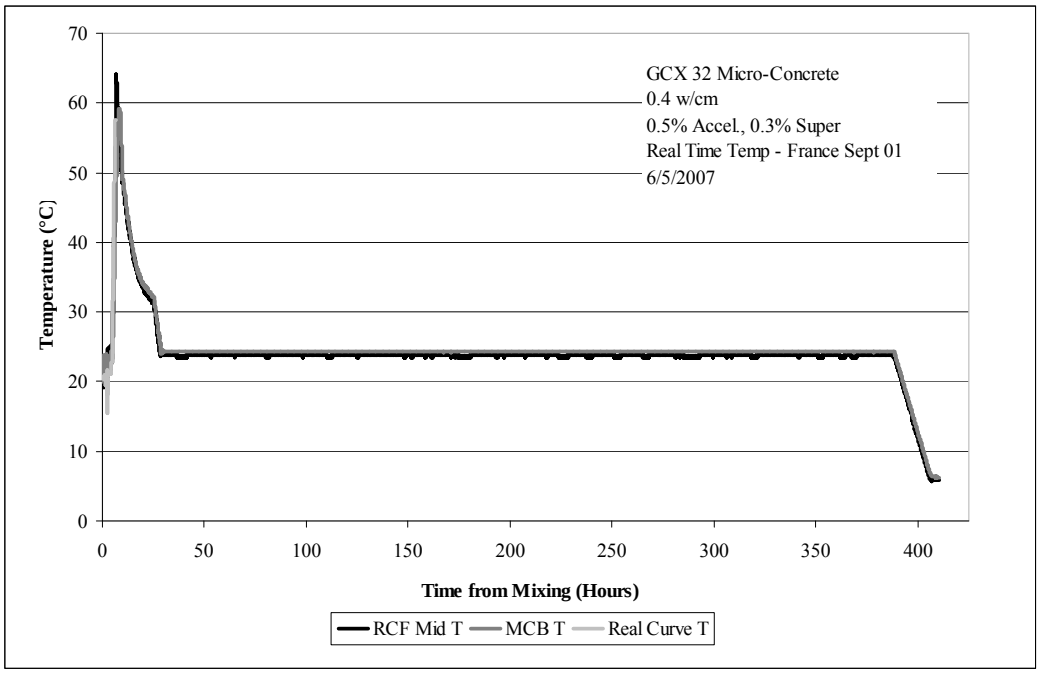

Figure 5.88: Temperature profile for real temperature history, GCX 32

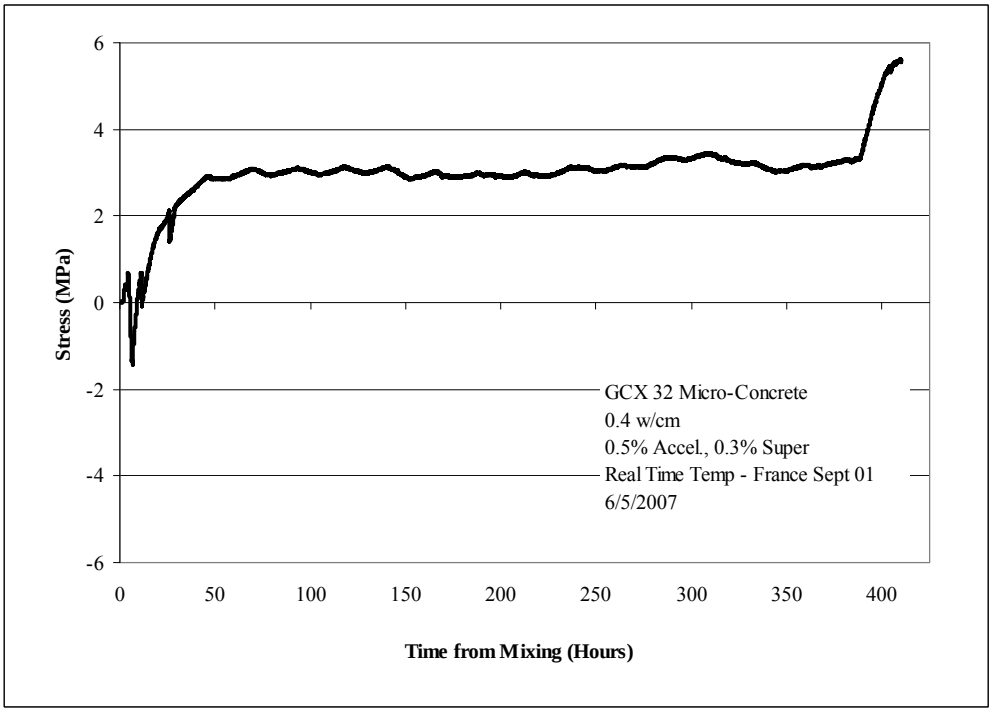

Figure 5.89: Stress generation for real temperature history, GCX 32

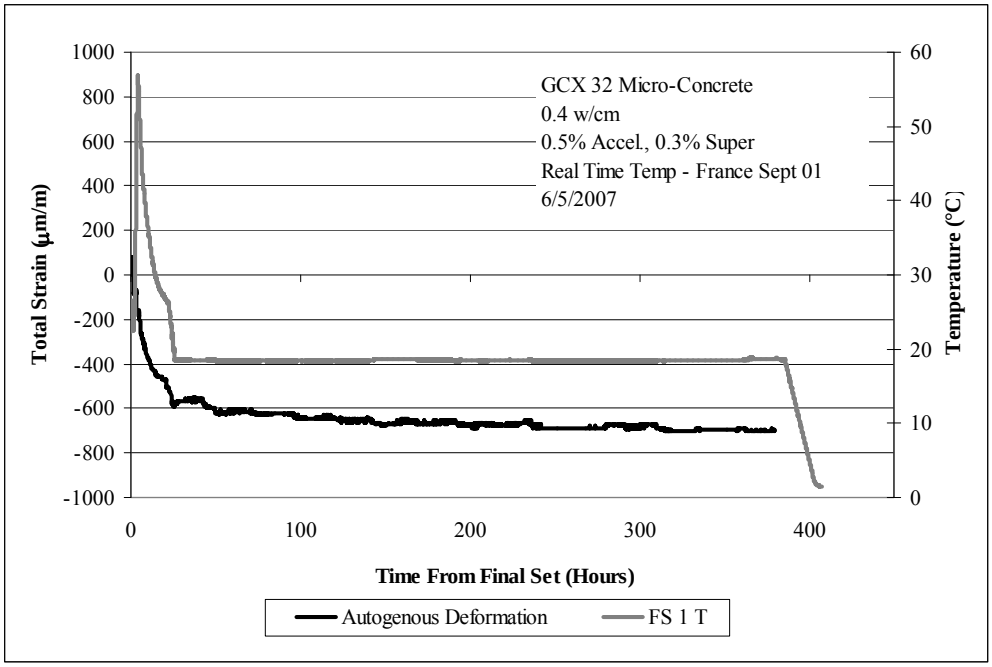

Figure 5.90: Free deformation for real temperature history, GCX 32

Table 5.29: Mechanical properties for real temperature history, GCX 32

Age (days)	Compressive Strength (MPa)	Elastic Modulus (GPa)	Tensile Strength (MPa)
0.3	42.0	-	4.8
1.2	37.5	33.6	5.8
3.2	31.8	38.7	4.3
7.2	41.7	34.3	6.5
17.2	43.1	33.71	5.9
28.3	49.8	37.2	8.7

The temperature profile for this mixture followed very closely along the desired real temperature history. However, this mixture set in 2.8 hours, which was much faster than GCX 30 which set in 4.7 hours and was more in line with the setting time of the actual mixture in the field trial. This is a result of an increased dosage of accelerator, 0.5% in GCX 32 compared to 0.2% in GCX 30. Due to the mixture setting about 2 hours before the imposed increase of temperature (to follow the desired time-temperature history), the mixture was artificially held roughly around 20 °C for 2 hours, and this had

significant impact on the remainder of the test. The stress generation profile shows that the mixture initially went into tension during this 2 hour time period where metastable hydrates were rapidly forming. Then upon heating the mixture went into compression and developed a maximum compressive stress of -1.3 MPa at 6.8 hours. However, at this point the mixture began to cool down as it would have in the actual field concrete and the mixture went into tension to a maximum value of +3.5 MPa and it stayed consistently around this value for the remainder of the isothermal portion of the testing regime. This behavior is confirmed by movement in the free deformation frame where the mixture expanded slightly to 100 μm/m and then was always in a state of shrinkage, even during the heating portion of this test. The ultimate free strain before artificial cooling was 694 μm/m. While this test may not be indicative of how true CACC concrete performs in the field (i.e. held isothermally at low temperature after setting) it was an important finding that demonstrates the profound effect that even a small perturbation in temperature has on volume change at early-age. Since the formation of CAC hydrates is through solution, meaning a rapid dissolution of ionic species into solution is followed by precipitation of hydration products, the temperature at which the hydration products forms and for how long the material remains within a temperature range to promote formation of certain products (e.g., metastable versus stable) have significant impact on early-age volume change and on the duration of conversion throughout the lifespan of the concrete.

The mechanical properties further elucidate these findings. The compressive strength of 42.0 MPa at 0.3 days is rather high indicating the amount of time spent at low temperature after setting encouraged rapid strength gain from the deposition of metastable hydrates (mixtures of CAH_{10} with some C_2AH_8). After this point the compressive strength gradually decreased to a minimum of 31.8 MPa at 3.2 days and

increased thereafter to a value of 49.8 at 28 days. The elastic modulus showed a decrease in strength between 7 and 17 days and tensile strength fluctuated between 3 and 17 days.

The next mixture tested was a repetition of mixture GCX 30 where the temperature was held isothermally for 2 hours after setting at a temperature of 20 °C, before the heating portion of the real temperature history was induced. The temperature profile for this mixture is shown in Figure 5.91 and the stress generation is shown in Figure 5.92. Free deformation and mechanical properties are shown in Figure 5.93 and Table 5.30 respectively.

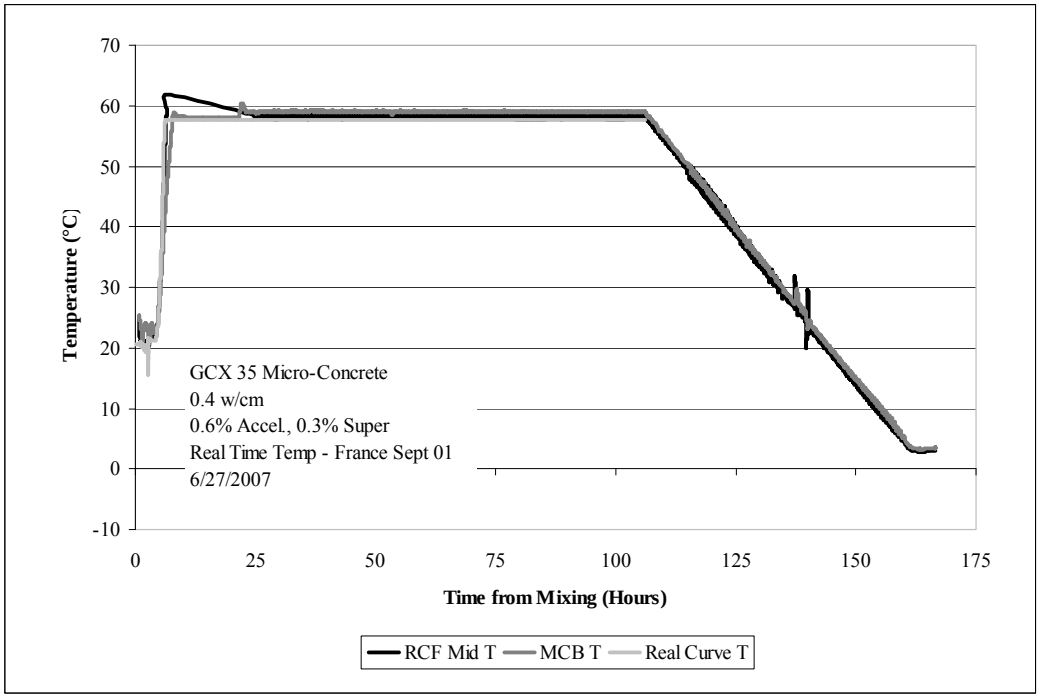

Figure 5.91: Temperature profile for real temperature history, GCX 35

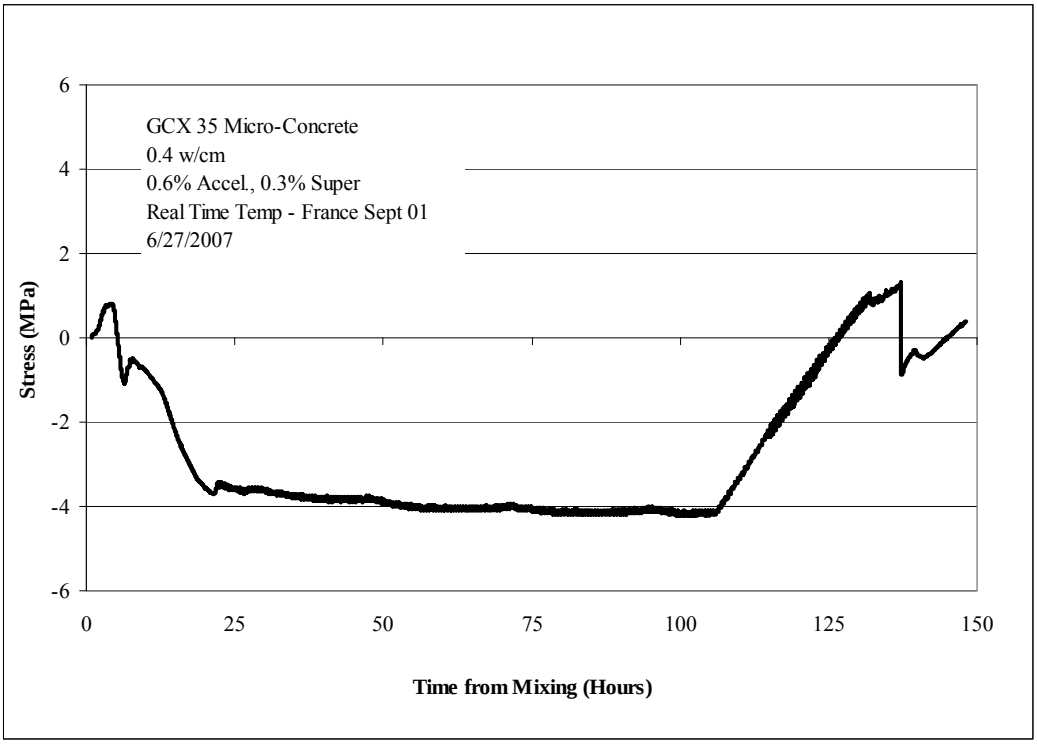

Figure 5.92: Stress generation for real temperature history, GCX 35

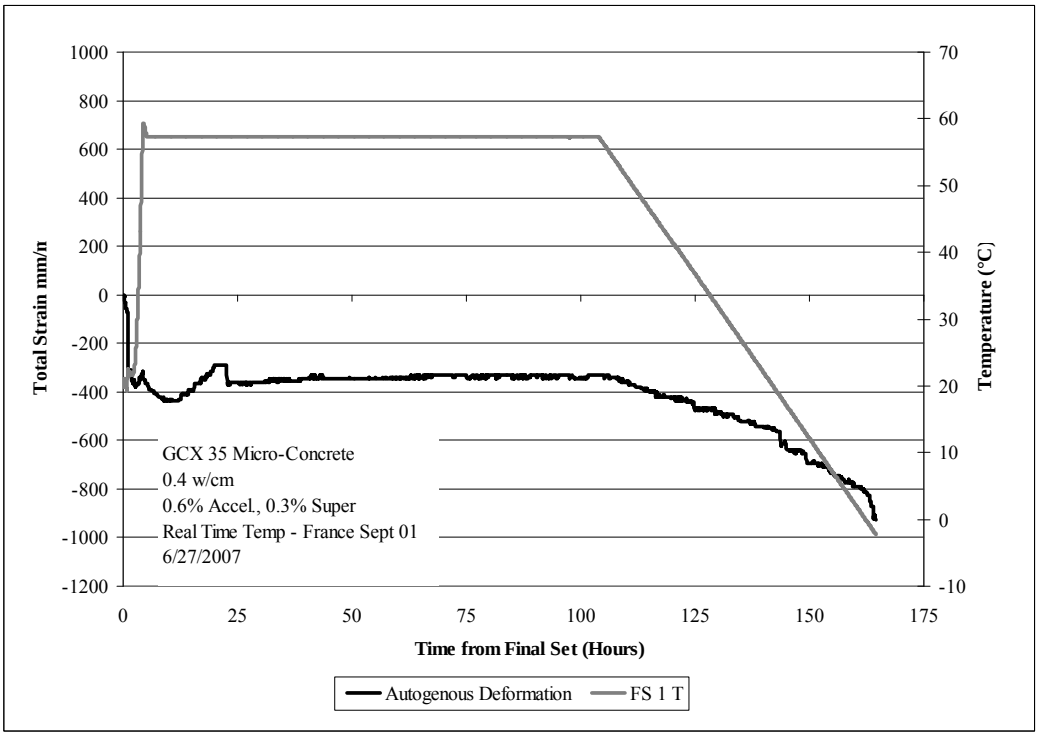

Figure 5.93: Free deformation for real temperature history, GCX 35

Table 5.30: Mechanical properties for real temperature history, GCX 35

Age (days)	Compressive Strength (MPa)	Elastic Modulus (GPa)	Tensile Strength (MPa)
0.2	33.0	25.1	4.6
1.2	21.9	29.1	3.6
6.3	25.3	27.4	4.6
7.2	26.0	26.51	4.9
126.1	31.9	35.0	4.4

The temperature profile for this mixture is very similar to GCX 30 with an isothermal hold at the maximum temperature attained of 57 °C until cooling at 110 hours. The stress generation profile shows that the mixture develops tensile stress while the mixture is held isothermally at 20 °C for 2 hours after final setting. Then compressive stresses develop as the mixture is heated to the maximum temperature during hydration of 57 °C. Then the mixture begins to go into tension again (while at high temperature) before fully developing compressive stress. The maximum compressive stress attained was -4.1 MPa at 106 hours (just prior to artificial cooling). Upon cooling the mixture did not exhibit cracking.

The free deformation data indicates similar behavior where the mixture exhibits shrinkage until the heating portion of the curve begins. However, the increase from this temperature rise is extremely small as shown in Figure 5.93. Then the mixture exhibits shrinkage again just as the mixture in the rigid cracking frame developed tensile forces for a several hours at high temperature before compressive stresses developed commensurate with fully converting the material to stable hydrates. This further demonstrates the profound influence of temperature on conversion. Once a substantial amount of metastable hydrates have formed (e.g., 2 hours of isothermal hold at 20 °C after setting, plus the additional time to cross a nominal threshold of 30 °C, above which stable hydrates are favored) it may be necessary to maintain high temperature for a specific amount of time to enable conversion of metastable to stable hydrates.

The mechanical properties evaluated on micro-concrete cast from this mixture show that a converted strength of 21.9 MPa was attained 1.2 days after casting (e.g., the end of conversion as evidenced by stress generation and free deformation). Compressive strength gradually increased thereafter. The elastic modulus decreased slightly to 26.5 GPa at 7.2 days, and increased thereafter. Tensile strength also decreased at 1.2 days and gradually increased thereafter. However, a slightly lower tensile strength of 4.4 MPa was measured 126 days after casting.

The notion that mixtures in the field that reach high temperature (55 °C and above) have fully converted strengths may be a misconception. The amount of time spent at high temperature is just as important a factor as the maximum temperature attained. The implications for field concrete will be discussed in the final chapter of this dissertation where field trials in Austin, Texas are discussed.

The next set of real time-temperature histories investigated were based on outdoor slabs cast at The University of Texas at Austin as mentioned at the beginning of this section. The real temperature history chosen to investigate was from an insulated slab to encourage self-heating and to replicate a heat signature typically of larger hydrating field elements. The first temperature profile investigated followed Option 3 where the mixture was allowed to heat and cool following the real temperature curve and then was held isothermally at 20 °C for the remainder of the testing period. Figure 5.94 and Figure 5.95 show the temperature profile and stress generation for this mixture, respectively. The free deformation and mechanical properties are shown in Figure 5.96 and Table 5.31.

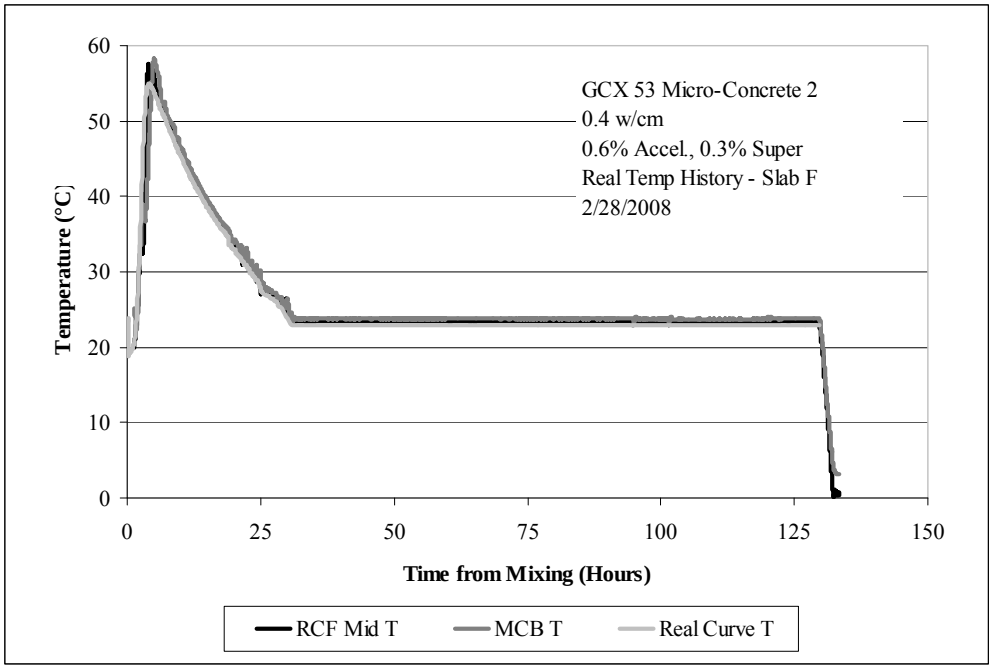

Figure 5.94: Temperature profile for real temperature history, GCX 53

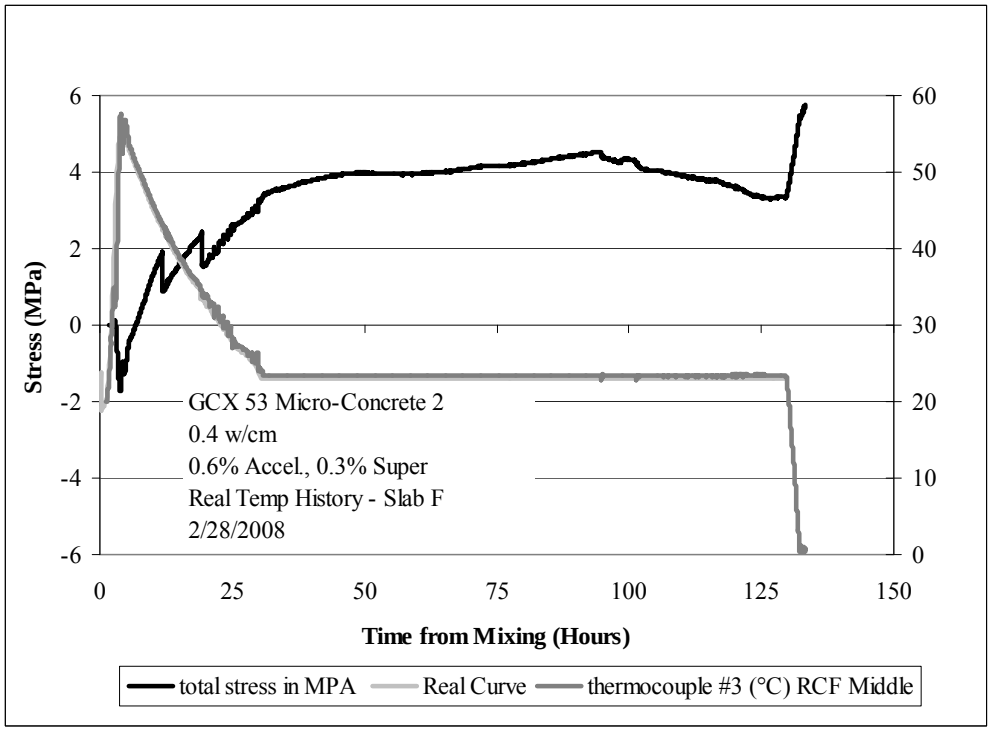

Figure 5.95: Stress Generation for real temperature history, GCX 53

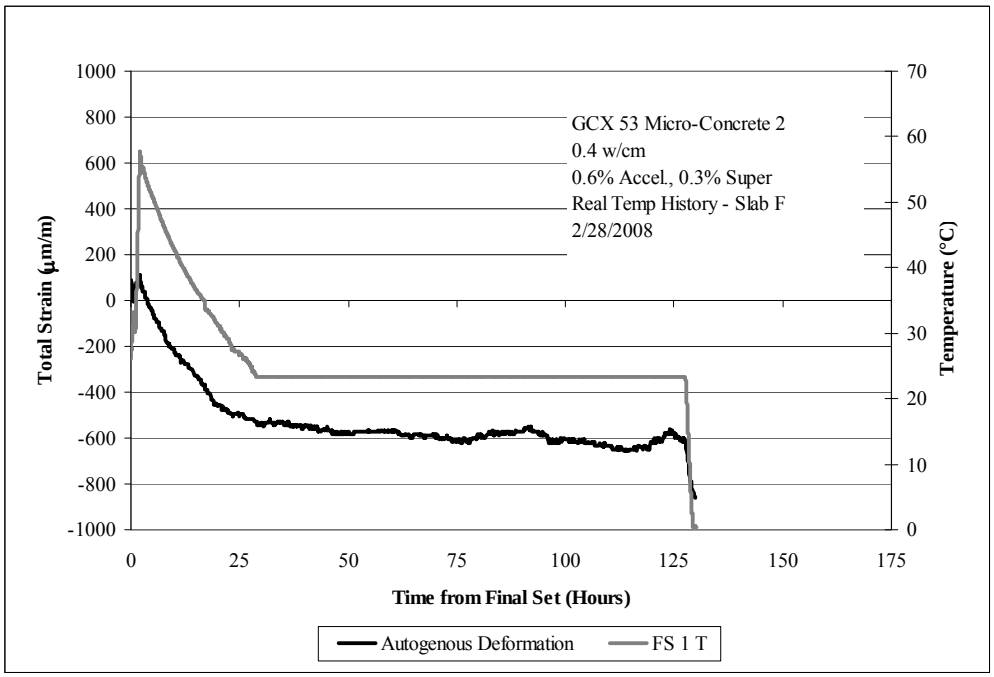

Figure 5.96: Free deformation for real temperature history, GCX 53

Table 5.31: Mechanical properties for real temperature history, GCX 53

Age (days)	Compressive Strength (MPa)	Elastic Modulus (GPa)	Tensile Strength (MPa)
0.2	36.9	35.9	6.6
1.2	46.1	35.0	7.8
5.0	50.6	40.3	9.0

GCX 53 set in approximately 2 hours and corresponded almost identically with the increase in temperature seen from the real temperature history. Furthermore, the water baths maintained excellent temperature control. The stress generation for GCX 53 shown in Figure 5.95 shows interesting results in that the material initially went into compression in line with the heat generation portion of the temperature profile to a maximum of -1.5 MPa at 4 hours. Upon cooling the mixture developed tensile stress and exhibited microcracking at a stress of +1.9 MPa at 11.9 hours and again at +2.4 MPa at 19.4 hours with continual increase in stress to a maximum value of +4.4 MPa at 95.1

hours. Upon cooling the mixture reached a maximum tensile stress of +5.7 MPa at 133.4 hours, but did not develop a full crack. Tensile strength at the end of the testing period was 9.0 MPa and is likely why the mixture did not show a full crack. At the earlier points of microcracking (11.9 and 19.4 hours) the tensile strength of the mixture was somewhere between 6.6 and 7.8 MPa. This is strength much higher than the tensile stress at which micro-cracking occurred and it is not fully understood why the material would be less resistant to cracking given that the tensile strength was so high. Compressive strength also showed marked increase to a maximum value of 50.6 MPa at 5.2 days. It is likely that these are unconverted strengths. Free deformation showed an initial expansion followed by shrinkage commensurate with the cooling phase of the material and after cooling to 20 °C the mixture showed very little movement until artificial cooling.

The next mixture followed the temperature profile for Option 1 where the entire real temperature profile with rise and fall in temperature after hydration owed to the change in ambient temperature. Figure 5.97 shows the temperature profile for this mixture with the temperature history of Slab F shown in red. Figure 5.98 and Figure 5.99 show the stress generation for this mixture. Figure 5.100 and Table 5.32 show the free deformation and mechanical properties for this mixture, respectively.

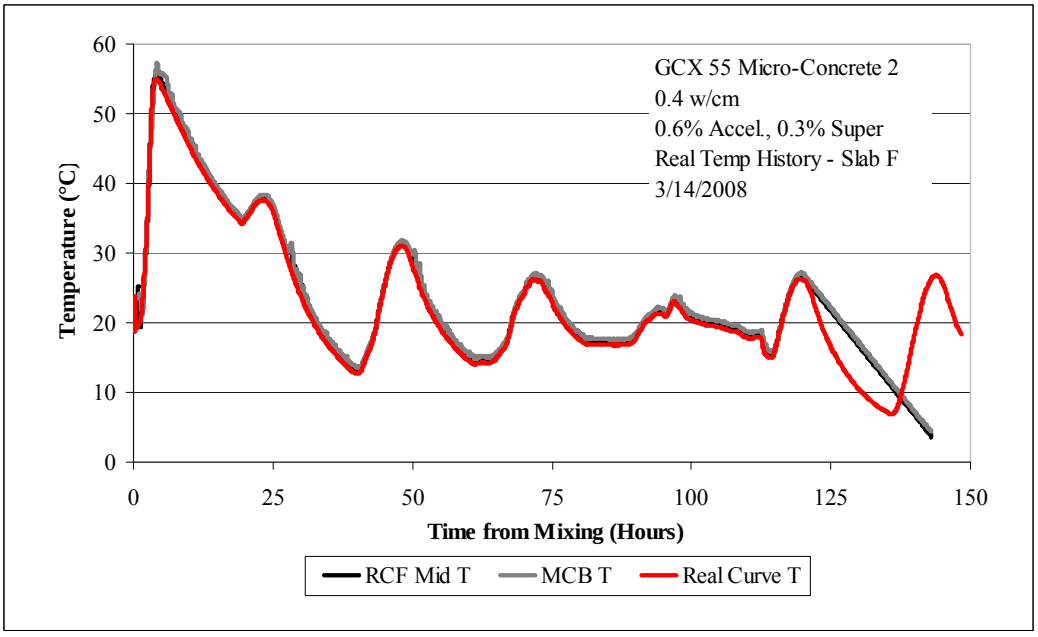

Figure 5.97: Temperature profile for real temperature history, GCX 55

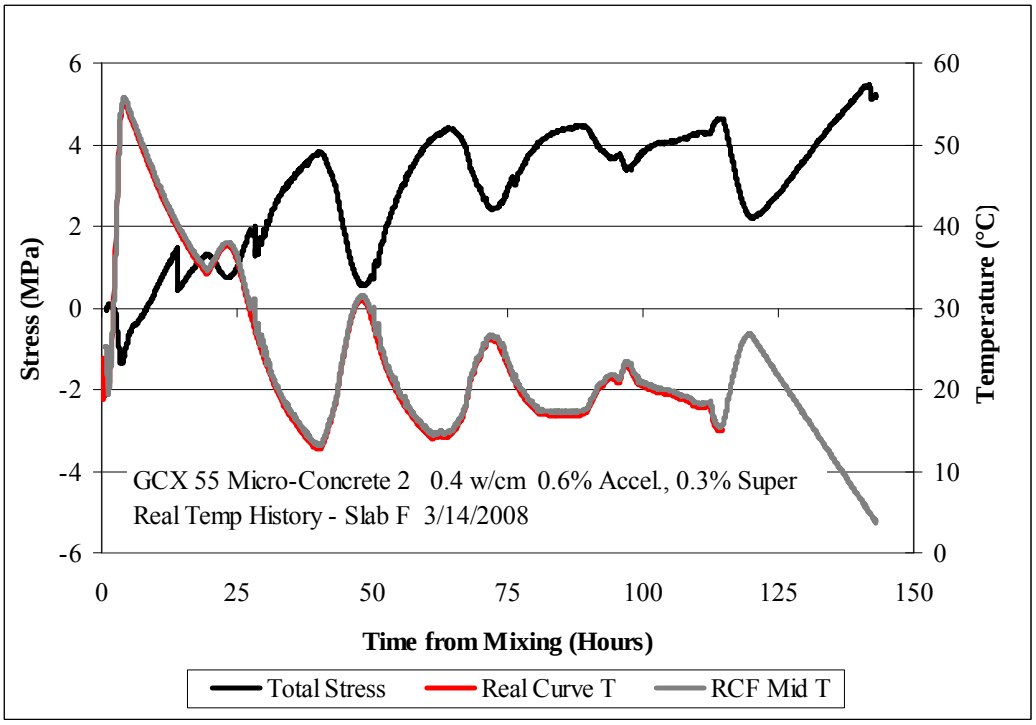

Figure 5.98: Stress generation for real temperature history, GCX 55

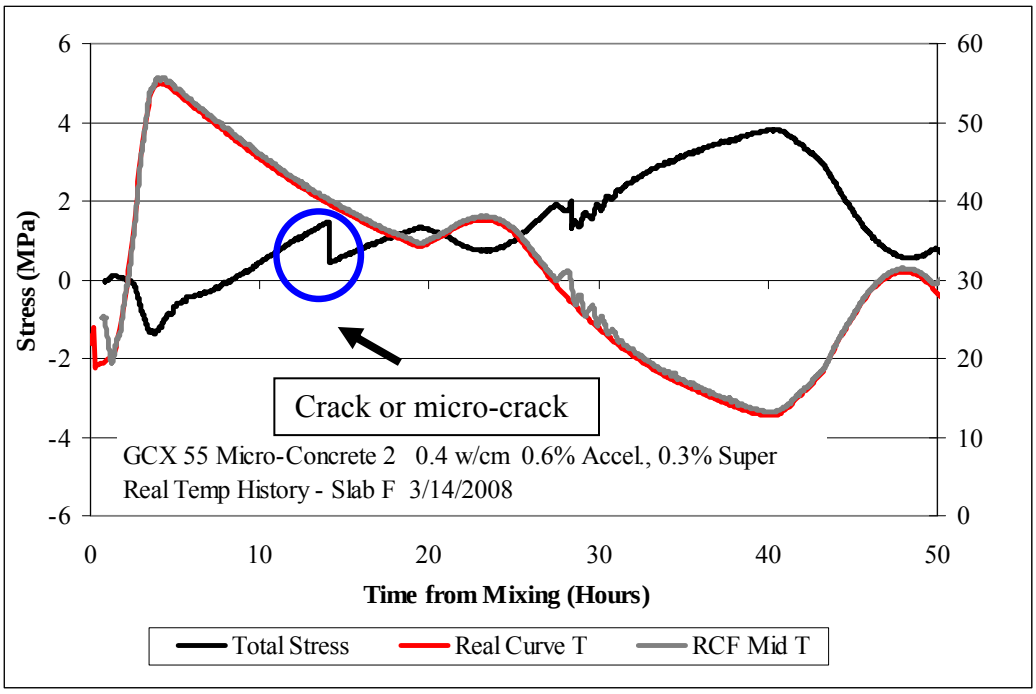

Figure 5.99: Stress generation for real temperature history, GCX 55, up to 50 hours

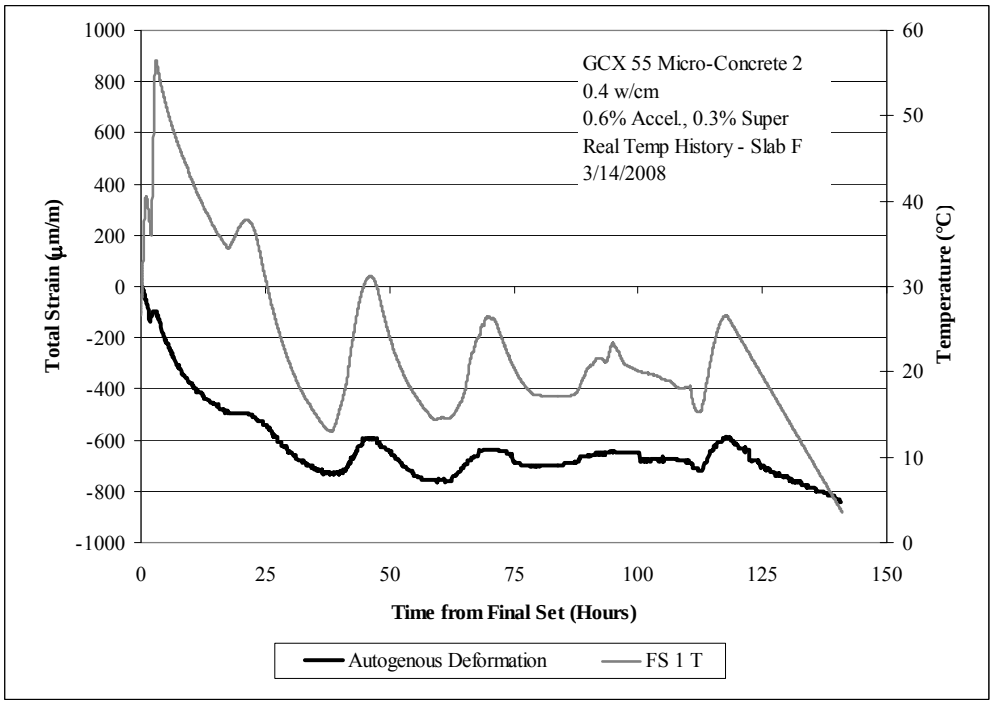

Figure 5.100: Free deformation for real temperature history, GCX 55

Table 5.32: Mechanical properties for real temperature history, GCX 55

Age (days)	Compressive Strength (MPa)	Elastic Modulus (GPa)	Tensile Strength (MPa)
0.2	33.3	28.7	5.9
1.2	41.1	36.4	7.0
3.2	34.6	36.2	7.3
6.2	44.3	*37.1*	7.2

Italics indicates only one test performed

This is the first temperature profile shown that replicates long-term temperature flucations for a CACC concrete cast with GCX Binder. The temperature profile shows that the water baths did an excellent job of following the entire real time temperature history. The mixture was artificially cooled at 120 hours as indicated in Figure 5.97. The stress generation for this mixture shows an almost immediate development of compressive stress followed by tensile stress generation commensurate with cooling. The mixture exhibited microcracking at a tensile stress of +1.5 MPa, 14 hours after casting. After this point the fluctuations in ambient temperature resulted in fluctuations between tensile and compressive stress, however the material remained on the tensile side of stress for the duration of this test. Again the free deformation frame showed mostly shrinkage with only a slight expansion during the period of initial heating of the material. After 24 hours the free deformation frame fluctuated between -600 and -800 μm/m. Mechanical property evolution indicates that some conversion may occur around 3.2 days as there is a decrease in compressive strength and elastic modulus at this age from 41.1 MPa to 34.6 MPa and 36.4 to 36.2 GPa, respectively. Tensile strength shows a gradual increase from a low value at 1.2 days of 5.9 MPa to 7.2 MPa at 6.2 days.

The next two mixtures investigated were part of a follow-up to the real temperature histories were inspired by an interest in determining the duration of exposure to high temperature (maximum 57 °C for this testing) that would promote complete conversion of the metastable hydrates to stable hydrates. Chemical shrinkage testing at

55 °C indicated that a minimum of 8-10 hours were needed to fully convert hydrating paste samples, keeping in mind that these samples are constantly exposed to water throughout the duration of the test. As a result, this time period at high temperature was doubled for the first mixture investigated so that the maximum temperature of 57 °C was held for 20 hours. Figure 5.101 shows the temperature history for this mixture and Figure 5.102 shows the stress generation. Figure 5.103 shows the free deformation and the mechanical properties are shown in Table 5.33.

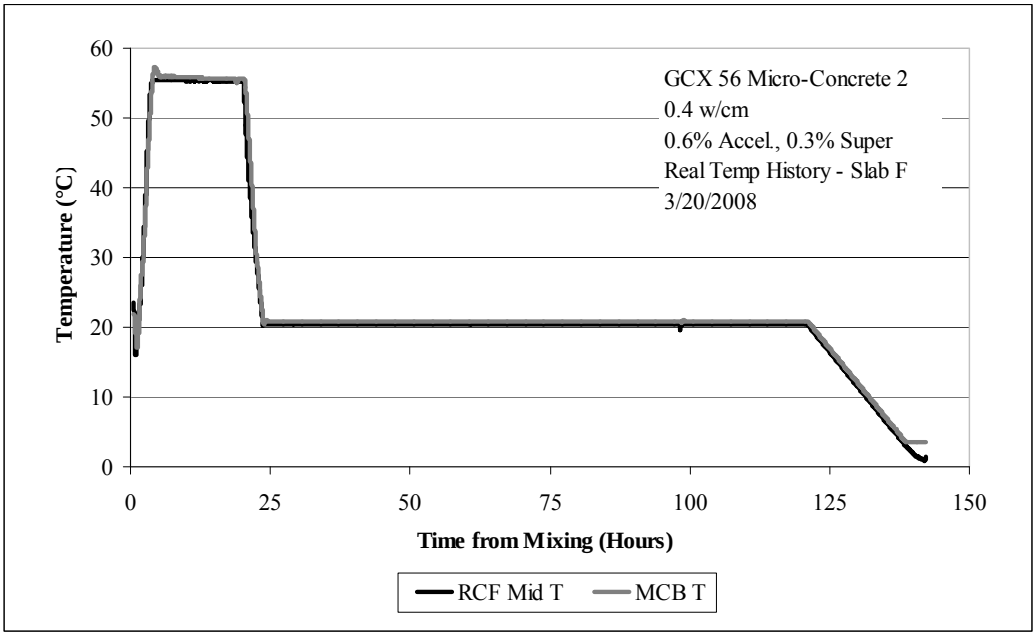

Figure 5.101: Temperature profile for real temperature history, GCX 56

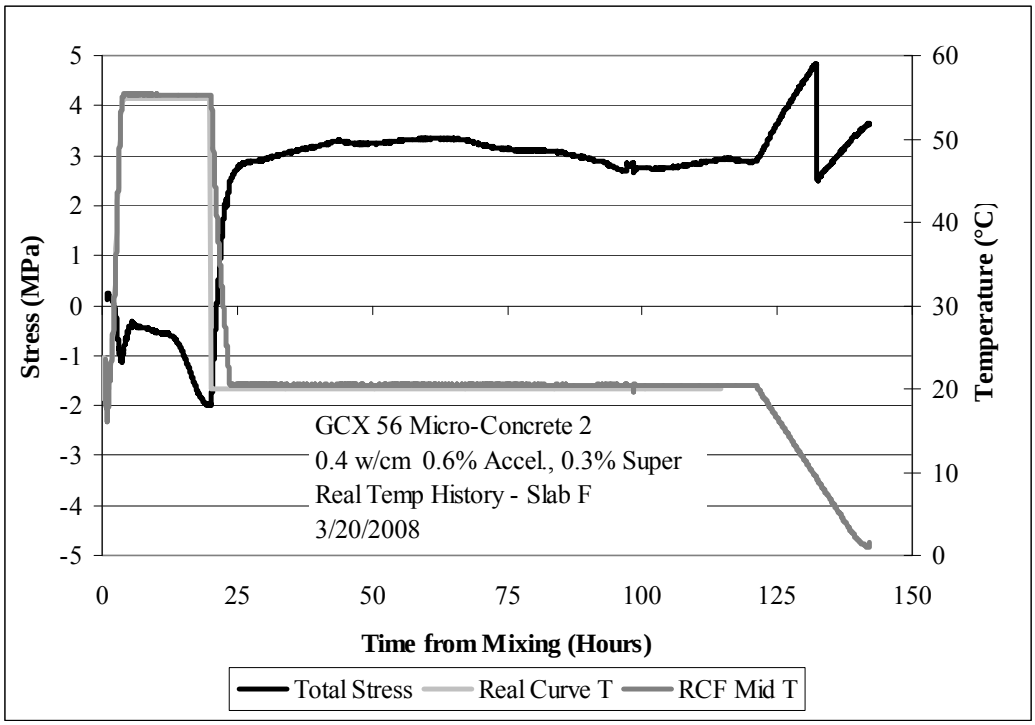

Figure 5.102: Stress generation real temperature history, GCX 56

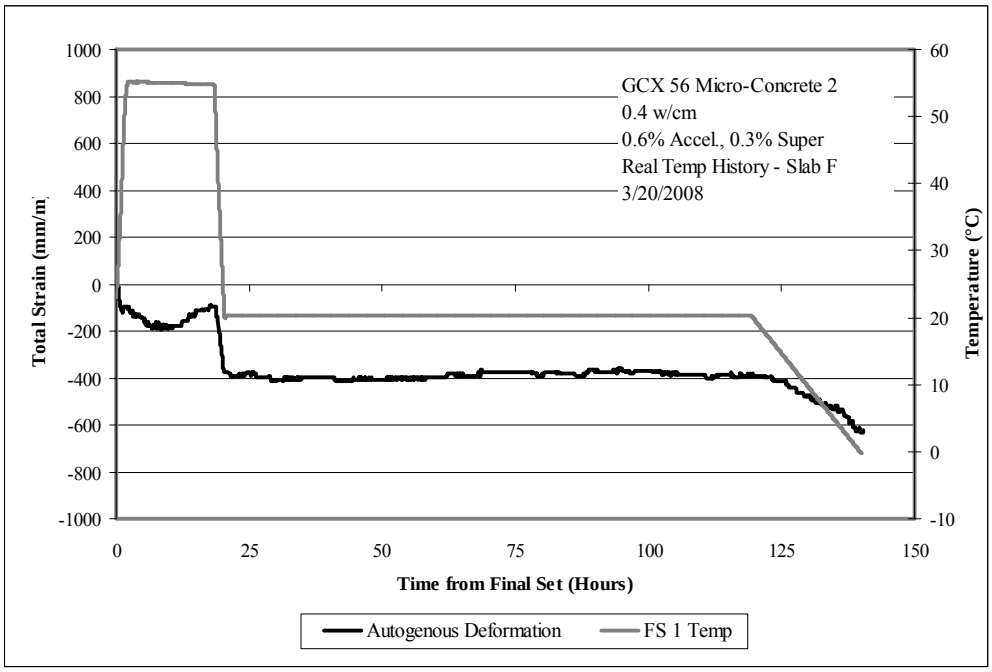

Figure 5.103: Free deformation for real temperature history, GCX 56

Table 5.33: Mechanical properties for real temperature history, GCX 56

Age (days)	Compressive Strength (MPa)	Elastic Modulus (GPa)	Tensile Strength (MPa)
0.2	24.5	21.9	3.9
0.8	17.3	24.3	3.7
1.1*	25.0	-	-
4.1	20.3	27.1	4.0
7.2	21.0	32.8	4.5

Note: (*) Denotes compression tests after cooling to 20°C

The temperature profile for this mixture shows the maximum temperature of 57 °C was held for 20 hours before cooling the mixture to 20 °C. Then the mixture remained at 20 °C until 120 hours at which point it was artificially cooled by 1 °C/hour. The stress generation shows an initial phase of expansion followed by a reduction in stress with a gradual movement to compression over the next 12 hours. Upon cooling the mixture returns to a state of tensile stress; however, the stress shows little change once the isothermal temperature of 20 °C was reached. Upon cooling the mixture cracked at a tensile stress of +4.8 MPa at 132 hours after casting. This was in good agreement with the tensile strength of the mixture which was roughly 4.5 MPa at this age. Free deformation showed an initial shrinkage to -178 μm/m followed by slight expansion to -106 μm/m by the end of the high temperature isothermal phase. The mixture shrank commensurate with cooling to 20 °C to a value of -389 μm/m and remained nominally at this value until final artificial cooling at 120 hours.

Mechanical properties of match-cured samples from this mixture in Table 5.33 show a minimum in compressive strength at 0.8 days (17.3 MPa). After cooling to 20 °C the compressive strength increased to 25.0 Mpa but decreased at 4 days of testing to 20.3 MPa and increased again to 21.0 MPa at 7 days. Elastic modulus gradually increased throughout the duration of the test to 32.8 MPa. After a slight drop in tensile strength at 0.8 days (3.7 MPa) it also increased to a value of 4.5 MPa at 7.2 days.

The same mixture was repeated but the maximum temperature of 57 °C was held until the stress generation leveled off, indicating the end of conversion. The temperature profile and stress generation are shown in Figure 5.104 and Figure 5.105, respectively. Free deformation results are shown in Figure 5.106. This was confirmed by testing mechanical properties of companion cylinders shown in Table 5.34.

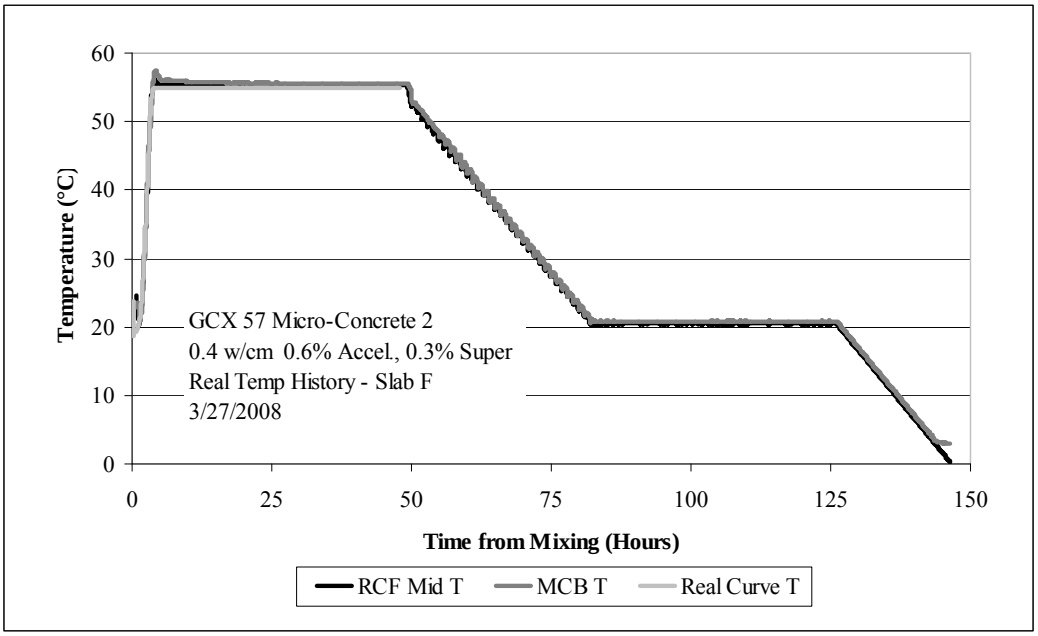

Figure 5.104: Temperature profile for real temperature history, GCX 57

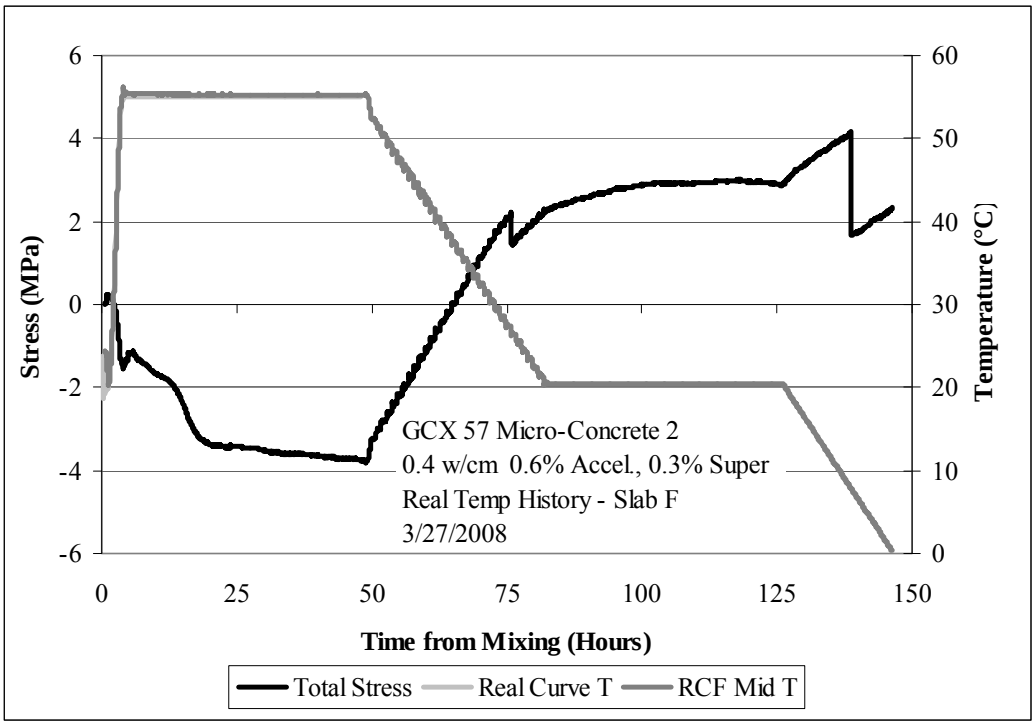

Figure 5.105: Stress generation for real temperature history, GCX 57

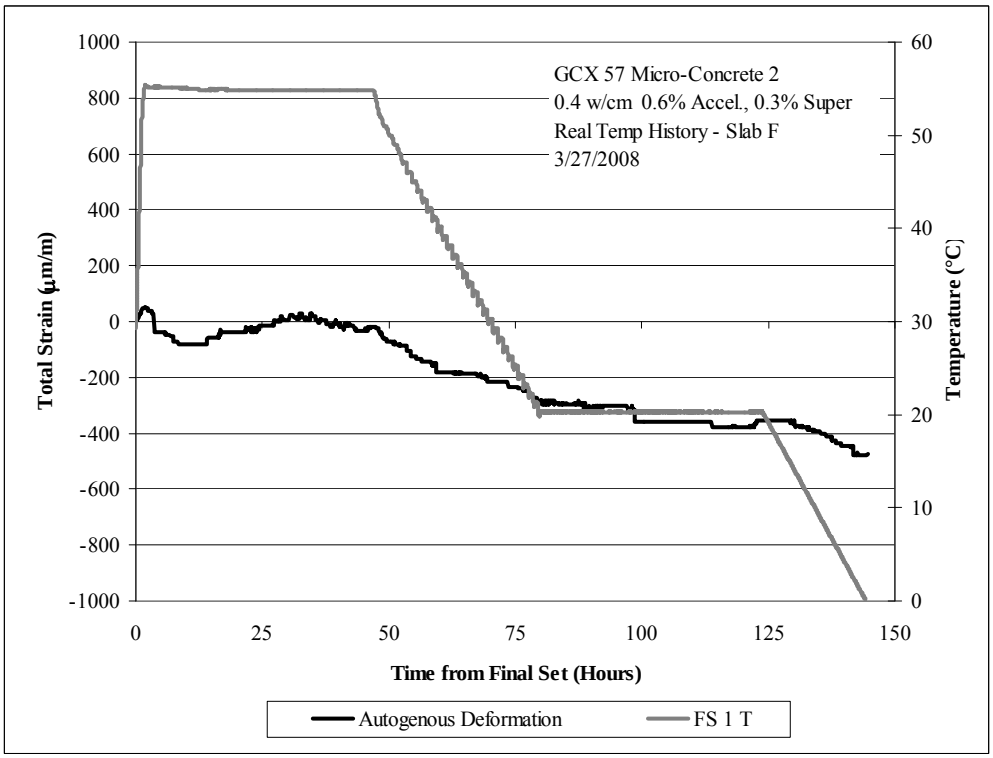

Figure 5.106: Free deformation for real temperature history, GCX 57

Table 5.34: Mechanical properties for real temperature history, GCX 57

Age (days)	Compressive Strength (MPa)	Elastic Modulus (GPa)	Tensile Strength (MPa)
0.3	32.9	30.2	5.7
1.2	28.5	32.9	4.8
3.5	29.4	32.7	5.8
5.4	29.4	36.1	5.4
7.2	27.1	32.4	5.7

Note: (*) Denotes compression tests after cooling to 20°C

The stress generation for this mixture shows that the stress had leveled off at a value around -3.5 MPa by 25 hours into the testing. After 25 hours there was little further decrease in stress. The mixture was cooled to 20 °C at this point and held there for 43 hours before artificially cooling by 1 °C /hour. The mixture exhibited micro-cracking at 75 hours after casting a tensile stress of +2.2 Mpa and again 138 hours after casting at a tensile stress of +4.2 MPa. After the specimen was demolded two cracks could be seen emanating from the teeth in the cross-heads on opposite ends and sides (e.g., diagonally) of the frame; however, the most desired location for a crack to occur, is in the middle of the rigid cracking frame. The free deformation data for this mixture showed an initial expansion to 38 μm/m at 3 hours followed by shrinkage -79 μm/m at 1.5 hours and then it expanded again to a nominal value of 0 μm/m. Upon cooling to 20 °C the mixture shrank to -290 μm/m at 82.3 hours.

Mechanical property evolution for this mixture shows a minimum strength of 28.5 MPa at 1.2 days with gradual increase to 29.4 MPa at 5 days. However, at 7.2 days the compressive strength showed a slight reduction to 27.1 MPa. The elastic modulus also decreased at this age to 32.4 MPa. Tensile strength showed a minimum value of 4.8 MPa at 1.2 days. However, tensile strength decreased again to 5.4 MPa at 5.4 days.

5.6 SUMMARY

The results of all testing from rigid cracking and free deformation frames are summarized in Table 5.35, Table 5.36 and Table 5.37.

Table 5.35: Summary of results from rigid cracking and free deformation frame testing (1)

Mix ID	Admixtures	Material Designation	Date Cast	Temperature	Initial set	Free Deformation	Max Stress before cooling (MPa)	Stress at Cooling (MPa)	Final Stress or at Cracking (MPa)	Figure References (Stress, FD)
GCX 14	0.3% Accel., 0.4% Super	Micro-concrete	7/12/2006	Iso 20°C	NR	NR	+ 2.4 (15 hr)	+ 2.4 (15 hr)	+2.9 (cracked)	5.4
GCX 15	0.3% Accel., 0.4% Super	Micro-concrete	7/14/2006	Iso 38°C	NR	NR	- 2 (29 hr)	- 0.45 (107 hr)	+ 1 (cracked)	5.28
GCX 16	0.3% Accel., 0.4% Super	Micro-concrete	7/21/2007	Iso 38°C	NR	NR	- 2.6 (12 hr)	- 1 (53 hr)	+ 2.3 (67 hr)	5.31
GCX 18	None	Micro-concrete	11/17/2006	Iso 38°C	3.5 hr	NR	-3 (15 hr)	-0.8 (53 hr)	+ 2.0 Mpa (65 hr)	5.33
GCX 19	None	Concrete	11/21/2006	Iso 38°C	-	Expansion up to 150 µm/m at 100 hours, before cooling in large free deformation		- 2 (96 hr)	+ 1.4 (142 hr)	5.39. 5.40
GCX 19	None	Sieved Mortar	11/21/2006	Iso 38°C	3.75 hr	NR		-3.2 (96 hr)	+ 4.4 (125)	4.35
GCX 20	None	Sieved Mortar	11/29/2006	Iso 38°C	4.43 hr	NR	- 5.6 (128 hr)	-5 (145 hr)	+ 3.6 (185 hr)	5.37
GCX 21	None	Concrete	12/12/2006	Iso 20°C-23°C	3.7 hr	Shrinkage to 700 µm/m before cooling in large free deformation frame	+ 2.5 (96 hr)	+ 2.5 (96 hr)	+ 2.7 (cracked)	5.8, 5.9
GCX 21	None	Sieved Mortar	12/12/2006	Iso 20°C	3.7 h	NR		+ 4.2 (120 hr)	+ 4.4 (cracked)	5.6
GCX 22	None	Micro-concrete	1/10/2007	Iso 70°C	35 min	NR	-	-	-	-
GCX 23	None	Micro-concrete	1/12/2007	Iso 50°C	3.58	NR	- 5.4 (16 hr)	- 4.7 (96 hr)	+ 2.2 (143 hr)	5.68
GCX 24	None	Micro-concrete	02/14/2007	Iso 25°C-30°C	6.6 h	NR	- 2.9 (45 hr)	- 2.1 (48 hr)	- 2.1 (48 hr)	5.58
GCX 25	None	Micro-concrete	02/19/2007	Iso 30°C	18 h	NR	- 0.6 (6 hr)	+ 3 (96 hr)	+ 3.5 (102 hr)	5.60

Table 5.36: Summary of results from rigid cracking and free deformation frame testing (2)

Mix ID	Admixtures	Material Designation	Date Cast	Temperature	Initial set	Free Deformation	Max Stress before cooling (MPa)	Stress at Cooling (MPa)	Final Stress or at Cracking (MPa)	Figure References
GCX 26	None	Micro-concrete	02/27/2007	Iso 34°C	9.8 h	NR	- 3.1 (32.5 hr)	-1.7 (109 hr)	+ 1.8 (148 hr)	5.65
OPC 1 (0.32 w/cm)	None	Sieved Mortar	3/7/2007	Iso 20°C	-	NR	+ 3.7 (145 hr)	+ 3.7 (145 hr)	+ 8.2 (164 hr)	5.2
GCX 27	0.2% Accel., 0.4% Super	Micro-concrete	03/21/2007	Iso 30°C	3.4 h	Shrinkage to 650 µm/m before cooling	- 1.25 (14hr)	+ 1.43 (120 hr)	+ 4.9 (cracked)	5.62, 5.63
GCX 28	0.2% Accel., 0.4% Super	Micro-concrete	4/2/2007	Iso 38°C	2.08 hr	Expansion to 885 µm/m before cooling	- 7.2 (105 hr)	- 6 (130 hr)	+ 1.8 (169 hr)	5.43, 5.44
GCX 29	0.2% Accel., 0.4% Super	Micro-concrete	04/18/2007	Iso 38°C	3.5 hr	Expansionto 485 µm/m before cooling	-5.6 (104 hr)	-4 (168 hr)	+2.7 (172 hr)	5.46, 5.47
OPC 2 0.32 w/cm	None	Sieved Mortar	5/23/2007	Iso 20°C	-	NR	+0.9 (123.5 hr)	+0.9 (123.5 hr)	+5.4 (141.5)	5.22
OPC 2 0.32 w/cm	None	Concrete	5/23/2007	Iso 20°C	-		+1.4 (243 hr)	+1.4 (243 hr)	+2.9 (264 hr) no crack	5.23, 5.24
GCX 30	0.2% Accel., 0.4% Super	Micro-concrete	5/30/2007	Real Time Temp without cooling	4.7 hr	NR	-3.6 (62.8 hr)	-3.6 (62.8 hr)	+2.1 (93.1 hr) cracked	5.86, 5.87
GCX 32	0.5% Accel., 0.3% Super	Micro-concrete	6/5/2007	Real Time Temp with cooling	2.8 hr	shrinkage to 694 µm/m at 380 hours	-1.3 (6.8 hr)	-1.3 (6.8 hr)	+3.5 (389.6 hr)	5.89, 5.90
GCX 35	0.6% Accel., 0.4% Super	Micro-concrete	6/27/2007	Real Time Temp without cooling	2.1 hr (final)	slight expansion after 12.5 hours,shrinkage to 346 µm/m before cooling	-4.1 (106 hr)	-4.1 (106 hr)	+1.3 (137.2 hr) cracked	5.92, 5.93
GCX 36 (AEA)	0.6% Accel., 0.4% Super, 0.15% AEA	Micro-concrete	7/5/2007	Iso 38°C	2.4 hr (final)	Expansion up to 623 µm/m (95 hr)	-5.7 (45.9 hr)	-4.3 (96.8 hr)	-2.1 (122 hr)	5.49, 5.50
Fondu 37	0.2% Accel., 0.3% Super	Micro-concrete	7/11/2007	Iso 38°C	2.6 hr (final)	Expansion up to 412 µm/m (165 hr)	-5.4 (46.9 hr)	-3.24 (169.4 hr)	no crack	5.55, 5.56
GCX 38	0.6% Accel., 0.3% Super	Micro-concrete	7/27/2007	Iso 20°C	2.3 hr (final)	Shrinkage to 1000 µm/m (122 hours)	+2.3 (28 hr)	not cooled	+1.5 (50 hr) cracked	5.11, 5.12

Table 5.37: Summary of results from rigid cracking and free deformation frame testing (3)

Mix ID	Admixtures	Material Designation	Date Cast	Temperature	Final Set	Free Deformation	Max Stress before cooling (MPa)	Stress at Cooling (MPa)	Final Stress or at Cracking (MPa)	Figure References
GCX 39	0.6% Accel., 0.3% Super	Micro-concrete	8/17/2007	Iso 55 °C	2.1 hr (final)	Expansion to 765 μm/m (28.4 hr)	-4.9 (88.9 hr)	-4.9 (88.9 hr)	+4.6 (138.0 hr)	5.71, 5.72
GCX 43 30% FA	0.6% Accel., 0.3% Super	Micro-concrete	8/24/2007	Iso 20°C	2.5 hr	Shrinkage to 680 μm/m (72 hours)	+1.3 (13.8 hr)	+2.8 (96.2 hr)	13.8 hr (micro-crack)	5.74, 5.75
GCX 45 30% FA	0.6% Accel., 0.3% Super	Micro-concrete	9/5/2007	Iso 38°C	2.6 hr	Expansion to 240 μm/m (124.2 hr)	-5.4 (128.9 hr)	-4.8 (247.8 hr)	+3.7 (287 hr)	5.80, 5.81
GCX 46 30% FA	0.6% Accel., 0.3% Super	Micro-concrete	10/3/2007	Iso 20°C	2.2 hr	Shrinkage to 632 μm/m (118 hr)	+2.2 (120.8 hr)	+2.2 (120.8 hr)	+2.2 (120.8 hr)	5.77, 5.78
GCX 47 30% FA	0.6% Accel., 0.3% Super	Micro-concrete	10/10/2007	Iso 38°C	2.25 hr	Expansion to 183.8 μm/m (127.3 hr)	-4.1 (224 hr)	-3.5 (251.6 hr)	+4.8 (289 hr)	5.83, 5.84
OPC 3 0.4 w/cm	None	Micro-concrete	10/31/2007	Iso 20°C	5.2 hr	Expansion to 56 μm/m at 19.5 hr, then shrinkage to -200 μm/m at 145 hr	-2.65 (148 hr)	-2.65 (148 hr)	-5.27 (169 hr)	5.17, 5.18
GCX 51	0.6% Accel., 0.4% Super	Micro-concrete	11/9/2007	Iso 38°C	1.73 hr	Expansion to 614 μm/m at 124 hours, then shrinkage to +314 μm/m at 166 hr	-4.24 (78 hr)	-3.43 (128.45)	+2.74 (165 hr)	5.52, 5.53
GCX 53	0.6% Accel., 0.4% Super	Micro-Concrete 2	2/28/2008	Slab F	2.0 hr	shrinkage to 648.4 μm/m (115.5 hr), shrinkage to 860 mm/m at 130 hr	+4.4 (95.1 hr)	+3.5 (130 hr)	+5.8 (133 hr)	5.95, 5.96
GCX 55	0.6% Accel., 0.4% Super	Micro-Concrete 2	3/14/2008	Slab F Complete Real Time	2.0 hr	shrinkage to 758 μm/m (62 hrs), movement with ambient temperature, shrinkage to -840 mm/m (140.7 hr)	+4.5 (115 hr)	+2.36 (121.2 hr)	+5.4 (142 hr)	5.98, 5.99
GCX 56	0.6% Accel., 0.4% Super	Micro-Concrete 2	3/20/2008	Slab F	1.72 hr	shrinkage to -178.7 μm/m (10.3 hr), shrinkage to -373 μm/m at 20.8 hours upon cooling to 20 C, shrinkage to 624.7 μm/m at	-1.8 (20.8 hr) at cool to 20C	+3.0 (121.6 hr) at cool to 0 C	-4.8 (132 hr) cracked	5.102, 5.103
GCX 57	0.6% Accel., 0.4% Super	Micro-Concrete 2	3/27/2008	Slab F Hold 48 hours then cool to 20C.	2.16 hr	flucuated around 0, then shrinkage with cooling to 20 C to -356 μm/m then shrinkage to -472 μm/m upon cooling to 0 C	-3.6 (49.5 hr) at cool to 20C	+3.0(127 hr) at cool to 0 C	+4.2 (138.6 hr) cracked	5.105, 5.106
GCX 58	0.6% Accel., 0.3% Super	Micro-Concrete	4/4/2008	Iso 20 C	3.0 hr	shrinkage to 576 μm/m at 123.4 hours before cooling	+2.4 (14.8 hr) microcrack	+1.9 Mpa (124.8 hr)	already micro-cracked	5.14, 5.15

5.7 CONCLUSIONS

From the inception of this research wide range of evaluation techniques were investigated to determine the best way to accurately characterize early-age volume change in calcium aluminate cement systems. Ultimately the best methodology utilized the rigid cracking and free deformation frame in conjunction with mechanical property testing on match-cured samples. While other results have been presented in this dissertation which have provided useful information about early-age volume change (chemical shrinkage, drying shrinkage, autogenous deformation), only the work with the frames has allowed the quantification of early-age volume change investigated through wide range of isothermal temperatures and realistic temperature histories. A total of 38 mixtures were tested in rigid cracking and free deformation frames as part of this study resulting in a total of 5600 hours (233 days) of evaluation in these apparatus. The following list summarizes the main conclusions and findings from the testing utilizing this equipment:

- Testing at discrete isothermal temperature *at* or below 30 °C promoted the formation of metastable hydration products (predominantly CAH_{10}) that led to the generation of shrinkage as evidenced by tensile stress development in rigid cracking frame testing and shrinkage phenomena in the free deformation frame.
- Mixtures cured *at* or below 30 °C often exhibited cracking in the rigid cracking frame as a result of the tensile stress developed during hydration.
- Testing at discrete isothermal temperature *above* 30 °C promoted the formation of mixtures of metastable and stable hydration products (mixtures of C_2AH_8 and C_3AH_6) and led to the generation of expansive

forces as evidenced by compressive stress development in the rigid cracking frame and expansion phenomena in the free deformation frame.

- Testing in the rigid cracking and free deformation frames further elucidated the profound impact that temperature has on calcium aluminate cement systems particularly during the hydration immediately after setting when hydration products rapidly precipitate.
- Replacement of GCX Binder with 30 % class C fly ash had little impact on behavior at 20 °C isothermal testing (tensile stress development in rigid cracking frame testing and shrinkage in free deformation testing).
- Replacement of GCX Binder with 30 % class C fly ash had more pronounced effects at 38 °C isothermal testing. While compressive stress still developed in the rigid cracking frame, the amount of expansion in free deformation testing was reduced by approximately one-third. This has important implications for field applications of this material where it may still be possible to benefit from a potential "pre-compression" of the material, with less expansive movement from the incorporation of 30 % class C fly ash.
- Testing following realistic temperature histories provided some of the most interesting results and demonstrated that while the material is hydrating it typically passes through a range of temperatures that, at least initially, promote the formation of metastable hydrates (temperatures at or below 30 °C). This is an inevitable process in the field and the duration of time spent at temperatures below 30 °C has profound impact on the amount of time required at temperatures above 30 °C to promote formation of stable hydrates.

- In fact, the duration of time maintained at high temperature determines how much benefit of pre-compression may be obtained for a given mixture. In other words reaching a high temperature for only a short period of time before cooling back to a temperature which promotes formation of metastable hydrates may not “lock-in” the desired beneficial pre-compressive stress possible with calcium aluminate cement concrete

6 Drying Shrinkage

This chapter summarizes a study of drying shrinkage of calcium aluminate cement concrete. Two different types of testing regimes were used to evaluate drying shrinkage: restrained ring testing (ASTM C 1581) and shrinkage measurements of concrete prisms (ASTM C 157).[26, 27] The goal of this testing was to answer the following questions:

- Could drying shrinkage be a potential reason for early-age volume change in CAC concrete at an earlier age compared to OPC concrete? This difference in drying shrinkage at early-age may be due to the rapid hydration, strength gain and potential for conversion at early-age and resulting rapid water consumption and/or release upon conversion in CACC (either early on or at later age depending on converted state of concrete).
- Could either of these testing strategies (ASTM C 157 or 1581) be modified to encourage self-heating in CAC systems so that CAC concrete that had converted (or gone through conversion during the measurements) could be evaluated for drying shrinkage.

6.1 ASTM C 1581 – RESTRAINED RING TESTING

In restrained ring testing (ASTM C 1581), concrete is cast between two cylindrical molds. The inner mold is made of steel (13 mm thick by 152 mm high) with an outer diameter of 330 mm and the outer mold is made of PVC with an inner diameter of 406 mm to give a total concrete thickness of 38 mm. Four strain gages are attached to the inner steel ring and strain monitoring may begin almost immediately after casting (if measurements are started then). The concrete is wet cured for 24 hours, at which point the outer mold is removed. A waterproofing coating is applied to the top surface of the

cylindrical concrete ring so that drying can only occur from the outer cylindrical face of the concrete sample. If enough shrinkage occurs in the mixture due to moisture loss, the tensile strength of the concrete may be overcome by the tensile stress due to drying. At this point a crack occurs and a sharp decrease in compressive strain (typically 30 μm/m or greater) is observed. Strain is monitored and recorded for at least 28 days unless cracking occurs prior to 28 days. It is also advised to visually inspect the rings at frequent intervals for cracks.[26]

6.1.1 Testing procedure and results

A total of five drying shrinkage rings were cast: three composed of calcium aluminate cement concrete (GCX binder) and two composed of ordinary portland cement concrete. Mixture proportions are shown in Table 6.1. The CACC mixtures contained 0.3% accelerator and 0.4% superplasticizer. No admixtures were used for the OPCC mixture.

Table 6.1: Mixture proportions for ASTM C 1581 testing

Mixture Component	**Concrete (wt%)**	**kg/m^3**
Coarse Aggregate (4.75-20 mm)	44.8	1054.0
Fine Aggregate (0-4.75 mm)	31.4	739.8
Cement content (kg/m^3)	17.0	400.0
Water	6.8	160.0
Total	100.0	2353.8

Thermocouples were placed in several locations in the fresh concrete and on the shrinkage ring walls. All thermocouples were placed at mid-height (76 mm): inside the fresh concrete, on the steel ring (at steel/concrete interface) and on the PVC (at PVC/concrete interface). In the interior portion of one of the rings, dense polystyrene was placed to promote self-heating so that a higher temperature rise in these specimens would occur compared to the two rings without insulation.

Figure 6.1 shows the heat generation in this testing regime. The ring that was insulated to encourage self-heating is shown as "ADB" and the rings without insulation are referred to as "AMB". The abbreviation "CON" means that a thermocouple was placed in the middle of the concrete for this specimen. The abbreviation (STL) means that the thermocouple was placed on the inner part of the steel ring and the abbreviation (PVC) means that the thermocouple was placed on the inner part of the PVC ring. The concrete in the insulated ring (ADB) generated no more heat than the non-insulated rings. Therefore all three rings using the GCX binder show essentially the same temperature profile and as a result have are all likely unconverted samples when placed into the shrinkage environment. The shrinkage rings were stored in a controlled environmental chamber with a temperature of 23 ± 1.0 °C and a relative humidity equal to or less than 50% after demolding. To minimize transport of the rings at early age (particularly OPCC) the shrinkage rings were cast inside the environmental chamber and it took approximately 20 hours for the room to return to the appropriate temperature limits after casting.

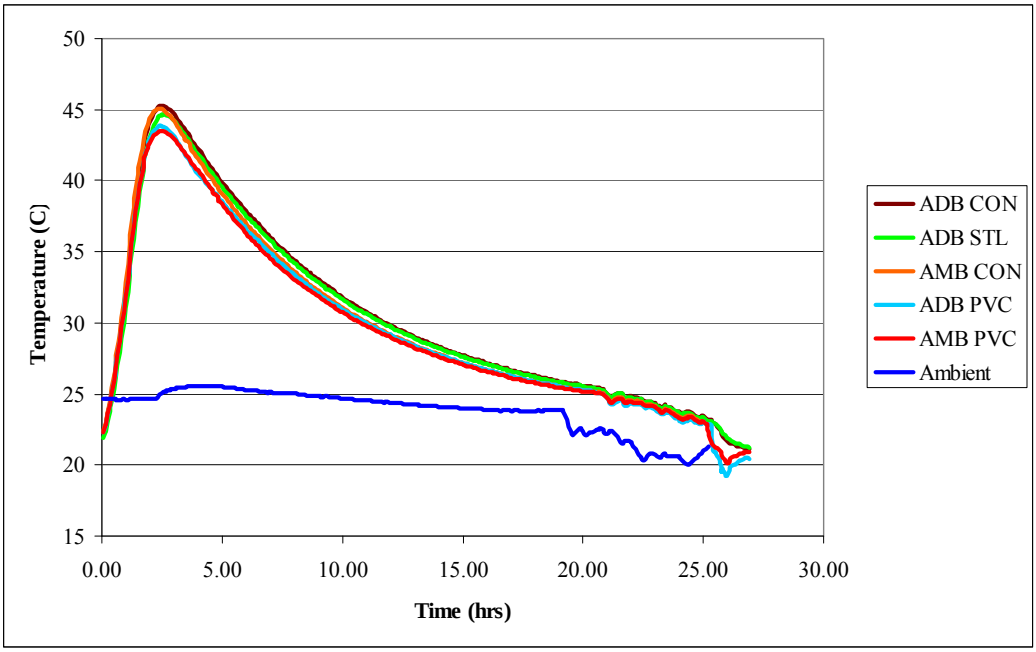

Figure 6.1: Heat Generation in Shrinkage Rings, self-heating (ADB), ambient cure (AMB) and room temperature (Ambient)

Figure 6.2 and Figure 6.3 show the strain generated by CAC AMB2 (CACC cured without added insulation) and OPC 1 (ordinary portland cement concrete cured without added insulation) samples under restrained shrinkage testing according to ASTM C 1581.

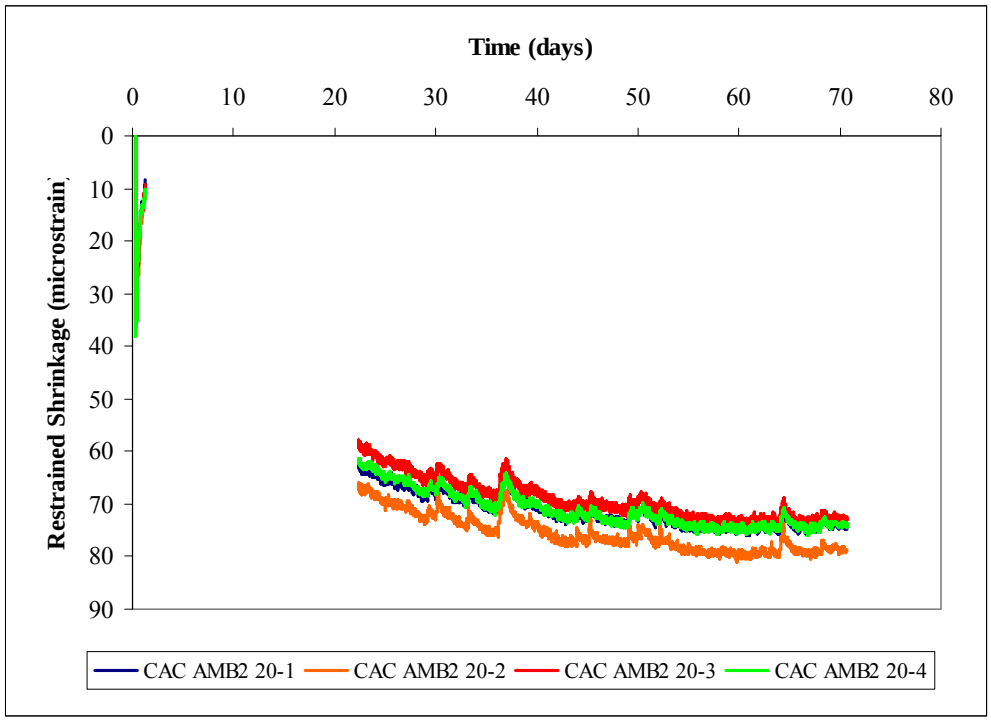

Figure 6.2: Strain generation in shrinkage rings for CAC AMB2

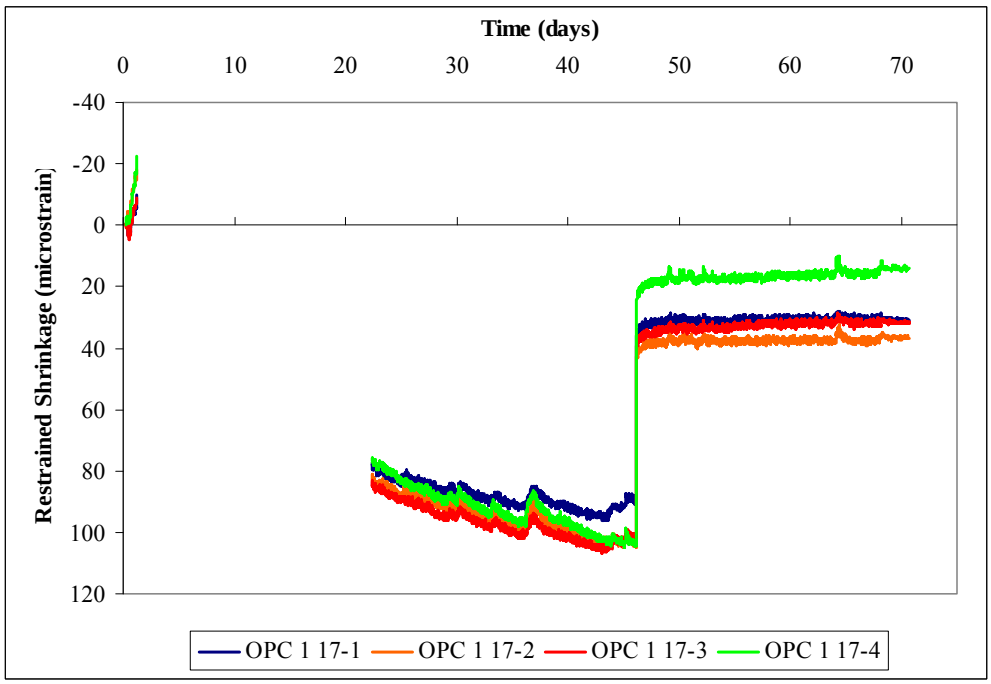

Figure 6.3: Strain generation in shrinkage rings for OPC 1

Strain data was recorded every 30 minutes as one point, and these graphs represent a total of just over 70 days of measurements. There is a large gap in the data from one day to 21 days. The data acquisition system can hold about 40 hours worth of data depending on how many shrinkage rings are hooked up to the system. Therefore an external computer program is needed to download the data at regular intervals from the data acquisition system. However, this was inadvertently mis-programmed and the error was not realized until 21 days, as the program appeared to be working properly, and no visible cracks had yet occurred in the samples.

While it is unfortunate these data were missing, it can be seen that the rings did go into compressive strain at some point after casting between 1 and 21 days, which was expected. Results from this testing showed that both CACC and OPCC at a 0.4 w/cm showed a similar amount of strain due to drying shrinkage. However, one of the two OPC replicates cracked at approximately 100 microstrain after 46 days of testing, while none of the three CAC replicates cracked by 70 days of testing. This test suggests that long-term drying shrinkage for these CAC concretes are no more susceptible (and in fact may be less so) than similar OPC concrete mixtures cured under ambient conditions.

Perhaps the most significant outcome from this testing was that it confirmed the need for modified testing strategies (e.g., specific temperature control for the rapidly hydrating CAC concrete). Often the small temperature rise in OPC concrete is either ignored or has passed (after the first 24 hours) before any measurements are taken on the material. However, the rapid strength gain and associated temperature rise are characteristics that make CAC concrete both an appealing material and an exceedingly difficult one to characterize with traditional laboratory tests.

6.2 ASTM C 157 – SHRINKAGE PRISMS

Companion ASTM C 157 shrinkage prisms were cast from the same mixtures outlined in section 6.1.1 for restrained ring testing. Prisms measuring 76 x 76 x 285 mm were cast in steel molds and typically demolded after 24 hours according to this testing protocol. The prisms were then placed in a limewater bath for 28 days, before they were placed in a drying environment.[27] However, variations in demolding and storage up to 28 days were made for these mixtures due to the rapid curing of CAC concrete. These variations are summarized as follows; three prisms were cast for each outlined description. The time at which the calcium aluminate cement concrete increases in temperature by 1 degree Celsius from the initial temperature while still in a fresh state is referred to as "T_{off}" (short for temperature take-off). This is used by the manufacturer of the calcium aluminate cement to denote the point at which setting of the material occurs.

- OPC (OPC 2) – ambient cure, demold at 24 hours, take initial reading, place in environmental chamber (drying shrinkage room) for subsequent storage and measurement
- GCX (GCX 13 AMB) – ambientcure, demold at 24 hours, take initial reading, place in environmental chamber (drying shrinkage room) for subsequent storage and measurement
- GCX (GCX 13 AMB Toff + 2) – ambient cure, demold at Toff + 2 hours, take initial measure, put back in molds and ambient wet-cure environment, final demolding at 24 hours, second measurement, place in environmental chamber (drying shrinkage room) for subsequent storage and measurement

- GCX (GCX 13 ADB) – cure in an insulated box to promote self-heating after casting, demold at 24 hours, take initial reading, place in environmental chamber (drying shrinkage room) for subsequent storage and measurement
- GCX (GCX 13 ADB Toff + 2) – cure in an insulated box to promote self-heating after casting, demold at Toff + 2 hours, take initial measure, put back in molds and back in insulated box, final demolding at 24 hours, second measurement, place in environmental chamber (drying shrinkage room) for subsequent storage and measurement.

Figure 6.4 shows the drying shrinkage of these prisms with the zero point as the initial measurement after the first demolding (two dashed lines representing measurements at Toff + 2 hours).

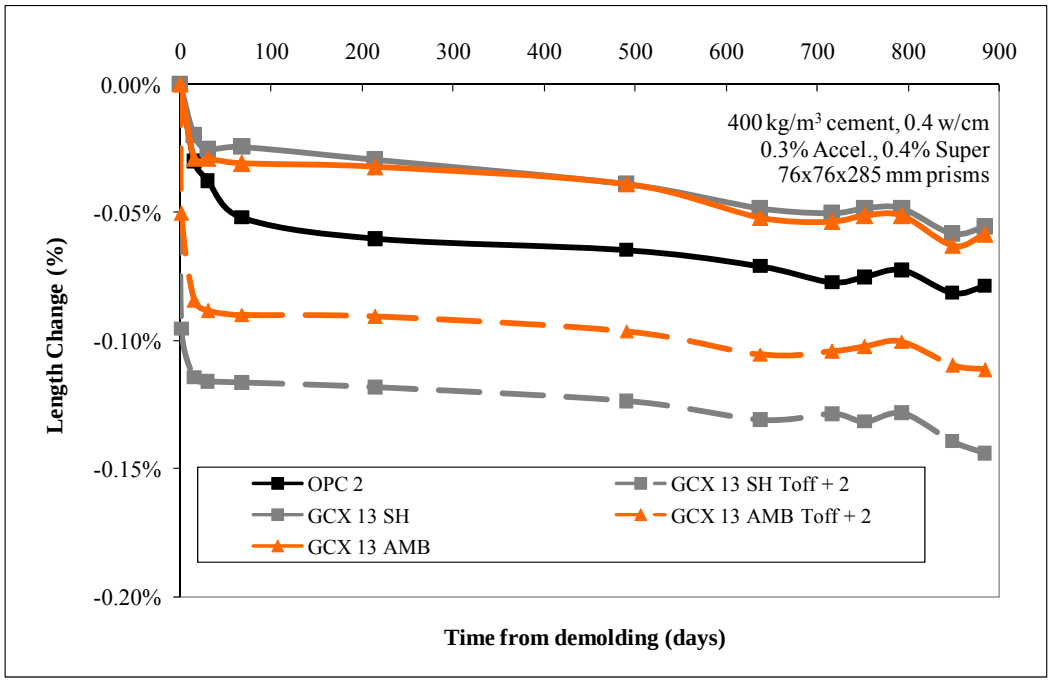

Figure 6.4: Drying shrinkage of CAC and OPC prisms following a modified ASTM C 157 procedure

Figure 6.4 shows that CACC prisms demolded at 24 hours shrink less than companion OPCC prisms demolded at the same age and subjected to a drying shrinkage environment. However, the bottom two dashed lines representing measurements for CACC prisms (self heating and ambient cure) seem to indicate that drying shrinkage is more significant for prisms demolded at earlier age. However, there is a thermal component of shrinkage in these prisms that is also not captured in this graph. At the time of demolding (Toff+2), samples in both curing regimes were at a temperature of 38 °C. In fact the efforts made to encourage self heating resulted again in no appreciable temperature rise in those samples compared to samples cured in ambient conditions. Figure 6.5 shows the same data with the zero point taken as the measurement at 24 hours after casting, i.e., when all samples were roughly at 23 °C.

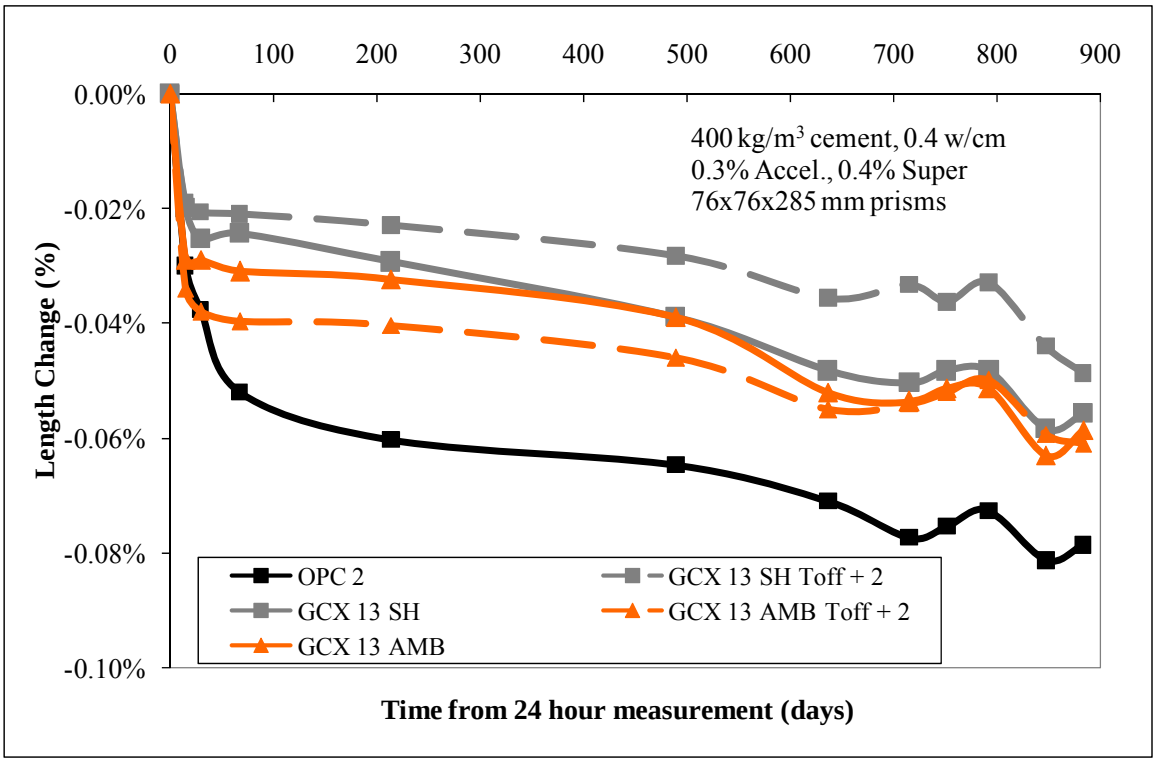

Figure 6.5: Drying shrinkage of CACC and OPCC prisms, from 24 hours

This figure shows a clearer trend for the CACC prisms compared to OPCC prisms indicating that drying shrinkage measured from demolding at 24 hours is less for CACC than OPCC. The drying shrinkage for the companion sets of CACC prisms is very similar, particularly in the case of the ambient cure samples. The least amount of shrinkage is seen in the GCX 13 SH Toff+2 samples for the majority of the test. However, by 884 days the drying shrinkage of all the CACC prisms is very similar. The mass loss of the prisms was also monitored and is shown in Figure 6.6.

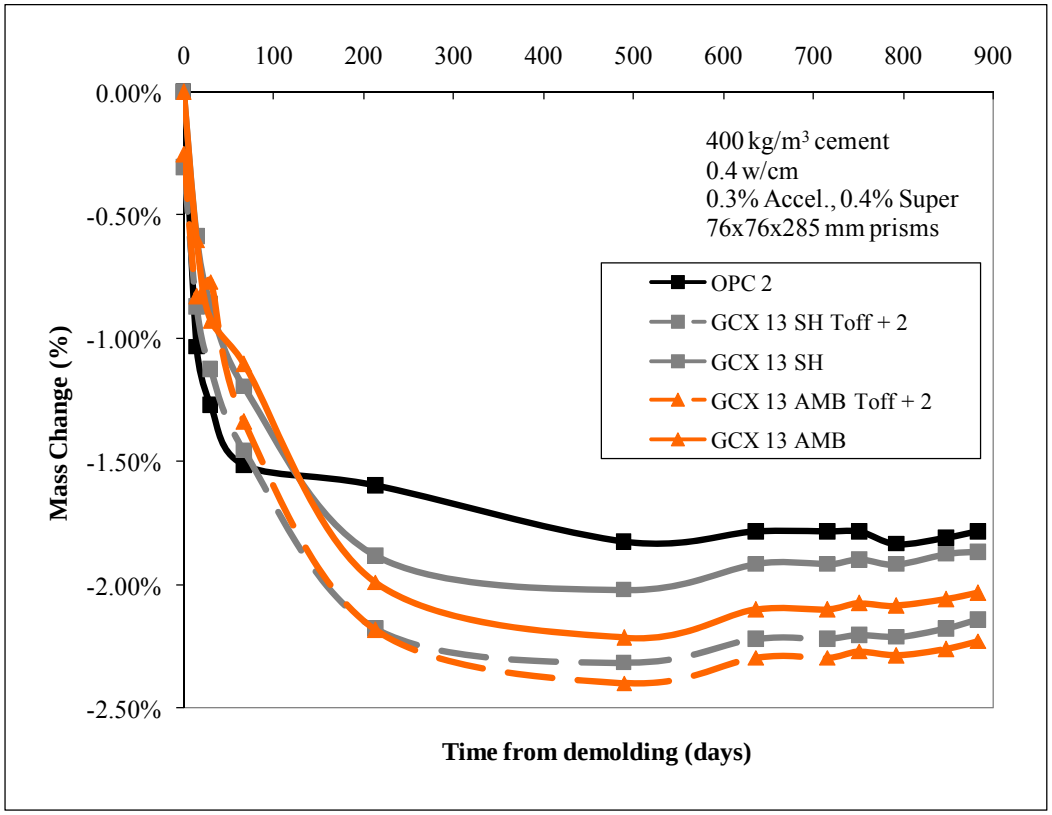

Figure 6.6: Mass loss of OPCC and CACC drying shrinkage prisms

Figure 6.6 shows an important trend that indicates that while mass loss (i.e., more prism drying) is greater for CACC, the resulting shrinkage (shown in Figure 6.5) is less than a comparative OPCC which shows less mass loss, yet the resulting shrinkage is

greater. This trend is further elucidated by a plot that shows mass loss versus length change in Figure 6.7. These results may be indicative of a coarser pore structure in the calcium aluminate cement concrete that is less susceptible to shrinkage upon drying due to the relative pore size compared to OPC. A separate study confirmed this finding through the use mercury intrusion porisimetry (MIP), which showed a coarser pore structure in CACC compared to OPCC.[49]

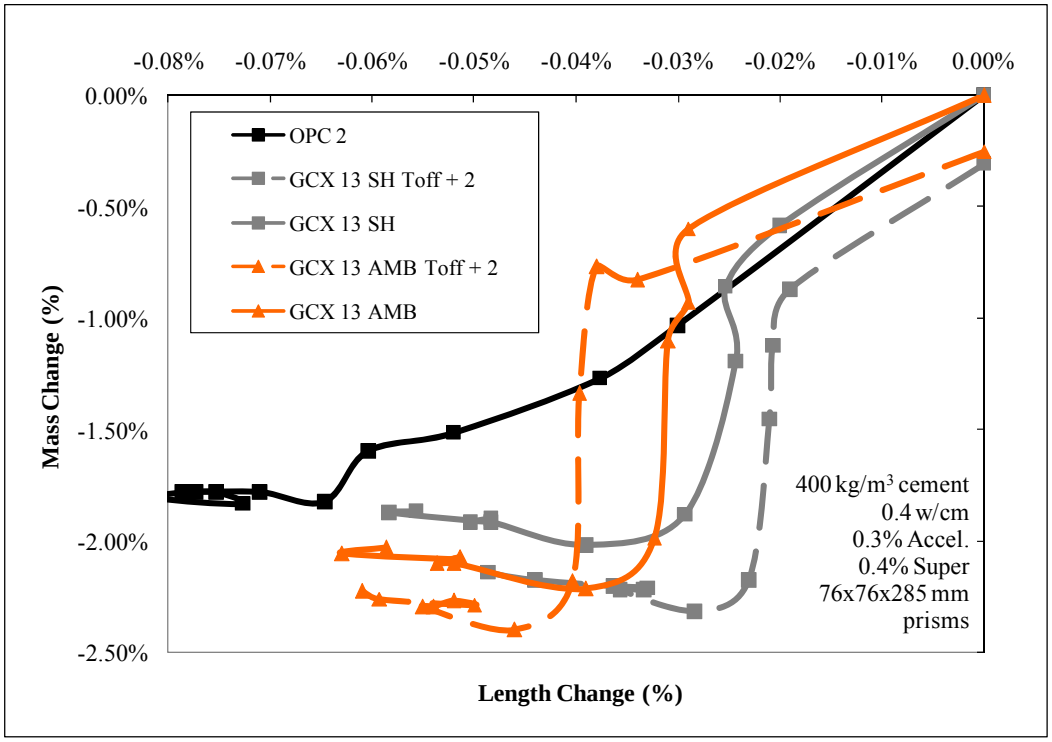

Figure 6.7: Mass loss versus length change for drying shrinkage prisms

Normally in OPCC, a mass loss is expected at early ages but there is little corresponding shrinkage. This is because water is first lost from large voids that do not contribute to shrinkage. However, as water is lost from subsequently smaller pores, specifically those that are ~50 nm or smaller, then shrinkage is likely to occur. Therefore, different pore sizes and even pore size distribution will have significant impacts on shrinkage. The most interesting piece of knowledge gained from this

experiment was that even though the CAC specimens showed more pronounced decrease in weight (due to moisture loss) compared to the OPC prisms, there was not a subsequent shrinkage associated with this weight loss, as was seen in the OPC samples. This may be due to the conversion process which continually releases water to the system as metastable hydrates dissolve and convert to stable hydrates. This water may either be lost through drying or may help to fill voids which would otherwise restrict upon drying and could result in a further shrinkage.

For the limited amount of samples cast as part of this study, several key trends can be identified. First, neither testing strategy (evenwith modifications including added insulation and curing inside a well insulated chamber) was capable of encouraging the type of heat development necessary to induce conversion within the first 24 hours after curing the samples. As a result, all samples essentially experienced a similar temperature gain to 40 °C and thus little if any conversion was expected at early age in the compared samples. The resulting drying shrinkage results confirmed this as ultimate shrinkage was similar for all CACC concrete investigated.

6.2.2 ASTM C 157 Drying Shrinkage: Unconverted CACC

Two subsequent studies on drying shrinkage were performed to further elucidate the effects of temperature on drying shrinkage in CACC samples that were still hydrating when demolded at early-ages and thus had higher temperature than the standard specimens taken at 23 °C.

The first set of CACC concrete specimens were cast with the same mixture proportions shown in Table 6.1. However, the accelerator dosage was increased to 0.6%. At this point in the project a new shipment of GCX Binder and admixtures was received. To retain a similar workability to previous mixtures the accelerator dosage was increased from 0.3 to 0.6% to provide a slightly stiffer mixture. Samples were cured in ambient

laboratory conditions and demolded at T_{off} + 2 hours and at 24 hours after casting. Thermocouples were placed in one prism from each of two sets of samples to monitor temperature change. Samples demolded at T_{off} + 2.5 hours were wrapped in heavy plastic sheeting to minimize moisture loss until the temperature reached nominally 23 °C. Samples were also cast and cured in large ovens at elevated temperature to force conversion so that drying shrinkage could be compared between converted and unconverted samples. Thermocouples were also placed in one prism in this set of samples. However, after further evaluation of the heat generation it was decided that the temperature rise was too rapid in these samples to truly replicate hydration in a field sample and therefore no results will be shown for these prisms. The temperature data acquisition system used for all temperature monitoring needed to be in close proximity to both sets of samples (those cured in the oven and those cured in ambient laboratory conditions). The room in which the ovens reside remained close to 28 °C throughout the testing period, and as a result, the samples cured in ambient conditions (28 °C) and demolded at T_{off} + 2 hours did not return to 23 °C until 24 hours after testing. As a result the drying shrinkage shown in Figure 6.8 represents two essentially identical ambient-cured sets of samples. The OPCC samples from the previous set of experiments are shown for comparison.

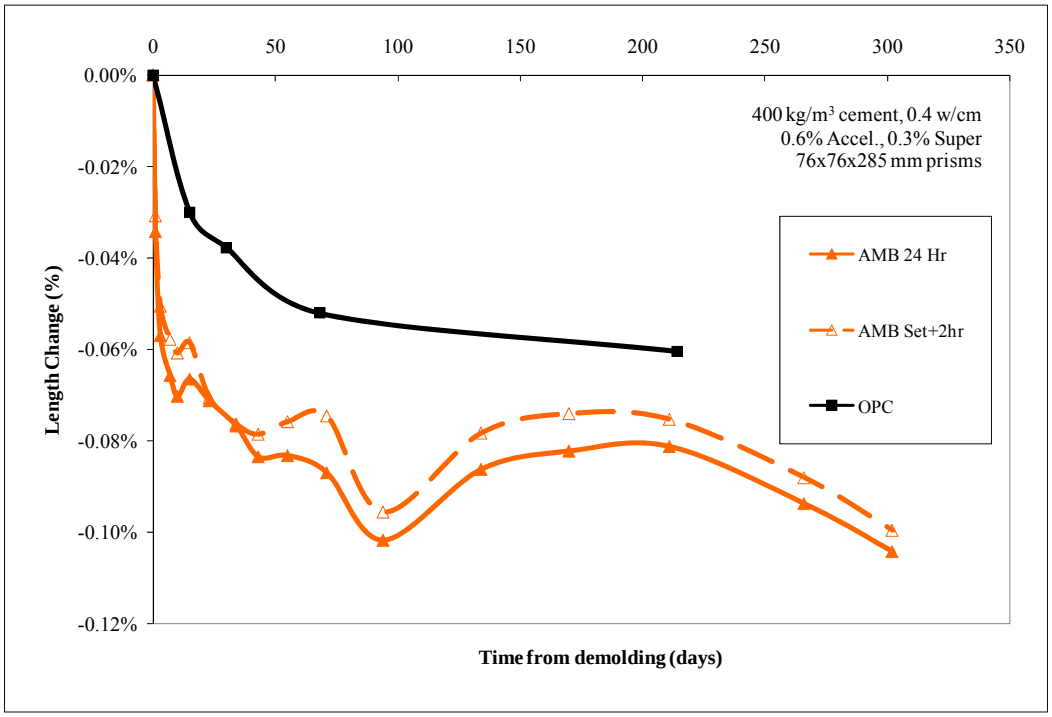

Figure 6.8: Drying shrinkage of CACC cured at Ambient Temperature

In contrast to the first set of experiments, the data in Figure 6.8 show that drying shrinkage of unconverted CACC prisms was greater than that of OPCC prisms. These data also show an expansion around 100 days of testing followed by shrinkage beginning between 150 and 200 days of testing for the CACC prisms. However, the samples shrank more than the companion OPCC samples. This expansion may be a result of conversion occurring in these specimens; however an increase in expansion was not observed in the first set of drying shrinkage prisms which have been measured for a longer period of 884 days. Mass changes are shown in Figure 6.9 for this set of drying shrinkage prisms.

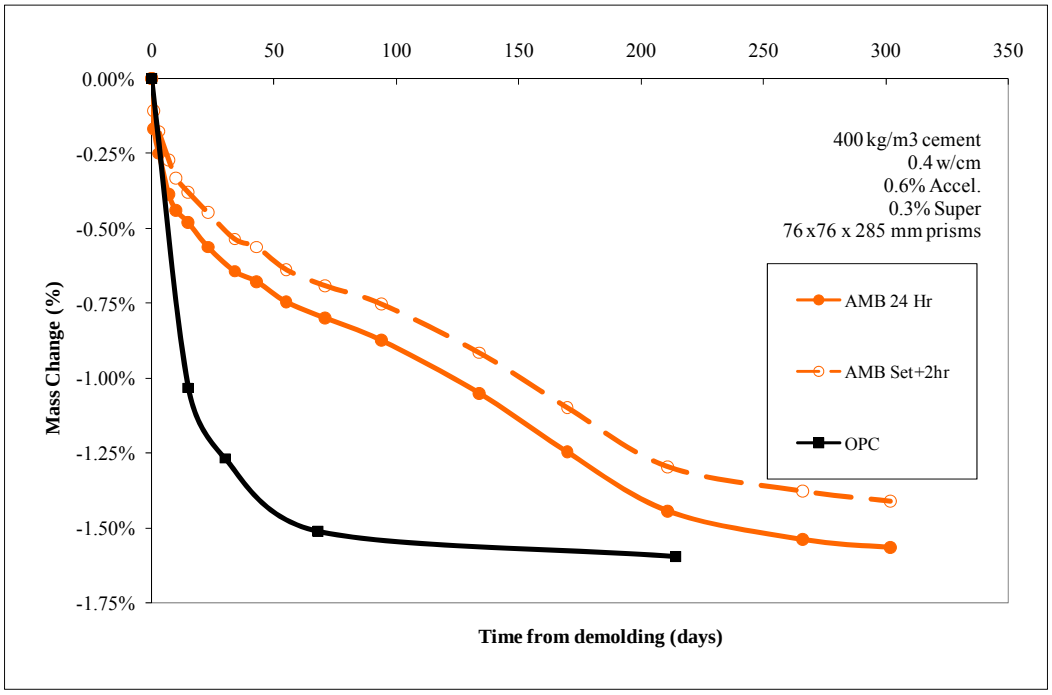

Figure 6.9: Mass change of CACC prisms cured at ambient temperature

Figure 6.9 shows that there is continued mass loss for the prisms throughout the testing period. Since mass loss continues (evidence of drying) this may support the theory of expansion being linked to conversion processes where hydrates change from metastable to stable phases actually resulting in a noticeable change in length, evidenced by expansion. The rate of mass loss also decreased between 50 and 100 days. If conversion is occurring during this time period, released water from the conversion process may be able to reduce the overall rate of drying in the prisms. Mass change versus length change is shown in Figure 6.10.

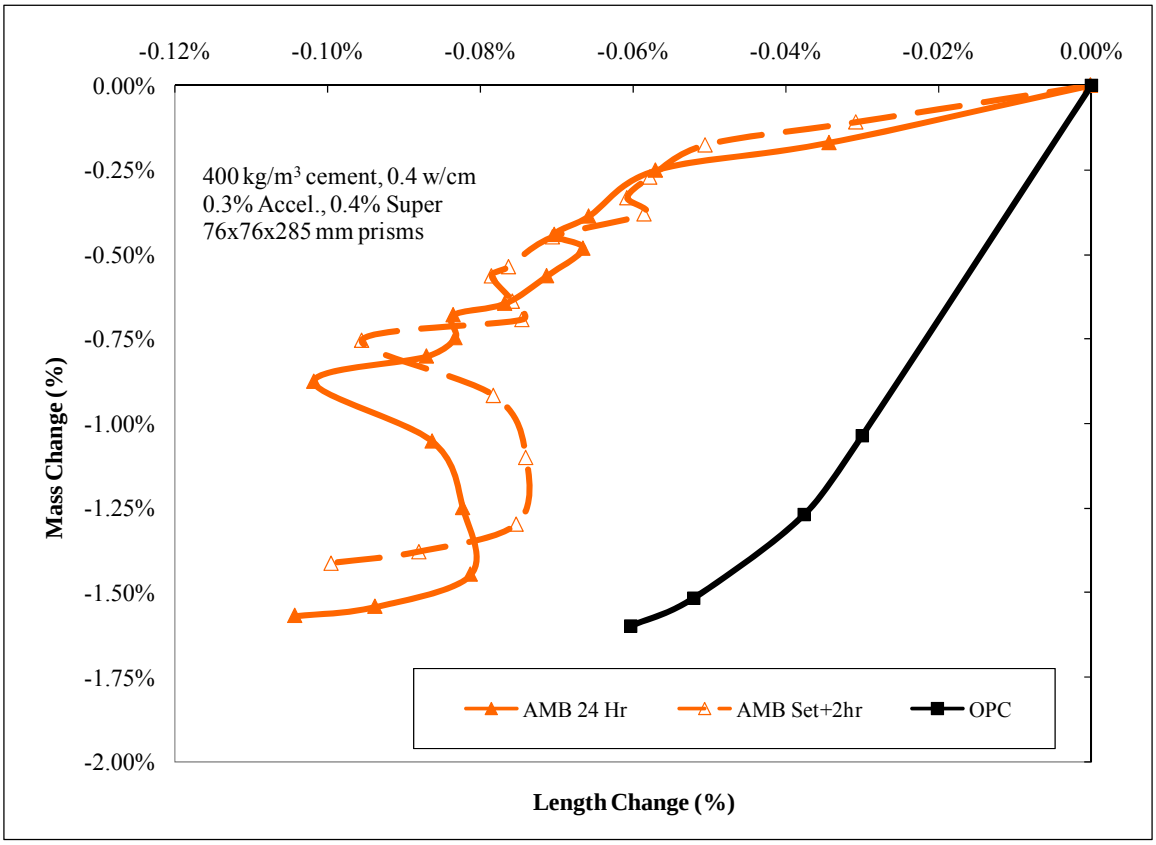

Figure 6.10: Comparison of mass change versus length change, CACC prisms, Ambient cure

Figure 6.10 further demonstrates that while mass loss continued in the CACC prisms an apparent increase in length (expansion) was observed (between 100 and 200 days). Due to the discrepancy in results between the first and second set of drying shrinkage experiments a third set of experiments was initiated. While results are preliminary ongoing long-term measurements should further clarify the drying shrinkage characteristics of CACC concrete and will be completed before any further conclusions can be made from the results of drying shrinkage of CACC.

The first part of this set of experiments investigated CACC concrete prisms cured in ambient conditions. In fact specimens were cured in steel prism mold wrapped with wet burlap in the environmental chamber used for drying shrinkage. At T_{off} + 2.5 hours

four prisms were demolded and measured for initial length. A thermocouple embedded in one of the samples allowed for continual monitoring of temperature which was recorded until temperature reached 23 °C. The samples were measured approximately every 2 hours until the temperature of the sample with the thermocouple reached 23 °C. However, in contrast to previous measurements (where prisms were returned to steel molds), the prisms were placed directly into drying conditions within the environmental chamber. This was done in an effort to determine the thermal component of drying shrinkage measurements made at early age with CACC. The second set of four prisms were demolded at 24 hours after casting as was done previously and it was confirmed that temperature of the prisms was constant at 23 °C.

Figure 6.11 shows the length change of CACC prisms demolded at T_{off} + 2.5 hours.

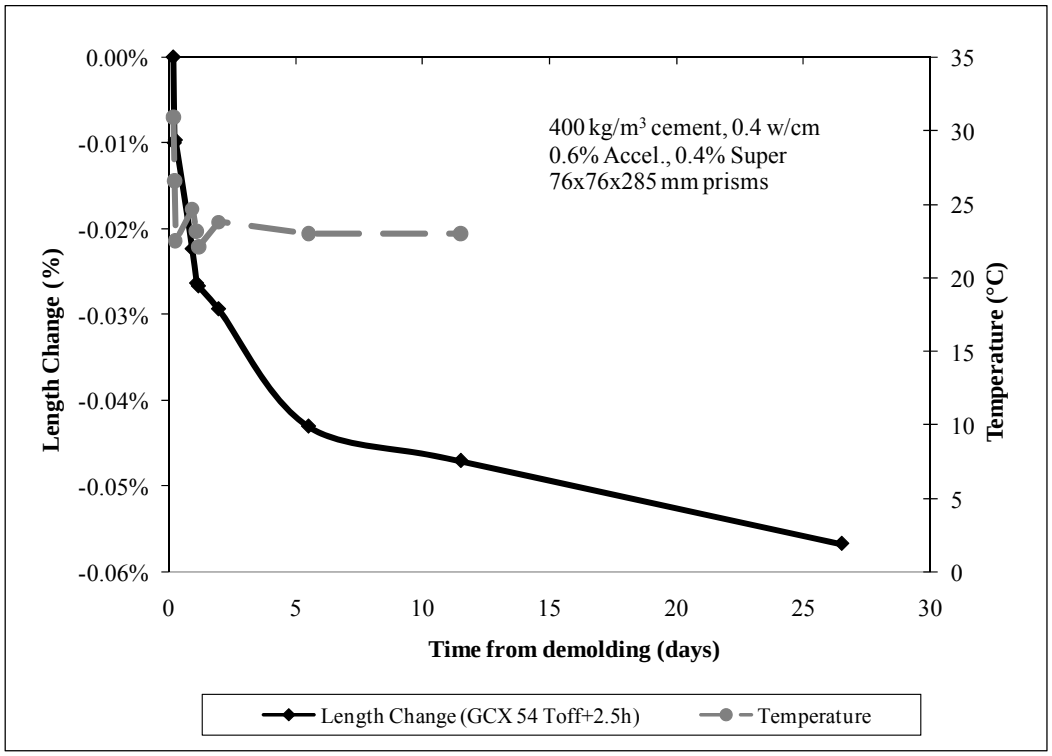

Figure 6.11: Drying shrinkage for CACC (GCX 54 Toff+2.5hr)

Measurements shown in Figure 6.11 were initiated 2.5 hours after T_{off} of the CACC prisms, mixture GCX 54. This figure shows that temperature at the time of demolding was 31 °C and gradually decreased to 23 °C four hours later (6.5 hours after mixing, 4 hours after demolding). Length change is shown throughout this period and a shrinkage of 0.01% (100 μm/m) is reached in the first four hours. This length change is a combination of thermal effects (cooling from 35 °C to 23 °C) and drying shrinkage. The coefficient of thermal expansion (CTE) on hardened unconverted CACC was measured to be 7.48 x 10^{-6} or 7.48 microstrain/°C according to TEX-428-A.[50] Taking into account the temperature decrease of (-8.45 °C); this represents a thermal shrinkage of approximately 63 microstrain or 0.0063%, meaning that of the length decrease of 0.01%, 0.0063% is due to thermal effects and the remaining 0.0037% is due to drying shrinkage. If the drying shrinkage is then normalized, taking into account the initial length change due to thermal effects, this results in representation of the actual drying shrinkage of the CACC demolded at T_{off}+2.5 hrs.

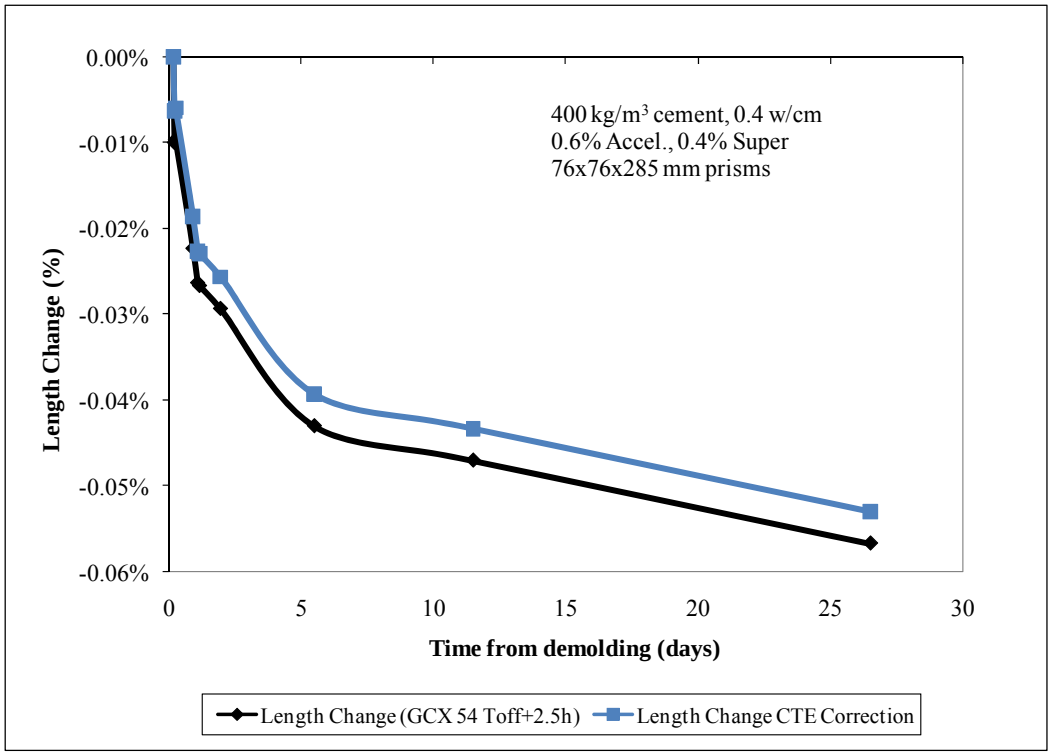

Figure 6.12: Corrected length change for temperature, GCX 54 T_{off}+2.5h

Figure 6.12 demonstrates two important concepts for early-age measurements of drying shrinkage on CACC. The first is that the thermal component of shrinkage in this experiment is relatively minor compared to the drying shrinkage that occurs before 24 hours (e.g., if samples are demolded at T_{off} + 2.5 hours and placed in a drying environment). The second is that the component of drying shrinkage that is not captured in the first 24 hours is shown as 0.053% (500 microstrain) for CACC cured in ambient conditions. This has important engineering application as structures which are not properly cured immediately after placement may have significant propensity for drying shrinkage as evidenced by these results.

Figure 6.13 shows mass change and normalized length change on the same graph for CACC cured in ambient conditions.

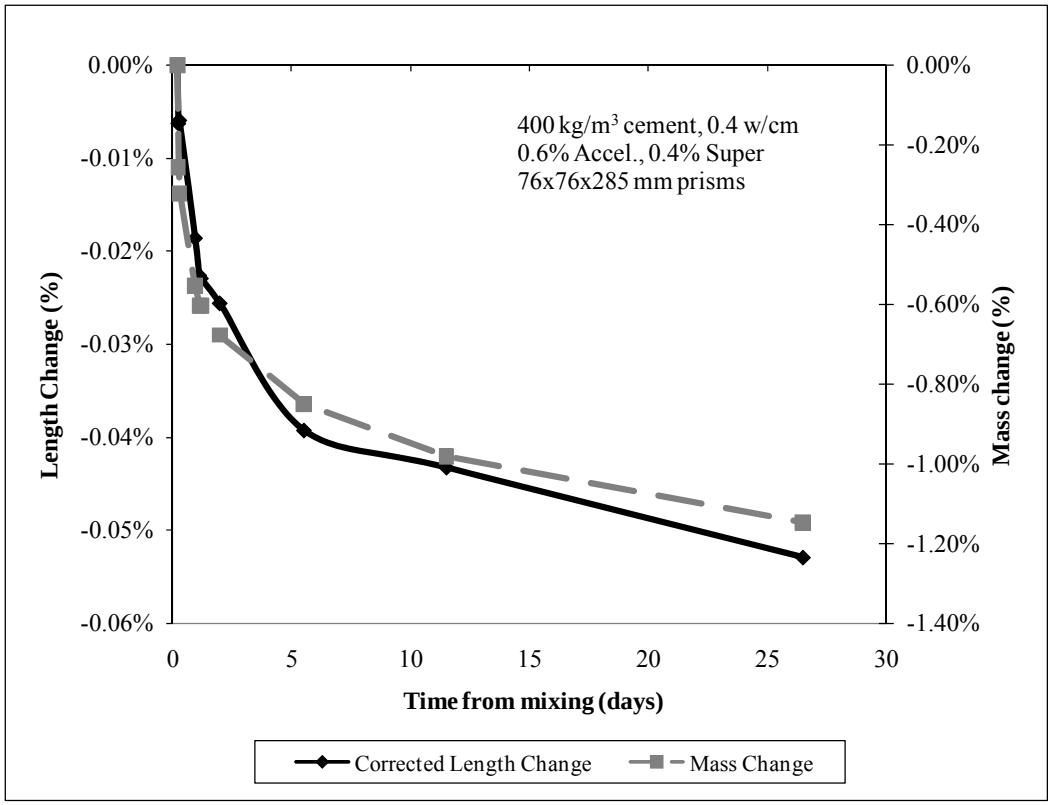

Figure 6.13: Length and mass change for GCX 54, demolded at T_{off} + 2.5 h

While the mass change for the prisms is of a different order of magnitude than the shrinkage, the data in Figure 6.13 indicate the profound effect of mass loss on shrinkage, particularly at early age for CACC drying shrinkage prisms. Figure 6.14 shows the length change and mass change for unconverted CACC prisms demolded 24 hours after casting, followed by subsequent storage in a drying shrinkage environment.

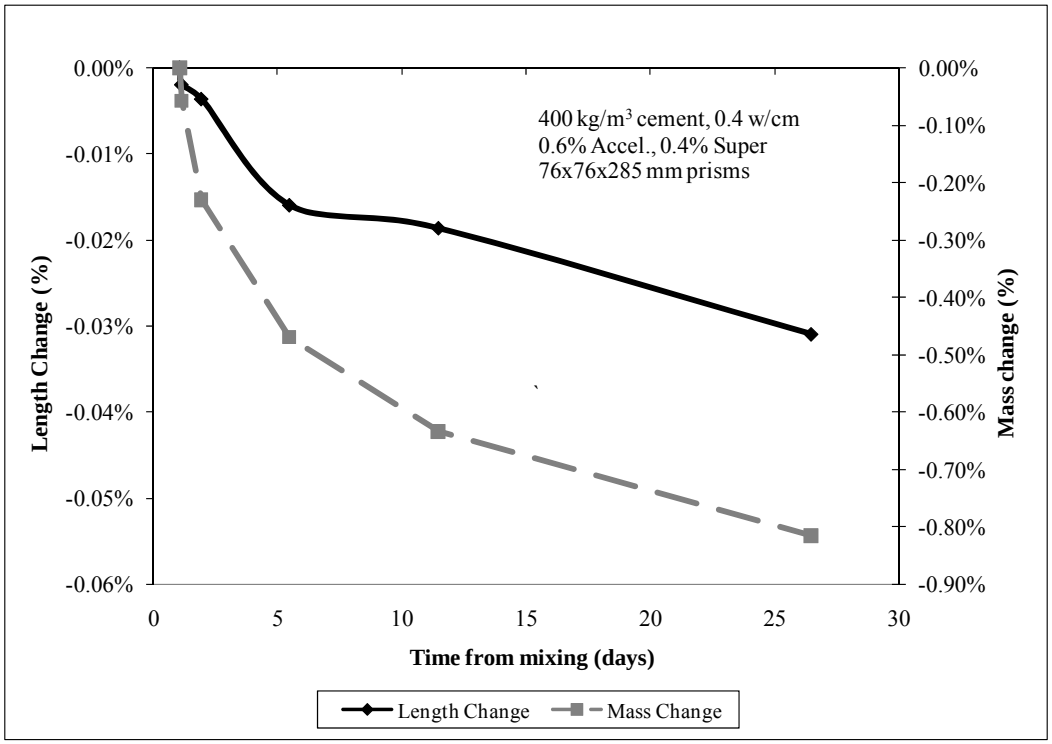

Figure 6.14: Length and mass change for GCX 54 demolded at 24 hours

Drying shrinkage for CACC prisms (GCX 54) demolded at 24 hours is shown at 0.03% at an age of 26 days, compared to a value of 0.05% for prisms from the same mixture demolded at T_{off} + 2.5 hours. Mass change is also lower at a value of 0.82% at 26 days compared to 1.15% for prisms demolded at T_{off} + 2.5 hours.

The results of this set of drying shrinkage measurements on unconverted CACC prisms has shown the importance of capturing drying shrinkage at early ages with CACC prisms. This is not captured if prisms are demolded and an initial measurement is taken at 24 hours. The thermal component related to ongoing hydration at early age can be easily corrected with the appropriate CTE value, assuming a hardened CTE applies to early-age CACC. Due to the rapid strength gain of CACC it is likely that early-age CTE is much less variable in these systems than CTE for OPC.[51]

6.2.3 ASTM C 157 Drying Shrinkage: OPCC

Drying shrinkage was also investigated further on ordinary portland cement concrete prisms with two different measuring regimes. A total of 8 prisms were cast for this mixture. All prisms were demolded at 24 hours after casting. The first four prisms were then measured for initial length and placed in an environmental chamber for subsequent drying shrinkage measurements. The second set of prisms followed ASTM C 157 where prisms are cured for 28 days in a saturated lime bath (3 g CaO/L of H_2O). Then prisms are placed in the environmental chamber for subsequent drying shrinkage measurements. Figure 6.15 shows length change and mass change for OPCC prisms measured beginning 24 hours after casting.

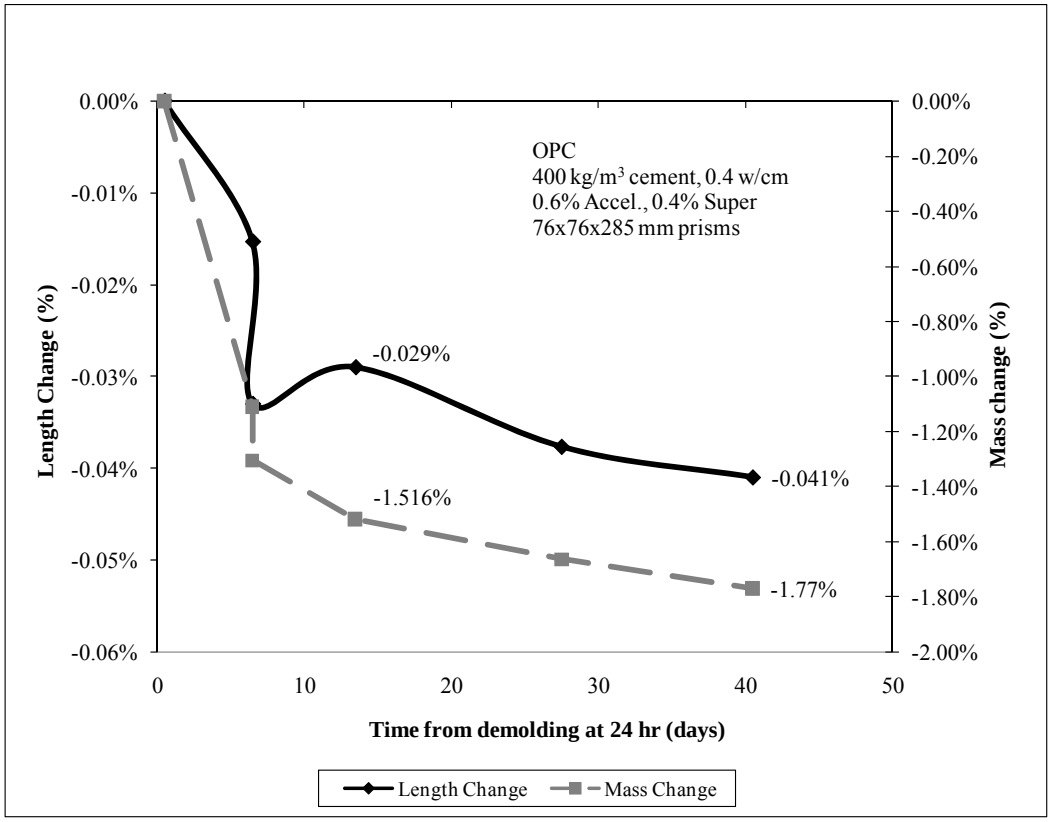

Figure 6.15: Drying shrinkage of OPCC prisms, measured at 24 hours

The results of this testing show a drying shrinkage at 40 days of approximately 0.041% for OPCC prisms subjected to a drying environment 24 hours after casting. At 28 days the shrinkage for these prisms averaged 0.038%, which is slightly greater than that of CACC prisms at the same age and storage condition (e.g., 0.031% at 28 days). However, mass change was almost -1.70% at 28 days which is about twice as much as that for comparative CACC prisms

Figure 6.16 shows length change and mass change for OPCC prisms where drying shrinkage testing began 28 days after testing.

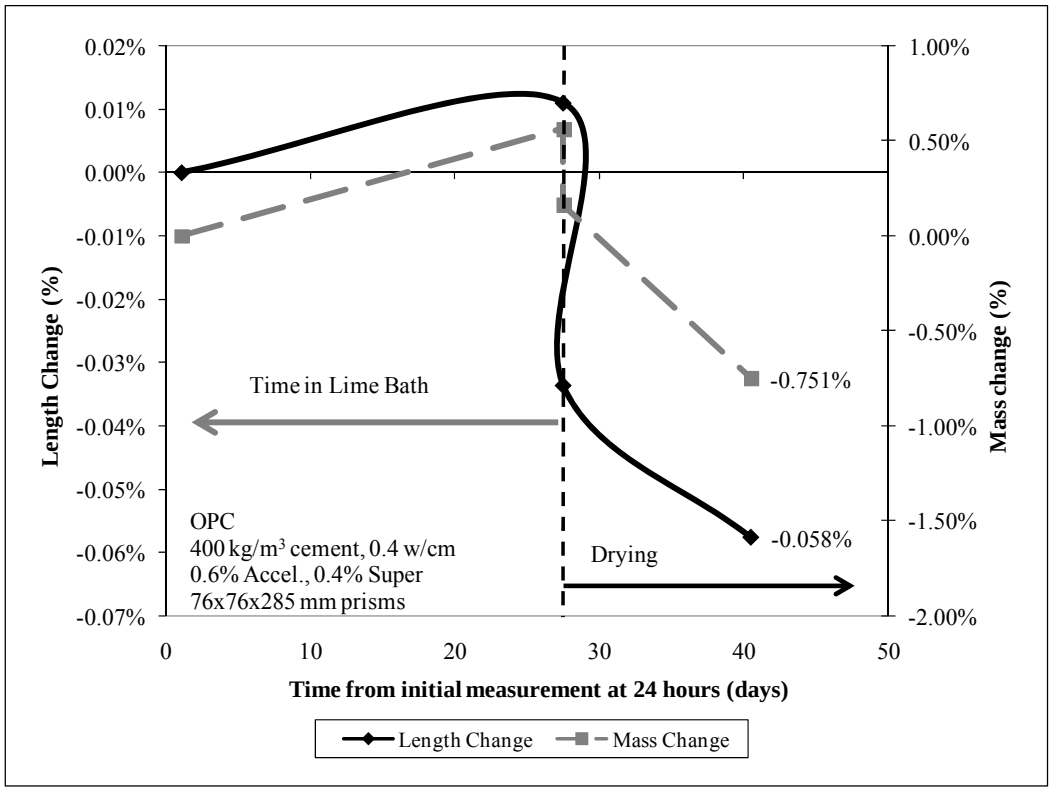

Figure 6.16: Drying shrinkage of OPCC prisms, measured after 28 days

This figure indicates that during the course of a 28 day lime water storage condition for OPCC prisms that the mass of the prisms increases (commensurate with water uptake during this soaking period) by 0.5% followed by a mass loss of 0.751%

after 12 days of storage in a drying environment. Length change indicates a slight expansion to 0.01% after 28 day storage in lime water followed by shrinkage to 0.058% after 12 days of exposure to the drying shrinkage environment. In comparison, the data for OPC prisms demolded at 24 hours and then placed in the drying environment mass loss at 12 days was 1.516% with a shrinkage of 0.029%. The mass loss is almost twice as much as that for OPC prisms cured for 28 days and may be a result of a more well-refined pore structure (i.e. lower permeability and porosity) after 28 days which limits the rapid moisture loss seen in prisms subjected to drying 24 hours after casting. However, the shrinkage for prisms subjected to drying 24 hours after casting is less at the same age, possibly indicating that moisture loss from the larger, less refined pore structure results in less drying shrinkage. While the current version of this test for OPCC concrete recommends a 28 day wet cure in saturated lime solution, it may in fact be appropriate to subject companion prisms at earlier age (e.g., 24 hours after demolding) to a drying shrinkage environment as real structures are often subjected to drying shrinkage environments at relatively early age for OPCC systems. This may provide more "engineering" value to the results of drying shrinkage measurements.

6.2.4 ASTM C 157 Drying Shrinkage: Converted CACC

The last set of drying shrinkage measurements performed on CACC prisms was performed to determine the drying shrinkage of converted (e.g., stable hydrates). Previous studies as part of this dissertation used an oven to promote self-heating in prisms, however the temperature rise in these samples was deemed too rapid and too high (e.g., 90 °C in 2 hours after setting) to truly replicate field samples. Therefore a set of four prisms was cured isothermally at 38 °C immediately after casting. These samples were cast in the same steel molds used for previous drying shrinkage experiments; however the molds were individually double wrapped with large 6 mil polyethylene

storage bags for the first 24 hours after casting to prevent evaporation of moisture. At 24 hours samples were demolded and an initial length change measurement was taken. The CACC prisms were then placed back in the water bath at 38 °C and stored for 7 days. Companion cylinders were tested for strength until conversion was evident from strength data. Then samples were artificially cooled to 23 °C in the same water bath (~ 2 hours to cool) by monitoring the temperature of an embedded thermocouple in one of the samples. An initial measurement at 23 °C was taken and then samples were subjected to a drying shrinkage environment. Figure 6.17 shows the length change of prisms cured isothermally at 38 °C for 7 days (to ensure conversion) prior to placement in an environmental chamber for drying shrinkage measurements.

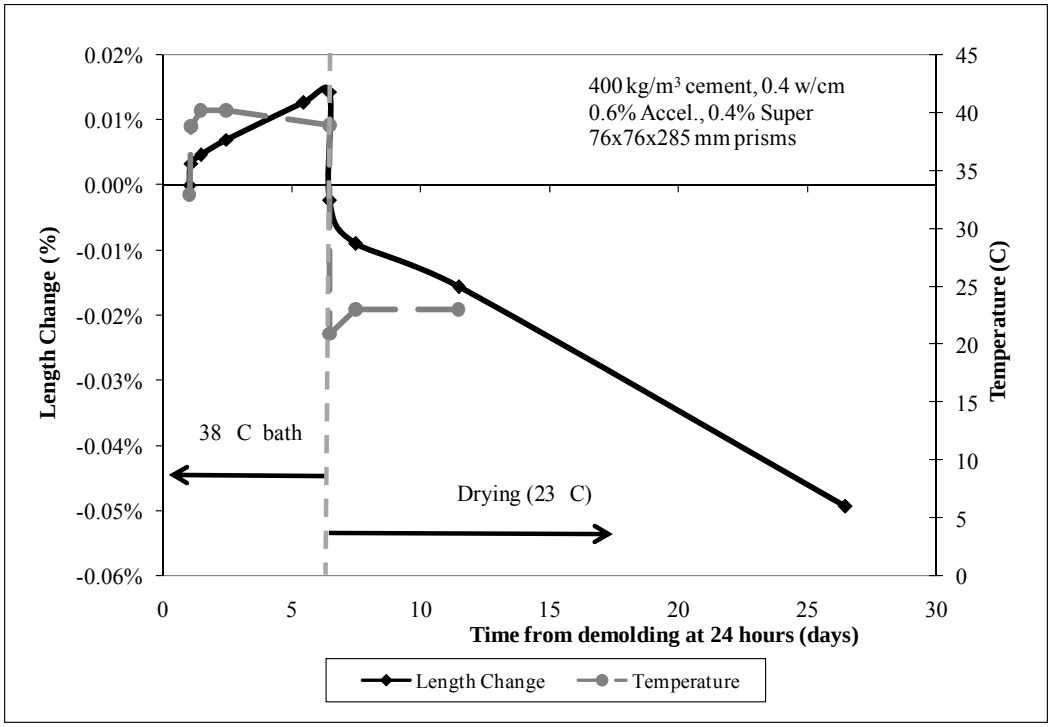

Figure 6.17: Length change and temperature for converted CACC prisms

In this figure the temperature of the prisms is shown by the gray dashed line and increases to a roughly constant 38 °C after the initial measurement (temperature around

34 °C due to demolding of specimens in ambient laboratory conditions prior to initial measurement). There is also a slight increase in length over this 7 day curing period at elevated temperature. This is a combination of water uptake and may be also due to expansion related to conversion of metastable hydrates to stable hydrates (as discussed in section 5.5.2). After seven days the specimens were rapidly cooled in the water bath to 23 °C before drying shrinkage conditions were imposed upon the samples. After 20 days of exposure to drying conditions the prisms shrank by approximately 0.05% (500 microstrain). While this is an ongoing test this level of shrinkage is in line with values for converted CACC at similar age (0.05% at 26 days after exposure to drying shrinkage environment). Figure 6.18 shows length change and mass change for the same series of converted prisms.

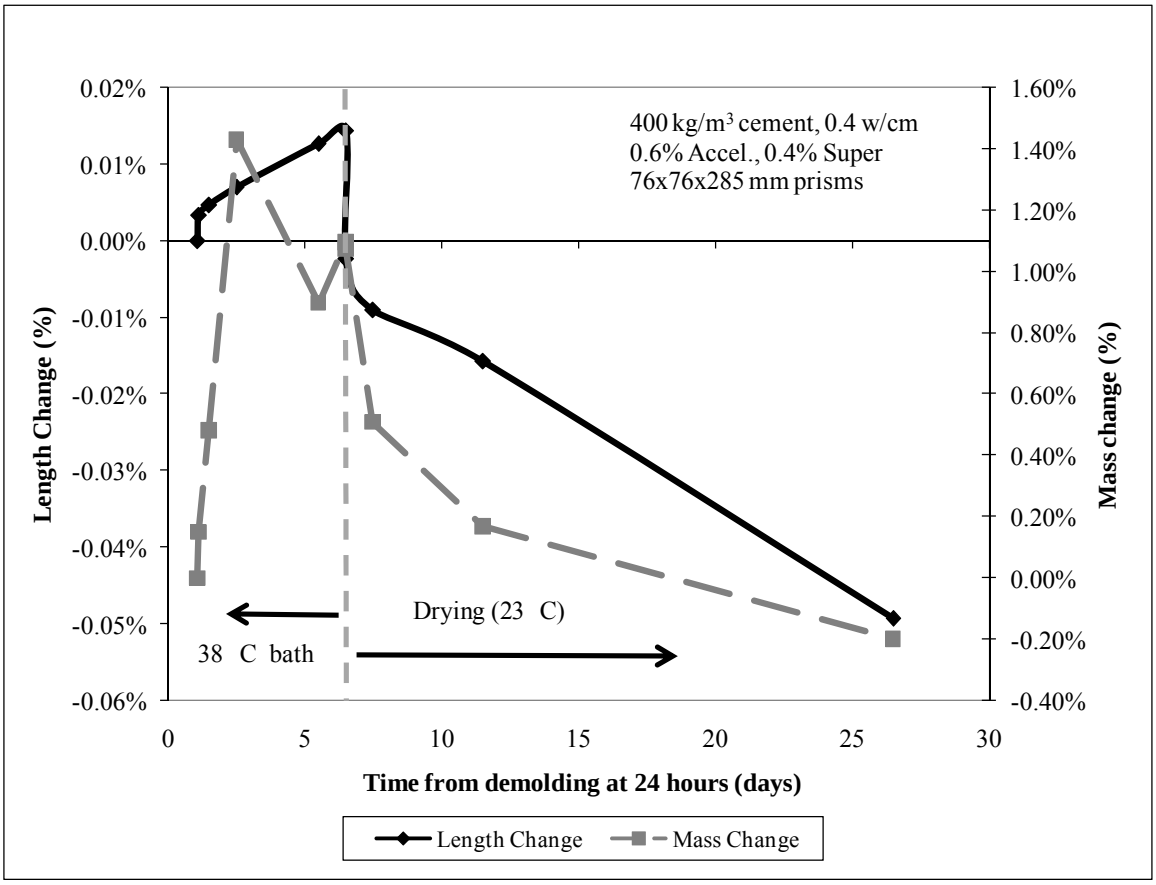

Figure 6.18: Length change for converted CACC Prisms

CACC prisms stored in the 38 °C water bath are shown to gain approximately 1.40% mass during the 7 day storage period with a slight decrease to 0.90% at 6 days after storage in the water bath. After storage in an environmental chamber, the same prisms lose approximately 1.3% water and correspondingly shrink to approximately 0.05% after 20 days of storage in this environment. This testing is ongoing and will be reported with more long-term data in future publications from this dissertation research.

6.2.5 Discussion

Long-term drying shrinkage measurements on initially unconverted CACC and OPCC prisms initially indicated that while CACC prisms evidenced more mass loss than OPCC prisms following the same testing regime they also shrank less than the

counterpart OPCC prisms. However, a second repetition of this testing showed a different behavior where shrinkage was greater for initially unconverted CACC prisms than OPCC prisms tested in the same regime. There was evidence of potential conversion in these CACC samples from an increase in length between 50 and 100 days of testing with no subsequent increase in mass. However, this still does not explain the discrepancy between these two sets tests. Further testing on a third set of samples demonstrated that drying shrinkage that can occur with CACC concrete at early-age is not captured in the traditional version of the ASTM C 157 test. In fact prisms for accurate testing should be demolded several hours (2-3) after T_{off} (roughly commensurate with initial set) and then subjected to a drying shrinkage environment. Measurements of both length change and temperature should be taken roughly every hour until the temperature of the hydrating samples reaches equilibrium with the temperature of the drying shrinkage environmental chamber. Using a hardened CTE value the component of shrinkage due to thermal cooling can be calculated and shrinkage of the prisms can be normalized to only take into account shrinkage due to mass loss. While shrinkage in the first 24 hours after casting calcium aluminate cement concrete may be due to thermal effects as well as drying shrinkage, autogenous deformation is a third factor contributing to shrinkage at early-age. Additional testing to isolate this component of shrinkage would useful in future work to further elucidate the causes for shrinkage so that any adverse effects from such movement may be appropriately mitigated. Long-term measurements on this third set of samples will further elucidate the conflicting results with respect to the amount of drying shrinkage evidenced for CACC versus OPCC.

6.3 DRYING SHRINKAGE ON FREE DEFORMATION SPECIMENS

After several successful rigid cracking and free deformation tests on CACC mortar at UT Austin it was decided to take the free deformation specimens at the end of a

testing period and fit them for long-term drying measurements. This was done to provide a linkage between testing following ASTM C 157 on concrete and long-term drying on CACC mortar specimens. It was also hoped to further delineate any potential difference in drying shrinkage between converted and unconverted microstructures.

6.3.1 Procedure

At the end of the testing period for the rigid cracking and free deformation tests the specimen was removed from the autogenous environment and modified for long-term drying measurements. Two holes nominally 6 mm in diameter by 12 mm in depth were drilled into opposite ends of the specimen. The location of the previously embedded LCP Invar rod for monitoring length change during the free deformation made the perfect "pilot" hole at either end for these newly drilled holes. A stainless steel gage stud (5 mm in diameter by 20 mm in length) was placed in either end and secured with rapid set, high strength epoxy. The effective gage length (inner distance between embedded stainless steel pins) was 135 mm. An initial measurement of the prism for length and weight was taken immediately after the rapid set epoxy had hardened; typically this occurred within 30 minutes of removing the specimen from the free deformation set-up.

6.3.2 Results of drying shrinkage on free deformation specimens

The results of this testing are shown in Table 6.2. The mixture identification, admixtures and curing temperature are given. Then the nominal 6-month shrinkage and mass loss are given for each prism. The shrinkage and mass loss at the latest measured age is also given for each prism. For more recently cast mixtures the latest measurement (shrinkage and mass loss) are provided. The table is arranged in order of isothermal temperature followed by mixture ID.

Table 6.2: Drying shrinkage of free deformation prisms at 6 months and latest measurement

Mix ID	Accel.	Super	Isothermal Temp. (°C)	Real Temp. History	Drying Shrinkage ("6 month")	Mass Change (%)	Age (days)	Drying Shrinkage (ultimate)	Mass Change (%)	Ultimate Age (days)
GCX 38	0.6	0.3	20	-	-0.087	-3.4	191	-0.068	-3.8	241
GCX 43 FA	0.6	0.3	20	-	-0.115	-3.18	168	-0.085	-3.1	218
GCX 46 FA	0.6	0.3	20	-	-0.064	-2.31	176	-0.064	-2.31	176
OPC (1) 0.32	-	-	20	-	-0.064	-0.71	181	-0.085	-1.11	377
OPC (2) 0.32	-	-	20	-	-0.047	-1.56	171	-0.049	-1.83	309
OPC (3) 0.4	-	-	20	-	-	-	-	-0.107	-3.24	146
GCX 27	0.2	0.4	30	-	-0.066	-1.3	174	-0.085	-1.61	372
GCX 26	-	-	34	-	-0.122	-0.86	198	-0.147	-1.07	394
Fondu 37	0.2	0.4	38	-	-0.083	-2.22	167	-0.075	-2.11	251
GCX 28	0.2	0.4	38	-	-0.105	-0.83	182	-0.12	-0.82	357
GCX 29	0.2	0.4	38	-	-0.096	-0.71	171	-0.102	-0.71	330
GCX 36 AEA	0.6	0.4	38	-	-0.119	-1.87	183	-0.115	-1.82	267
GCX 45 FA	0.6	0.3	38	-	-0.124	-1.48	174	-0.105	-1.45	196
GCX 47 FA	0.6	0.3	38	-	-0.075	-1.38	159	-0.075	-1.38	159
GCX 51	0.6	0.4	38	-	-	-	-	-0.075	-3.09	138
GCX 39	0.6	0.3	55	-	-0.055	-0.85	168	-0.032	-0.8	218
GCX 30	-	-	-	Real 57C Hold	-0.068	-1.75	165	-0.066	-1.78	303
GCX 32	0.5	0.3	-	Real with cool	-0.085	-3.48	178	-0.113	-0.366	263
GCX 35	0.6	0.4	-	Real 57C Hold	-0.053	-1.28	189	-0.047	-1.23	273

6.3.3 Discussion

A trend in drying shrinkage is difficult to ascertain from the long-term exposure to drying for free deformation specimens. General trends are summarized as follows:

- Specimens that have lower amounts of drying shrinkage (D.S. ≤ 0.8% at 6 months) are:
    - GCX 46 FA (20 °C isothermal)
    - OPC 1 (0.32 w/cm, 20 °C isothermal) (sieved mortar)
    - OPC 2 (0.32 w/cm, 20 °C isothermal) sieved mortar
    - GCX 27 (30 °C isothermal)
    - GCX 47 FA (38 °C isothermal)
    - GCX 39 (55 °C isothermal)
    - GCX 30 (Real time-temperature history hold at 57 °C)
    - GCX 35 (Real time-temperature history hold at 57 °C)
- Specimens that have higher amounts of drying shrinkage (D.S. > 0.8% at 6 months) are:
    - GCX 38 (20 °C isothermal)
    - GCX 43 FA (20 °C isothermal)
    - GCX 26 (34 °C isothermal)
    - GCX 28 (38 °C isothermal)
    - GCX 36 AEA (38 °C isothermal)
    - GCX 45 FA (38 °C isothermal)
    - GCX 32 (Real time-temperature history with cool to 20 °C)

Samples cured at high isothermal temperature (i.e., fully converted specimens) show the lowest values for drying shrinkage. However free deformation specimens from 38 °C isothermal testing are also fully converted by the end of the testing regime (rigid cracking and free deformation testing) prior to placement in the drying shrinkage environmental chamber. The majority of these specimens show drying shrinkage greater than 0.08% after 6 months of testing which is an incongruous result compared to the other fully converted samples that shrink less than 0.08% after 6 months of testing.

6.4 CONCLUSIONS

Drying shrinkage testing as part of this dissertation illustrated the importance of capturing early-age shrinkage for calcium aluminate cement concrete which occurs rapidly after setting due to the rapid hydration and subsequent strength gain of the material. Traditional testing methods such as ASTM C 1581 showed that unconverted calcium aluminate cement concrete samples were less susceptible to cracking than companion ordinary portland cement concrete samples. The majority of the drying shrinkage work was performed with various modifications to test method ASTM C 157 to determine the difference in drying shrinkage between converted and unconverted samples, if one existed. One of the major findings was that most testing methods developed to OPCC systems had to be modified so that measurements began within several hours of setting for CACC or a significant portion of shrinkage (which may be a combination of autogenous and drying) was not captured by the testing method. Some of the results indicate that drying shrinkage of unconverted CACC may be less than OPCC. Even though greater mass loss in CACC was observed less drying shrinkage than OPCC was measured. This may be due to water lost from a coarser pore structure in CACC resulting in the generation of less shrinkage forces upon loss of this water compared to OPCC. Contrary results were also shown where other CACC prisms exhibited more

drying shrinkage than their counterpart OPCC prisms subjected to the same storage conditions. A final set of experiments is underway to elucidate the causes behind these anomalous results and to properly highlight the difference between converted and unconverted CACC. The final set of testing most importantly demonstrated that shrinkage in the first 24 hours after casting is predominantly due to drying rather than thermal contraction of the specimens due to cooling after the temperature peak from hydration.

7 Field Trial: CACC Slabs Cast to Generate Real Time-Temperature Histories

Full-scale calcium aluminate cement concrete slabs were cast at The University of Texas at Austin in an outdoor exposure field. The slabs were cast with the aim of generating real time-temperature histories that could be used to drive the temperature profile of rigid cracking and free deformation frames. It was also desired to measure the movement (strain change) of these slabs, both in the short- and long-term. In addition, the internal relative humidity of the slabs was monitored beginning 2.5 hours after final set of the outdoor slabs to evaluate the impact of hydration and drying on internal moisture content. These slabs were heavily instrumented with thermocouples to measure temperature, vibrating wire gages to track deformations, embedded gage studs to provide additional length change measurements and embedded plastic sleeves at various depths to enable relative humidity measurements with the Vaisala system.

The first section of this chapter will briefly describe the six different slabs that were cast, including details related to formwork, instrumentation and concrete placement. The second part of the chapter will discuss the measured temperature profiles, strain, relative humidity and the results of mechanical properties tested on laboratory-cast cylinders that were cured isothermally in a 38 °C water bath (for quality control purposes).

7.5 SLAB DETAILS

Six slabs were cast as part of this study. The slabs measured 0.9 x 0.9 x (0.1, 0.2 or 0.3) m. The slabs were referred to as A, B, C, D, E and F. The mixture designs for each slab were identical and followed the mixture proportions for concrete shown in Table 7.1.

Table 7.1: Mixture proportions for outdoor slabs A-F

Mixture Component	**Concrete (wt%)**	**kg/m^3**
Coarse Aggregate (4.75-20 mm)	44.8	1054.0
Fine Aggregate (0-4.75 mm)	31.4	739.8
Cement content (kg/m^3)	17.0	400.0
Water	6.8	160.0
Total	100.0	2353.8

Formwork was constructed from commercially available plywood and lumber. A summary of the each of the slab depths, curing and mechanical testing for quality control is shown in Table 7.2. The quality control for slabs A, B, C and F involved curing cylindrical specimens (100 x 200 mm) in a 38 °C water bath according to the standard methodology used for testing under this temperature regime. Compressive strength (f'c), elastic modulus (E) and splitting tensile strength (f't) were evaluated at 1, 3, 5, (6), (7), and 28 days for all specimens cured at 38 °C isothermally according to the ASTM C 39, 469 and 496, respectively.[52-54] Slabs D, E and F were all cast on the same day from the same materials and with identical mixture proportions. As a result it was decided to only test compressive strength on cylinders cured in a 38 °C water bath from slabs D and E. In addition to the full suite of testing on slab F at 38 °C, samples were also cured in an insulated box to encourage self heating (referred to as ADB for adiabatic) and samples were also cured in ambient laboratory conditions (referred to as AMB for ambient). Only compressive testing was performed on samples cured in ADB or AMB conditions. Results of mechanical property testing will be discussed at the end of the results section for each slab.

Table 7.2: Summary of slab properties and testing procedures

Slab	Depth (m)	Curing	Quality Control Curing Regime	Testing
A	0.1	plastic sheeting	38 C	f'c, E, f't
B	0.2	plastic sheeting	38 C	f'c, E, f't
C	0.3	plastic sheeting	38 C	f'c, E, f't
D	0.1	plastic sheeting	38 C	f'c only
E	0.1	none	38 C	f'c only
F	0.1	insulated	38 C	f'c, E, f't
F	0.1	insulated	ADB	f'c
F	0.1	insulated	AMB	f'c

Three vibrating wire gages were cast in each slab. One gage was placed in the center of each slab at mid-depth. The other two vibrating wire gages were offset by 150 mm from either side (laterally) of the center gage. One of these gages was located higher than the center gage and the other gage was placed lower. For slabs measuring 100 mm in depth (A, D, E and F) this offset distance in the z direction (out of the slab or into the slab) was nominally 25 mm so that vibrating wire gage was placed at a depth of 25, 50 and 75 mm in the slab. For slab B (200 mm depth) this distance was 50 mm so that a vibrating wire gage was placed at a depth of 50, 100 and 150 mm in the slab. Finally for slab C (300 mm depth) an offset distance of 75 mm was used so that a vibrating wire gage was placed at a depth 75, 150 and 225 mm in the slab. Vibrating wire gages were secured to 20 mm diameter PVC hollow PVC pipe. On each of these three PVC pipes thermocouples were located at the same respective offset distances so that on each PVC pipe there were two thermocouples and one vibrating wire gage. An additional PVC pipe was placed in one of the corners of the slab at an offset of 152 mm from other side. This PVC pipe had three thermocouples attached to it so that temperature was monitored at an appreciable distance from the center of the hydrating slab and through a range of depths the same as the thermocouples in the center of the slabs.

Plastic sleeves measuring nominally 12 mm in diameter were cast into the fresh concrete for slabs A, B, C, D and E. These sleeves were cast to enable future measurement of relative humidity once the concrete had set by the (Vaisala) probe relative humidity measurement system. For slabs A, D and E, probes were placed at depths of 25, 50, and 76 mm. For Slabs B and C an additional probe was placed at a depth of 100 mm (maximum depth possible for the type of sleeve available).

7.6 SLAB A

Slab A was cast on January 22, 2008 in Austin, Texas. This slab was the only one cast on this date and was done as a trial or "proof of concept" to ensure that the data acquisition system and instrumentation were working properly and to bring to light any potential improvements that could be made before casting the remaining slabs. Figure 7.1 shows the formwork and instrumentation layout prior to placing the calcium aluminate cement concrete into the formwork. Figure 7.2 shows a close-up of the instrumentation where the vibrating wire gages (3 total) and thermocouples are highlighted. Figure 7.3 shows a side view of the vibrating wire gages and thermocouples for Slab B and illustrates the different depth placement of these gages. Figure 7.4 shows the data acquisition system set up to retrieve and store data from the vibrating wire gages and thermocouples.

Figure 7.1: Slab A formwork and instrumentation

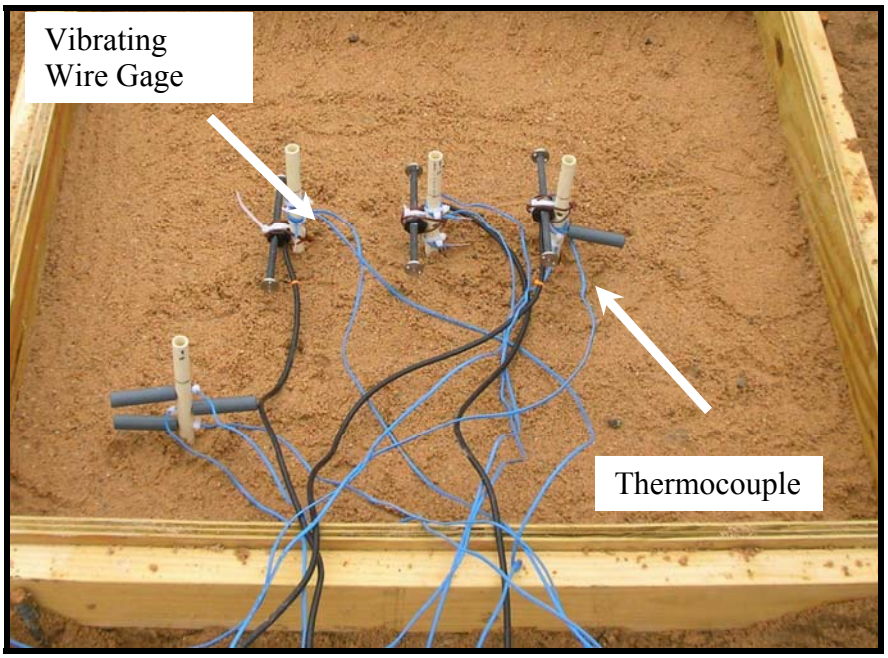

Figure 7.2: Slab A, thermocouple and vibrating wire gages

Figure 7.3: Side view of thermocouple and VBWG layout for Slab B

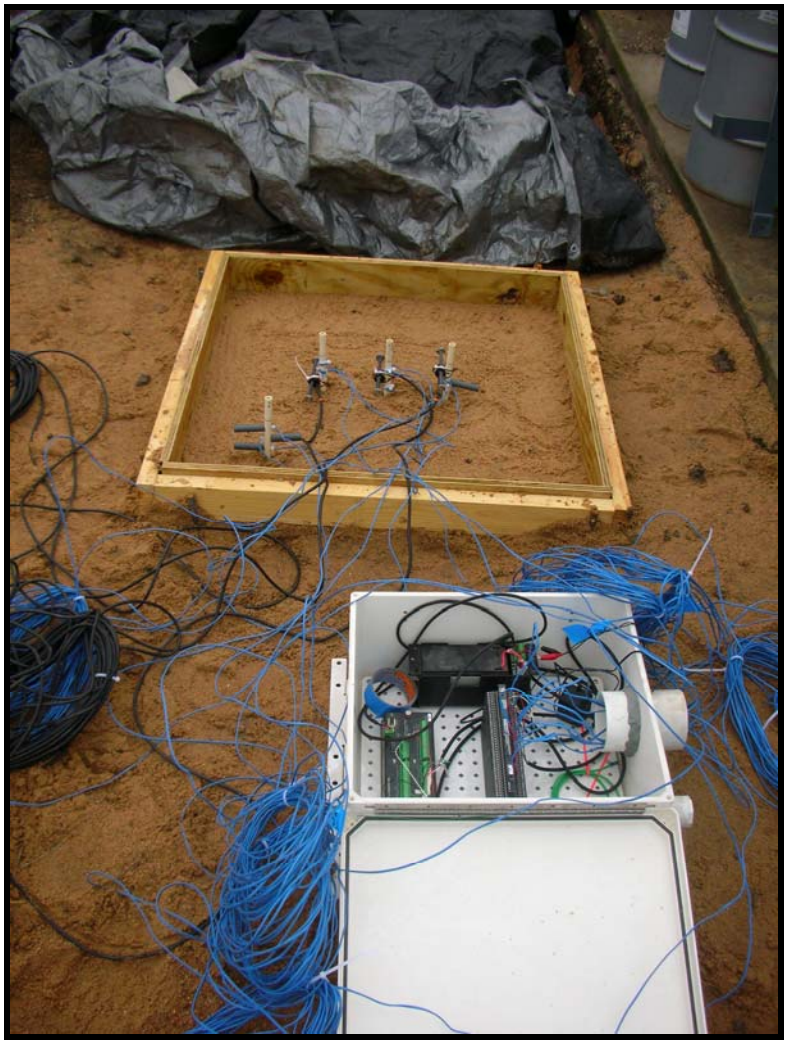

Figure 7.4: Data acquisition system for Slab A

Figure 7.5 shows the vibrating wire gage and thermocouple schematic for Slab A to aid in the interpretation of vibrating wire gage and in particular temperature profiles. On the square representing the slab, TC, 1, 2 and 3 represent a location of a PVC pipe that has either vibrating wire gages and thermocouples on it (1, 2, or 3) or just thermocouples (TC). This will be the same nomenclature used for the schematics for the other slabs shown in this chapter. Figure 7.6 shows vibration of the concrete placed in the form for slab A.

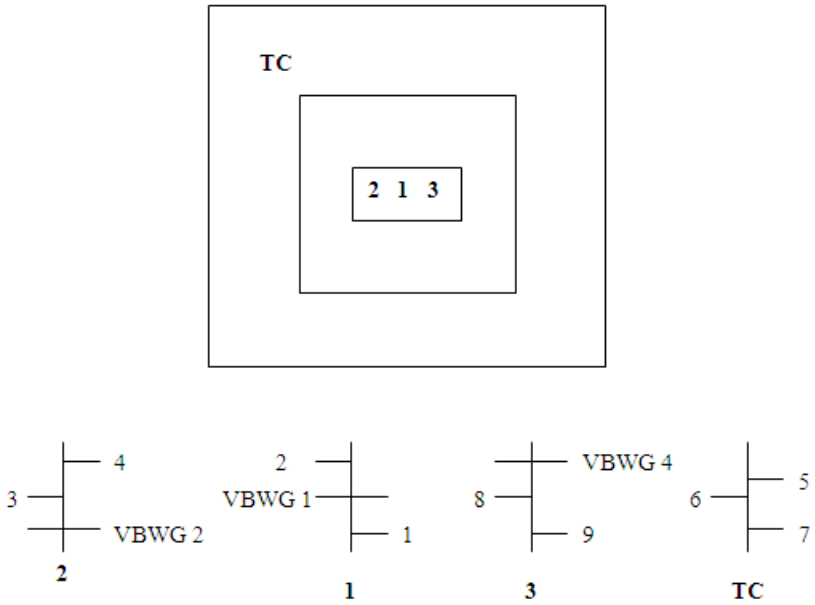

Figure 7.5: Schematic of VBWG and Thermocouple layout for Slab A

Figure 7.6: CACC placement in Slab A

The temperature profile for slab A up to 150 hours of testing is shown in Figure 7.7. An expanded view of the first 50 hours is shown for the temperature profile for slab A in Figure 7.8.

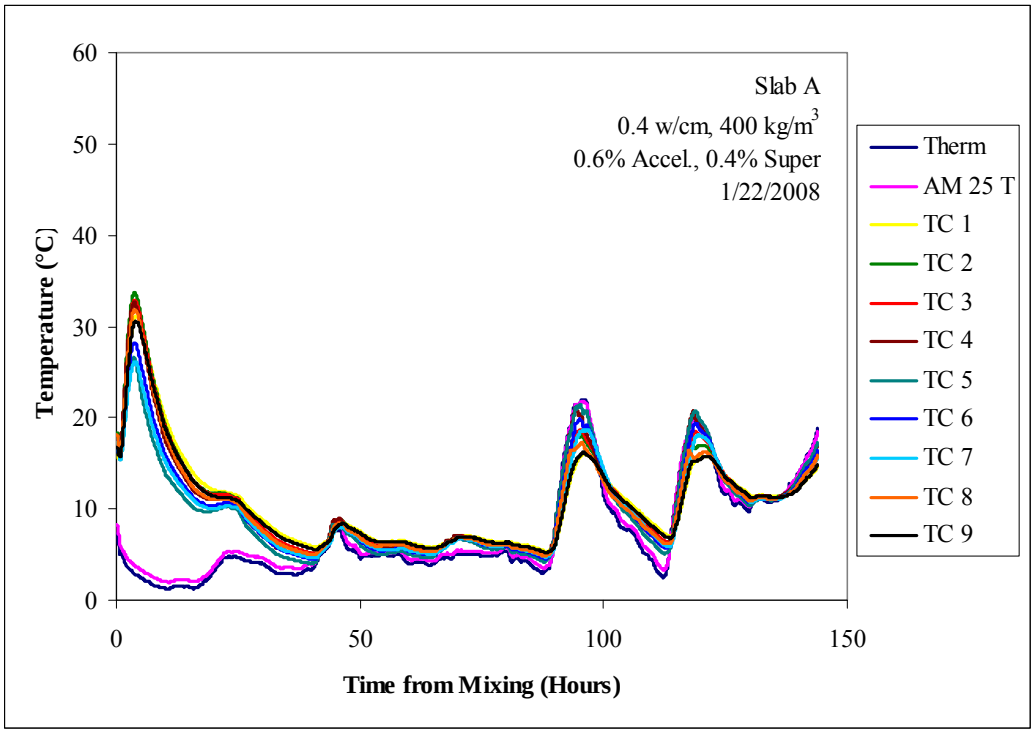

Figure 7.7: Temperature profile for Slab A, 0.1 m thick

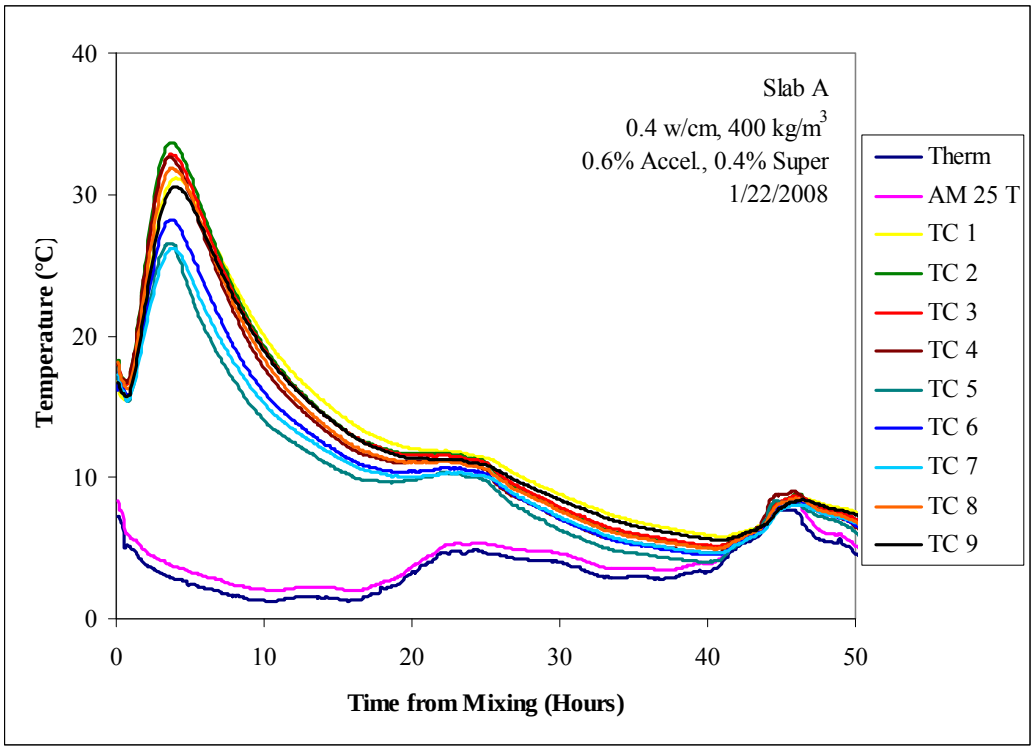

Figure 7.8: Temperature profile for Slab A, 0.1 m thick, 50 hours

Figure 7.8 shows that Slab A reached a maximum temperature averaging just around 30 °C roughly 6 hours after mixing. The hottest part of the slab was the center as expected (TC 1 through 4 and TC 8 and 9). The coolest part of the slab that was measured was for TC 5 through 7 which were located closer to the corner of the slab. It can also be seen from the thermocouples for "therm" and "AM 25 T" (ambient thermocouples in data acquisition system housing box) that the ambient temperature was very cool during the casting of Slab A and is likely why the temperature rise for this slab was relative low at just around 30 °C.

The strain measurements from the VBWG are shown in Figure 7.9.

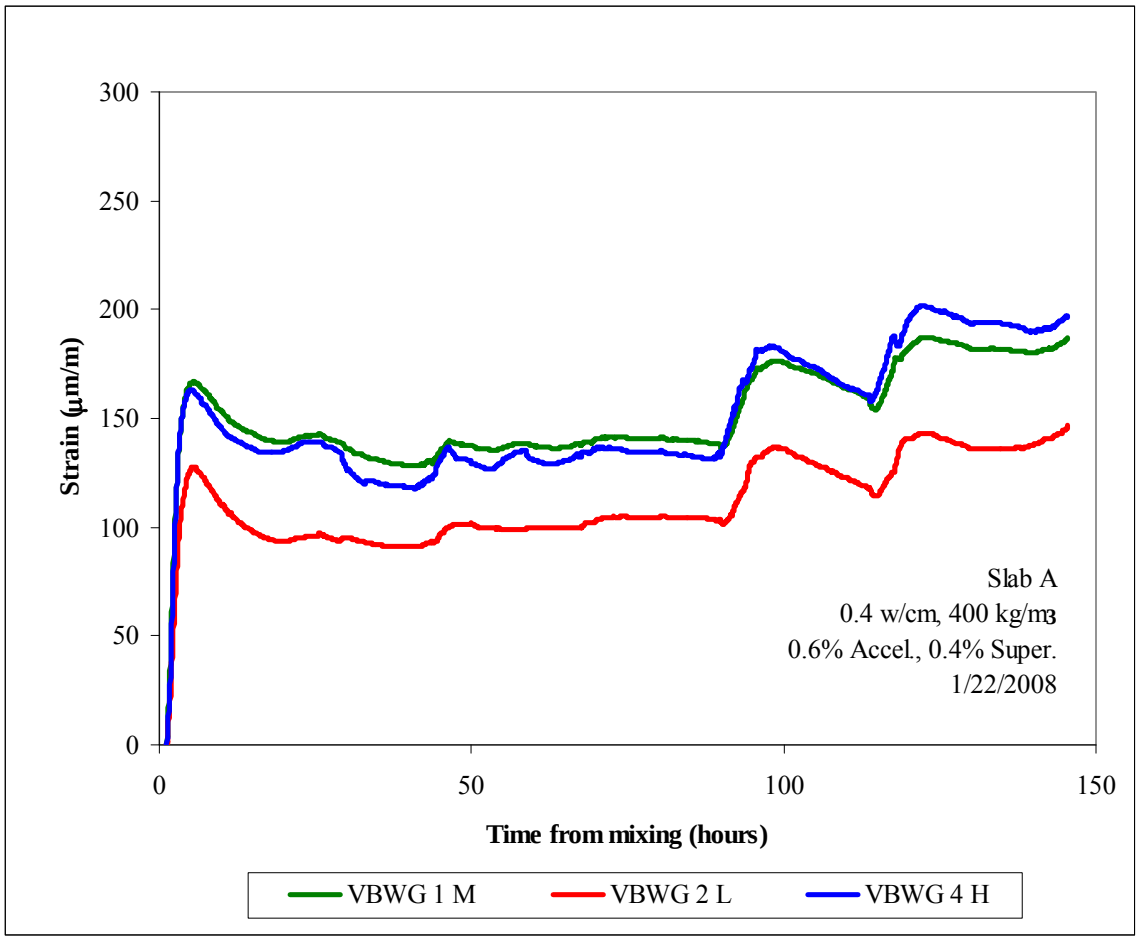

Figure 7.9: VBWG strain readings for Slab A, 0.1 m thick

Figure 7.9 shows very interesting results for the strain generated during hydration of Slab A in that the concrete expanded with the rise in temperature due to hydration to a maximum value of ~ 170 μm/m and then upon cooling the material shrank but only by approximately 50-70 μm/m. For up to 6 days of testing the material remained in a state of positive strain and with a commensurate increase in temperature it continued to show overall slight expansion. The least amount of strain was observed from the lowest placed vibrating wire gage (VBWG 2 L).

The change in relative humidity for slab A is shown in Figure 7.10.

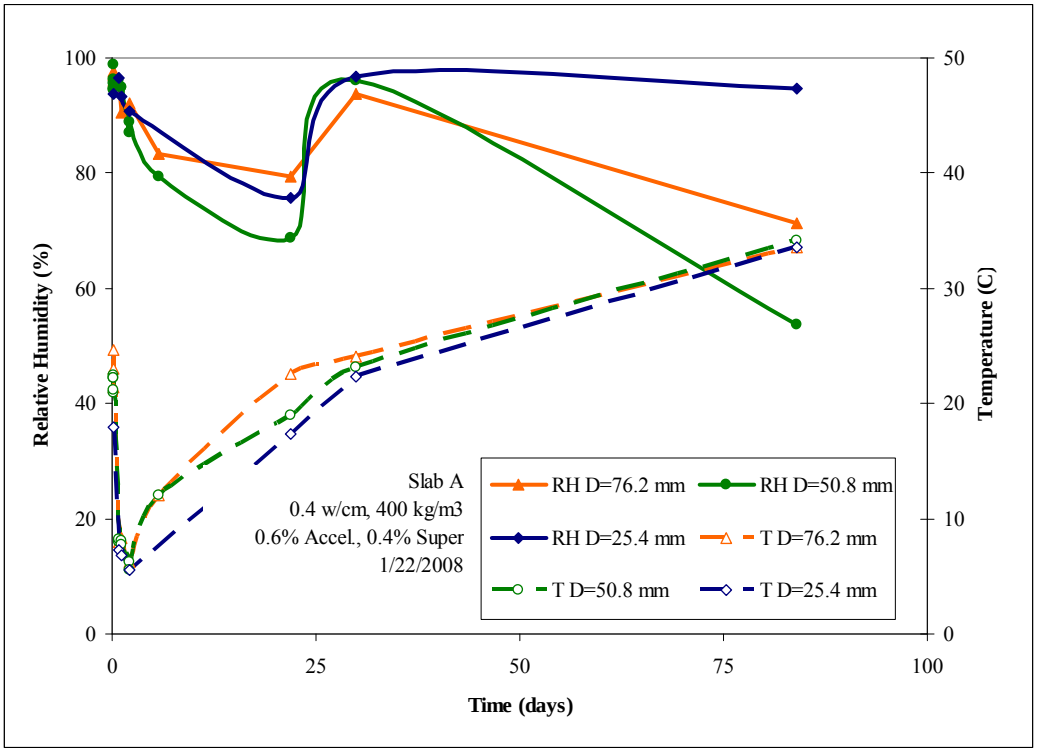

Figure 7.10: Relative humidity values for Slab A, 0.1 m thick

Figure 7.10 shows that after a rapid decrease in relative humidity just after hydration the relative humidity continued to decrease to a minimum value around 70 % at a depth of 50.8 mm in the slab and then the relative humidity increases again. It was noted at the time of measurements at 24 days after casting there had been a heavy period of rain. This indicates that after initial rapid-drying of the CACC concrete commensurate with hydration relative humidity is then affected more so by the environment to which it is exposed.

Mechanical properties for the concrete cylinders cured from slab A in the 38 °C isothermal water bath environment are shown in Table 7.3.

Table 7.3: Mechanical property data for Slab A cylinders -38 °C water bath cure)

Age (days)	Compressive Strength (MPa)	Elastic Modulus (GPa)	Tensile Strength (MPa)
1	31.5	57.0	4.8
3	30.1	50.7	4.4
5	25.7	54.6	3.6
6	28.9	50.5	4.3
28	31.1	56.4	4.6

The data shown in Table 7.3 show that conversion occurs at five days with a reduction in compressive strength to 25.7 MPa. Splitting tensile strength also shows a reduction at this age. A reduction in elastic modulus is not observed until the next day of testing at 6 days of age however.

7.7 SLAB B

Slab B was cast on the 29th of January, 2008 and measured nominally 200 mm in depth. Figure 7.11 shows a schematic diagram for the vibrating wire gage and thermocouple layout for slab B. Figure 7.12 shows slab B just after casting, covered with plastic sheeting, which is typical of how CACC slabs are cured in field applications.

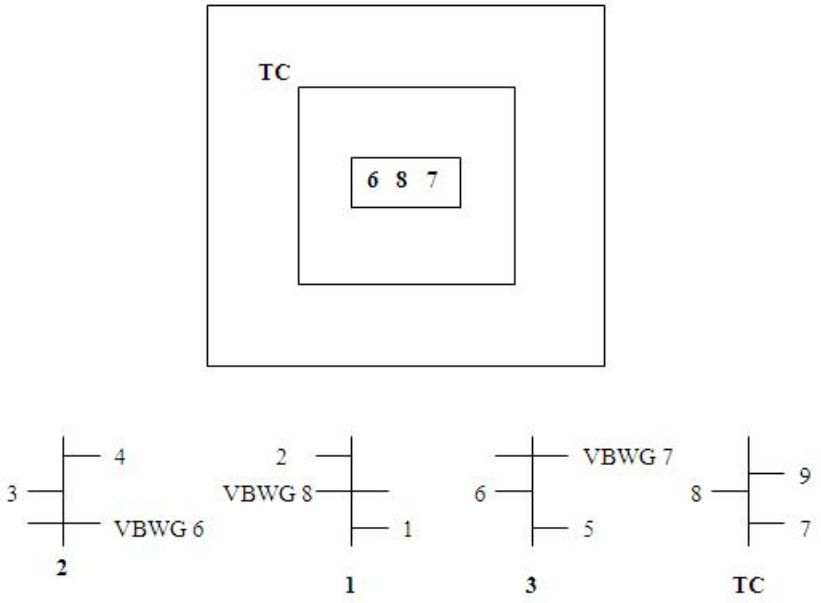

Figure 7.11: Schematic of VBWG and thermocouple layout for Slab B

Figure 7.12: Plastic sheeting covering Slab B after casting

The temperature profiles in Figure 7.13 and Figure 7.14 show that a higher maximum temperature (above 60 °C) was attained for slab B in comparison to slab A where the maximum temperature was just 30 °C. This is due to the larger size of slab B and also to the fact that ambient temperatures at placement were roughly 10-15 °C higher when slab B was cast. The lowest temperatures around 50 °C were observed for TC 1, 7 and 5 which were all thermocouples located closest to the bottom of the slab. Due to the cooler temperature of the ground and the insulating properties of the ground mass, concrete within 50 mm of the bottom of the slab was 10 °C cooler than concrete in the center of the slab. This temperature gradient increased with increased depth toward the ground.

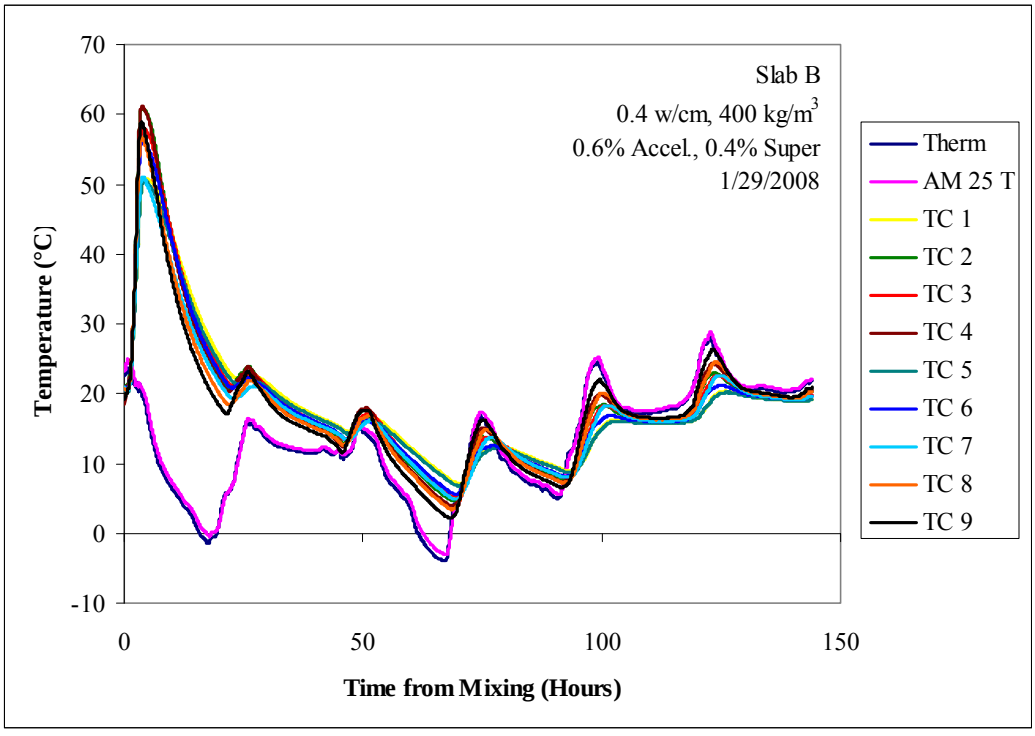

Figure 7.13: Temperature profile for Slab B, 0.2 m thick

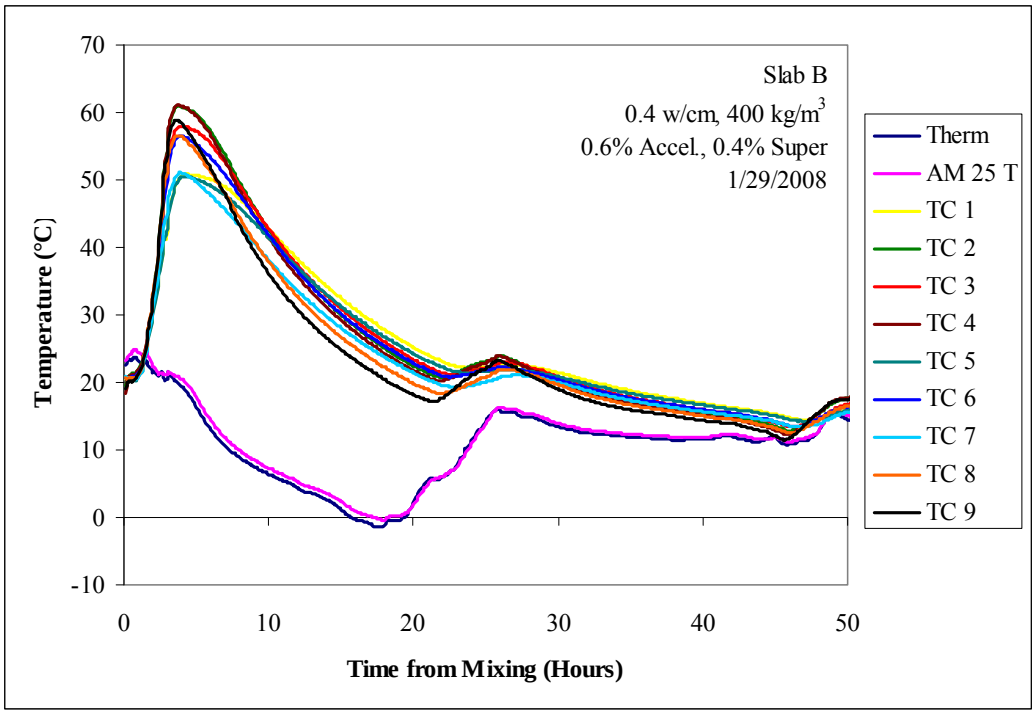

Figure 7.14: Temperature profile for Slab B, 0.2 m thick

Figure 7.15 shows the strain generated in slab B. There is a gap in the data between 24 hours and 48 hours as the data logging storage module overwrote existing data to continue recording data.

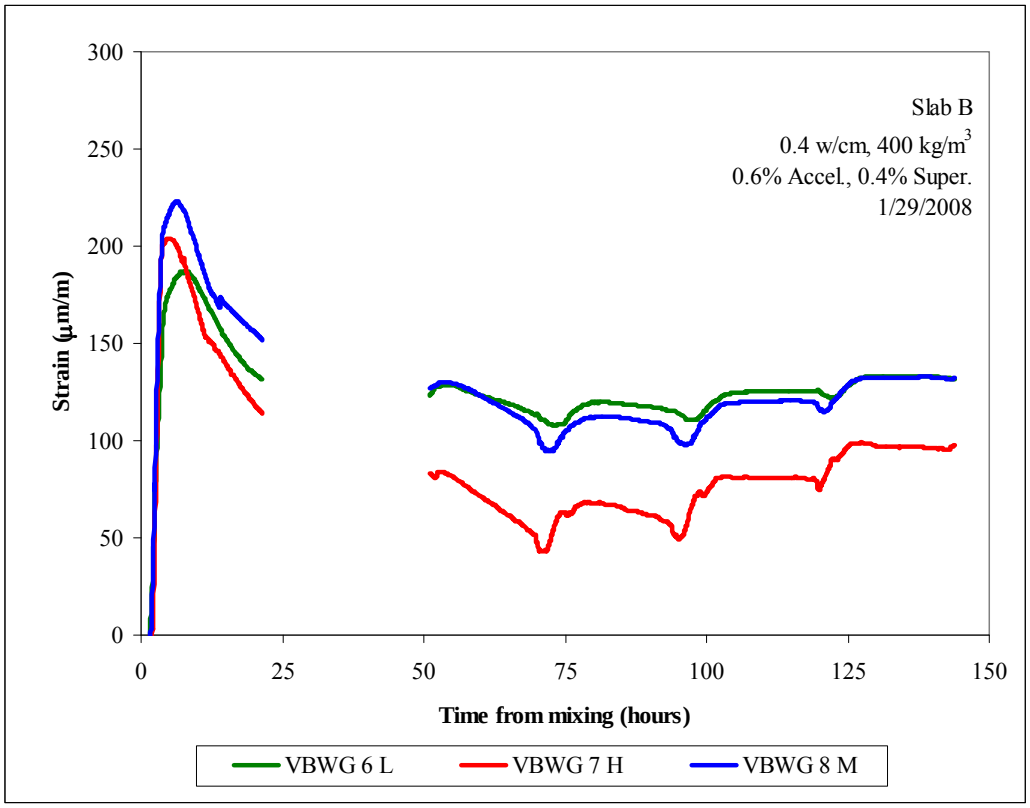

Figure 7.15: Strain generated for Slab B, 0.2 m thick

Compared to the strain seen for Slab A, Slab B generated more expansive strain, around 200 µm/m. Upon cooling the concrete in this slab shrank, but similar to Slab A stayed in a state of expansive strain, even with ambient rise and fall of temperature (after heat of hydration in the first 24 hours had evolved). Relative humidity is shown in Figure 7.16 and Figure 7.17.

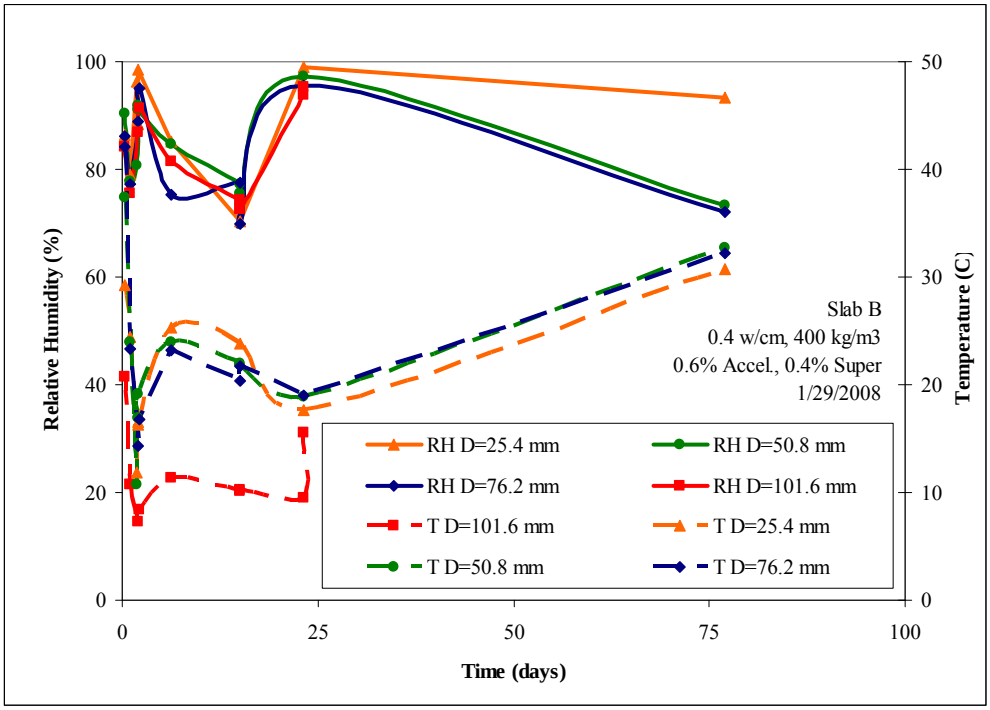

Figure 7.16: Relative humidity and temperature in Slab B, 0.2 m thick

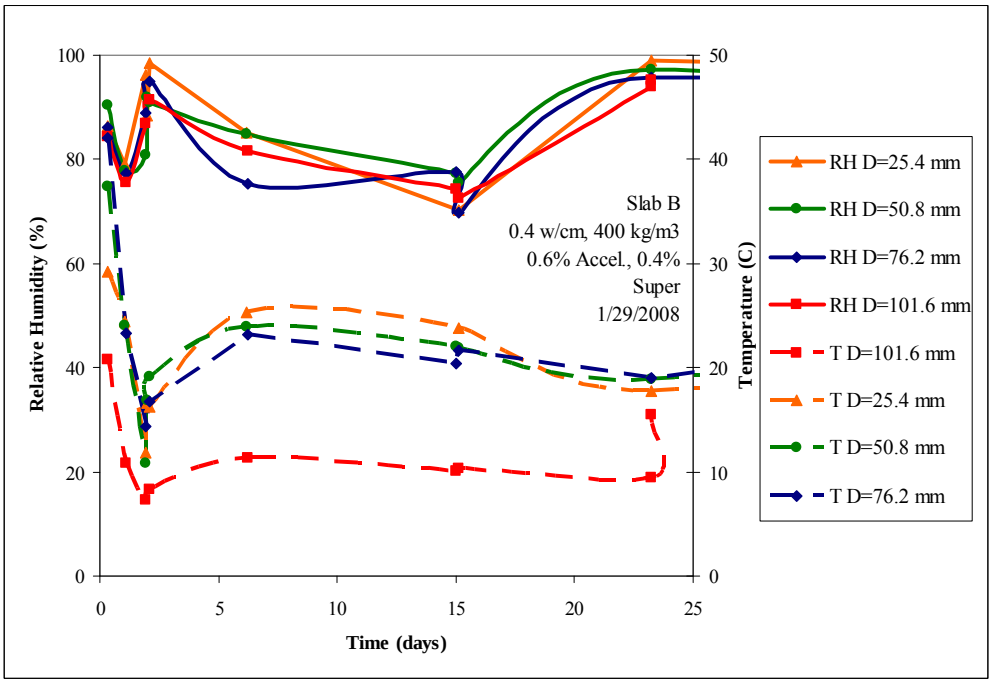

Figure 7.17: Relative humidity and temperature in Slab B, 0.2 m thick, 25 days

After a rapid decrease in internal relative humidity to just below 80% the relative humidity rapidly increased over the next three days commensurate with more rainfall in Austin, Texas during this time. Relative humidity fluctuated over the next 70 days. It is interesting to note that the internal relative humidity of CAC concrete rapidly decreased during initial hydration to below 80%; a value that may never be attained in ordinary portland cement concrete except in exceedingly dry climates or with externally applied coatings.

Mechanical property development for concrete cast from this mixture and cured isothermally at 38 °C is shown in Table 7.4.

Table 7.4: Mechanical property data for Slab B cylinders -38 °C water bath

Age (days)	Compressive Strength (MPa)	Elastic Modulus (GPa)	Tensile Strength (MPa)
1	29.2	51.5	4.3
3	29.8	46.3	3.8
5	24.5	49.2	3.6
7	27.4	51.7	4.3
28	30.9	55.0	4.2

Conversion as evidenced by a decrease in compressive strength was observed at 5 days for the calcium aluminate cement concrete cylinders cast from the mixture for Slab B and cured in a 38 °C water bath. Elastic modulus showed a slight reduction from 51.5 GPa at 1 day to 46.3 GPA at 3 days and steadily increased thereafter to a value of 55 GPa at 28 days. Tensile strength also decreased commensurate with conversion.

7.8 SLAB C

Slab C was the largest slab cast with a 0.3 m depth and was cast immediately after Slab B on the same day. Figure 7.18 shows a schematic for the vibrating wire gage and thermocouple layout for slab C.

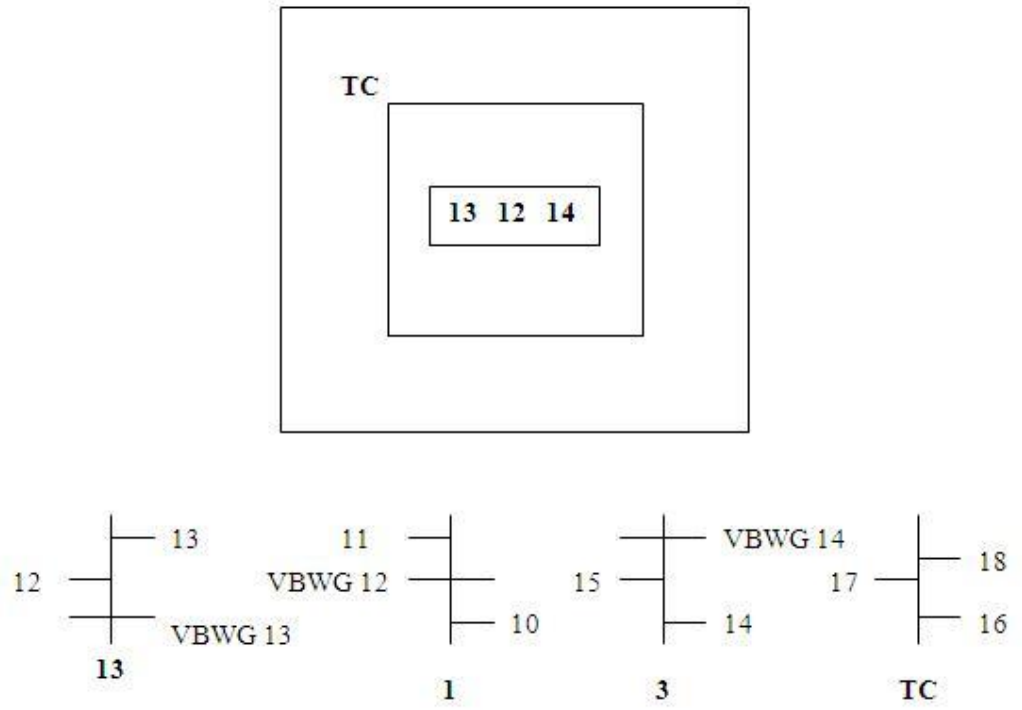

Figure 7.18: VBWG and thermocouple schematic for Slab C

The temperature profile shown in Figure 7.19 and Figure 7.20 is actually very similar to the heat generation for Slab B with a maximum temperature of 60 °C. Despite the thicker size of Slab C, it was cast at point in the day when the temperature was rapidly falling (with the onset of nightfall) and this likely had a pronounced effect on the maximum heat attained for slab C.

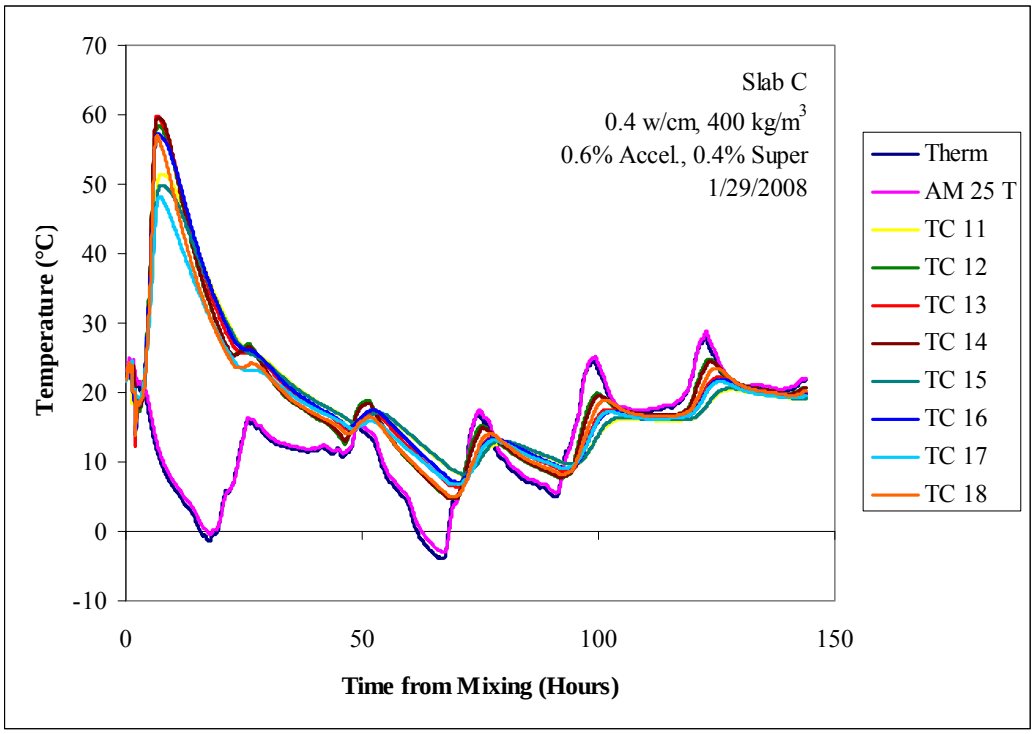

Figure 7.19: Temperature profile for Slab C, 0.3 m thick

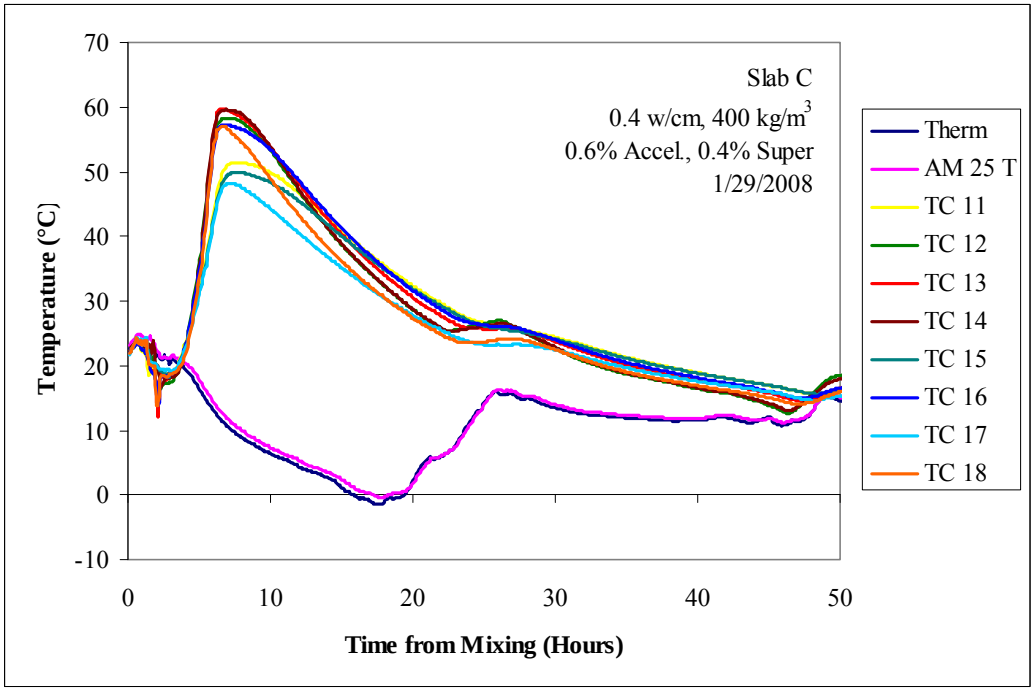

Figure 7.20: Temperature profile for Slab C, 0.3 m thick, 50 hours

Figure 7.21 indicates a wide range of expansive strain for Slab C. The highest strain was shown for VBWG 14 which was the gage closest to the surface of the concrete. The least amount of strain was observed in the lowest vibrating wire gage at roughly 150 µm/m. This early expansion remained "locked" into the system;s even upon cooling the material stays in this state of expansive strain.

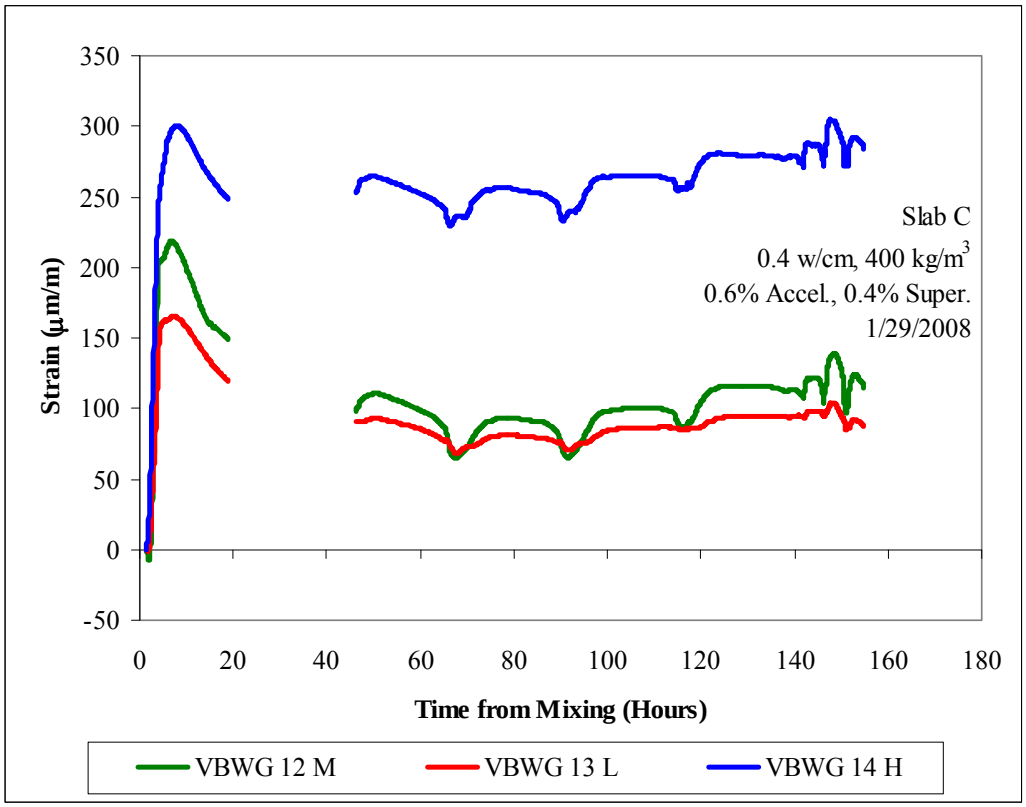

Figure 7.21: Strain generation for Slab C, 0.3 m thick

Figure 7.22 and Figure 7.23 show perhaps most clearly for all the slabs tested that relative humidity, decreased more rapidly at shallow concrete depths (potential evidence of drying shrinkage coupled with rapid hydration and self-dessication in the first day after casting).

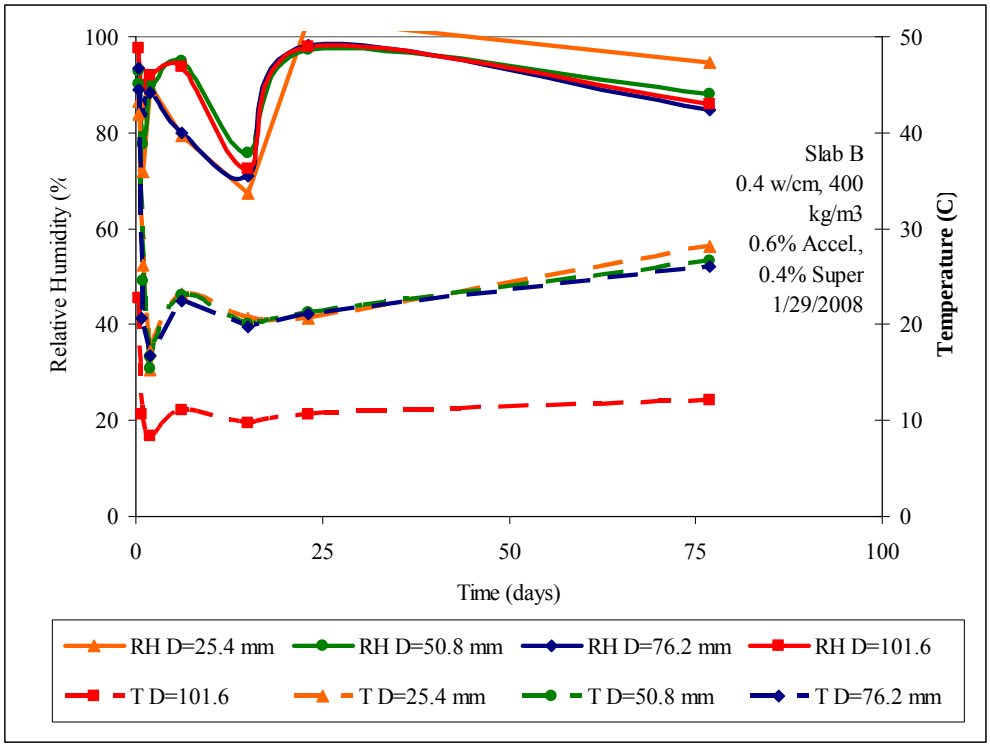

Figure 7.22: Relative humidity and temperature for Slab C, 0.3 m thick

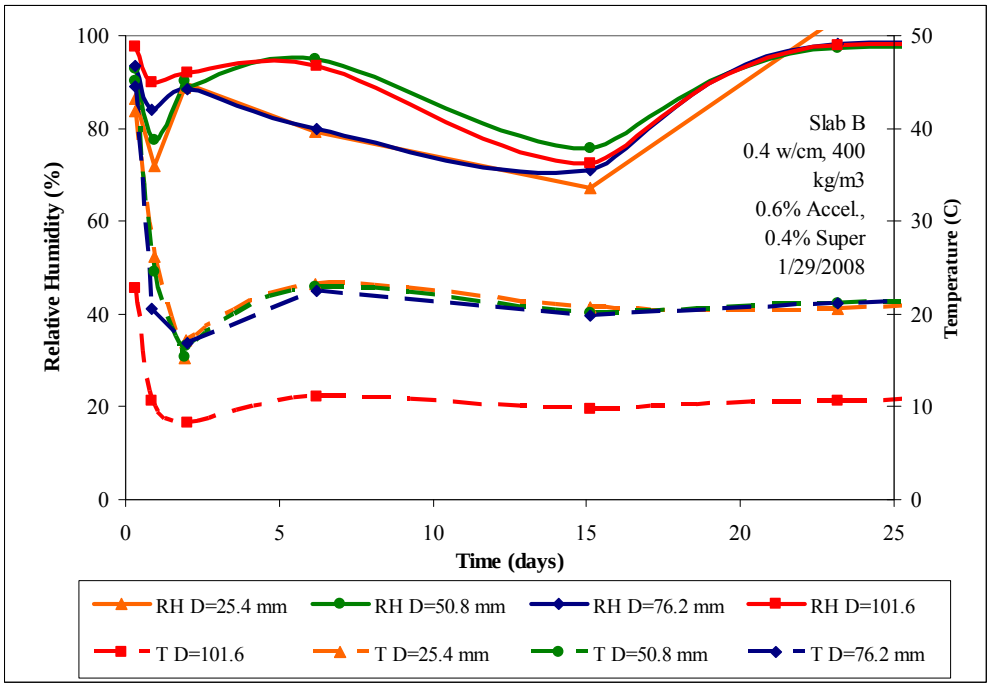

Figure 7.23: Relative humidity and temperature for Slab C, 0.3 m thick 25 hours

Mechanical properties for cylinders cured from this mixture at 38 °C isothermally are shown in Table 7.5. In line with previous results conversion occured at 5 days for concrete cylinders cured in a 38 °C isothermal water bath cast from the same mixture as Slab C. A reduction in both elastic modulus and tensile strength occurred at the same time as decrease in compressive strength due to conversion.

Table 7.5: Mechanical property data for Slab C concrete – 38 °C cure

Age (days)	Compressive Strength (MPa)	Elastic Modulus (GPa)	Tensile Strength (MPa)
1	37.6	49.8	3.8
3	31.1	46.3	4.1
5	29.7	52.8	4.2
7	34.2	52.6	4.8
28	39.5	58.5	5.2

7.9 SLAB D, E, F

Slabs D, E, and F were all cast on 7 February 2008 and were all 0.1 m in depth. Slab D was covered with plastic sheeting immediately after finishing. Slab E was not cured and was left open to cure in ambient conditions. Slab F was insulated with a 0.9 x 0.9 x 0.5 m piece of high density polystyrene and was then wrapped with heavy-duty curing blankets to promote self-heating in this slab to not only reach a high temperature but to maintain that temperature for as long as possible. Figure 7.24, Figure 7.25 and Figure 7.26 show the schematic diagrams for the VBWG and thermocouple layouts for slabs D, E and F.

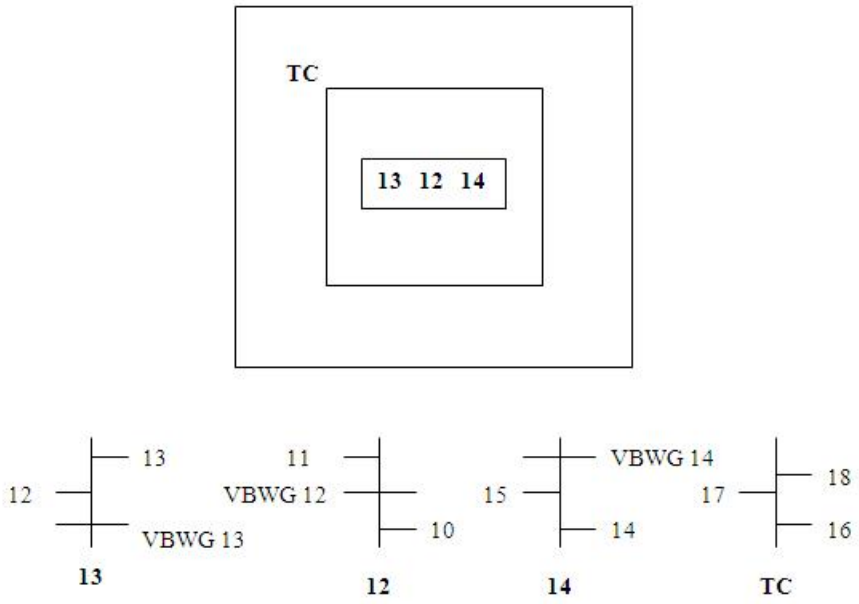

Figure 7.24: Slab D VBWG and thermocouple schematic

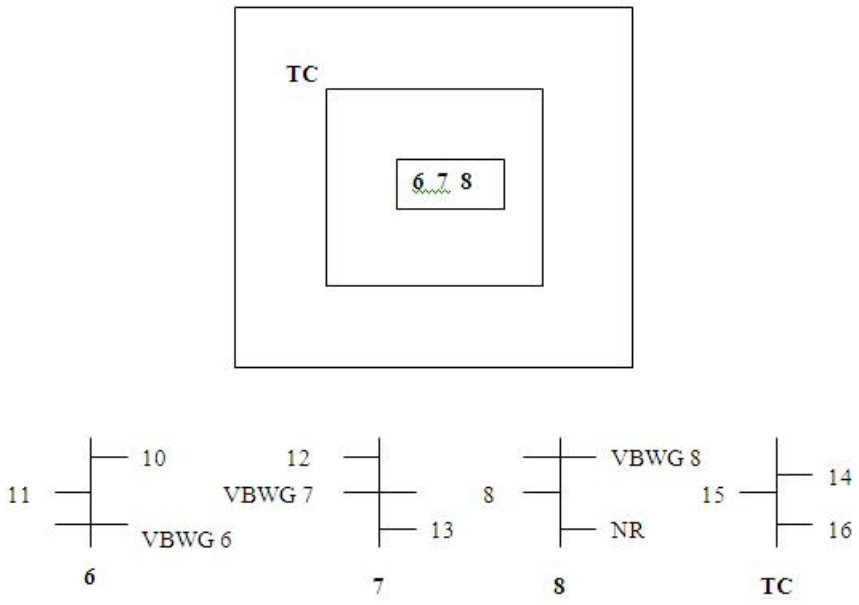

Figure 7.25: Slab E VBWG and thermocouple schematic

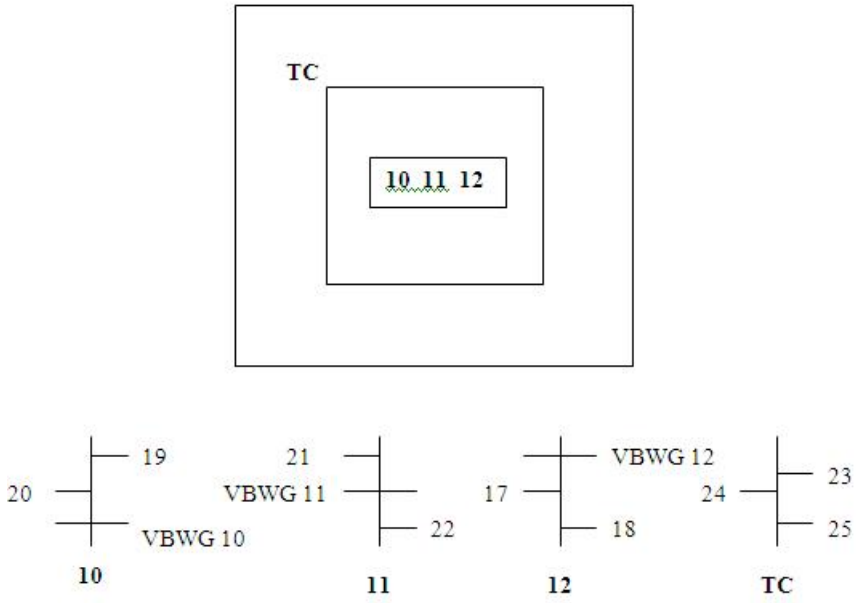

Figure 7.26: Slab F VBWG and thermocouple schematic

The temperature profiles for these slabs are shown in Figure 7.27, Figure 7.28 and Figure 7.29. It is useful to compare the temperature histories of these three slabs as it demonstrates the profound effect that even seemingly small changes in insulation play in increasing heat generation in calcium aluminate cement concrete. Perhaps the most interesting comparison is between Slab D (covered with plastic sheeting after finishing) and Slab E, which was never covered. These two slabs were placed within thirty minutes of one another so the effects of ambient temperature decrease are very similar for both slabs. The maximum temperature reached for Slab D was 57 ° C, whereas the maximum temperature reached for Slab E was 37 °C, an almost astonishing difference of 20 °C almost solely attributed to the presence of plastic sheeting covering Slab D. The insulated slab, F, reached a maximum temperature essentially the same as Slab D, however the cooling rate for this slab was much slower and as a result it remained at high temperature for the longest of any slabs investigated as part of this study. Thermocouple

19 was chosen as the reference thermocouple to provide a real temperature history for rigid cracking and free deformation testing in the laboratory. Figure 7.30 shows the temperature readings from thermocouple 19 from Slab F that were used for testing in the rigid cracking and free deformation frames.

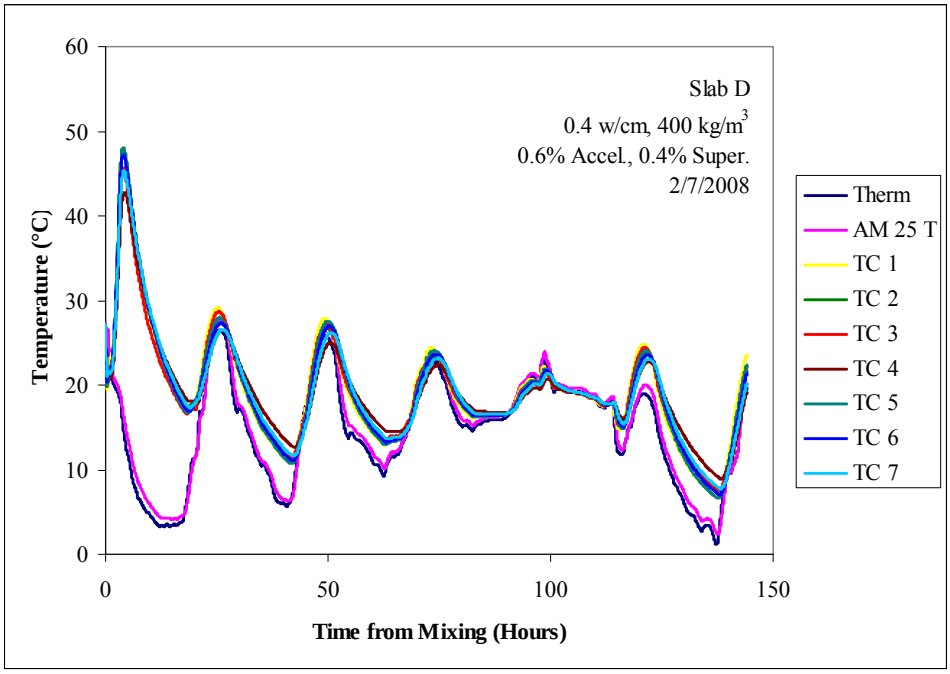

Figure 7.27: Temperature profile for Slab D, 0.1 m thick

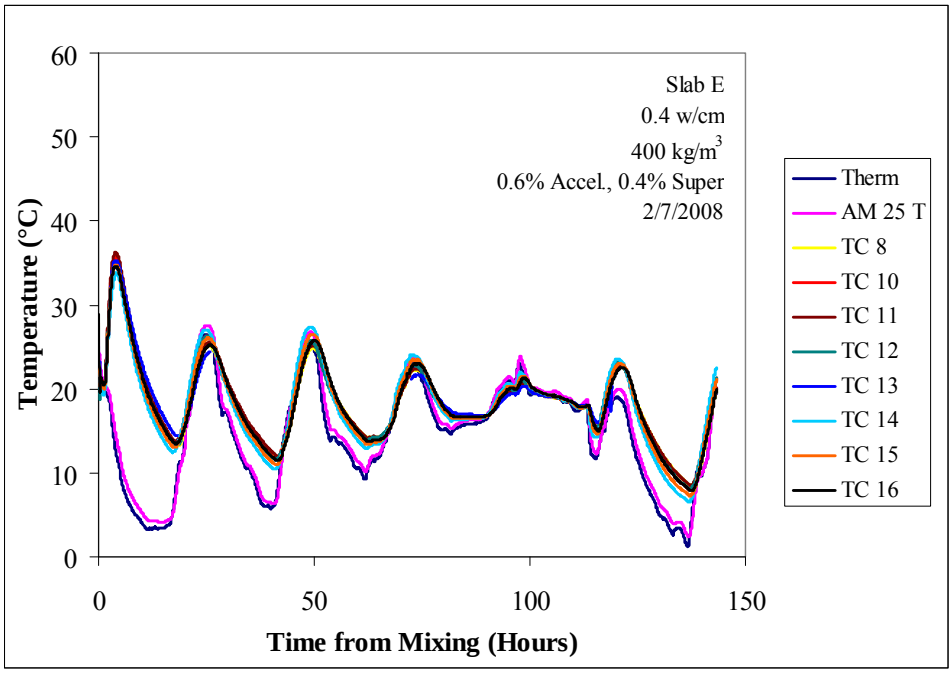

Figure 7.28: Temperature profile for Slab E, 0.1 m thick

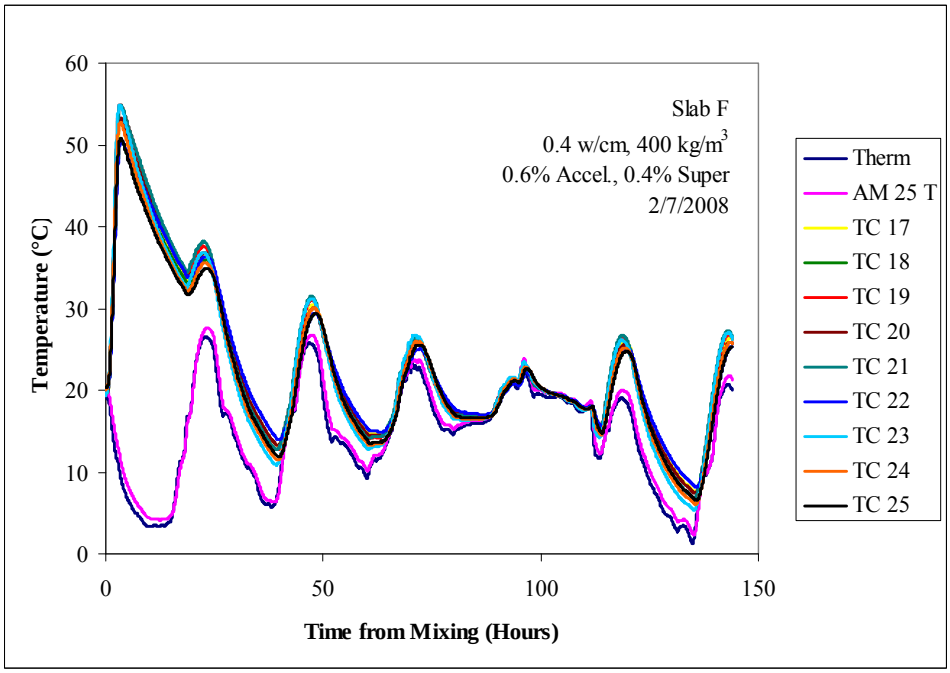

Figure 7.29: Temperature profile for Slab F, 0.1 m thick

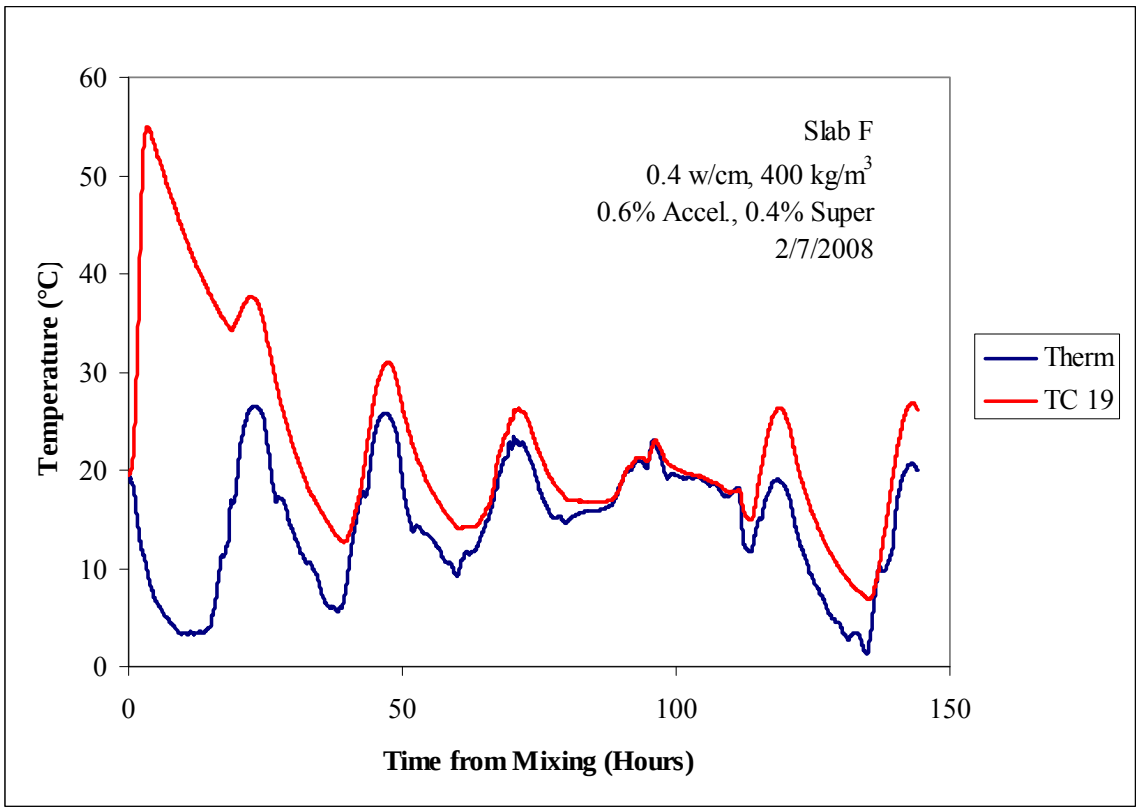

Figure 7.30: Temperature evolution for TC 19

Strain generation for each slab is shown in Figure 7.31 and Figure 7.32 and Figure 7.33. The strains generated in Slab D and F showed the most uniform deformation of these three slabs. It is not surprising that this is the case for Slab F since it was well-insulated and therefore temperature rise was the most uniform in this slab. The results for Slab E which showed the lowest temperature rise are somewhat surprising. The upper and lower VBWG showed less movement than the other slabs (D and F); this may be a result of the smaller temperature rise in slab F. However, the middle VBWG showed almost twice as much movement as the upper and lower gages and continued to deviate further away from the other two gages. There could be a problem with placement of the gage, proximity to larger aggregate particles, or this could be a gage that was not properly calibrated from the factory.

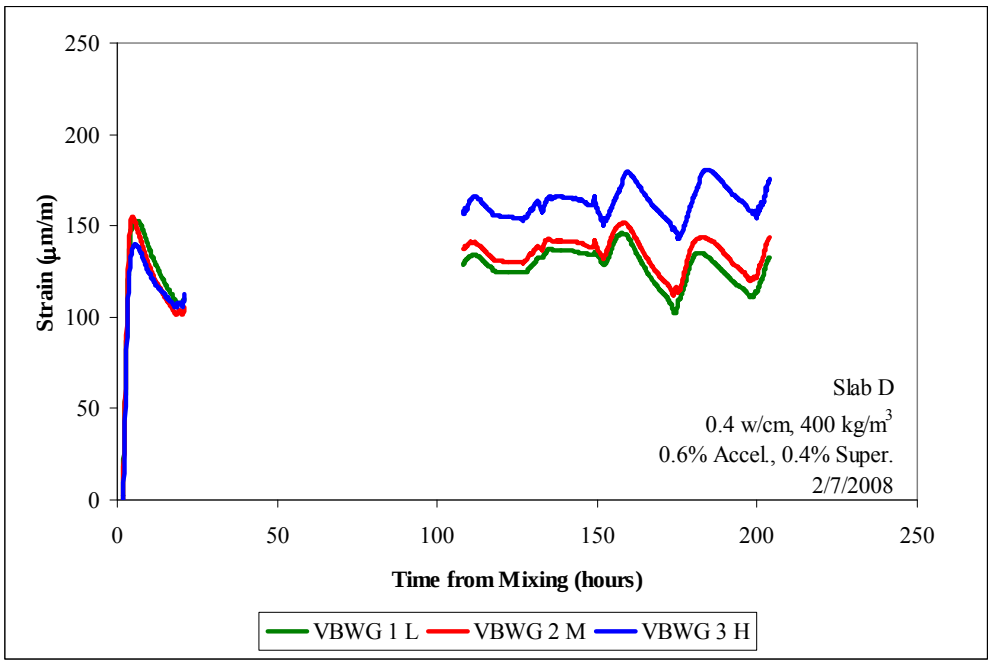

Figure 7.31: Strain generation for Slab D, 0.1 m thick

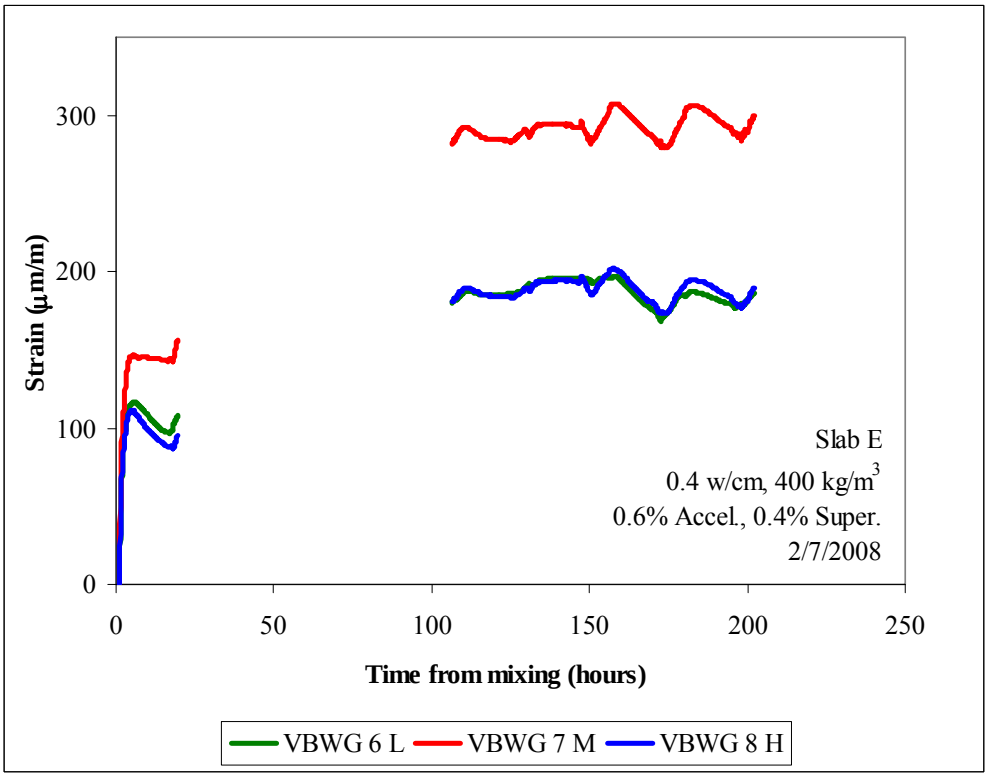

Figure 7.32: Strain generation for Slab E, 0.1 m thick

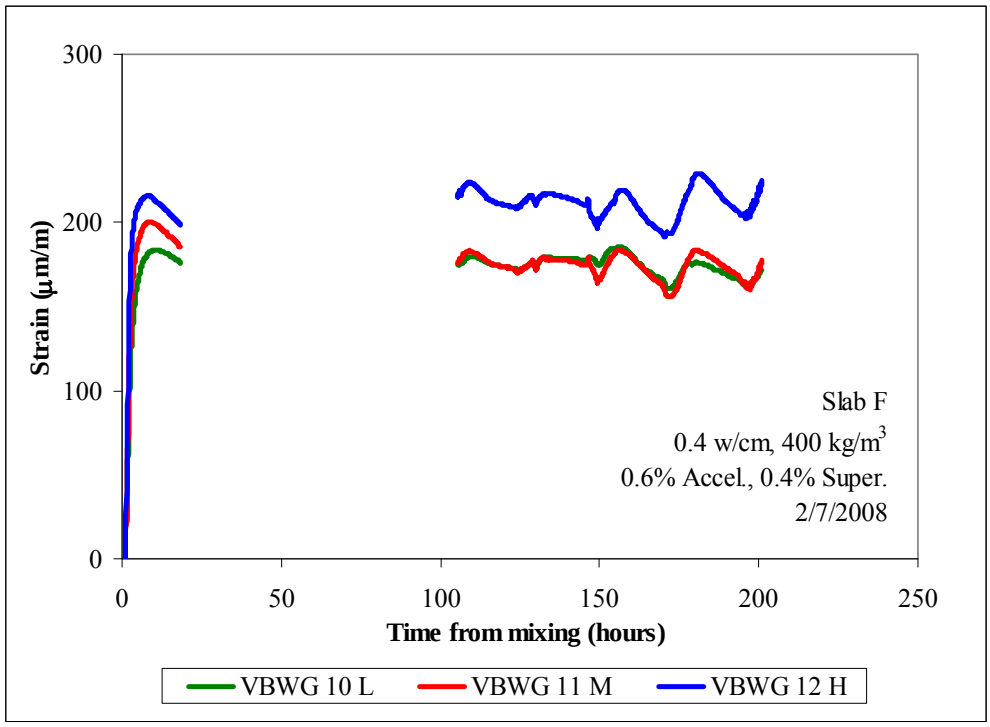

Figure 7.33: Strain generation for Slab F, 0.1 m thick

Relative humidity was only monitored on Slabs D and E and these results are shown in Figure 7.34 and Figure 7.35. It was expected to see a lower relative humidity in Slab E since it was not cured or kept covered with plastic sheeting after casting in the same fashion as Slab D. However, the relative humidity decreased rapidly in both slabs to values just below 80% one day after casting. This suggested that the lowering of internal relative humidity in CACC slabs may be more a function of rapid hydration and internal self dessication, with a loss of moisture to the environment a smaller factor in this early-age decrease in relative humidity.

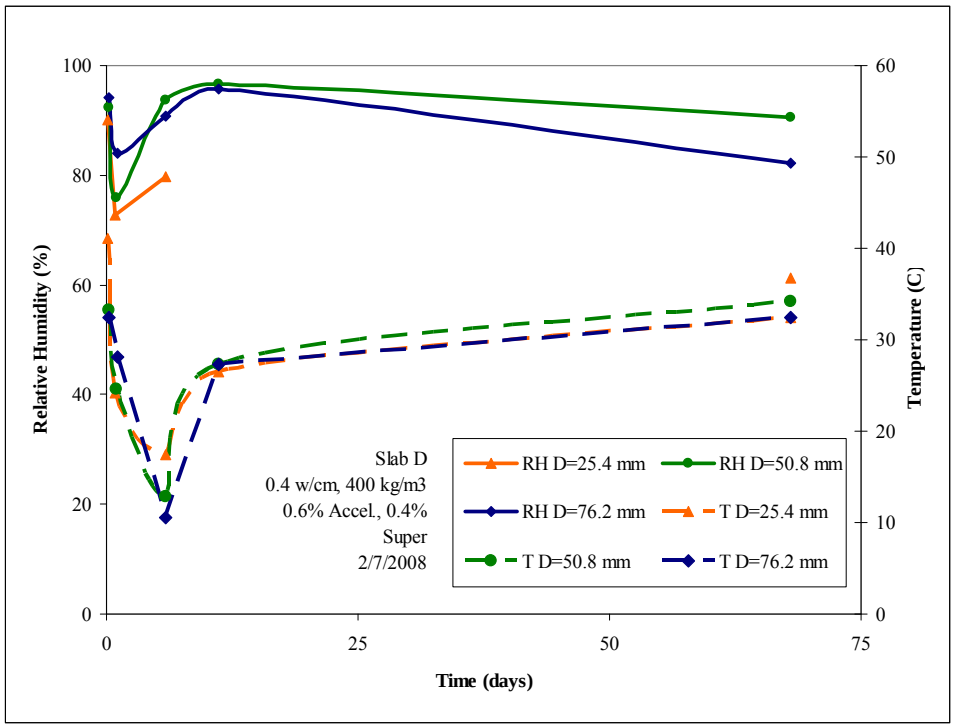

Figure 7.34: Relative humidity and temperature for Slab D, 0.1 m thick

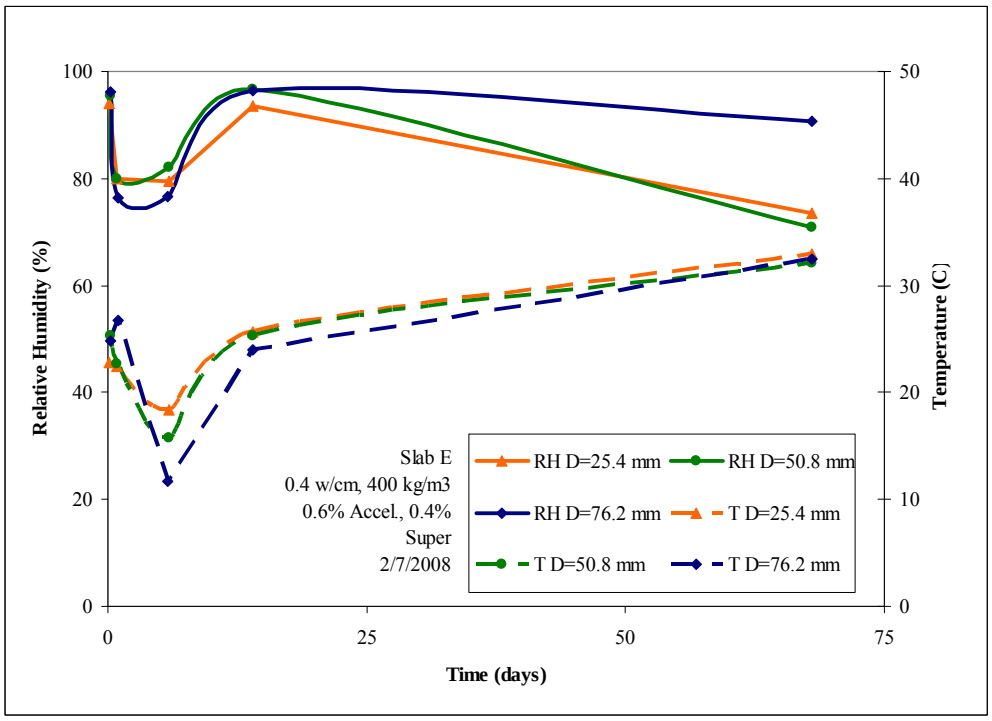

Figure 7.35: Relative humidity and temperature for slab E, 0.1 m thick, 75 hours

Table 7.6 and Table 7.7 show the development of compressive strength for concrete cast from slabs D and E, respectively and cured isothermally in a 38 °C water bath. The concrete from Slab E was not well consolidated (observed upon demolding at 24 hours) and is the probable cause for the decreased strength for cylinders from Slab E.

Table 7.6: Mechanical property data for Slab D concrete – 38 °C cure

Age (days)	Compressive Strength (MPa)
1	23.1
5	21.1
7	22.4
28	29.2

Table 7.7: Mechanical property data for Slab E concrete – 38 °C cure

Age (days)	Compressive Strength (MPa)
1	24.1
5	16.6
7	19.7
28	23.5

Table 7.6 and Table 7.7 show that conversion in these cylinders occurred at five days and increased at 7 and 28 days of testing. Table 7.8, Table 7.9 and Table 7.10 show mechanical properties for the concrete cylinders cast from concrete for slab F and represent the three curing conditions outlined in section 7.1: semi-adiabatic insulated box, 38 °C water bath and ambient conditions.

Table 7.8: Mechanical property data Slab F concrete, Adiabatic Cure

Age (days)	Compressive Strength (MPa)
1	22.6
7	25.9
28	29.9

Table 7.9: Mechanical property data Slab F concrete, Ambient Cure

Age (days)	Compressive Strength (MPa)
1	37.9
7	45.5
28	54.2

Table 7.10: Mechanical property data Slab F concrete-38 °C water bath

Age (days)	Compressive Strength (MPa)	Elastic Modulus (GPa)	Tensile Strength (MPa)
1	29.9	49.9	4.8
3	29.8	48.5	4.0
5	25.2	45.4	3.9
7	27.3	47.9	4.6
28	31.3	52.4	---

Concrete cured in quasi-adiabatic conditions (Table 7.8) shows a low strength evident of full conversion of this concrete 1 day of age. Strength then increased from 22.6 MPa to 29.9 MPa at 28 days after casting. On the other hand concrete cured in ambient laboratory conditions (low temperature, low self heating) showed strength increase through 28 days of testing to a value of 54.2 MPa. This represented an unconverted strength of this concrete mixture.

Concrete cured under 38 °C isothermal conditions in a water bath converted at 5 days with a minimum compressive strength of 25.2 MPa followed by subsequent strength gain up to 28 days. Elastic modulus and splitting tensile strength also converted at five days with strengths of 45.4 GPa and 3.9 MPa, respectively.

7.10 CONCLUSIONS

Casting real field scale slabs of calcium aluminate cement concrete outdoors generated several useful pieces of information for the dissertation research. Temperature profiles used to “drive” temperature in rigid cracking and free deformation frames were

generated and the results of this testing were shown in Chapter 5. For all of the slabs cast strain was recorded with the use of vibrating wire gages. Interestingly, all slabs exhibited generation of expansive strain that was effectively "locked-in" to the slabs for the monitored duration of the slabs. In other words strain never reached a point of exhibiting shrinkage for the CACC slabs. Relative humidity measurements indicated that a rapid decrease in relative humidity to values below 80% within the first 24 hours is largely due to the rapid hydration and uptake of water by hydration products in CACC systems. Unconverted versus covered slabs exhibited the essentially the same decrease in relative humidity, thereby reducing the implications of moisture lost to the surrounding environment.

8 Conclusions

This chapter summarizes the main findings from this research study on the early-age behavior of calcium aluminate cement systems, including concrete, micro-concrete and pastes. Lastly, recommendations for future research on this innovative and unique material are presented to further advance the work presented in this dissertation.

8.1 SUMMARY

Compared to the vast amount of knowledge that exists for early-age behavior of ordinary portland cement concretes, relatively little knowledge in this area exists for calcium aluminate cement concrete. Even though there is a large amount of information for early-age behavior of ordinary portland cement there is still much debate about the complexities of interaction at the nano, micro, meso and macro scale at early-age in these "well-understood systems". In fact, there has been resurgence in the past 10-15 years to better quantify early-age properties using new methodologies and new testing approaches in an effort to provide better input for computer models to predict heat of hydration and volume change and to estimate and/or model the cracking risk of concrete structures.

To initiate similar fundamental data generation for calcium aluminate systems, a scientific network at several leading universities across the world was started in the fall of 2004 by Kerneos Aluminate Technologies (formerly Lafarge Aluminates). As part of this research initiative, Kerneos sponsored the dissertation research for one doctoral student at each of the identified universities. The University of Texas at Austin was the first university chosen as part of this network. The goal for research at UT Austin was to investigate early-age volume change of CAC systems and to specifically elucidate the possibility for cracking risk compared to OPC systems. Since 2004, two additional PhD research projects have been sponsored by Kerneos, one at Ecole Polytechnique Federale

de Lausanne (EPFL) in Lausanne, Switzerland under the direction of Dr. Karen Scrivener investigating CAC microstructure and another at the University of New Brunswick under the direction of Dr. Michael Thomas investigating CAC durability.

At the onset of this project, one of the goals was to generate relevant data on CACC as inputs to a software program developed at UT-Austin known as "ConcreteWorks."[29] In this highly customizable computer model, the heat generation in a mass OPC concrete element may be predicted and recommendations to limit cracking risk due to thermal gradients, concrete maturity and other parameters is given. However, it was soon realized that not only did calcium aluminate cement concrete behave quite differently from ordinary portland cement concrete, but generation of fundamental material properties were not possible within the scope of this current research project.

It was realized that one of the key aspects of this research project would be to advance the state knowledge for this unique material through generation of fundamental information/data to characterize parameters such as chemical shrinkage, drying shrinkage, autogenous deformation, restrained cracking risk and early-age volume change. There is a learning curve when investigating any material and the learning curve with this material was steep at the initiation of the project. The first year of the project was centered on familiarization and ease of working with this new (to this research group) and unique material that had properties that varied significantly from ordinary portland cement concrete. Calcium aluminate cement systems are highly temperature dependent and hydration is complicated by the fact that metastable hydrates, stable hydrates or a combination thereof may be formed at different temperatures during hydration. The conversion of metastable hydrates is inevitable and highly dependent upon time, temperature and moisture availability. In addition, the hydration of CACC is highly exothermic on a much shorter time scale than OPCC. As a result, the need for

active temperature control for the majority of testing techniques was realized early in the research program. A variety of testing techniques that had been applied successfully to portland cement concrete systems were applied to calcium aluminate cement concrete. Some of these attempts at implementing established techniques were successful, whereas others were found to be ineffective for CACC-based systems, either resulting in modifications to these techniques or abandonment of them.

It was decided early on in the project that the best way to characterize volume change and assess the cracking risk of this material was to use a scaled down version (1/3 scale) of rigid cracking and free deformation frames (formerly referred to as free deformation frames) that had already seen success in an on-going project at The University of Texas at Austin. The design, procurement, fabrication, and construction of formwork, as well as the procurement and programming of appropriate data acquisition systems to run this highly complex and innovative testing apparatus took approximately 1.5 years before the first successful test was performed in these devices. During this time, research focusing on drying shrinkage, chemical shrinkage, and autogenous deformation testing was initiated. As was later born out, the rigid and free deformation frames became vital to the success of this research project and provided much information that was previously unknown for this material. This is one of the only types of test set-ups that allows for active (and reactive) temperature control to either maintain isothermal testing conditions for rapidly hydrating samples such as the CAC micro-concrete investigated as part of this dissertation.

As part of this project we (Folliard and Ideker) were fortunate to spend 4 months of residency in the spring/summer of 2006 in Lausanne, Switzerland at Ecole Polytechnique Federale de Lausanne working with Dr. Karen Scrivener and her research group. This included another PhD student, Christophe Gosselin, who is a student

working as part of the Scientific Network on research also funded by Kerneos Aluminate Technologies specifically investigating early-age microstructural development in CAC systems (pastes and micro-concrete). The time spent in Switzerland was a key component to the future direction of the research project. Collaboration with the researchers at EPFL, in particular Dr. Scrivener, whose expertise in the area of calcium aluminates was essential to discussion and interpretation of results as well as guidance and direction for future testing. The first testing with the rigid cracking and free deformation frames was conducted in Switzerland and was a direct result of the support from the laboratory staff at EPFL. In addition, isothermal calorimetry through a wide range of temperatures was investigated in that time period. The use of an automated chemical shrinkage set-up at EPFL was later replicated for further study at UT Austin and was instrumental in determining the chemical shrinkage characteristics of CAC pastes.

At the time of publication of this dissertation, 38 rigid cracking and free deformation tests have been conducted as part of this dissertation research, equaling a total of 5600 hours of time that micro-concrete or concrete was evaluated with the use of these innovative testing apparatus. A wide range of isothermal temperatures were investigated as well as realistic time-temperature histories. To provide realistic time-temperature history information necessary for rigid cracking and free deformation frame mixtures some of the final research done as part of this dissertation project was to cast CACC slabs (0.9 x 0.9m with varying depth) outdoors. These slabs were heavily instrumented and monitored for temperature, strain (vibrating wire gages) and relative humidity. The temperature profiles were used to drive the temperature of hydrating CAC micro-concrete in the rigid cracking and free deformation frames.

8.2 CONCLUSIONS

The major findings from this research project have further elucidated the profound effect of temperature on hydration of calcium aluminate cement systems. The key findings from the project are summarized below:

- Chemical shrinkage of calcium aluminate cement pastes is significantly greater (2 to 4 times higher) than ordinary portland cement pastes through a range of isothermal temperatures.

- The lowest chemical shrinkage occurs for metastable hydrates at 20 °C, whereas the highest chemical shrinkage occurs for stable hydrates at a temperature of 45 °C .

- Curing isothermally at 30 °C and below illustrated that metastable hydrate formation (particularly CAH_{10}) resulted in shrinkage in free deformation testing and the generation of tensile stresses in rigid cracking frame testing. The generation of tensile stress at temperatures less than 30 °C typically resulted in cracking (within the first 48 hours) of the CAC micro-concrete before artificial cooling was induced on the specimens.

- Maximum free deformation was observed at approximately 1000 μm/m for samples cured isothermally at 20 °C, and corresponding tensile stress generation was approximately 2 – 2.5 MPa in rigid cracking frame testing.

- Curing isothermally at temperatures above 30 °C promoted the formation of metastable (predominantly C_2AH_8) and stable hydrates that generated expansion in free deformation testing and led to development of compressive stress in rigid cracking frame testing. The maximum

compressive stresses obtained were just over 6 MPa for a fully converted micro-concrete mixture cured isothermally at 55 °C.

- Realistic time-temperature history investigations in rigid cracking frame testing showed evidence of cracking during the cooling phase of the material after the peak temperature during hydration was reached.

- While isothermal curing at high temperature leads to accelerated formation of metastable hydrates and generation of potentially beneficial compressive stress (pre-compression), actual CAC concrete elements cast in a field application typically undergo a temperature history where at least for a short time period (~30 minutes to 1 hour), the material passes through a temperature range where the formation of metastable hydrates is favored before eventually crossing a temperature threshold of about 30 °C, where the formation of stable hydrates or the process of conversion from metastable to stable hydrates is favored.

- The time spent at low temperature ($T < 30$ °C) has significant impact on the volume change of the material, later age conversion and ultimate volume stability as evidenced by investigation into realistic time temperature histories as part of this dissertation

- The replacement of 30 % Class C fly ash for CAC had little impact on shrinkage and tensile stress development in 20 °C isothermal testing in rigid cracking and free deformation frames.

- The replacement of 30 % Class C fly ash for CAC showed little impact on compressive stress development in 38 °C isothermal testing in rigid

cracking frame testing. However, a reduction in autogenous expansion by 2/3 was observed due to incorporation of the Class C fly ash

- CACC was shown to be more crack resistant than OPCC in ASTM C 1581 (restrained ring drying shrinkage testing)
- Drying shrinkage measurements using modified ASTM C 157 testing on CACC demonstrated that measurements should be taken at much earlier age (e.g., 2-3 hours after T_{off}) than comparative OPCC samples. A major portion of the drying shrinkage is not captured if measurements are started 24 hours after casting

8.3 FUTURE WORK

The following are some recommendations for future research to build on what was learned and presented in this dissertation:

- Investigation into hydrate development with XRD and/or TGA/DTA on chemical shrinkage samples cured at 20 °C (sampled at several discrete time intervals during the high rate of chemical shrinkage and after this rate flat lines) and 38 °C, to monitor and confirm the progress of conversion

- SEM work on chemical shrinkage samples cured at 20 and 38 °C to further qualify the pore structure of the system and the theory of a dense and essentially low permeability microstructure at 20 °C that severely limits the ingress of water (e.g., evidence of abrupt change in slope of chemical shrinkage curve)

- Extension of work with SCMs to include more work with Class C fly ash and slag as replacement for CAC in rigid cracking and free deformation testing

- Separation of the thermal component during realistic time-temperature histories from stresses generated due to microstructural formation and concomitant autogenous deformations.

- Continued long-term measurements on drying shrinkage samples cast toward the end of this dissertation research to further elucidate the potential difference in drying shrinkage between CACC and OPCC

- Generation of addition data to better provide crack prediction models for CACC, including:
    - creep of converted versus unconverted CACC
    - thermal "signatures" of CACC systems, based on potential application of activation energy approach
    - semi-adiabatic and adiabatic calorimetry to provide necessary inputs for computer modeling programs such as ConcreteWorks

- Evaluations of a range of realistic time-temperature histories to further investigate the necessary duration of high temperature (at various high temperatures) to promote full conversion

- Investigations into microstructural gradients that may exist in field structures where the hottest part of the element may actually be of the lowest strength and the coolest part of the element may be the highest

- Development of a reliable field method for predicting converted versus unconverted strength prediction

- Development of a method similar to the “maturity” method used for OPCC to predict property development and strength for CACC

9 References

1. Scrivener, K.L. and Capmas, A., *Lea's Chemistry of Cement and Concrete*. Fourth ed. Calcium Aluminate Cements, ed. P.C. Hewlett. 1998, Arnold: New York and Toronto. 69 p.
2. *Calcium Aluminate Cements in Construction: A Reassessment*, Concrete Society, 1997.
3. Argandona, A., *Ethical Aspects of an Urban Catasrophe*, Journal of Business Ethics, 1995, 14 (7): p. 511-530.
4. Fryda, H., Scrivener, K.L., and Chanvillard, G., *Relevance of Laboratory Tests to Field Applications of Calcium Aluminate Cement Concretes*, in Proceedings of the International Conference on Calcium Aluminate Cements (CAC), Heriot-Watt University, Edinburgh, Scotland, UK. 2001, IOM Communications Ltd, p. 215-247.
5. Cong, X. and Kirkpatrick, R.J., *Hydration of calcium aluminate cements. A solid-state 27Al NMR study*, Journal of the American Ceramic Society, 1993, 76 (2): p. 409-416.
6. Gessner, W. and Moehmel, S., *Effects of the Aluminate Quality on Hydration and Thermal Behaviour of Calcium Aluminate/Aluminate Mixes*, in Calcium Aluminate Cements 2001, Edinburgh, Scotland, U.K. 2001, IOM Communications, p. 291-317.
7. Gessner, W. and Moehmel, S., *Recent Researches on Calcium Aluminate Hydration*, in Calcium Aluminate Cements 2001, Edinburgh, Scotland, UK. 2001, IOM Communications, p. 151-154.
8. Guirado, F., Gali, S., Chinchon, S., and Rius, J., *Crystal Structure Solution of Hydrated Alumina Cement from X-ray Powder Diffraction Data*, Angewandte Chemie - International Edition, 1998, 37 (1-2): p. 72-78.
9. Banfill, P.F.G., *Superplasticizers for Ciment Fondu. Part 2: Effects of temeprature on the hydration reactions*, Advances in Cement Research, 1995, 7 (28): p. 151-157.
10. Bushnell-Watson, S.M., *On the Cause of the Anomalous Setting Behaviour With Respect to Temperature of Calcum Aluminate Cements*, Cement and Concrete Research, 1990, 20 (5): p. 677-686.
11. Capmas, A., Sorrentino, D., and Damidot, D., *Effect of Temperature on Setting Time of Calcium Aluminate Cements*, in Proceedings of the International Symposium on Calcium Aluminate Cements, London, England. 1990, p. 65-80.
12. Fryda, H., 2006, *personal communication*
13. Fryda, H., 2005, *personal communication*
14. Riding, K.A. and Poole, J., *Unpublished Review*. 2005.
15. ACI Committee 318, ACI 318, *Structural Building Code*, ACI, Farmington Hills, Michigan, 2008.

16. ACI 224R-01, *Control of Cracking in Concrete Structures*, ACI, Farmington Hills, Michigan, 2001.

17. ACI Committee 209, ACI 209R, *Prediction of Creep, Shrinkage, and Temperature Effects in Concrete Structures*, ACI, Farmington Hills, Michigan, 1992.
18. Gajda, J. and McGee, T.D., *Elastic Properties of a Calcium Aluminate-Cement-Based Concrete*, American Ceramic Society Bulletin, 1997, 76 (4): p. 81-85.
19. Neville, A.M., *Properties of Concrete*, Fourth Edition ed. 1996, Essex, England: Pearson Education Limited, 844 p.
20. Shaeles, C.A. and Hover, K.C., *Influence of mix proportions and construction operations on plastic shrinkage cracking in thin slabs*, ACI Materials Journal, 1998, 85 (6): p. 495-504.
21. Bentur, A., Igarashi, S.-I., and Kovler, K., *Prevention of autogenous shrinkage in high-strength concrete by internal curing using wet lightweight aggregates*, Cement and Concrete Research, 2001, 31 (11): p. 1587-1591.
22. Sellevold, E., Bjøntegaard, Ø., Justnes, H., and Dahl, P.A., *High Performance Concrete: Early Volume Change and Cracking Tendency*, Thermal Cracking in Mass Concrete, RILEM Report 25, E.F. Spon, London 1995,
23. Bjøntegaard, O., *Thermal Dilation and Autogenous Deformation as Driving Forces to Self-Induced Stresses in High Performance Concrete*, in *Division of Structural Engineering*. 1999, The Norwegian University of Science and Technology.
24. Burrows, R.W., *The Visible and Invisible Cracking of Concrete*, ACI Monograph No. 11, American Concrete Institute, Farmington Hills, Michigan 1998,
25. AASHTO PP34-99, *Standard Practice for Estimating the Cracking Tendency of Concrete*, AASHTO, 1998.
26. ASTM C 1581, *Standard Test Method for Determining Age at Cracking and Induced Tensile Stress Characteristics of Mortar and Concrete under Restrained Shrinkage*, ASTM International, West Conshohocken, PA, 2004.
27. ASTM C 157, *Standard Test Method for Length Change of Hardened Hydraulic-Cement Mortar and Concrete*, ASTM International, West Conshocken, Pennsylvania, 2006.
28. Springenschmid, R., Brietenbücher, R., and Mangold, M., *Development of the Cracking Frame and the Temperature-Stress Testing Machine*, Rilem Report 25, Thermal Cracking in Mass Concrete, E & FN Spon, 1994.
29. Riding, K.A., *Early Age Concrete Thermal Stress Measurement and Modeling*, in *Civil, Environmental and Architectural Engineering*. 2007, The University of Texas at Austin: Austin, Texas. p. 588.
30. ASTM C 618, *Standard Specification for Coal Fly Ash and Raw or Calcined Natural Pozzolan for Use in Concrete*, ASTM International, West Conshocken, Pennsylvania, 2008.

31. La Chatelier, H., *Sur les Changements de Volume qui Accompagent le durcissement des Ciments*, Bulletin Societe de l'Encouragement pour l'Industrie Nationale, 1900, Seme Serie (Tome 5).
32. Geiker, M., *Studies of Portland Cement Hydration: Measurements of Chemical Shrinkage and a Systematic Evaluation of Hydration Curves by Means of the Dispersion Model*. 1983, Technical University of Denmark: Copenhagen, Denmark.
33. Knudsen, T. and Geiker, M., *Chemical Shrinkage as an Indicator of the State of Hardening*, in International Conference on Concrete at Early Ages. 1982, p. 163-165.
34. Boivin, S., Acker, P., Rigaud, S., and Clavaud, B., *Experimental Assessment of Cemical Shrinkage of Hydrating Cement Paste*, in Autoshrink '98 Proceedings of the INternational Workshop on Autogenous Shrinkage of Concrete. 1998, p. 77-88.
35. Justnes, H., Clemmens, F., Depuydt, P., Van Gemert, D., and Sellevold, E.J., *Correlating the deviation point between extrenal and total chemical shrinakge with setting time and other characteristics of cement pastes*, in Shrinkage 2000 - International RILEM Workshop on Shrinkage of Concrete, Paris, France. 2000, p. 57-73.
36. Sant, G., *Measurement of volume change in cementitious materials at early ages review of testing protocols and interpretation of results*, in Transportation Research Record, Washington, D.C. 2006, p. 21-29.
37. ASTM C 1608, *Test Method for Chemical Shrinkage of Hydraulic Cement Paste*, ASTM International, West Conshocken, Pennsylvania, 2005.
38. ASTM C 989-06, *Standard Specification for Ground Granulated Blast-Furnace Slag for Use in Concrete and Mortars*, ASTM International, West Conshocken, Pennsylvania, 2006.
39. ASTM C 150, *Standard Specification for Portland Cement*, ASTM International, West Conshocken, Pennsylvania, 2007.
40. ASTM C 305, *Standard Practice for Mechanical Mixing of Hydraulic Cement Pastes and Mortars of Plastic Consistency*, ASTM International, West Conshocken, PA, 2006.
41. Whigam, J., *Evaluation of Restraint Stresses and Cracking in Early-Age Concrete with the Rigid Cracking Frame*. 2005, Auburn University: Auburn, Alabama.
42. Poole, J., *Modeling temperature sensitivity and heat evolution of concrete* in *Civil Engineering*. 2006, The University of Texas at Austin: Austin.
43. Mangold, M., *Methods for Experimental Determination of Thermal Stresses and Crack Sensitivity in the Laboratory*, Prevention of Thermal Cracking in Concrete at Early Ages, E & Fn Spon, 1998.
44. ASTM C 403-05, *Standard Test Method for Time of Setting of Concrete Mixtures by Penetration Resistance*, ASTM International, West Conshocken, Pennsylvania, 2005.
45. Bushnell-Watson, S.M. and Sharp, J.H., *Further Studies of the Effect of Temperature Upon the Setting Behaviour of Refractory Calcium Aluminate Cements*, Cement and Concrete Research, 1990, 20 (4): p. 623-635.

46. Emborg, M., *Developing Early Age Mechanical Behaviour*, Prevention of Thermal Cracking in Concrete at Early Ages, Rilem Report 15, R. Springenschmid, E.F. Spon, London, U.K. 1998, p. 76-148.
47. Mindess, S., Young, J.F., and Darwin, D., *Concrete*, 2nd ed. 2003, Upper Saddle River: Pearson Education, Inc. 644 p.
48. Lamour, V.H.R., Monteiro, P.J.M., Scrivener, K.L., and Fryda, H., *Mechanical Properties of Calcium Aluminate Cement Concretes*, in Proceedings of the International Conference on Calcium Aluminate Cements (CAC), Heriot-Watt University, Edinburgh, Scotland, UK. 2001, IOM Communications Ltd, p. 199-213.
49. Lamberet, S.F., H., Saucier, F., and Mouchot, A., *Drying and Shrinkage of CAC-Based Concrete*, in Calcium Aluminate Cements: Proceedings of the Centenary Conference Avignon, France 2008, IHS BRE Press.
50. TEX-428-A, *Determining the Coefficient of Thermal Expansion of Concrete*, TxDOT, 2001.
51. Viviani, M., Glisic, B., and Smith, I.F.C., *Separation of Thermal and Autogenous Deofrormation at Varying Temperatures using Optical Fiber Sensors*, Cement and Concrete Composites, 2007, 29 (6): p. 435-447.
52. ASTM C 39, *Standard Test Method for Compressive Strength of Cylindrical Concrete Specimens*, ASTM International, West Conshocken, Pennsylvania, 2005.
53. ASTM C 469, *Standard Test Method for Static Modulus of Elasticity and Poisson's Ratio of Concrete in Compression*, ASTM International, West Conshocken, Pennsylvania, 2002.
54. ASTM C 496, *Standard Test Method for Splitting Tensile Strength of Cylindrical Concrete Specimens*, ASTM International, West Conshocken, Pennsylvania, 2004.

10 Vita

Jason Henry Ideker was born on March 12, 1979 in Brevard, North Carolina. He graduated from Brevard Senior High School in 1997. He then attended the Georgia Institute of Technology and received a Bachelor of Science in Civil Engineering in 2002, with high honors. During his time at Georgia Tech he was employed with Willmer Engineering Inc., as part of the cooperative employment program for undergraduates. In September of 2002 he pursued higher education at The University of Texas at Austin. He received a Master of Science in Engineering in 2004 under the advisement of Dr. Kevin J. Folliard and Dr. Maria C.G. Juenger while working as a graduate research assistant at the Concrete Durability Center. While pursuing his doctoral degree he was a visiting Ph.D. Candidate at École Polytechnic Fédérale de Lausanne (EPFL) in Lausanne, Switzerland in 2006.

Permanent address: 280 Pleasant Hill Drive, Brevard, North Carolina 28712

This dissertation was typed by Jason Henry Ideker.